

Leonel António Almeida Fernandes

Licenciado em Ciências da Engenharia Química e Bioquímica

Development of a new solution to attain a controlled decrease of fluids density

Dissertação para obtenção do Grau de Mestre em Engenharia Química e Bioquímica

Orientador: Stéphanie Branco Leal, GEO-Ground Engineering Operations Co-orientador: Ana Isabel Nobre Martins Aguiar de Oliveira Ricardo, Professora Catedrática, FCT-UNL

Júri:

Presidente: Mário Fernando José Eusébio, Doutor, Professor Auxiliar, FCT/UNL Arguente(s): Pedro Miguel Calado Simões, Doutor, Professor Associado, FCT/UNL Vogal(ais): Stéphanie Leal, GEO-Ground Engineering Operations





Leonel António Almeida Fernandes

Licenciado em Ciências da Engenharia Química e Bioquímica

Development of a new solution to attain a controlled decrease of fluids density

Dissertação para obtenção do Grau de Mestre em Engenharia Química e Bioquímica

Orientador: Stéphanie Branco Leal, GEO-Ground Engineering Operations Co-orientador: Ana Isabel Nobre Martins Aguiar de Oliveira Ricardo, Professora Catedrática, FCT-UNL

Júri:

Presidente: Mário Fernando José Eusébio, Doutor, Professor Auxiliar, FCT/UNL Arguente(s): Pedro Miguel Calado Simões, Doutor, Professor Associado, FCT/UNL Vogal(ais): Stéphanie Leal, GEO-Ground Engineering Operations



Development of a new solution to attain a controlled decrease of fluids density

Copyright ©Leonel António Almeida Fernandes, Faculdade de Ciências e Tecnologia, Universidade Nova de Lisboa.

A Faculdade de Ciências e Tecnologia e a Universidade Nova de Lisboa têm o direito, perpétuo e sem limites geográficos, de arquivar e publicar esta dissertação através de exemplares impressos reproduzidos em papel ou de forma digital, ou por qualquer outro meio conhecido ou que venha a ser inventado, e de a divulgar através de repositórios científicos e de admitir a sua cópia e distribuição com objetivos educacionais ou de investigação, não comerciais, desde que seja dado crédito ao autor e editor.

Agradecimentos

Terminada uma etapa da minha vida, gostaria de agradecer a todas as pessoas que tornaram este feito possível, pois sem elas teria sido um caminho muito árduo.

Em primeiro lugar, gostaria de agradecer à minha orientadora, Stéphanie Leal, por toda a sua disponibilidade, dedicação, ajuda, motivação, pela sua paciência interminável e atenção ao detalhe. Gostaria também de agradecer aos meus co-orientadores, prof. Dra Ana Aguiar Ricardo, pela sua disponibilidade, apoio e pelas sugestões dadas ao longo do percurso, e Leandro Parada, pela sua paciência, ajuda e pontos de vista que foram crucias para a navegação da dissertação.

Quero também agradecer à GEO pelo seu ambiente relaxado, amigável e motivador. Um agradecimento especial ao Eng.º Jorge Capitão-Mor, pela sua disponibilidade em transmitir o seu conhecimento valioso e inspirador para novas ideias, pelo seu sentido crítico e pelo seu interesse contínuo no tema. Quero também agradecer aos meus colegas durante o meu percurso na GEO, Carla Rodrigues e Joana Bernardo, pelo seu apoio.

Em segundo lugar, quero agradecer a todas as pessoas que me apoiaram directamente ou inderetamente. Aos meus colegas de curso, João Freira, Carolina Spranger, Eliana Amaral, Bernardo Rodrigues, Rafaela Neves, e restantes, pela sua amizade e pelo seu apoio durante todos estes anos que estivemos juntos.

Por último, gostaria de agradecer aos meus familiares, os maiores contribuidores para o meu sucesso académico, aos meus pais, Fortunato Mendes e Eunice Fernandes, pelo seu apoio, motivação e amor incondicional durante todos os momentos difíceis e por sempre acreditarem em mim. Ao meu irmão, Valdir Fernandes, pela sua amizade, motivação e oportunidades que me forneceu durante todo este percurso. Sem eles, nunca teria chegado ao ponto em que estou nem que alguma vez estarei. Estou-lhes eternamente grato.

Abstract

The objective of this work was to achieve a controlled density reduction of a support fluid within the intervals of 0.02, 0.06, 0.09 and 0.12 g/cm³, while: (1) reducing the Marsh viscosity by 5 s/quart or less, (2) generating a density gap between the middle and bottom of the recipient by less than 0.03 g/cm³ (3) generating a collectable deposit, (4) performing in a density range within 1.00-1.20 g/cm³, and (5) performing within 30 minutes or less.

Coagulants, flocculants, and combinations of these products were tested on two clays: A and B.

For clay A, a density reduction interval of 0.02 g/cm³ was achieved using aluminum sulfate at the concentration of 600 mg/L, producing density gaps inferior to 0.03 g/cm³ and collectable deposits. The density reductions of 0.06 g/cm³ and 0.09 g/cm³ were achieved using aluminum sulfate and polyferric sulfate at the concentrations of 1000 mg/L, with collectable deposits.

For clay B, the density reduction intervals of 0.02 g/cm³ and 0.06 g/cm³ were attained. The simultaneous achievement of the density reduction interval of 0.02 g/cm³ and the reduction of the Marsh viscosity equal or less than 5 s/quart was achieved using: (1) TelSun 5153 at the concentration of 150 mg/L, (2) aluminum sulfate and ferrous sulfate at the concentrations of 150 mg/L with TelSun 5153 at the concentration of 150 mg/L. The density reduction of 0.06 g/cm³ was attained using anionic flocculant A0410 at the concentration of 1000 mg/L with hydrochloric acid at the concentrations of 3.3 - 4.7 mM. For this clay, the final density gaps created between the bottom and middle were lower than 0.03 g/cm³.

A great disparity was observed between the results obtained for both clays, thus, for future work, tests should be performed on soils with different clays and compositions (with sands and silts) to simulate real-world conditions.

Keywords: Controlled density reduction, coagulation, flocculation, soil stabilization, support fluids

Resumo

O objetivo deste trabalho foi atingir uma redução controlada da densidade de uma solução nos intervalos de 0,02, 0,06, 0,09 e 0,12 g / cm³, enquanto: (1) reduz a viscosidade de Marsh por 5 s/quarto ou menos, (2) gera um diferencial de densidade entre o meio e o fundo do recipiente inferior a 0,03 g/cm³, (3) gera um depósito coletável, (4) opera numa gama de densidades de 1,00-1,20 g/cm³, e (5) que atua em 30 minutos ou menos.

Coagulantes, floculantes e combinações desses produtos foram testados em duas argilas. Com a argila A, um intervalo de redução de densidade de 0,02 g/cm³ foi obtido utilizando sulfato de alumínio com uma concentração de 600 mg/L, produzindo diferenciais de densidade inferiores a 0,03 g/cm³ e depósitos coletáveis. A redução de densidade de 0,06 g/cm³ foi atingida utilizando sulfato de alumínio e de 0,09 g/cm³ foi obtida utilizando sulfato poliférrico, ambos nas concentrações de 1000 mg/L, com depósitos coletáveis.

Para a argila B, foram atingidos os intervalos de redução da densidade de 0,02 g/cm³ e 0,06 g/cm³. A obtenção simultânea do intervalo de redução de densidade de 0,02 g/cm³ e a redução da viscosidade de Marsh igual ou inferior a 5 s/quarto foi obtida usando: (1) TelSun 5153 com uma concentração de 150 mg/L, (2) sulfato de alumínio, sulfato poliférrico e sulfato poliférrico nas concentrações de 150 mg/L com TelSun 5153 na concentração de 150 mg/L. A redução da densidade de 0,06 g/cm³ foi obtida utilizando o floculante não-iónico A0410 com uma concentração de 1000 mg/L com ácido clorídrico nas concentrações de 3,3 – 4,7 mM. Para esta argila, os diferenciais de densidade foram menores que 0,03 g/cm³.

Foi observada uma grande disparidade entre os resultados obtidos para ambas as argilas e assim, para trabalho futuro, devem ser feitos ensaios em solos com diferentes argilas e composições (com areias e siltes) para melhor simular condições reais.

Palavras-chave: Redução controlada da densidade, coagulação, floculação, estabilização de solos, fluidos de escavação.

Contents

1.	Introduc	tion1
	1.1 Soil St	abilization1
	1.1.1	Support fluids1
	1.2 Soil pr	operties4
	1.2.1	Clay mineralogy5
	1.2.2	Clay colloid interactions
	1.3 Solid-l	_iquid Separation methods13
	1.3.1	Physical methods13
	1.3.2	Chemical methods
	1.3.3	Field Assisted Methods
	1.4 Outline	э
2.	Material	s and Methods33
	2.1 Reage	ents
	2.2 Equipr	ment
	2.3 Execu	tion protocols34
r	2.3.1 mixing time	Density reduction as function of coagulant type, coagulant concentration, mixing speed, initial densities and introduction method
	2.3.2	Density reduction as a function of agitator type35
r	2.3.3 method and	Density reduction as a function of coagulant and flocculant type, introduction dimixing speeds
	2.3.4	Density reduction as function of flocculant charge (cationic and non-ionic),
(concentration	on, and solution pH and temperature38

2.3.5	Density reduction as function of HCl concentration and solution volume	
olay/3aric	7 TIIX (10	55
2.4 Cha	racterization protocols	40
2.4.1	Marsh viscosity measurement	40
2.4.2	Density measurement	40
2.4.3	Brookfield viscosity measurement	41
2.4.4	pH measurement	41
2.4.5	Electrical conductivity measurement	42
2.4.6	Analogic density measurement	42
3. Result	ts and discussion	44
3.1 Influ	ence of the coagulant concentration and mixing time on density reduction	44
3.2 Influ	ence of the coagulant dispersion on the density reduction	55
3.2.1	Study of the coagulant concentration and mixing speed	55
3.2.2	Study of agitator type	60
3.2.3	Study of coagulant introduction method	66
	ence of the increase of the solution's initial density and coagulant types on dens	-
3.3.1	Study of the solution's initial density and coagulant types	68
3.3.2	Study of the coagulant types and concentration	75
3.4 Stud	dy of the use of flocculants	82
3.4.1	Study of flocculant type	82
3.4.2	Study of density charge and molecular weight of anionic polyacrylamides us	ed
as floccu	lants	88

	3.4.3	Study of the coagulant and flocculant concentration on DR	92
	3.4.4	Study of the mixing speed and introduction method	107
	3.5 Influe	nce of clay type	112
	3.6 Study	of different coagulants and flocculants and their combinations	120
	3.7 Study	of calcium and sodium salts	124
	3.8 Study	of the reduction of dispersant	127
	3.9 Study	of nonionic and cationic polymers as flocculants and their solution pH	135
	3.9.1	Study of the use of cationic polymer 6605	135
	3.9.2	Study of the use of non-ionic polymers	140
	3.9.3	Influence of the solution temperature	151
	3.9.4	Use of clay/sand solutions	154
4.	Conclus	sions	163
5.	Referen	ces	165
6	Annend	iy	181

List of Figures

Figure 1.1 - Cased shaft construction process – from Texas Shafts Inc., 2013 [14] Error! Bookmark not defined.
Figure 1.2 - Sketch representation of (a) a single silica tetrahedron and (b) a sheet of silica tetrahedrons – adapted from [33]
Figure 1.3 - Clay mineral structures – adapted from Serhiy, 2015 [191]. 1:1 structures are alternated sheets while 2:1 structures are the repetition of two tetrahedral sheets surrounding an octahedral sheet.
Figure 1.4 - Stern model of the electrical double layer – adapted from Miller, 2011 [204]7
Figure 1.5 - Swelling of montmorillonite clays: interlayer distances when dry and hydrated – Adapted from EFFC, 2019 [15]9
Figure 1.6 - Schematic diagram showing (a) polymer bridging and (b) steric stabilization – Adapted from Gregory, 1993 [40]12
Figure 1.7 - Schematic representation of membrane processes – Adapted from Jhaveri et al.(2016) [96]16
Figure 1.8 - Classification of coagulants and some examples - Adapted from Bratby, 1980 [141]23
Figure 1.9 - Mole fraction of the hydrolyzed products of iron (III) coagulants [150]24
Figure 1.10 - Schematic representation of some flocculant properties [157] [91]26
Figure 2.1 - Jacketed reactor side view (A), top view (B), and the recirculating bath (C) 34
Figure 2.2 - Soil mixing apparatus35
Figure 2.3 - (A) - Agitator "P1"; (B) - Agitator "P2"; (C) - Agitator "P3"; (D) - Agitator "P4"; (E) - Agitator "P5"; (F) – Agitator "P6"; (G) – Agitator "P7"; (H) – Agitator "P8"

Figure 2.4 - Marsh cone40
Figure 2.5 - Mettler Toledo Densito PX-3040
Figure 2.6 - DV2T Brookfield viscometer41
Figure 2.7 - PHS - 3CW pH meter42
Figure 2.8 - DDS-307 Electrical conductivity meter
Figure 2.9 - Analog densimeter
Figure 3.1 - Effect of $Al_2(SO_4)_3$ concentration and mixing time on DR (at a mixing speed of 200rpm)
Figure 3.2 - Deposits on the blades for 8 minutes mixing time and different concentrations of Al ₂ (SO ₄) ₃ : (A) - mg/L, (B) – 50 mg/L, (C) – 200 mg/L, (D) – 600 mg/L
Figure 3.3 - Deposits retained on the net of the Marsh funnel for 8 minutes mixing time and different concentrations of Al ₂ (SO ₄): (A) – 5 mg/L, (B) – 50 mg/L, C – 200 mg/L, D – 600 mg/L
Figure 3.4 - Deposits retained on the net of the Marsh funnel for 16 minutes mixing time and different concentrations of Al ₂ (SO ₄): (A) – 5 mg/L, (B) – 50 mg/L, C – 200 mg/L, D – 600 mg/L
Figure 3.5 - Deposits on the blades for 16 minutes mixing time and different concentrations of Al ₂ (SO ₄) ₃ . (A) – 5 mg/L, (B) – 50 mg/L, C – 200 mg/L, D – 600 mg/L
Figure 3.6 - Deposits retained on the net of the Marsh funnel for 24 minutes mixing time and different concentrations of Al ₂ (SO ₄): (A) – 5 mg/L, (B) – 50 mg/L, C – 200 mg/L, D – 600 mg/L
Figure 3.7 Deposits on the blades for 24 minutes mixing time and different concentrations of Al ₂ (SO ₄) ₃ . (A) – 5 mg/L, (B) – 50 mg/L, C – 200 mg/L, D – 600 mg/L51
Figure 3.8 - Effect of the coagulant concentration on DR, for 8 minutes of mixing time 52
Figure 3.9 – Deposits retained in a sieve net for 8 minutes mixing time and different concentrations of Al ₂ (SO ₄): (A) – 900 mg/L, (B) – 1200 mg/L, C – 1500 mg/L54

Figure 3.10 – Deposits on the blades for 8 minutes mixing time and different concentrations of	
Al ₂ (SO ₄) ₃ . (A) – 900 mg/L, (B) – 1200 mg/L, C – 1500 mg/L	54
Figure 3.11 - Effect of Al ₂ (SO ₄) ₃ concentration and mixing speed on DR (8 minutes)5	55
Figure 3.12 - Deposits on the blades for 250 rpm and different concentrations of Al ₂ (SO ₄) ₃ . (A) $_{-}$ 5 mg/L, (B) $_{-}$ 50 mg/L, C $_{-}$ 200 mg/L, D $_{-}$ 600 mg/L	
Figure 3.13 - Deposits retained on the net of the Marsh funnel for 250 rpm. (A) – 5 mg/L, (B) – 50 mg/L, C – 200 mg/L, D – 600 mg/L5	
Figure 3.14 - Deposits on the blades for 300 rpm and different concentrations of Al ₂ (SO ₄) ₃ . (A) \sim 5 mg/L, (B) \sim 50 mg/L, C \sim 200 mg/L, D \sim 600 mg/L	
Figure 3.15 - Deposits retained on the net of the Marsh funnel for 300 rpm. (A) – 5 mg/L, (B) – 50 mg/L, C – 200 mg/L, D – 600 mg/L5	
Figure 3.16 - (A) - Agitator "P1"; (B) - Agitator "P2"; (C) - Agitator "P3"; (D) - Agitator "P4"; (E) Agitator "P5"; (F) – Agitator "P6"; (G) – Agitator "P7"; (H) – Agitator "P8"6	
Figure 3.17 – Effect of agitation levels and mixing speed on DR for 8 minutes of agitation 6	3
Figure 3.18 - Deposits retained on the net of the Marsh funnel for: (A) - single level agitator, 200 rpm; (B) - single level agitator, 300 rpm; (C) - two level agitator, 200 rpm; (D) – two level agitator, 300 rpm at 600 mg/L	35
Figure 3.19 - Deposits on the blades for (A) - single level agitator, 200 rpm; (B) - single level agitator, 300 rpm; (C) - two level agitator, 200 rpm; (D) – two level agitator, 300 rpm at 600 mg/L	35
Figure 3.20 - Effect of the coagulant introduction method on DR6	6
Figure 3.21 - Deposits retained on the net of the Marsh funnel and in the sieve for: (A) - external introduction; (B) - internal introduction6	3 7
Figure 3.22 - Effect of coagulant type on DR at 8 min, 250 rpm at different initial densities 6	39
Figure 3.26 – Effect of Al ₂ (SO ₄) ₃ and PFS concentration on DR7	'5
Figure 3.27 - Effect of coagulant type on DR7	' 6

Figure 3.47 - Effect of Al ₂ (SO ₄) ₃ concentration, clay type, and Microbond concentration for 8 minutes and 200 rpm
110
Figure 3.46 - Flocs taken from the solutions treated with $Al_2(SO_4)_3$ and Telsun 5153 at 150 mg/L when introduced at: (A) – top, 200 rpm; (B) – bottom, 200 rpm, and (C) – bottom, 20 rpm
Figure 3.45 – Side view of the solutions treated with Al ₂ (SO ₄) ₃ and Telsun 5153 at 150 mg/L when introduced at: (A) – external introduction, 200 rpm; (B) – bottom, 200 rpm, and (C) – bottom, 20 rpm
Figure 3.44 - Effect of the introduction type and mixing speed of the flocculant in DR 108
Figure 3.37 - Effect of Al ₂ (SO ₄) ₃ and Telsun 5153 concentrations on DR95
Figure 3.36 – Effect of different concentrations of Al ₂ (SO ₄) ₃ and Telsun 5153 on DR93
Figure 3.35 - Flocs taken from the solutions treated with (A) – Telsun 5153; (B) – 9233; (C) – Telsun N23; (D) – Flonex 934
Figure 3.34 - Side view of the solutions treated with (A) – Telsun 5153; (B) – 9233; (C) – Telsun N23; (D) – Flonex 93490
Figure 3.33 – Effect of charge density and molecular weightof anionic flocculants (Telsun 5153, 9233, Telsun N23 and Flonex 934)
Figure 3.32 - Side view of the solutions treated with (A) - Microbond; (B) – 6610; (C) – Telsun 5153 after overnight
Figure 3.31 - Side view of the solutions treated with the coagulant Al ₂ (SO ₄) ₃ and -(A) - Microbond; 6610 - (B) -; Telsun 5153 - (C)
Figure 3.30 – Effect of flocculant type on DR82
Figure 3.29 - Deposits retained on the net of the sieves for (A) - Al ₂ (SO ₄) ₃ , 200 mg/L; (B) - PFS, 200 mg/L;(C) - Al ₂ (SO ₄) ₃ , 600 mg/L; (D) – PFS, 600 mg/L; (E) – Al ₂ (SO ₄) ₃ , 1000 mg/L; (F) – PFS, 1000 mg/L; and on the agitator blades for: (G) – Al ₂ (SO ₄) ₃ , 1500 mg/L; (H) – PFS, 1500 mg/L
(B) - 1000 mg/L; (C) – 1500 mg/L and PFS at (D) – 200 mg/L; (E) – 1000 mg/L; (F) – 1500 mg/L
Figure 3.28 – Side by side comparison of solutions treated with $Al_2(SO_4)_3$ at: (A) – 200 mg/L;

Figure 3.48 - Deposits on the nets and blades for (A) - Al ₂ (SO ₄) ₃ , 600 mg/L (clay A); (B) - Al ₂ (SO ₄) ₃ , 600 mg/L (clay B); (C) - Al ₂ (SO ₄) ₃ + Microbond, 600/75 mg/L (clay A); (D) - Al ₂ (SO ₄) ₃ + Microbond, 600/75 mg/L (clay B); (E) - Al ₂ (SO ₄) ₃ , 2000 mg/L (clay A); (F) -
Al ₂ (SO ₄) ₃ , 2000 mg/L (clay B);
Figure 3.49 - Side view of the solutions treated with 2000 mg/L of Al ₂ (SO ₄) ₃ on: (A) - clay A; (B) - clay B
Figure 3.50 – Effect of clay types and mixing speeds on DR
Figure 3.51 – Al ₂ (SO ₄) ₃ + Telsun 5153 at :(A) – Clay A (200 rpm); (B) –Clay A (20 rpm), 20 rpm (Terracota); (C) –Clay B (200 rom); (D) – Clay B (20 rpm)
Figure 3.52 – Effect of Al ₂ (SO ₄) _{3,} 5153 and Microbond at 150 mg/L
Figure 3.53 – Effect of Al ₂ (SO ₄) ₃ , PFS and FeSO ₄ combined with Telsun 5153 on DR 121
Figure 3.54- Side view of the runs performed with (A) – Microbond; (B) - Al ₂ (SO ₄) ₃ ; (C) – Telsun 5153; (D) – Al ₂ (SO ₄) ₃ + Telsun 5153; (E) – PFS + Telsun 5153; (F) – FeSO4 + Telsun 5153
Figure 3.55 – Effect of NaCl and CaCl ₂ at different concentrations with clay B on DR 124
Figure 3.56 - Side view of the solutions treated with (A) – NaCl, 584 mg/L; (B) – NaCl, 5844 mg/L; (C) – CaCl ₂ , 1110 mg/L; (D) – CaCl ₂ , 2775; (E) – CaCl ₂ , 5549 mg/L; (F) – CaCl ₂ , 11100 mg/L
Figure 3.58 – Side view of the solutions treated with Al ₂ (SO ₄) ₃ at: (A) – 0 mg/L (no GPlus); (B) – 300 mg/L (no GPlus); (C) – 600 mg/L; (D) – 600 mg/L (no GPlus); (E) – 2000 mg/L; (F) – 2000 mg/L (no GPlus)
Figure 3.59 – Effect of coagulant and flocculant type on DR at the concentration of 0 mL/L of GPlus
Figure 3.60 - Side view of the solutions treated with (A) - Al ₂ (SO ₄) ₃ ; (B) - PFS; (C) - A0410.131
Figure 3.62 – Side view of the solutions treated with (A) – NaCl + Microbond and (B) – NaCl + 6610
Figure 3.63 - Effect of HCl concentration combined with 6605 on DR
Figure 3.66 – Effect of HCl concentration with Nonionic 513 on DR

Figure 3.68 – Effect of HCI concentration on DR in conjunction with A0410	143
Figure 3.69 - Effect of HCl concentration on DR in conjunction with A0410 for mM of HCl	
Figure 3.71 - Effect of A0410 concentration on DR	149
Figure 3.72 - Effect of solution temperature on DR	151
Figure 3.76 - Effect of A0410 + HCl solution volume on DR	158
Figure 3.77 - Effect of A0410 + HCl solution volume on mean DR	159

List of Tables

Table 1.1 - Effect of molecular weight on different charge polymer adsorption rates [67] [68]
[69] [70]11
Table 1.2 - Influence of clay cation exchange capacity on different polymers with different charges [61] [72] [73]11
Table 1.3 - Advantages and disadvantages of screening [86] [87] [89]14
Table 1.4 - Advantages and disadvantages of deep-bed filters [82] [94] [95]15
Table 1.5 - Some characteristics about pressure-driven membranes [82] [98] [99] [100] 16
Table 1.6 - Advantages and disadvantages of membrane separation processes – Adapted from Crini, 2013 [94]
Table 1.7 - Advantages and disadvantages of plain settling – Adapted from World Health Organization, 2002 [116]18
Table 1.8 – Advantages and disadvantages of centrifugation - Adapted from Xu-Ming et al. 2017 [123]19
Table 1.9 - Advantages and disadvantages of flotation processes [94] [130] [133]21
Table 1.10 - Some advantages and disadvantages of the adsorption process [94] [136] 22
Table 1.11 - Advantages and disadvantages of coagulation and flocculation - Adapted from Crini, 2013 [94]
Table 1.12 - Advantages and disadvantages of the magnetic field assisted separation process – Adapted from Zaidi et al. 2014 [173]29
Table 1.13 - Advantages and disadvantages of ultrasonic wave separation [178] [179] 30
Table 2.1 - Runs and agitators tested37
Table 3.1 - Solution objectives for the present work Error! Bookmark not defined.
Table 3.2 – Initial densities, coagulant concentration, Marsh Viscosity gaps and final density of the runs performed at 8 minutes. ^{a)} Marsh gap is calculated from the difference between final

and initial values. ^{b)} Final density gap is calculated from the difference between middle and
bottom values
Table 3.3 – Initial densities, coagulant concentration, Marsh Viscosity gaps and final density of the runs performed at 16 minutes. ^{a)} Marsh gap is calculated from the difference between final and initial values. ^{b)} Final density gap is calculated from the difference between middle and bottom values. 48
Table 3.4 – Initial densities, coagulant concentration, Marsh Viscosity gaps and final density of the runs performed at 24 minutes. ^{a)} Marsh gap is calculated from the difference between final and initial values. ^{b)} Final density gap is calculated from the difference between middle and bottom values. 50
Table 3.5 – Initial densities, Marsh Viscosity gaps and final density of the runs performed at 8 minutes for the concentrations of 900, 1200 and 1500 mg/L. ^{a)} Marsh viscosity gap is calculated from the difference between final and initial values. ^{b)} Final density gap is calculated from the difference between middle and bottom density values after the coagulant effect. ^{c)} Impossible to measure, due to clogging of the Marsh funnel
Table 3.6 - Initial densities, coagulant concentration, Marsh Viscosity gaps and final density of the runs performed at 250 rpm. ^{a)} Marsh viscosity gap is calculated from the difference between final and initial values. ^{b)} Final density gap is calculated from the difference between middle and bottom density values after the coagulant effect
Table 3.7 - Initial densities, coagulant concentration, Marsh Viscosity gaps and final density of the runs performed at 300 rpm. ^{a)} Marsh viscosity gap is calculated from the difference between final and initial values. ^{b)} Final density gap is calculated from the difference between middle and bottom density values after the coagulant effect. ^{c)} Impossible to measure, due to clogging of the Marsh funnel
Table 3.8 - Time required for colorant uniformization with the different paddles tested 62
Table 3.9 - Initial densities, coagulant concentration, Marsh Viscosity gaps and final density of the runs performed using a single level agitator (8 and 26) and a two level agitator (39 and 40). a)Marsh viscosity gap is calculated from the difference between final and initial values. b)Final density gap is calculated from the difference between middle and bottom density values after the coagulant effect. c)Impossible to measure, due to clogging of the Marsh funnel
Table 3.10 - Initial densities, coagulant concentration, Marsh Viscosity gaps and final density of the runs performed with external introduction and internal introduction. ^{a)} Marsh gap is

calculated from the difference between final and initial values. ^{b)} Final density gap is calculated from the difference between middle and bottom values
Table 3.11 - Initial densities, coagulant concentration, Marsh Viscosity gaps and final density of the runs performed with Al ₂ (SO ₄) ₃ , FeSO ₄ , PFS and (NH4) ₂ SO ₄ at densities below and within the objective range. ^{a)} Marsh viscosity gap is calculated from the difference between final and initial values. ^{b)} Final density gap is calculated from the difference between middle and bottom density values after the coagulant effect. ^{c)} Impossible to measure, due to clogging of the Marsh funnel.
Table 3.12 - Coagulants and concentrations for the runs shown in Figure 4.2676
Table 3.13 - Initial densities, coagulant concentration, Marsh Viscosity gaps and final density of the runs performed with Al ₂ (SO ₄) ₃ and PFS. ^{a)} Marsh gap is calculated from the difference between final and initial values. ^{b)} Final density gap is calculated from the difference between middle and bottom values. ^{c)} Impossible to calculate due to inability to draw samples. ^{d)} Not measured
Table 3.14 - Clean strip heights for the solutions presented on Figure 3.31
Table 3.15 - Clean strip heights for the solutions on Figure 3.31 30 minutes and 18 hours after their completion
Table 3.16 - Initial densities, coagulant concentration, Marsh Viscosity gaps and final density of the runs performed with Al ₂ (SO ₄) ₃ and when combined with Microbond, 6610 and Telsun 5153. a)Marsh gap is calculated from the difference between final and initial values. b)Final density gap is calculated from the difference between middle and bottom values. c)Impossible to
measure, due to clogging of the Marsh funnel. d)Impossible to calculate86
Table 3.17 – Initial and final Brookfield viscosity for the selected runs performed using performed with Al ₂ (SO ₄) ₃ and when combined with Microbond, 6610 and Telsun 5153. a)Impossible to measure due to the inability to draw samples. b)Not measured
Table 3.18 - Molecular weights and charge densities of the anionic flocculants tested88
Table 3.19 - Initial and final Brookfield viscosity for the selected runs performed using performed with Al ₂ (SO ₄) ₃ when combined with Telsun 5153, 9233, Telsun N23 and Flonex 934. a)Impossible to measure due to the impossibility of drawing samples
Table 3.20 - Coagulant and flocculant concentrations for the runs shown on Figure 3.36 93
Table 3.21 - Coagulant and flocculant concentrations for the runs shown on Figure 3.37 95

Table 3.22 - Clean fluid height of the solutions treated with $Al_2(SO_4)_3$ and Telsun 5153 at: (A) - 50/75 mg/L; (B) - 100/37.5 mg/L and (C) - 175/37.5 mg/L
Table 3.23 - Clean fluid height of the solutions treated with Al ₂ (SO ₄) ₃ at 200 mg/L with Telsun
5153 at (A) - 15 mg/l; (B) – 37.5 mg/L and (C) – 75 mg/L
Table 3.24 - Clean fluid height of the solutions treated with Al ₂ (SO ₄) ₃ at 150 mg/L with Telsun
5153 at (A) - 37.5 mg/l; (B) - 75 mg/L; (C) $-$ 150 mg/L and (D) $-$ 300 mg/L
Table 3.25 - Initial densities, coagulant concentration, Marsh Viscosity gaps and final density of
the runs performed with Al ₂ (SO ₄) ₃ combined with Telsun 5153. ^{a)} Marsh gap is calculated from
the difference between final and initial values. ^{b)} Final density gap is calculated from the
difference between middle and bottom values. © Impossible to measure, due to clogging of the
Marsh funnel. d)Impossible to calculate due to the inability to draw samples. e)Not measured103
Table 3.26 - Initial and final Brookfield viscosity for the selected runs performed using
performed with Al ₂ (SO ₄) ₃ when combined with Telsun 5153. ^{a)} Impossible to measure due to the
inability to take samples. b)Not measured
Table 3.27 - Introduction method and clean fluid height for the solutions treated with $Al_2(SO_4)_3$
and Telsun 5153
Table 3.28 - Initial and final Brookfield viscosity for the selected runs performed using
performed with Al ₂ (SO ₄) ₃ when combined with Telsun 5153. ^{a)} Not measured due to the
impossibility of drawing samples
Table 3.29 - Initial densities, coagulant concentration, Marsh Viscosity gaps and final density
gaps of the runs performed with Al ₂ (SO ₄) ₃ . ^{a)} Marsh gap is calculated from the difference
between initial and final values. ^{b)} Density gap is calculated from the difference between middle
and bottom values. c)Impossible to measure due to blockage of the Marsh funnel net.
d)Impossible to calculate. e)Not measured
Table 3.30 - Initial densities, concentrations, Marsh and final density gaps and Brookfield
viscosities for the runs performed with $Al_2(SO_4)_{32}$ at different mixing speeds, for clay A and clay
B. ^{a)} Marsh gap is calculated from the initial and final values. ^{b)} Final density gap is calculated
from the difference between middle and bottom values. c)Impossible to measure due to
blockage of the Marsh funnel net. ^d Impossible to calculate. ^{e)} Not measured117
Table 3.31 - Coagulants and flocculants for the runs performed on Figure 3.53

Table 3.42 - Initial densities, flocculant concentrations, initial and final Brookfield values and
final density gaps for the runs performed. ^a Density gap is calculated from the difference
between middle and bottom values
Table 3.43 - Initial densities, Brookfield viscosities and final zone gaps for the runs performed.
^a Density gap is calculated from the difference between middle and bottom values
Table 3.44 - Initial densities, spindles and initial Brookfield values for the control run performed
for confirmation
Table 3.45 - Initial densities, HCl concentrations, Brookfield viscosities and final density gaps
for the runs performed with A410 at 1000 mg/L with 0-2.5mM HCl on clay/sand mix. a)Density
gap is calculated between the difference between the middle and the bottom values 156
Table 3.46 - Initial densities, solution volumes, Brookfield viscosities and final density gaps for
the runs performed with A0410 and HCl on clay/sand mixture. ^{a)} Density gap is calculated from
the difference between middle and bottom values

List of Abbreviations

DR Density reduction

PFS Polyferric sulfate

1. Introduction

As the world population and living standards increase, the necessity for taller buildings and larger industrial complexes also grows. Thus, larger and deeper foundations are needed to support these large structures. To avoid structural problems that could compromise the process viability and personnel/community safety, it is imperative to guarantee soil stability when dealing with problematic and weak soils [1].

1.1 Soil Stabilization

Soil stabilization is the process of improving soil properties such as strength, permeability, stiffness, swelling capacity, compressibility, water sensitivity and volume change. It can be done physically, mechanically, thermally or electrokinetically [2]. To achieve stabilization, chemicals labeled as stabilizers are used to increase their resistance to stress and their load-carrying capacity [3] [4]. Soil stabilization can be applied in areas such as agriculture [5], oil exploration [6] [7], and construction [8].

Historically, constructions in expansive and unstable soils have caused several structural problems in infrastructures such as cracking due to foundation movements [9]. In the United States, expansive soils have reportedly inflicted billions of dollars in damages and repairs of structures [10].

Stabilization of soils in foundations is important to ensure a long-lasting foundation that does not require excessive maintenance and can resist different types of weather and volume variations due to moisture [11].

1.1.1 Support fluids

Support fluid, also known as drilling mud or drilling fluid, is a generic term used to describe a mix of manufactured materials, that support the walls of open and deep excavations for concrete filling [15]. A support fluid's function is to control subsurface pressure, transport cuttings, support and stabilize the wellbore, seal permeable formations, cool, lubricate and support the drilling assembly [16].

Support fluids used are separated into three classifications [16]:

- Pneumatic
- Oil-based
- Water-based

Water-based are the most used support fluids. These are also divided in three major categories according to their influence on clay swelling behavior:

- Inhibitive
- Non-inhibitive
- Polymeric

Inhibitive support fluids, as the name suggests, inhibit clay swelling through the presence of cations such as Na⁺. Examples of inhibitive support fluids are starch, carboxymethyl cellulose and polyanionic cellulose [17].

Non-inhibitive support fluids do not suppress clay swelling – they are generally comprised of clays, such as bentonite [16].

Polymeric fluids, depending on their nature, such as partially hydrolyzed polyacrylamides and carboxymethyl cellulose, can be inhibitive or non-inhibitive [15] [16]. They are very diverse and are used to viscosify fluids, control filtration properties, and deflocculate or encapsulate solids. In these systems, solids can be major threats to its use [16].

1.1.1.1 Support fluid Properties

For optimal performance, a support fluid should be able to sustain enough stress to maintain the cuttings at the surface, whilst having low enough viscosity to be pumpable and high enough to transport cuttings [16] [18]. In construction sites, Marsh viscosity is used to characterize fluids. This measurement represents the ratio of the speed of the sample fluid as it passes through the outlet tube to the amount of force that is causing the fluid to flow. It is reported as the number of seconds a quart of fluid takes to flow out of the funnel. For water, this value is 26 s/quart [19]. Acceptable viscosities for polymeric fluids are between 40-80 s/quart [20]. Yield stress values are very wide: from 0.048 to 50.06 Pa [21]. Viscosity can be increased by viscosifiers such as pre-hydrated bentonite, guar gum, attapulgite and polyanionic cellulose (PAC) [16].

A support fluid should also have high yield point, which is a desirable property in hole cleaning. Higher yield point increases the mud's capacity to carry solid particles and cuttings. The yield point is the minimum force required to impart movement on a fluid when the shear rate, the velocity gradient between two successive layers of fluid, is 0. The required value to suspend a 1mm particle is usually 2.8-6.7 Pa [22, 23]. Support fluids tend to perform better at higher pH due to the increase of viscosity and yield point [24].

Density is another important factor in the support fluid's performance. Its increase generally correlates to a higher capacity to carry solids and cuttings through buoyancy [16]. Density can be increased by weighing agents such as barite, pyrite, siderite, or galenite [25]. An increase of

suspended solids also causes an increase of density, upwards to 1.25 g/cm³. Fluid density should not be too high, or the fluid might not be efficiently displaced by the upward flow of concrete [25]. Lam et al. [12] claim that prior to concreting, the fluid's density should not be over 1.20 g/cm³. If the fluid's density is close to the cement's density, problems that may affect the cement's quality and integrity may occur when it is replacing the support fluid [26].

1.1.1.1.1 Inhibitive support fluids

While the swelling of soils is a desirable effect that enables the suspension of clays in boreholes, this effect can also be a major cause of soil instability in areas such as shale drilling. When clays present in shales absorb water, the volume variation can cause undesirable such as wellbore instability and formation damage. Inhibitive support fluids combat this problem by exhibiting low reactivity with the soil and preventing its swelling [27]. These fluids use sodium, calcium and potassium salts to achieve inhibition. Examples of inhibitive support fluids are lime muds (calcium-based), saltwater muds (sodium-based) and KOH-lignite muds (potassium-based muds). Since these fluids are formulated with salts, a large cost is associated with the disposal [16].

1.1.1.1.2 Non-inhibitive support fluids

Non-inhibitive support fluids are simple and non-expensive, but their application is limited when drilling dispersive soils, since they cannot stop the swelling. These fluids are also less adept at dealing with contaminants and high temperatures, or at increasing fluid density, if needed [16].

Bentonite clay is a common mineral additive for support fluids. It is mainly composed of montmorillonite clays, which can absorb water up to many times their weight. The addition of small amounts of bentonite to water causes the formation of colloidal suspensions that increase the viscosity of the mixture. Besides the viscosity increase, bentonite also has another beneficial property of forming a filter cake on the walls of the excavation, restricting fluid loss [15] [16].

1.1.1.1.3 Polymeric support fluids

Polymers used in support fluids are often synthetic with high molecular weights, typically 15 million Dalton or more. These polymers interact with each other, with the soil and with the water, increasing the viscosity of the fluid [15] [12]. These interactions cause the formation of a polymeric membrane on the excavation walls, reducing fluid loss [25]. Partially hydrolyzed polyacrylamides (PHPA) are the most used synthetic polymers, although, historically, some natural polymers such as carboxymethyl cellulose and xanthan gum were used [28] [12].

Natural polymers have two main advantages: they are biodegradable and prevent fluid losses by forming gel-like cross linking structures [15]. Being biodegradable is also a disadvantage in itself, as microorganisms can cause alterations in these fluid's properties [13].

Synthetic polymers have the advantage of being customizable according to the job at hand can be repeatedly reused, if adequate management is in place [13] [25]. Nonetheless, these fluids are sensitive to free Ca²⁺ and Mg²⁺ in the solution, as these can cause attraction of polymeric chains and consequently, their agglomeration [25].

Throughout this introduction, a larger focus will be given to this type of support fluids.

1.2 Soil properties

Understanding the soil's physical properties is the first step towards understanding how the soil will interact with the polymer, when using polymeric support fluids. Soil texture is a very important property in classifying its profiles and suitability for development. Texture describes the sizes of the finer individual soil particles: these can be as large as 2 mm (sands) and as small as 10⁻⁶ m (submicroscopic clays) [29].

Particles between 0.05 mm and 2 mm are denominated as sand. Most sands are constituted by quartz (SiO₂). They are visible to naked eye and due to the larger size, larger interstitial spaces and lower adsorptive capacity due to their negligeable electric charge and low specific surface areas when compared to smaller particles sandy soils cannot hold water [29] [30].

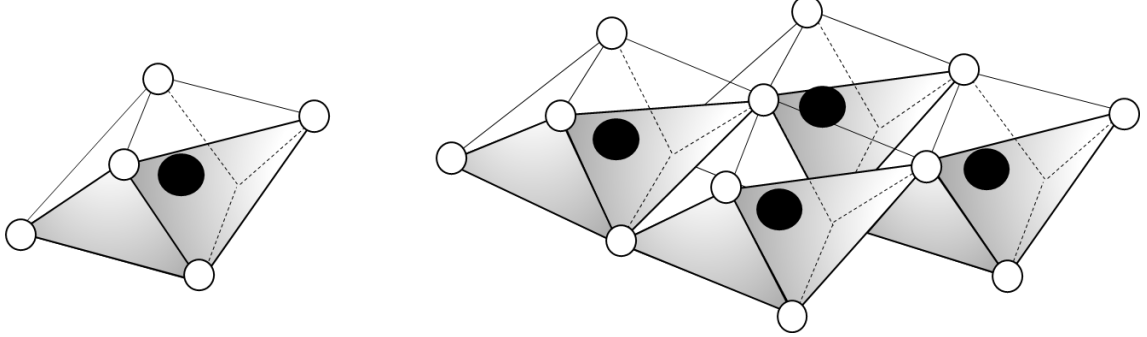
Particles between 0.02 mm and 0.05 mm are classified as silts. Silt is visually and compositionally like sand (being that they are compositionally made of quartz), although individual particles are small enough to be invisible to the naked eye. Silt has higher capacity to adsorb water particles than sand but much of it is due to adhesion of clays [29].

Particles smaller than 0.02 mm are called clays. These exhibit the highest water adsorption capacity due to the very large surface areas and unique composition that yields a surface charge 5 to 20 times higher than sands and silts [29] [30].

Meozzi [31], in 2011, developed a relationship between soil properties and clay content and concluded that soil with high clay content have higher turbidity values. Density, turbidity and suspended clays can be correlated as turbidity is by definition the blockage of light caused by the presence of colloidal and suspended solids [32]. This means that increasing the amount of suspended clays increases the turbidity and consequently, the density of the solution.

1.2.1 Clay mineralogy

In 1979, Theng defined clays as hydrous silicates and aluminosilicates arranged in crystalline tetrahedral or octahedral structures and as the mains constituents of the colloidal fraction of soils. These majority of clay minerals form sheets composed of silica or aluminum stacked on top of each other, thus they are frequently labeled as layer silicates or phyllosilicates. A silica sheet contains two plains of oxygen/hydroxyl ions, one on the base and one on the tip of the Si(OH)₄ tetrahedral structure. Figure 1.2 represents a sketch of a silica tetrahedron and its arrangement in sheets.



Conversely, the octahedrally coordinated aluminum sheet has a lower and upper plane, both

Figure 1.1 - Sketch representation of (a) a single silica tetrahedron and (b) a sheet of silica tetrahedrons – adapted from [34]

consisting of hydroxyl groups, in between which is a plane of Al3+ ions [32].

These sheets can be stacked in different manners: often aluminum and silica sheets are organized in an alternated order. Their arrangement is shown in Figure 1.3.

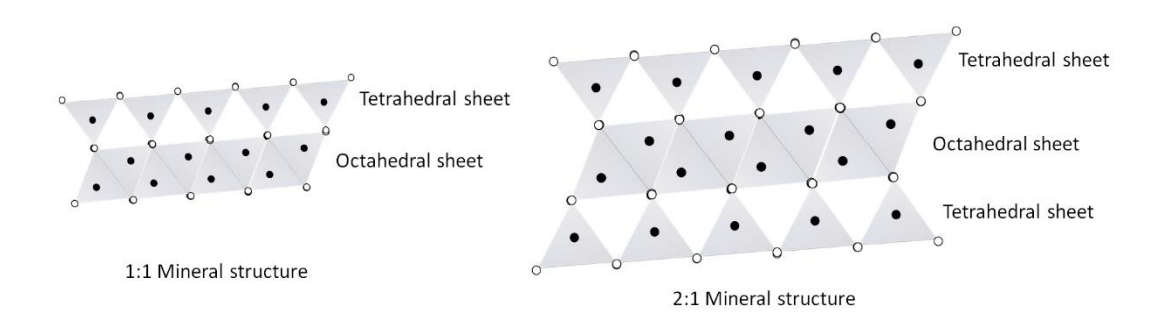


Figure 1.2 - Clay mineral structures – adapted from Serhiy, 2015 [205]. 1:1 structures are alternated sheets while 2:1 structures are the repetition of two tetrahedral sheets surrounding an octahedral sheet.

As the sheets hold a residual negative charge, a cation holds them together. These cations are known as interlayer cations [33]. In the crystalline structure, an important process known as isomorphous substitution occurs, in which Si⁴⁺ is substituted by Al³⁺ or Mg²⁺. The substitution of a higher valence cation for one of lower valence leads to negative charges on the clay particle

[34]. The arrangement and substitution occur in a different manner throughout the clay minerals, hence their division in groups, which will be subsequently detailed.

The kaolinite group

Kaolinites are organized in a 1:1 structure. The basal siloxane (Si-O) structure is hydrophobic and the other basal aluminol (Al-OH) surface is hydrophilic. They are dioctahedral, non-swelling minerals in aqueous solutions [35]. These minerals do not show interlayer expansion due to the superposition of oxygen and hydroxyl planes, causing Van der Waals attractions and hydrogen bonding. Kaolinites carry a negative surface charge [32].

The smectite group

This group contains a very important dioctahedral mineral: montmorillonite. This 2:1 mineral shows extensive interlayer expansion and isomorphic substitution is fairly common, therefore it is also used as an adsorbent due to the large, exposed surface area [32]. These are the only clays where simultaneously, the interlayer cations are exchangeable, hydratable and the interlayer surfaces are also hydratable, making these very reactive with water and easily swellable [36]

The vermiculite group

Vermiculites are usually dioctahedral or trioctahedral with a 2:1 structure [32]. They have limited swelling due to divalent Mg²⁺ interlayer ions and have high layer charge density [37]. In these minerals, isomorphic substitution only occurs in the tetrahedral sheet [33].

The mica and chlorite group

Micas are 2:1 clay minerals and they are either dioctahedral or trioctahedral whilst chlorites can also be di-tri-octahedral with a 2:1:1 structure where an hydroxide layer also joins the alternate structure. Micas and chlorites are generally not found in soils, but only as minerals [32].

The palygorskite-sepiolite group

Palygorskites and sepiolites are highly sorbent, high surface area minerals that form stable suspensions that are very little affected by electrolytes. Due to these properties, they are generally used as catalysts and viscosifiers. [38]

In this group, palygorskites known as attapulgites are the most important. Attapulgites are 2:1, di-tri-octahedral or trioctahedral minerals [32]. Attapulgites are commonly used as visosifiers

due to their gel forming capabilities and high viscosities in solutions (upwards to 40000 cP). [13] [39].

1.2.2 Clay colloid interactions

Soil colloids are stabilized due to a balance of attractive and repulsive forces. Such forces can be explained by electrical double layer repulsion, van der Waals attractive forces between particles, hydrogen bonds, hydration effects, hydrophobic/hydrophilic interactions, steric interactions and polymer bridging [33] [40].

As previously mentioned in chapter 1.2.1, the phenomenon of isomorphous substitution leads to creation of negative charges, which is then compensated by adsorption of cations in the surface layer. Another property of clays is cation exchange capacity (CEC), in which the adsorbed cations may be replaced by other cations (counter-ions) in an aqueous solution [41].

Since the system is electrically neutral, the medium must contain an equivalent number of opposite charges. As such, around the particle's negatively charged layer, a positively charged layer must exist, thus, forming the electrical double layer [42], first observed by Gouy, in 1910 [43] and Chapman, in 1913 [44]. In 1924, Stern [45] further modified the Gouy-Chapman model by defining a rigid layer surrounding the particle solely comprised by cations, while further away from the solid particle, another layer consisting of both positive and negative ions. Figure 1.4 schematically represents the constitution of an electric double layer.

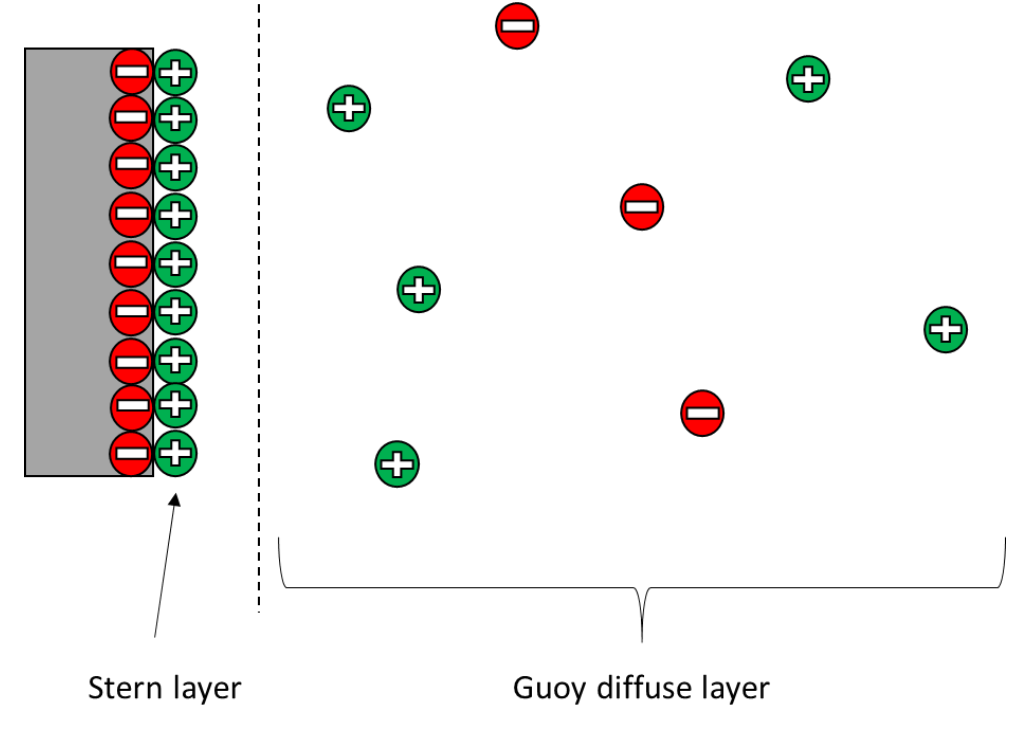


Figure 1.3 - Stern model of the electrical double layer – adapted from Miller, 2011 Fonte especificada inválida.

The surface charge of the clay particles is fixed, therefore, increasing the electrolyte concentration of the opposite sign will simply compress the double layer [46], thus reducing the double layer repulsion force. At high electrolyte concentration, attractive forces prevail, while at low concentrations, repulsive forces dominate [33]. The type of cation in solution not only affects the thickness of the double layer but also the internal spacing of the clay minerals: increasing the valence of the counter ion further shrinks the double layer and compresses the sheets due to their residual negative charge and the electrostatic attraction between these and the cations in solution [33] [47] [48].

Hydrogen bonds are formed when a hydrogen ion forms the positive end of a dipole attracted by a negative charge, generally formed by strongly electronegative atoms, such as oxygen, fluoride and nitrogen [49]. The electron transferred from the hydrogen to the oxygen travels between both atoms, forming a permanent dipole between clay particles and oxygen on their surface [41]. Hydrogen bonds are responsible for important mechanisms such as the interaction of clays and water molecules and the adsorption of non-ionic and ionic polymers on clays [33].

Van der Waals forces can be described as the totality of non-covalent forces or as intermolecular forces. These forces act between stable molecules and are weaker than chemical bonding and hydrogen bonds [50]. Unlike hydrogen bonds' permanent dipole, van der Waals forces are a consequence of a fluctuating dipole, which correlate to the molecules coming closer to each other. van der Waals forces are the dominant attractive forces at long distances. They are responsible for the attraction of clay sheets. At high counter ion concentrations, attractive forces prevail due to the shrinking of the double layer and the decrease of repulsive forces. This way, when repulsive forces are low, van der Waals are the main driving forces explaining the phenomenon of flocculation [41] [33] [50].

The behavior of water near a solid particle can be very different from water in bulk phase. Since clay particles end in oxygens or hydroxyls, hydrogen bonds are believed to be the main bonding mechanisms of water adsorption [41]. The approach of two particles with hydrated surfaces will generally be hindered by an additional repulsive interaction, distinct from electrical double layer repulsion. This effect arises from the need for the surfaces to become dehydrated if contact is to occur. The range of this interaction is appreciable compared to double layer repulsion and it is expected that it would have some effect on colloid stability [40].

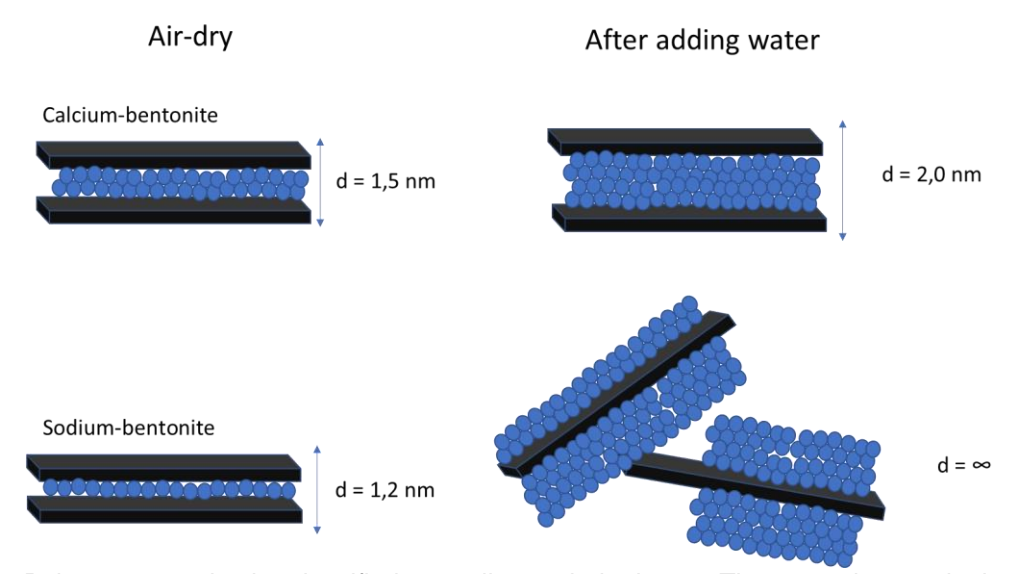
Swelling is a hydration effect observed in some clay minerals, such as montmorillonite, where they disjoint or move apart in order to accommodate water molecules. The hydroxyl groups of clays will interact with hydrogens from the water and create repulsive forces on the surface. This repulsive force causes the separation of clay sheets and the incorporation of water molecules in the interlayer space, and consequently, hydration [51]. Minerals with strong interlayer bonding such as kaolinite or absence of isomorphic substitution such as pyrophyllite experience much less swelling [32]. Interlayer bonding strength is influenced by the interlayer cation valence: clays with monovalent cations in the interlayer space tend to swell more. This effect is represented on Figure 1.5.

1.2.2.1 Polymer nature and their interactions with soils

Polymers have only weak interactions with silts and sands, mostly due to the weak charge these particles exhibit [22, 52]. As such, this section will only cover polymer-clay interactions since polymers tend to only bind directly to the latter.

Regarding their nature, polymers can be categorized as natural, synthetic or semi-synthetic. Natural polymers occur in nature, and some examples are silk, DNA, cellulose and proteins, while synthetic are man-made petroleum derivates such as polyethylene, nylon and epoxy [53]. Semi-synthetic polymers are chemically modified natural polymers such as cellulose nitrates and cellulose acetates [54].

Figure 1.4 - Swelling of montmorillonite clays: interlayer distances when dry and hydrated – Adapted from EFFC, 2019 [15]



Polymers can also be classified according to their charge. These can be non-ionic, cationic or anionic, depending on their functional groups [55]. Non-ionic polymers carry no net charge. Cationic polymers carry a net positive charge while anionic polymers carry a net negative charge [56].

1.2.2.1.1 Charge influence

In an aqueous medium, adsorption of uncharged (non-ionic), flexible polymers onto clay particles leads to a displacement of water molecules [57] [58]. The desorption of water molecules leads to an entropy gain. The polymer polar group will create hydrogen bonds with the oxygens of the silicate layer, reducing the free energy of the system. The adsorption of non-ionic polymers is therefore an enthalpy driven process [51]. Increasing electrolyte concentration shrinks the double layer, thus, the aggregation of the system increases and the spacing between clay particles decrease [59]. This aggregation reduces the surface area, therefore, also reduces the adsorption of polymer [60]. Adsorption of non-ionic polymers is not influenced by pH due to its lack of charges [61].

Cationic polymers are adsorbed mainly due to the interactions between the cationic groups and the negatively charged clay. These polymers also have the highest adsorption rates compared to neutral and anionic polymers [62]. Increase in electrolyte concentration reduces the adsorption rate due to the competition between soluble inorganic cations and the cationic polymer for the negative sites of the clay [62]. In 2018, Jacquet et al. [63] conducted experiments using FL22, a quaternary polyammonium cation on kaolinite clays and state that, by increasing pH from 6 to 10, an increase of adsorption rate of 75% is shown. They explained that this is due to the increase of the polymer's cationic charge and due to the ionization of the clay surface at high pH.

Anionic polymers tend to show a lower degree of adsorption due to the repulse between the clay palettes also carrying a negative charge. Adsorption is increased by the presence of polyvalent cations such as Ca²⁺ which act as a bridge between the polymer and the clay [64]. By increasing ionic strength, the polymer's negative charge is "screened" or neutralized by protonation. At the same time, soluble cations also create a bridge between the polymer and the clay negative sites. The electrostatic repulsions between the polymer chains are reduced, leading to a reduction of size and change of conformation [62]. Lee et al, [65] in 1991, conducted experiments with polyacrylamides and kaolinites. They found that increasing pH decreases adsorption. This is due to the dissociation of the acrylic groups, increasing the negative charge and pronouncing the electrostatic repulsions. Heller et al. (2002) [66] claimed that the electrostatic repulsions are responsible for the increase of viscosity in the clay suspensions due to the extension of the polymer molecules. This effect increases with hydrolysis degree.

1.2.2.1.2 Molecular weight influence

In Table 1.1, a synthesis of the effect of molecular weight increase on adsorption rates of polymers with different charges is shown.

Table 1.1 - Effect of molecular weight on different charge polymer adsorption rates [67] [68] [69] [70]

Neutral	Anionic	Cationic
Increase of adsorption rates until 10 ⁷ Da, followed by a decrease due to polymeric chain entanglements	No appreciable increase of adsorption rates	Increase for low cationicities, no influence on high cationicities.

Molecular weight has an influence on several polymer properties, such as viscosity. The latter tends to increase as molecular weight increases [71].

1.2.2.1.3 Influence of clay CEC on polymer adsorption

The substitution of the central cation in the octahedral matrix of clays has different effects on the adsorption of polymers, depending on their charge. Table 1.2 shows a summary of this property on adsorption.

Table 1.2 - Influence of clay cation exchange capacity on different polymers with different charges [61] [72] [73]

Neutral polymers (Polyethylene glycol and guar)	Anionic polymers (Poly (4-sodium styrene sulphonate) and polyacrylamide)	Cationic (Guar)
 Na+>Ca²⁺ Na+ clays are more dispersed therefore, have higher surface area for adsorption 	 Ca²⁺>Na⁺ Presence of polyvalent cations increases adsorption rate 	 Na+>Ca²⁺ Higher valence charge cations screen negative charges and reduce adsorption capacity

1.2.2.1.4 Steric Interactions

Steric stabilization occurs when flexible macromolecules (MW>>10³ Da) adsorb into clay particles and other colloids, creating a strong repulsion. This phenomenon only occurs in the presence of high concentrations of these polymers - high enough to completely cover the particles. These compounds are generally soaps constituted by a hydrophobic head that adsorb into the clay particles and a hydrophilic tail that extends onto the aqueous phase [40] [74]. As the particles approach each other, the hydrophilic chains tend to overlap. Since these chains are hydrated, the overlap would cause dehydration and, consecutively, an increase of free energy, which is not favorable. Thus, the particles will repel at close distances [75]. Increasing the number of hydrophilic groups increases this effect [76]. Both charged and uncharged polymers

engage in steric stabilization although, for charged polymers, electrostatic interactions also have an influence, thus for this case, this interaction is called electrosteric stabilization [75]. Zaman [77], in 2000, conducted experiments on the effect of polyethylene oxide adsorption on silica particles and concluded that steric stabilization reduces the viscosity of the suspension.

1.2.2.1.5 Polymer Bridging

Polymer bridging is essentially the simultaneous attachment of an individual polymer molecule to two or more particles or molecules [78]. If the polymer has high molecular weight or long chains, a protruding segment will extend to the solution and reach other particles, bridging them together as a floc [79]. Polymers used for bridging are usually non-ionic or partially hydrolyzed polyacrylamides (anionic) with molecular weights above 10⁷ Da [78]. For high concentrations of polymer, however, this effect can extend to steric stabilization, thus, an optimal amount is needed for each effect [40]. This effect is schematically shown in Figure 1.6. Polymer bridging increases the viscosity of the solution due to the formation of tridimensional networks [80].

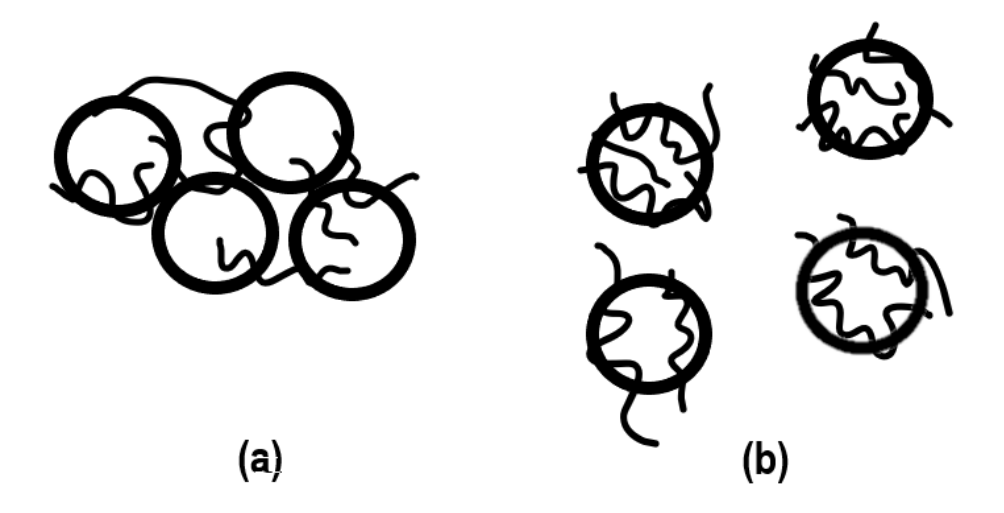


Figure 1.5 - Schematic diagram showing (a) polymer bridging and (b) steric stabilization – Adapted from Gregory, 1993 [41]

1.3 Solid-Liquid Separation methods

1.3.1 Physical methods

1.3.1.1 Filtration

Filtration is defined as a mechanical method of separating distinct phases using physical differences between them such as particle size, particle density or electric charge [81].

Filters can be categorized by: [82]

- Screens Filter media made from perforated plates, woven wire or wedge wire bars with coarse openings
- Demisters Devices that capture vapor or fine solids from gaseous streams using liquid droplets
- Scrubbers Wet or dry dust separators using liquid sprays or packed beds of granular solids
- Depth filters Vertical filters packed with fibrous or granular material that entrap particles in the pores
- Surface/cake filters Filters that rely on solids build-up on the filter medium. This build up causes a formation of a cake that in turn, acts as another filter medium.
- Gravity Simple filters that use gravity to move liquid through a filter
- Centrifugal Filters that recover solids from liquid suspensions using centrifuges with pores in their walls
- Fluid pressure Filters that use hydrostatic pressure to move liquid through the media
- Mechanical pressure Filters that use mechanical force such as squeezing to separate liquids from solids
- Cross-flow and membrane systems Filters that use membranes and tangential flow to avoid clogging and fouling
- Other force fields

Not all filtration processes will be discussed, since some such as demisters and scrubbers only apply to gas-solid separations. The concept of filtration is nearly identical for most process, i.e. separating two phases by placing a filter in between [81]. Hence, this section will not be an exhaustive approach to all filter types but, instead, the concept of filtering a solution using filters of different pore sizes/meshes.

In the filtration process, the fluid's viscosity is known to reduce filtration rates, although there are applications where filters have been emplaced in viscous, dense fluids [83] [84].

Screening

A screen is a simple coarse filter using regularly sized opening such as perforated plates and wired meshes as filtering medium. These are usually made of metal, although in some applications plastic can be used to reduce costs or gain corrosion resistance [82]. Vibration or oscillation is generally used to assist the movement of the particles through the openings [85].

There are several types such as the stationary water screen, the rotary screen, the intake screen, the well screen, and the vibratory screen. Stationary water screen has no moving parts and depends on low velocity (0.1-0.15 m/s), low viscosities and it is used to reduce the entrainment risk to aquatic life [86]. The rotary screen adds rotation effect to assist in the separation. The submerged part of the screen rotates, carrying the solids on the surface of the screen out of the water onto a collection device [87]. Intake and well screens are protective screens especially made to fit in intake pipes to prevent entry of particles [82]. Vibratory screen has an inbuilt motor to impart vibratory energy to avoid accumulation and assist the separation of finer particles [88] [89]. Meshes can be as course as 3-mesh (6.73 mm) and as small as 500 mesh $(25 \mu\text{m})$ [90].

Screens have been used in particle exclusion from sewage and drinking waters for decades [91].

Table 1.3 - Advantages and disadvantages of screening [86] [87] [89]

Advantages	Disadvantages
 Simple process Ability to separate solids into fractions of different sizes Efficient at removing visible solids 	 Fine, moist particles can clog the sieve openings Minimum practical mesh size is 25 µm

Deep bed filters

Commonly known as a sand filters due to the fact that the most common filter medium is sand, deep bed filter is a clarification filter which operates through gravity separation. As the liquid flows downward through a deep bed of granular filling, the particles are trapped between the interstitial space of the filter medium. When enough dirt is accumulated, the filter must be washed by flow reversal, expanding the bed and releasing the trapped particles through the top of the filter [82].

Deep bed filters exist in two types: slow rate and high rate. The differences between these two types are mainly the flow rates, bed depth and filling grade. Slow rate sand filters' depth are

usually 0.6-1 m deep and operate with liquid rates of 0.1-0.2 m/h and sand particle size between 0.35-0.5 mm, while fast beds are usually 0.75 m deep and operate with liquid rates between 5-15 m/h and filling particle size of 0.5-0.6 mm [82].

These filters have been used for over 100 years in drinking water treatment [82] and more recently on clarification of sugar refinery liquor [92]. Deep bed filters can also be used in the production of metallurgically clean aluminum, a very dense fluid (2.7 g/cm³) [93].

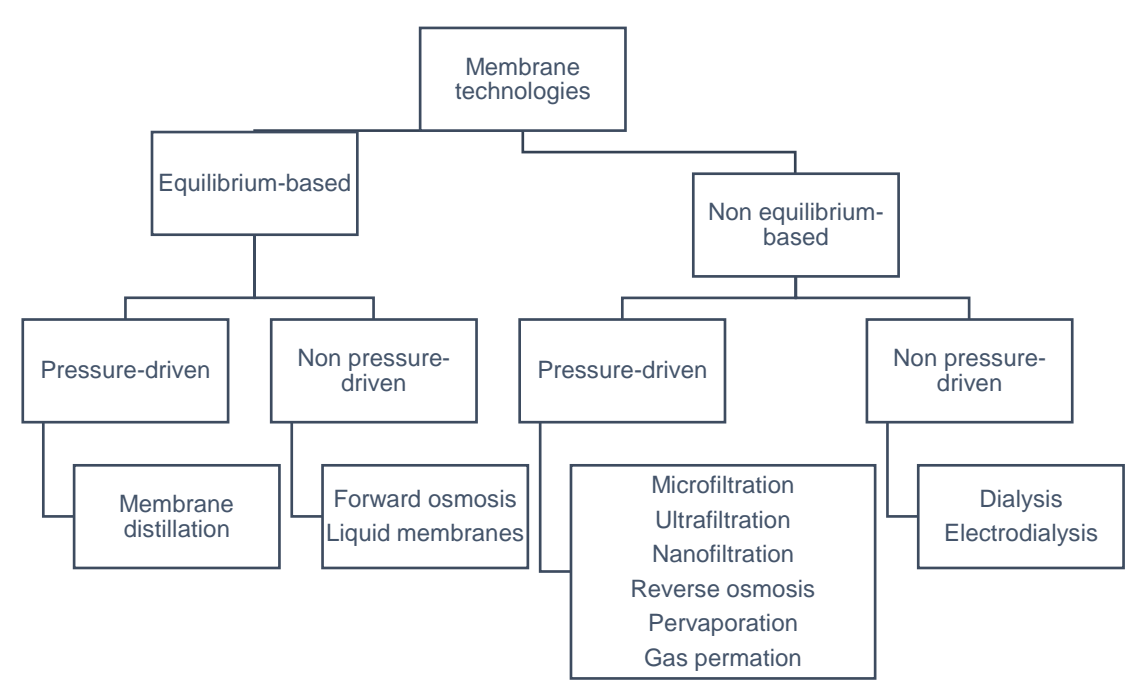
Table 1.4 shows the advantages and disadvantages of deep bed filters.

Table 1.4 - Advantages and disadvantages of deep-bed filters [82] [94] [95]

Advantages	Disadvantages
 Simple process Established and efficient at removing suspended particles 	 Medium is hard to clean due to its porosity Cleaning the filter involves stopping the operation Large space and manpower requirement

Cross-flow and membrane systems

Membrane filtration functions in two distinct modes: conventional depth filtration and crossflow filtration. In the latter, the liquid flows tangentially in relation to the medium and the filtration occurs in the surface. This semi-permeable surface filtering device, which may or may not be



thin, is denominated as a membrane. Membranes are also commonly defined as any cross-flow filter with cut-points below 0.1µm and are usually not designed specifically to accommodate depth filtration [82]. The different membrane technologies and their driving forces and exemplified on Figure 1.6.

Figure 1.6 - Schematic representation of membrane processes - Adapted from Jhaveri et al. (2016) [96]

Aside from their driving forces, membrane processes are also employed based on particle size ranges. Table 1.5 summarizes pressure driven membrane processes' differences and pore sizes, with the addition of forward osmosis, since the remaining membrane process only find applications in liquid-liquid processes such as membrane distillation and liquid membranes or gas processes such as gas permeation [97].

Table 1.5 - Some characteristics about pressure-driven membranes [82] [98] [99] [100]

Membrane process	Pore size (µm)	Operation mode
Microfiltration	10 ⁻¹ -10	Cross-flow / Dead-end
Ultrafiltration	10 ⁻³ -1	Cross-flow, dead-end in some cases
Nanofiltration	10 ⁻³ -10 ⁻²	Cross-flow is highly preferential due to fouling
Reverse osmosis/Forward osmosis	10 ⁻⁴ - 10 ⁻³	Cross-flow

Microfiltration (MF) is the membrane process with largest pores. It is applied in wastewater treatment as method to remove sediments and suspended solids [98, 101, 99]. This process is also used in the food industry for clarification and sterilization of juices [102], removal of dirt, coagulated protein and fats from gelatin [103], removal of suspended solids from syrups [104] and sweeteners and as a method of filtering antibiotics from the liquor [105].

Ultrafiltration (UF) is more suited to separation of suspended solids, colloids, proteins and microorganisms. Physical screening is considered to be the main mechanism of separation in this process, although, it is also believed that adsorption occurs on the surface of the membrane and in the pores [106].

This process in commonly used in the water treatment area, particularly in the drinking water treatment [106], in the production of ultrapure water for electronics, in dairy applications, in hemofiltration [107] and in the treatment of wastewater in agricultural sector [108].

Nanofiltration (NF) is distinguished by its ability to separate solutes and suspensions based on their charge and molecular weight. Since these membranes are usually negatively charged,

electrostatic effects are involved in nanofiltration.NF is a relatively new process that fills the gap between microfiltration and reverse osmosis [100].

Due to pore size, this process has limited applications. Nonetheless, it is still commonly used in the desalination of wastewaters [100], concentration of lactose and syrups, dyes [98] and recovery of sulphates from wastewaters [100]. Gönder et al [109]., in 2011, applied nanofiltration as a solid/liquid separation process and achieved a complete removal of suspended solids.

Forward Osmosis (FO) is a membrane process that uses osmotic pressure as driving force. Osmosis is defined as the movement of water across a selectively permeable membrane to a region of lower water chemical potential [110]. Reverse Osmosis (RO) is a more familiar process than FO. The difference between RO and FO is that the former uses hydraulic pressure to overcome the osmotic pressure. To accomplish this, a water pump is required to exert pressure on the feed solution [111]. FO/RO find applications in seawater desalination [110] [111], wastewater treatment [112], and concentration of food products [110].

Below, a summary of advantages and disadvantages for the membrane processes is shown.

Table 1.6 - Advantages and disadvantages of membrane separation processes – Adapted from Crini, 2013 [94]

Advantages Disadvantages Large number of applications Energy intensive Wide of commercial High maintenance costs, due to range membranes with different washing and membrane configurations available replacement Possible elimination of all suspended Rapid membrane clogging, along solids with fouling reducing permeate flow No chemicals required Limited flow rates Simple, rapid and efficient Not adequate for dense fluids, as cannot handle high concentrations of solids due to pore clogging and fouling.

1.3.1.2 Sedimentation

Sedimentation is, by definition, the settling of a particle or suspension of particles in a fluid due to external forces such as gravity, centrifugal force, or any force caused by an external body [113].

Settling velocity is given by Stokes law [114].

$$u = \frac{gD_p^2(\rho_s - \rho_l)}{18\mu} \tag{1}$$

where u is settling velocity (m/s), g is gravitational acceleration (m/s²), D is particle diameter (m), ρ is density (kg/m³), μ is viscosity (kg/(m.s)) and the subscripts p, s, l, represent, respectively, particle, solid and liquid.

The velocity of the particles depends on the particle diameter, particle density, fluid density and fluid viscosity. The larger and denser the particles are, the faster they settle, while the denser and more viscous the fluid is, the slower the particle settles. Temperature also indirectly influences settling velocity, since fluid density and viscosity vary with temperature [115]. Water's density and viscosity reduce as temperature increases.

In plain settling, suspended solids in water settle out by gravitational force for this purpose, large tanks designed to maintain low fluid velocities are used.

Sedimentation is widely used in primary water treatment of urban sewage, where thickeners, simple gravity sedimentation tank are used to settle out solids [91].

A summary of advantages and limitations of the plain settling process is presented on Table 1.7.

Table 1.7 - Advantages and disadvantages of plain settling – Adapted from World Health Organization, 2002 [116]

Advantages	Disadvantages
 Simple, low-cost process Can be used as a pre-treatment for other processes that require less solids content 	 Smaller/less dense particles do not settle Not feasible without addition o chemicals to speed up settling rates

1.3.1.3 Centrifugation

Centrifugation is the application of centrifugal force to assist sedimentation. Given that settling speed is based on difference between densities, some particles can take long periods to settle. Centrifugal force in centrifuges can be hundreds to millions of times higher than Earth's gravitational force, thus increasing substantially settling rates [117].

Centrifugation is very widely used and as such, several types of centrifuges are used for solid-liquid separation [118].

Although the hydrocyclone uses centrifugal force, it is not really a centrifuge – the separation is provoked by the tangential introduction of the feed. As the particles enter the hydrocyclone at high speeds, the heavier and larger particles will migrate rapidly downward and toward the walls, while smaller particles will be dragged upward and inward by the fluid toward the overflow [118].

On the other hand, a decanter centrifuge consists in a horizontal cylindrical bowl rotating at high speed to impart centrifugal force with a helical extraction screw placed coaxially. The differential speed between the screw and the bowl causes the solids to move towards the bowl wall and the liquid phase to form a concentrical inner layer [118] [119].

Decanter centrifuges have the advantages of having higher liquid capacities, higher separation efficiency and can handle higher solid concentration [118].

Known centrifuges are developed for low viscosity fluids, as this process' effectiveness is reduces as the liquid's viscosity increases [120]. However, studies on hydrocyclones have been made with liquids as viscous as 85 cP [121].

Centrifuges are widely used in the pharmaceutical industry [118] and food industry [122].

Since the principle of the different centrifuges is the same, the advantages and disadvantages are shared. These are shown on Table 1.8.

Table 1.8 – Advantages and disadvantages of centrifugation - Adapted from Xu-Ming et al. 2017 [123]

Advantages	Disadvantages
Requires less space than sedimentation tanks	High equipment cost
 Flexible process with many available equipment types 	
High separation efficiency	

1.3.1.4 Flotation

Packam et al [124], in 1973, defined flotation as the transfer of a suspended phase from the bulk of a dispersion medium to the atmosphere/liquid interface by means of bubble attachment. Flotation uses the density differential as separation and consists of four steps [125]:

- 1. Bubble generation
- 2. Contact between gas bubble and suspended particle
- 3. Attachment of the particle to the gas bubble
- 4. Rise of air/suspended particle combination to the surface

Bubble rise rate is given by the Stokes Law [126]:

$$v = \frac{gD_b^2(\rho_l - \rho_b)}{18\mu} \tag{2}$$

where v is bubble rise rate (m/s), D is diameter (m), ρ is density (kg/m3), μ is viscosity (Pa.s) and subscripts I and b stand for liquid and bubble, respectively.

By this equation it is possible to conclude that this process is negatively impacted by increasing the fluids viscosity and positively impacted by increasing the fluid's density. Flotation has been used to separate copper from aqueous solutions as dense as 3.1 g/cm³ [127].

Five types of flotation exist: dissolved air, induced air, electrolytic, froth and vacuum. Only the first three are used industrially. Froth flotation is not used due to the excessive amount of surfactant needed and vacuum flotation is not used due to high energy costs with similar performance compared to dissolved air [125]. Although froth flotation is not the most common process, it can be useful for separation of hydrophilic materials by using surfactants to make clays hydrophobic and improve their adhesion to bubbles [128]. This modification is only favorable for low concentrations of surfactant, since at higher concentrations (0.5% w/w), the use of surfactants decreases the viscosity of the suspensions [129].

Flotation is applied in urban water treatment [125] [130], mineral wastewater treatment [124], algae removal, food industry wastewaters [131] and wine clarification [132].

Below, in Table 1.9, are the advantages and disadvantages of this method when compared to other gravity-based separation process such as sedimentation.

Table 1.9 - Advantages and disadvantages of flotation processes [94] [130] [133]

Advantages	Disadvantages
 Does not require polyelectrolytes Wide variety of solids collected Lower retention time Efficient removal of small, unsettled particles with low densities Requires smaller tanks 	 Higher operating capital costs due to air and energy requirement

1.3.1.5 Adsorption

Adsorption can be defined as the selective adhesion of one or more components of a colloid or solution into a surface [134]. The forces involved can be as weak as van der Walls interactions (physical adsorption) or as strong as covalent bonds or ionic bonds (chemical adsorption)

For chemical adsorption, the medium is usually activated carbon due to its high surface area – usually 600 to 1000 m²/g [99] [135]. Adsorption is widely used in removal of reactive dyes from textile industry wastewater [136]. Amosa et al (2016) [137] also applied adsorption as an experimental process for removal of suspended solids, reaching an 89% removal rate.

Hydrodynamic chromatography

Hydrodynamic chromatography (HC) is an adaptation of the chromatography process for colloidal particles. It is based on the physical adsorption, through the size difference of colloidal particles, as these can be very different. If colloidal particles are to pass through a column filled with packing, van der Waals interactions can slow them down and effectively fraction the colloidal suspension intro fractions. The fractioning of the particles happens due to Brownian diffusion: a colloidal particle tends to flow throughout all the available void space. The larger the particle, the less its tendency to travel throughout smaller pores, and the higher its velocity along the column, while smaller particles will travel a longer path due to this diffusion effect. Small first described this process, using spherical beads of styrene divinylbenzene as packing and polystyrene latex suspensions particles as the mobile phase [138].

This process also depends on the ionic strength effect, as an increase of this effect causes the shrinkage of the electrical double layer, and the approximation of the colloidal polystyrene particles to the packing. [138]

Hydrodynamic chromatography is used as a particle sizing method to characterize polymers of high molecular weight [139].

In Table 1.10, advantages and disadvantages of the adsorption process as a solid-liquid separation process are described.

Table 1.10 - Some advantages and disadvantages of the adsorption process [94] [136]

Advantages	Disadvantages
 Technologically simple Highly effective process with fast kinetics Wide variety of target contaminants Excellent quality of treated water 	 Activated carbon is expensive, although recently, efforts have been made to obtain activated carbon from biomass Regeneration is costly and results in loss of material Rapid saturation and clogging of columns

1.3.2 Chemical methods

1.3.2.1 Coagulation

To achieve settlement in a colloid, a particle size increase is necessary [140]. Bratby [141], in 1980, defined coagulation as the process whereby a particle's size is increased through the destabilization of a given suspension or solution. In this process, the electrical double layer repulsion between particles shrinks through changes in the ionic nature and the concentration of ions in the solution [142]. Coagulation is possible through three methods: mechanical agitation, addition of inorganic salts, and addition of lower molecular weight polymers [142].

Alluminum salts

Ferric Salts

Natural

Synthetic

Guar gum

Microbond

Starches

Tannins

Sodium Alginate

Figure 1.8 shows the most common types of coagulant used.

Figure 1.7 - Classification of coagulants and some examples - Adapted from Bratby, 1980 [142]

Coagulation is used in sewage wastewater treatment [143], treatment of mining industry wastewater [144], textile water treatment [145] and support fluid treatment [146].

Most coagulants can be employed on multiple applications; however, their efficiency is dictated mostly by the water conditions and the impurity type and concentration [147]. Other factors that also affect the performance of coagulants are the medium pH, temperature, mixing time and speed.

Inorganic Coagulants

Metallic coagulants are employed due to their high valency, which leads to a charge neutralization of colloids, reducing its electrical double layer, thus promoting coagulation. Common inorganic coagulants are Al₂(SO₄)₃.18 H₂O (aluminum sulphate), Fe₂(SO₄)₃ (ferric sulphate), FeSO₄ (ferrous sulphate), and FeCl₃ (ferric chloride) [141] [143]. Chlorides are highly corrosive, but generally more efficient than the remaining inorganic coagulants. Iron-based coagulants tend to perform better at higher pH (>8), when compared to magnesium-based ones [141]. Önen et al.(2018) [148] compared several inorganic coagulants (FeCl₃, Al₂(SO₄)₃, MgCl₂, CaCl₂ and NaCl) to treat kaolin suspensions at pH 7.86 and with an initial turbidity of 301 NTU. Each coagulant showed distinct optimal concentration for the same conditions, which were 250 mg/L, 1000 mg/L, 500 mg/L, 2000 mg/L, 125 mg/L, respectively. For these conditions, the studied coagulants achieved a turbidity reduction of 91%, 90%, 76%, 64% and 25% at.

In high doses of inorganic coagulants, charge neutralization is overridden by a different form of coagulation called sweep floc, where the inorganic salts hydrolyze into metallic hydroxides and consequently entrap the impurities and precipitate from the solution, increasing the settling speeds of the flocs [149]. A simplified example of a coagulant reaction is given by:

$$Me_2^{3+}(SO_4)_3 + 6 Na(OH) \rightarrow Me_2^{3+}(OH)_6 + Na_6(SO_4)_3$$
 (3)

Where Me³⁺ represents a trivalent metallic cation.

pH is also an important factor in coagulation, as it affects the charge of the hydrolyzed species in solution. Figure 1.9 represents the mole fraction of the insoluble hydrolyzed products of iron (III) coagulants in function of pH.

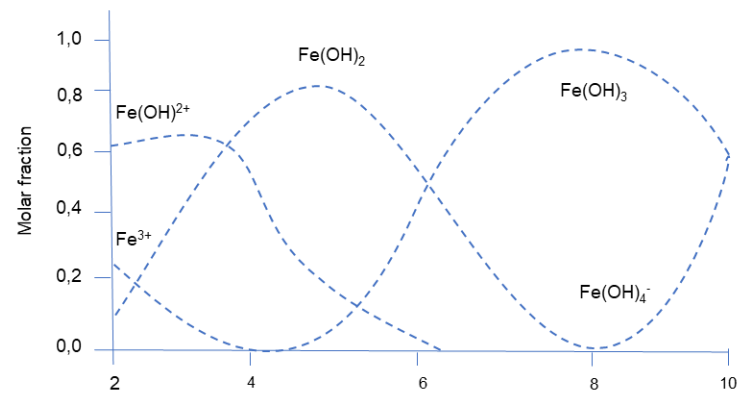


Figure 1.8 - Mole fraction of the hydrolyzed products of iron (III) coagulants [151]

As the pH increases, the positive charges of these species are reduced. Effective coagulation occurs when the insoluble, amorphous Fe(OH)₂ and Fe(OH)₃ are the predominant species. The pH range at which these species are predominant is different between coagulants. Presence of highly charged anions such as sulfates reduce the positive charge of the insoluble hydroxides in low pH ranges so that large flocs are formed in a larger pH range [150].

Bantcheva (2001) [151] used FeCl₃, Al₂(SO₄)₃ and FeSO₄ for treatment of paper and pulp and textile wastewaters. For the paper and pulp effluent, the initial turbidity was 229.4 NTU and the optimal doses were 10 mg/L, for both coagulants. Al₂(SO₄)₃ had the lowest residual turbidity (3.17 NTU) and FeSO₄ had the highest (90.8 NTU). For the textile effluent, the initial turbidity was 226.6 NTU and the optimal doses were 20 mg/L for FeCl₃, 25 mg/L for FeSO₄ and 20 mg/L for Al₂(SO₄)₃. The best performing coagulant was Al₂(SO₄)₃ again, with a residual turbidity of 6.13 NTU, while FeSO₄ was the worst performing, with a residual turbidity of 101.7 NTU. Optimal pH values for both effluents were 4.12 for FeCl₃, 7 for Al₂(SO₄)₃ and 8.15 for FeSO₄.

Ding et al. [152], in 2019, studied the influence of mixing speed using magnesium hydroxide and concluded that increasing the mixing speed from 250rpm to 350rpm, reduces the size of flocs from 8.39 µm to 8.04 µm. Mixing is usually done in two consecutive phases: one with faster

speed called "rapid mixing" and one with slower speeds called "slow" mixing. Yu et al. (2011) [153] tested the influence of mixing conditions on kaolin clay using Al₂(SO₄)₃. They claim that rapid mixing had an optimal length of 10 seconds, once residual turbidity increased with the increase of the mixing time. The authors concluded that by increasing the mixing time from 10 seconds to 60 seconds, floc size was reduced and the residual turbidity increased from 2.7 NTU to 3 NTU. Passing the mixing time over the 60 seconds caused an even higher reduction of floc size due to an increase of floc breakage, which lead to a residual turbidity of around 3.5 NTU. Zhang et al [154], in 2013, also conducted experiments using polyaluminum chloride on kaolin solutions with an initial turbidity of 68 NTU and concluded that the residual turbidity is reduced to 0.214 NTU when the slow mixing time is increased to 15 minutes but further beyond this point, the turbidity increases again.

Polymeric Coagulants

Polymeric coagulants are positively charged natural or synthetic based organic coagulants. These have the advantage of being highly charged independently of the pH of the water, once they are mainly quaternary amines [155].

Although natural polymers such as sodium alginate have the advantage of being practically toxicity-free. Synthetic polymers, like cationic polyacrylamides, polyDADMAC polyamines, and polyaluminum chloride have a more wide-spread use due to the possibility of being able to control fundamental properties important to coagulation such as molecular weight and charge density [141]. Increasing both these properties increases the efficiency of the coagulants, as they will enhance the interparticle bridging and effective destabilization of the solution. [155].

Zand and Hoveidi (2013) [156] conducted experiments on kaolinite suspensions using aluminum sulfate (Al₂(SO₄)₃) and polyaluminum sulfate (PAC) at pH 4-6. PAC demonstrated a superior turbidity reduction, particularly at higher turbidity values (500 and 1000 NTU). At optimal concentration, PAC produced a turbidity reduction of 94.1% and 94.6% at these initial turbidities while Al₂(SO₄)₃ produced 86.3% and 84.3%. The concentrations used were varied between 0 and 50 mg/L.

1.3.2.2 Flocculation

Flocculation is a physico-chemical process in which two or more particles are aggregated by adsorption on large polymer chains. There are three types of flocculation: bridging flocculation, network flocculation and charge neutralization [157].

As previously shown in chapter 1.2.2.1.5, bridging flocculation occurs when a large chain of polymer adsorbs simultaneously into multiple particles.

Network flocculation is the formation of three-dimensional gel-like structures formed by one or more linear polymer chain stabilized by hydrogen bonds [158].

The third type of flocculation is charge neutralization. This phenomenon is caused by the attraction of charged polymers towards opposite charge particles [159].

Anionic and cationic flocculants adsorb strongly to particles of opposite charge, resulting in charge neutralization but can still form flocs through the other two mechanisms, network flocculation and bridging flocculation. to different extents [157]. Flocculants are usually polymers with molecular weight range between 10⁵ to 10⁶ Da [91].

Below, in Figure 1.9, are presented different flocculants depending on their nature and charge.

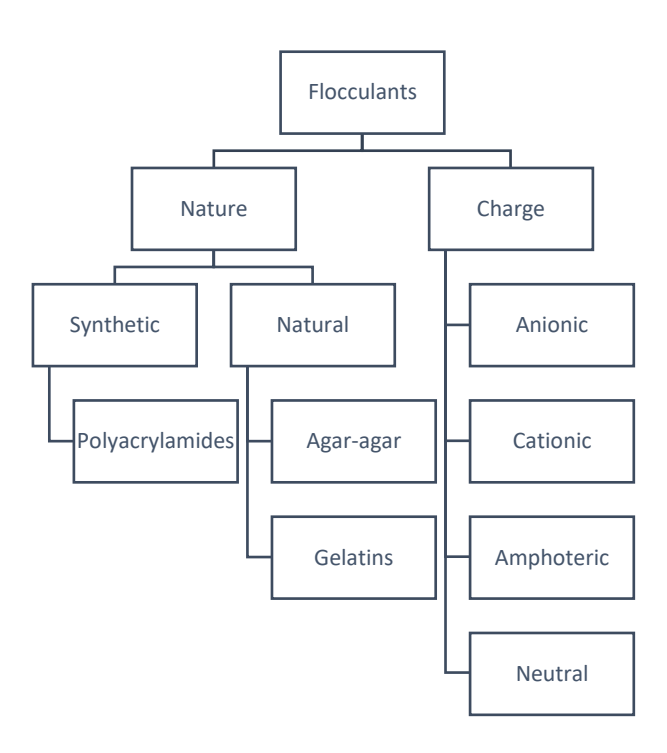


Figure 1.9 - Schematic representation of some flocculant properties [157] [91]

Synthetic flocculants have the advantage of being customizable according to the industrial needs. Industries where flocculation is used are mineral [148], pulp and paper mill [160], textile [161] and treatment of support fluids [162]. The most important characteristics when choosing a flocculant is molecular weight, the nature of their functional groups and their charge density [157]. Optimal molecular weight is 10⁶ kDa or more, once as longer chains are, the probability of reaching other particles increase. The functional groups will determine if the flocculant is ionic, anionic or non-ionic. Charge density also dependent on the functional group being ionizable or not. For anionic polyacrylamides, flocculation improves as molecular weight increases [157].

Nasser and James (2006) [163] evaluated the influence of charge density and molecular weight of flocculants on the treatment of kaolinite suspensions. They reported that by increasing the charge density of anionic polyacrylamides from 10% to 35%, settling speeds were reduced from 7.9 cm/min to 5.8 cm/min and turbidity reduction was lower with higher anionicity polymers. Similarly, for cationic polymers, increasing charge density from 10% to 35% decreased the settling speeds from 5.7 cm/min to 4.8 cm/min but had no effect on turbidity. The authors proposed that increasing charge density in cationic polymers can quickly saturate the surface of the clays, preventing further adsorption. Concerning the polymers molecular weight, by increasing it, turbidity suffered a decrease from 41 to 26 NTU and increased settling rates from 4.6 cm/min to 5.8 cm/min for anionic polymers. For cationic polymers, only the settling rate increased from 4.1 to 4.8 cm/min with the increasing of molecular weight.

Taşdemir et al. [164], in 2012, studied the importance of mixing conditions in flocculation. They claim that for an effective flocculation, the dual system of rapid mixing and slow mixing is needed. The former serves the purpose of dispersing the flocculant throughout the solution, while the latter promotes collision between flocs to increase their size. Even though the conditions may vary significantly from system to system, they concluded that optimal conditions were 250 rpm for rapid mixing of 5 minutes, 40 rpm for slow mixing of 10 minutes and obtained a settling time of 15 minutes. The rapid mixing was tested between 1 and 5 minutes at 75, 100, 150 and 250 rpm. Slow mixing was tested between 5 and 30 minutes at 20, 30 and 40 rpm. Settling times were 15 and 30 minutes.

Flocculation, while an independent process, is usually used in conjunction with coagulation. When the combination is employed, flocculants are sometimes referred as coagulant aids [99]. In these systems, coagulants can be paired with cationic, anionic, and non-ionic polymers, however cationic and anionic tend to be more effective [165]. In the study of Önen et al, (2013) [148], they also compared anionic, cationic and non-ionic polyacrylamides. The anionic polyacrylamide achieved the highest turbidity removal of 94.3%, compared to 93.9% and 82.8% of the cationic and non-ionic, respectively with the lowest dose of 1.25 mg/L, compared to 40 mg/L and 20 mg/L of the cationic and non-ionic. Cationic polymers can be used in conjunction with coagulants, reducing the latter's required dose, while anionic coagulants are generally added after the coagulant takes effect and promote the floc size increase through electrostatic attraction, as mentioned previously [166].

Because coagulation and flocculation have very similar advantages and disadvantages, they are grouped in Table 1.11.

Table 1.11 - Advantages and disadvantages of coagulation and flocculation - Adapted from Crini, 2013 [94].

Advantages	Disadvantages
 Simple process Can serve as a precursor to other separation processes Inexpensive 	 Require the addition of non- reusable chemicals Require physicochemical monitoring

1.3.3 Field Assisted Methods

1.3.3.1 Electric Field Assisted Separation

Most particles found in nature have an inherent electrical charge. This charge can be changed through variation of pH, conductivity, temperature, or composition of the solution to be separated.

For clay minerals, increasing pH increases their negative charge due to ionization of the basal hydroxyl group [63]. Conductivity can be improved through increase of their hydration [167].

In presence of a controlled electric field, it is possible to force particles of different charges to move in different directions. Electrophoresis is the movement of charged particles in a conductive liquid or colloidal suspension within an electric field applied. The movement of a liquid when an electric field is applied is called electroosmosis [168]. Using these properties, it is possible to force the water to migrate towards an electrode and the colloidal matter towards the opposite electrode, with a filtering medium in between [169]. Tchillingarian, in1952 suggested that electrophoresis can be a potential separation process for colloidal clays and determined that the cataphoretic velocity in presence of NaOH is inversely proportional to particle size [170]. Culkin, in EP 0.202.934, describes electrophoretic separation as a process to separate kaolin clay suspensions [168]. Later, electrokinetic effects have been used in combination with crossflow filtration to reduce membrane fouling. This assistance consists in applying an electric field gradient to direct the charged particles in a direction away from the filter [169]. Mostafazadeh et al [171], in 2016, combined these two processes and concluded that while this process reduces fouling and improves water quality, the low conductivity of the water stream, the high energy requirement and the heat generation, the large space requirements restrict the use of this process for industry use Another disadvantage for this process is that electrophoretic mobility is reduced as the fluid's viscosity increases [172].

1.3.3.2 Magnetic Field Assisted Separation

Magnetic field can be applied to separation purposes by affecting the magnetic properties of contaminants in water [173]. Magnetic separation usually involves passing a suspension through a non-uniform magnetic field. If the particles are susceptible to the magnetic field, they will move towards the regions of highest strength [169].

High Gradient Magnetic Separation is a process in which a magnetically susceptible wire bed is placed inside an electromagnet. Applying a magnetic field will create a heterogeneous magnetic field and produce large field gradient around the wires and trapping the magnetic particles. The collection of particles depends on their size, magnetic properties, and the magnetic force's capacity to dominate the fluid drag, gravitation, inertial and diffusional forces [173].

Magnetic fields have been applied in water treatment. The application of magnetic fields reduces settling times and promotes coagulation. Therefore, suspended solids removal increases as the magnetic field strength and exposure time are increased and as flow rate is decreased [173] [174]. Hibayashi et al. [175], in 2011, applied magnetic fields in separations with dense fluids (polyvinyl alcohol) with a measured viscosity of 800 cP and attained a velocity of 100 mm/s.

In Table 1.12 some advantages and limitations of this process are presented.

Table 1.12 - Advantages and disadvantages of the magnetic field assisted separation process – Adapted from Zaidi et al. 2014 [173]

•	Separation is more difficult or
not represent an environmental hazard and does not require chemical use Magnets can last many years	particles that are less susceptible to magnetic field

1.3.3.3 Separation Using Ultrasonic Waves

When ultrasonic waves are applied in a suspension, the waves propagate in as mechanical vibratory energy [169]. A standing wave is formed when a sinusoidal wave is reflected by a fixed point. As the waves travel in opposite directions, two distinct zones form: the nodes and the antinodes. The nodes are very low energy zones where particle velocities are closer to zero and the antinodes are high energy zones where particle velocities are high [176]. The scattering of the wave will produce what is known as primary acoustic radiation force, which acts on the

particles so that they are moved towards either the antinode or the node, depending on the acoustic contrast factor. The acoustic contrast factor depends on the density and compressibility of the particles and is given by:

$$\emptyset = \frac{5\rho_p - 2\rho_l}{2\rho_p + \rho_l} - \frac{\beta_p}{\beta_p} \tag{4}$$

Where ρ is the density, β is the compressibility and the subscripts p and l refer to the particle and the liquid, respectively. If the contrast factor is positive, the particles will move towards the pressure nodes. If the factor is negative, the particles will move towards the antinode. The positioning of the particles in the nodes or antinodes after applying the standing wave will cause them to aggregate into larger particles [177].

Bekker et al, in 1992, have used this principle to separate talc suspensions [176]. Fetyan & Attia [178], in 2020, described this process as extremely efficient in total solids removal in water treatment.

Table 1.13 - Advantages and disadvantages of ultrasonic wave separation [178] [179]

Advantages	Disadvantages
 Simple process, low capital cost No additives and no byproducts formed 	 Energy consumption Maintenance/replacement of the ultrasound probe
No environmental concerns	 Instruments can be damaged by the ultrasonic waves Ultrasound waves can reduce suspension viscosity up to 55%

1.4 Outline

The present work was done with the guidance of GEO. GEO is a global company whose mission is to improve the efficiency of the drilling and excavation processes in the foundation industry, through the application of unique products and techniques.

The foundation construction process is carried out in the following steps [23] [27]:

- 1. Pre-mixing of the support fluid, where the fluid is mixed with water or additives to grant its necessary properties such as density and viscosity.
- 2. Drilling and stabilization, where the hole is excavated, and the fluid is added.

- 3. Cleaning of the hole, where the solid cuttings are removed, as they can interfere with the cementing step.
- 4. Positioning and Casing, where a steel structure is placed to keep the hole open.
- 5. Cementing, where cement is added in the bottom of the hole, displacing the support fluid.
- 6. Post-cementing and treatment of the stabilizing fluid.

Steps 2-6 are represented in Figure 1.10. Fluid properties are measured during steps 1-4 and 6 [23]. Step 3 is crucial, since as mentioned previously, for effective cementing, density in the column cannot be higher than the density of the cement.

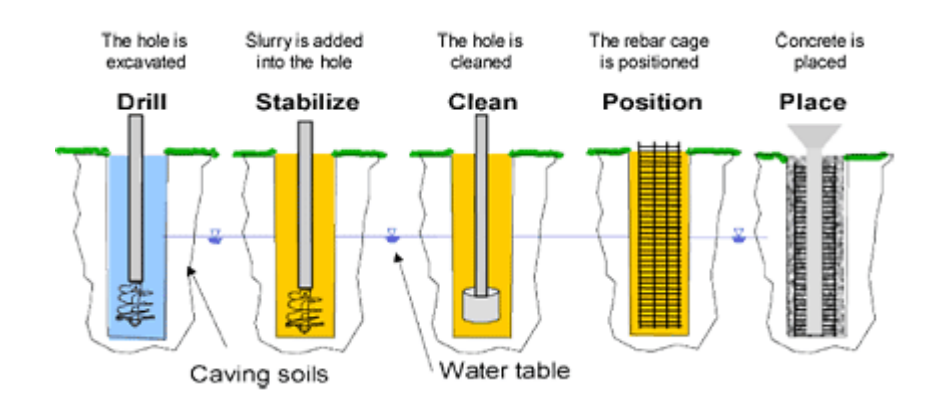


Figure 1.10 - Cased shaft construction process - from Texas Shafts Inc., 2013 [180]

Considering that the solution resulting from the present work must be applicable to the construction site, the purpose of this work is to create a new solution that focuses on the controlled reduction of the solution's density, while maintaining the stability of the column. As this is a novelty concept, the crossing of the study variables will be focused mainly on this goal without undermining the remaining objectives.

To accomplish this goal, the following set of objectives was established:

- A decrease on the Marsh viscosity lower or equal to 5 s/quart;
- A controlled decrease of the solids in suspension with the control of the dosage of the product(s), within the density intervals of 0.02g/cm³, 0.06g/cm³, 0.09g/cm³, and 0.12g/cm³ (DR) and an initial density between 1.15-1.20g/cm³. With a tolerance of +-0.01g/cm³;
- The deposit must be collected;
- After collecting the deposit from the bottom, all the column must have the same density (do not create a gradient on the column superior to 0.03g/cm³ between the middle and bottom of the column);
- The product(s) must work in a density range between 1.00-1.20g/cm³;

All the process of density decrease and deposit collection must take no longer than 30 minutes.

It is imperative that the stability of the column is also assured, as the failure to attain this objective poses a serious risk to the construction process and may collapse the column, This will be reflected on the solution's viscosity, DR results, density gradients and visual cues.

Therefore, to attain these objectives, coagulation and flocculation were selected as the main strategies due to their ease in diffusing in polymeric suspensions, their affinity to colloidal particles and their ability to neutralize and agglomerate clay particles. Furthermore, the specific components selected followed the following criteria:

- Effective at basic pH (>7)
- Low corrosiveness
- Able to apply uniformly in a viscous solution
- Small components (for coagulants)
- High valency (for coagulants)
- High molecular weight (for flocculants)

Thus, for the next chapters, suitable protocols were established in order to study these strategies on two clay types: clay A and clay B.

2. Materials and Methods

2.1 Reagents

Sodium hydroxide (NaOH, 98% purity, CAS n.° 1310-73-2, purchased from Labkem), calcium chloride (CaCl₂, 100.8% purity, CAS n.° 10035-04-8, purchased from VWR chemicals), sodium chloride (NaCl, 99.5% purity, CAS n.° 7547-14-5, purchased from ITW Reagents), hydrochloric acid (HCl, 35% purity, CAS n.º 7647-01-0, purchased from Labkem), aluminum sulfate (Al₂(SO₄)₃, 16-17.5% purity, CAS n.° 17927-65-0, purchased from VWR chemicals), (olyMud®, GNet® GPlus®, clay A (purchased from Terracota do Algarve), clay B (purchased from MCS), sand (from Costa da Caparica beach), ferrous sulfate (FeSO₄, 98.6% purity, CAS n.° 7782-63-0, purchased from Shandong Tongli Chemical Co., Ltd.), polyferric sulfate (PFS, 19-22% purity, CAS n.° 10028-22-5, purchased from Shandong Tongli Chemical Co., Ltd.), ammonium sulfate ((NH4)₂SO₄, 99% purity, CAS n.° 7783-20-2, purchased from Shandong Tongli Chemical Co., Ltd.), Microbond® (40% purity, CAS n.° 26062-79-3, purchased from GEO), Telsun 5153 (90% purity, CAS n.° 9003-05-8, purchased from VM Chemical Industry Co., Ltd.), 6610 (CAS n.° 9003-05-8 purchased from Shandong Tongli Chemical Co.), 9233 (CAS n.º 9003-05-8 CAS, purchased Xinxiang Boyuan Water Purifiyng Materials Co., Ltd.), TelSun N23 (90% purity, CAS n.° 9003-05-8, purchased from VM Chemical Industry Co., Ltd.), Flonex 934 (CAS n.° 9003-05-8, purchased from SNF Brasil Ltda.), A0410 (CAS n.º 9003-05-8, purchased from Shandong Right Fine Chemical Co., Ltd.), Nonionic 513 (CAS n.º 9003-05-8, purchased from Xinxiang Boyuan Water Purifiyng Materials Co., Ltd.), 6605 (CAS n.º 9003-05-8, purchased from Shandong Tongli Chemical Co.) and distilled water. All reagents were used without further purification.

2.2 Equipment

pH meter (model PHS-3CW), Brookfield viscometer (model DV2T), conductimeter (model DDS-307), magnetic stirrer (model SH-3), scale (model HD-150 from Scale-House), mixing rotors (model HD2004W), electrical bath (model TB-21 from Biobase Industry), 5L reactor, clay stirrer (model YN-90-60 from VTV Motor), micropipette (from VWR chemicals), peristaltic pump (model FPP6), digital densimeter (model Densito PX-30 from Mettler Toledo), analogic densimeter (model 100-0 from OFITE) and Marsh funnel (from OFITE).

2.3 Execution protocols

2.3.1 Density reduction as function of coagulant type, coagulant concentration, mixing time, mixing speed, initial densities and introduction method

The aim of this protocol is to reduce the density of a polymeric clay suspension within the intervals of 0.02 g/cm³, 0.06 g/cm³, 0.09g/cm³, and 0.12g/cm³ g/cm³, by studying coagulant concentrations between 5 and 600 mg/L, mixing times between 8 and 24 minutes, mixing speeds between 200 and 300 rpm, initial densities between 1.10-1.13 g/cm³ and 1.14-1.16 g/cm³, with internal and external introduction of coagulant.

For this, a 5L jacketed reactor (Figure 2.1) was filled with 3L of deionized water with a bath set at 22°C (in order to have the solution at 17-18°C). Mixing was maintained using a bubbling air agitator. 12mL of an aqueous solution of NaOH of 2.5M (pre-prepared) were added to the distilled water, to attain a pH of 11. Afterwards, 3g of PolyMud polymer were added to the solution and were dissolved for 1h. The solution was then transferred to a 7L bucket (Figure 2.2) and mixed using an agitator, like the one showed in Figure 2.2, at 200 rpm. 0 to4.51 mL of GPlus were added (see Appendix 1) and 20 minutes later, 750g-900g of clay were added and the solution was kept under agitation for 90 minutes. After this time, the solution was transferred to a 5L recipient and put to rest for 30 minutes.



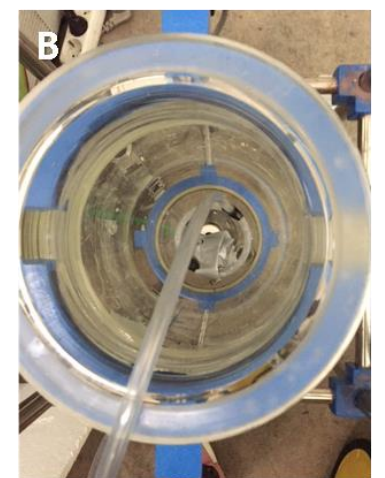




Figure 2.1 - Jacketed reactor side view (A), top view (B), and the recirculating bath (C).





Figure 2.2 - Soil mixing apparatus

Marsh viscosity of the solution was then characterized according to chapter 2.4.1, and the solution transferred to a 3L recipient and put to rest for 10 minutes. Passed this time, samples from the middle and bottom of the solution were collected using a peristaltic pump and characterized according to the protocols: density (2.4.2), Brookfield viscosity (chapter 2.4.3), pH (chapter 2.4.4), and electrical conductivity (chapter 2.4.5). 2L of the solution were put under agitation at 200-300 rpm and the agitation time and coagulant concentration were adjusted according to Appendix 1. After the agitation was stopped, the solution was kept at rest for 10 minutes and then samples were collected from middle and bottom zones to characterize again according to the protocols: density (2.4.2), Brookfield viscosity (chapter 2.4.3), pH (chapter 2.4.4), electrical conductivity (chapter 2.4.5) and Marsh viscosity (chapter 2.4.1).

2.3.2 Density reduction as a function of agitator type

The aim of this protocol is to observe the visual effect of different agitators (P1 to P8, Figure 2.3) at 200 rpm to determine which paddle generates the most uniform dispersion throughout the container's height using 1mL of red colorant.



Figure 2.3 - (A) - Agitator "P1"; (B) - Agitator "P2"; (C) - Agitator "P3"; (D) - Agitator "P4"; (E) - Agitator "P5"; (F) - Agitator "P6"; (G) - Agitator "P7"; (H) - Agitator "P8"

For this purpose, a 5L reactor was filled with 3L of deionized water was maintained in a 22°C bath (in order to have 17-18°C inside the 5L jacketed reactor). Mixing was maintained using a bubbling air agitator. 12mL of an aqueous solution of NaOH of 2.5M (pre-prepared) were added to the distilled water, in order to have a pH of 11. Afterwards, 3g of PolyMud polymer were added to the solution and were dissolved for 1h. 2L of the solution was transferred to a 3L recipient. The paddle was selected according to Table 2.1 and put under agitation at 200 rpm. 1 mL red colorant was added, and the dispersion was recorded. The agitation was stopped once the solution as homogeneous or after 90 seconds.

Table 2.1 - Runs and agitators tested.

Run	Agitator
31	P1
32	P2
33	P3
34	P4
35	P5
36	P6
37	P7
38	P8

2.3.3 Density reduction as a function of coagulant and flocculant type, introduction method and mixing speeds

The aim of this protocol is to reduce the density of a polymeric clay suspension within the intervals of 0.02 g/cm³, 0.06 g/cm³, 0.09g/cm³, and 0.12g/cm³, with the initial density of 1.15 – 1.20 g/cm³, by increasing settling speeds using flocculants (Microbond, 6610, Telsun 5153, 9233, Telsun N23 and Flonex 934)+ in addition to the coagulants Al₂(SO₄)₃ and PFS, by varying introduction method (internal and external) and by varying mixing speeds (20-200 rpm).

For this, a 5 L reactor was filled with 3 L of deionized water was maintained in a 22 °C bath (in order to have 17-18°C inside the 5L jacketed reactor). Mixing was maintained using a bubbling air agitator. 12mL of an aqueous solution of NaOH of 2.5M (pre-prepared) were added to the distilled water, in order to have a pH of 11. Afterwards, 3g of PolyMud polymer were added to the solution and were dissolved for 1h. The solution was then transferred to a 7L bucket (Figure 2.2) and mixed using an agitator, like the one showed in Figure 2.2, and at 200 rpm. 4.51 mL of GPlus were added and 20 minutes later, 900g of clay were added and kept under agitation for 90 minutes. After this time, the solution was transferred to a 5L recipient and put to rest for 30 minutes.

The Marsh viscosity of the solution was then characterized according to 2.4.1, then transferred to a 3L recipient and then put to rest for 30 minutes. Passed this time, samples from the middle and bottom of the solution were taken using a peristaltic pummp filtered using a sieve and then characterized according to the protocols Density (2.4.2), Brookfield viscosity (chapter

2.4.3), pH (chapter 2.4.4) and electrical conductivity (chapter 2.4.5). Flocculants were selected according to Appendix 2 and added to a 2L of solution, which put under agitation at 200 rpm. Flocculant introduction method was selected according to Appendix 2. Mixing speed was then adjusted to 20 rpm (when applicable). When cationic flocculants (Microbond and 6610) were used, they were introduced immediately after the coagulant and the agitation was stopped 8 minutes after the addition of the latter. When anionic flocculants (Telsun 5153, 9233, and Flonex 934 and Telsun N23) were used, they were added 3 minutes after the addition of coagulant and the agitation was stopped 4 minutes after the addition of the former. After stopping the agitation, the solution was put to rest for 30 minutes and then samples were collected from middle and bottom zones to characterize according to the protocols Density (2.4.2), Brookfield viscosity (chapter 2.4.3), pH (chapter 2.4.4), electrical conductivity (chapter 2.4.5) and Marsh viscosity (chapter 2.4.1).

Solutions were left overnight (about 18 hours) to settle out and were then characterized again according to Brookfield viscosity (chapter 2.4.3).

2.3.4 Density reduction as function of flocculant charge (cationic and non-ionic), concentration, and solution pH and temperature

The aim of this protocol is to reduce the density of a polymeric clay suspension within the intervals of 0.02 g/cm³, 0.06 g/cm³, 0.09g/cm³, and 0.12g/cm³, with the initial density of 1.15 – 1.20 g/cm³, by adding cationic and non-ionic flocculants in concentrations of 250-2000 mg/L combined with HCI, with solution temperature of 16-21°C.

For this, a 5L reactor was filled with 3L of deionized water was maintained in a 22°C bath (in order to have 17-18°C inside the 5L jacketed reactor). Mixing was maintained using a bubbling air agitator. 12mL of an aqueous solution of NaOH of 2.5M (pre-prepared) were added to the distilled water, in order to have a pH of 11. Afterwards, 3g of PolyMud polymer were added to the solution and were dissolved for 1h. The solution was then transferred to a 7L bucket (Figure 2.2) and mixed using an agitator, like the one showed in Figure 2.2, and at 200 rpm. 1.50 mL of GPlus were added and 20 minutes later, 900g of clay were added and were kept in agitation for 90 minutes. After this time, the solution was transferred to a 5L recipient and put to rest for 30 minutes. The solution was then transferred to a 3L recipient and put to rest for 30 minutes. Passed this time, samples from the top, middle and bottom of the solution were taken using a peristaltic pump and characterized according to the protocols Density (2.4.2), Brookfield viscosity (chapter 2.4.3), pH (chapter 2.4.4) and electrical conductivity (chapter 2.4.5).2L of solution were put under agitation. Agitation was set to 300 rpm. Flocculants were added according to Appendix 3 and after 15 seconds, the agitation was reduced to 50 rpm. After 8 minutes, the agitation was stopped, and the solution was put to rest for 30 minutes. Passed this

time, samples from the top, middle and bottom of the solution were taken using a peristaltic pump and characterized according to the protocols Density (2.4.2), Brookfield viscosity (chapter 2.4.3), pH (chapter 2.4.4) and electrical conductivity (chapter 2.4.5).

2.3.5 Density reduction as function of HCl concentration and solution volume on clay/sand mixture

The aim of this protocol is to reduce the density of a polymeric clay/sand suspension within the intervals of 0.02 g/cm³, 0.06 g/cm³, 0.09g/cm³, and 0.12g/cm³, with the initial density of 1.15 – 1.20 g/cm³, by adding cationic and non-ionic flocculants combined with HCl and by varying the volume of solution.

For this, a 5L reactor was filled with 3L of deionized water was maintained in a 22°C bath (in order to have 17-18°C inside the 5L jacketed reactor). Mixing was maintained using a bubbling air agitator. 12mL of an aqueous solution of NaOH of 2.5M (pre-prepared) were added to the distilled water, in order to have a pH of 11. Afterwards, 3g of PolyMud polymer were added to the solution and were dissolved for 1h. The solution was then transferred to a 7L bucket (Figure 2.2) and mixed using an agitator, like the one showed in Figure 2.2, and at 200 rpm. 1.50 mL of GPlus were added and 20 minutes later, 540g of clay were added and were kept in agitation for 90 minutes. The solution was put to rest for 30 minutes and characterized according to protocols Density (2.4.2) and Brookfield viscosity (chapter 2.4.3). The solution was then put under mechanical agitation at 200 rpm and 300g of sand were added. Agitation was stopped after 30 minutes and the solution was characterized according to protocols Density (2.4.2), Analogic Density (chapter 2.4.6) and Brookfield viscosity (chapter 2.4.3). After this time, the solution was put to rest for 30 minutes and characterized according to protocols Density (2.4.2), Analogic Density (chapter 2.4.6), Brookfield viscosity (chapter 2.4.3) and Marsh viscosity (chapter 2.4.1). Samples were drawn from the top, middle and bottom using a peristaltic pump and characterized according to protocols Marsh viscosity (chapter 2.4.1), Density (2.4.2), Brookfield viscosity (chapter 2.4.3), pH (chapter 2.4.4), electrical conductivity (chapter 2.4.5) and Analogic Density (chapter 2.4.6). The solution was put under mechanical agitation at 200 rpm and the A0410 + HCl solution was added according to Appendix 4. The mixing speed was set to 300 rpm for 15 seconds and reduced to 50 rpm. Agitation was stopped after 8 minutes and the solution was put rest for 30 minutes. Samples were drawn from the top, middle and bottom and characterized according to protocols Marsh viscosity (chapter 2.4.1), Density (2.4.2), Brookfield viscosity (chapter 2.4.3), pH (chapter 2.4.4), electrical conductivity (chapter 2.4.5) and Analogic Density (chapter 2.4.6).

2.4 Characterization protocols

2.4.1 Marsh viscosity measurement

The determination of the Marsh viscosity was done using a Marsh cone and cup, as shown on Figure 2.4. To do it, cover the base of the marsh cone with your index finger and add the solution to be measured until the line at the top of the cone. Place the cup under the outlet of the marsh cone and dismantle the base of the cone at the same time as the time counting starts with a chronometer. Stop the chronometer, by the time the solution reaches the cup mark, and the value obtained is the viscosity value in seconds/quart.



Figure 2.4 - Marsh cone

2.4.2 Density measurement

The determination of the density was done using the densimeter with model name Mettler Toledo Densito PX30. To do this, draw a 100mL sample of the solution into a cup. Slowly pull the sample until the internal tubes are filled. Read the density value on the screen.



Figure 2.5 - Mettler Toledo Densito PX-30

2.4.3 Brookfield viscosity measurement

The determination of the Brookfield viscosity was made by using the viscometer with model name DV2T. To do this, turn on the device and proceed to the calibration step. Make sure that the air bubble on the front of the equipment is centered and press "AUTO ZERO" without any spindle attached. Attach the spindle in the device and in the main menu, set the spindle (LV-01 or ULA) and rotation speed, with a 5 second data interval for 5 minutes. Measure around 50-100 mL, depending on the spindle and pour it into the measuring vessel. Press "RUN" and collect the results after 5 minutes.



Figure 2.6 - DV2T Brookfield viscometer

2.4.4 pH measurement

To determine the pH of the polymeric soil solution, turn on the pH meter (Figure 2.7) by pressing the power button. Rinse the electrode with deionized water and dry it. Dip the electrode in the solution and wait 5 minutes. Record the value and rinse the electrode with deionized water.



Figure 2.7 - PHS - 3CW pH meter

2.4.5 Electrical conductivity measurement

To determine the electrical conductivity of the polymeric soil solution, turn on the conductivity meter (Figure 2.8) by pressing the power button. Rinse the electrode with deionized water and dry it. Dip the electrode in the solution and wait 5 minutes. Record the value and rinse the electrode with deionized water.



Figure 2.8 - DDS-307 Electrical conductivity meter

2.4.6 Analogic density measurement

To determine the density of the polymeric soil solution, pour the solution into the densimeter cup until it is completely full. Confirm that the cup is correctly balanced and cover it with the lid. Make sure that some of the fluid is pushed out of the hole on the lid to remove the air. Wipe the excess fluid and put the cup on the scale. Adjust the weight of the scale in order to level the bubble. Record the value on the scale.



Figure 2.9 - Analog densimeter

3. Results and discussion

For the evaluation of the DR, initially, samples were taken from the middle and bottom and DR from each zone was analyzed individually until mentioned otherwise. From chapter 3.3.2 onward, the need to take samples from the top area arose. For these runs top, middle and bottom samples were evaluated, the mean and median between these three values were calculated to reduce the measurement errors and variability of the experiments, as detailed further bellow.

Furthermore, to guarantee the stability of the column in real-life scenarios, whenever a clean strip is formed and there is partial or total coagulation/flocculation throughout the column, this solution is deemed as inviable, as the viscosity and suspension capability of the column needs to be maintained to continue the construction process. Even so, the measurements and visual analysis will be performed to determine if the DR is representative of a controlled decrease or if the stability of the column is at risk.

3.1 Influence of the coagulant concentration and mixing time on density reduction

The purpose of this subsection is to study the influence of the concentration of the coagulant $Al_2(SO_4)_3$ (5, 50, 200 and 600 mg/L) and its mixing time (8, 16 and 24 minutes) on DR capacity, following protocol 2.3.1. Fixed variables are mixing speed (200 rpm), coagulant type ($Al_2(SO_4)_3$), clay type (clay A from Terracota do Algarve) and polymer type (PolyMud).

As detailed on protocol, 2.3.1. on each run, two samples were taken: from the middle and the bottom of the recipient to evaluate the variation of the density across the column with the addition of coagulant and to evaluate the density gradient between these two zones.

In Figure 3.1, the values of DR, for middle and bottom samples, are represented when varying the coagulant concentration and mixing times.

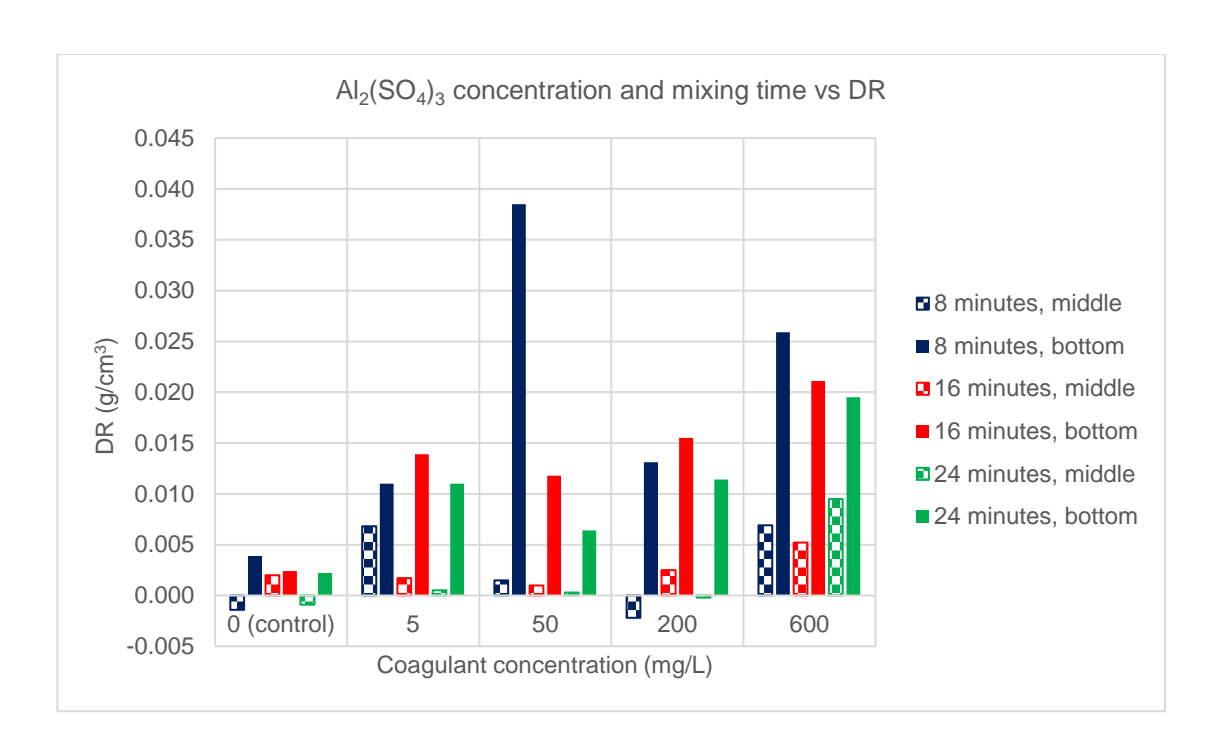


Figure 3.1 - Effect of Al₂(SO₄)₃ concentration and mixing time on DR (at a mixing speed of 200rpm).

It is possible to observe that DR for the middle samples is vastly inferior, for nearly all samples, when compared to the DR of the bottom samples. This may be due to the agitator configuration not allowing the uniform distribution of the coagulant, especially in the middle region.

Increasing the coagulant concentration, on average, leads to an increase of DR. For the middle samples, the trend between all concentrations is a DR lower than 0.005 g/cm³, for the concentrations of 5, 50 and 200 mg/L, except for 5 mg/L at 8 minutes. At the concentration of 600 mg/L, DR increased past 0.005 g/cm³ for all mixing times. For the bottom samples, increasing the coagulant concentration between 5 and 600 mg/L increases DR - 0.015 g/cm³ for 8 minutes, slightly over 0.05 g/cm³ for 16 minutes and over 0.015 g/cm³ for 24 minutes, all times considering that 50 mg/L is an outlier, since DR for this concentration is vastly superior to all other concentrations and for other mixing times for the same concentration.

Increasing mixing time for the middle samples decreased DR, except for the runs performed with 600 mg/L of coagulant, while for the bottom sample, increasing from 8 to 16 minutes, no pattern is observable, but from 8 to 24 minutes, the trend is for DR to decrease.

Hassan et al. (2009) claim that excessive mixing times reduce the efficiency of the flocculation process due to the floc breakage [181]. The results obtained are in accordance, as it was observed the decrease of DR with increasing mixing times. It might be a possibility that the floc breakage is contributing to local density increase, as the small flocs will not settle as easily as the bigger ones.

In conclusion, increasing the mixing time reduces DR. A DR of 0.02 g/cm³ is achieved using 600mg/L of (Al₂(SO₄)₃) and 16 minutes of mixing, and 0.025g/cm³ with 600mg/L and 8 minutes of mixing.

In addition to the DR, and as presented above, other objectives must be taken into consideration, so they will be presented and discussed below.

Table 3.1 – Initial densities, coagulant concentration, Marsh Viscosity gaps and final density of the runs performed at 8 minutes. ^{a)}Marsh gap is calculated from the difference between final and initial values. ^{b)}Final density gap is calculated from the difference between middle and bottom values.

Run	Zone	Coagulant concentration (mg/L)	Initial density (g/cm³)	Marsh viscosity gap (s/quart) ^{a)}	Final density gap (g/cm³) ^{b)}
	Middle	E	1.1026	2	0.0024
9	Bottom	5	1.1102	-2	0.0034
7	Middle	50	1.1125	_	0.0120
7	Bottom	50	1.1375	-5	
40	Middle	000	1.1051		0.0044
10	Bottom	200	1.1190	1	0.0014
	Middle	000	1.0974		0.0067
8	Bottom	600	1.1231	6	

Table 3.1 represents the initial densities, Marsh viscosity gap and density gradient between middle and bottom for the selected runs performed for 8 minutes of mixing time at different concentrations of the coagulant (Al₂(SO₄)₃).

For a mixing time of 8 minutes, Marsh viscosity has a maximum decrease of 5s/quart when 600mg/L of coagulant are applied, the final density gap between the bottom and middle of the column is lower than 0.03g/cm³ for the four runs presented, meaning that the objectives related to these two points were accomplished.

Initial densities are not within the objective (1.15-1.20 g/cm³) due to the difficulty of handling higher density solutions (clogging of the volumetric pipette when collecting the samples). Nonetheless, it was necessary to establish a comparability criterion. Arbitrarily, it was established that the runs are comparable if the initial densities are within a 0.03 g/cm³ range. From chapter 3.3, the protocol was altered to use densities within the values established in the objective, since the handling was altered.

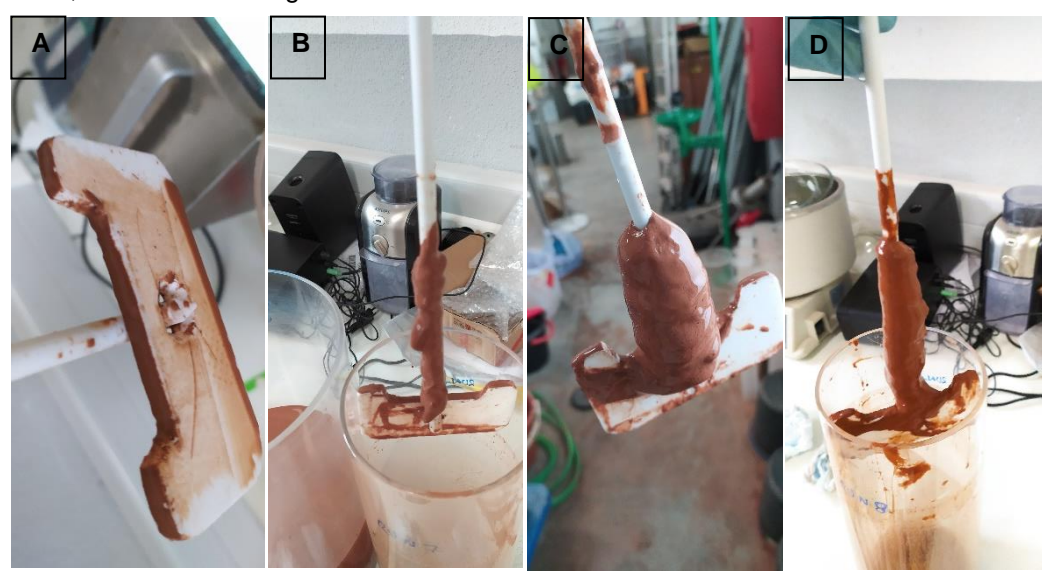


Figure 3.2 - Deposits on the blades for 8 minutes mixing time and different concentrations of $Al_2(SO_4)_3$: (A) - mg/L, (B) - 50 mg/L, (C) - 200 mg/L, (D) - 600 mg/L.

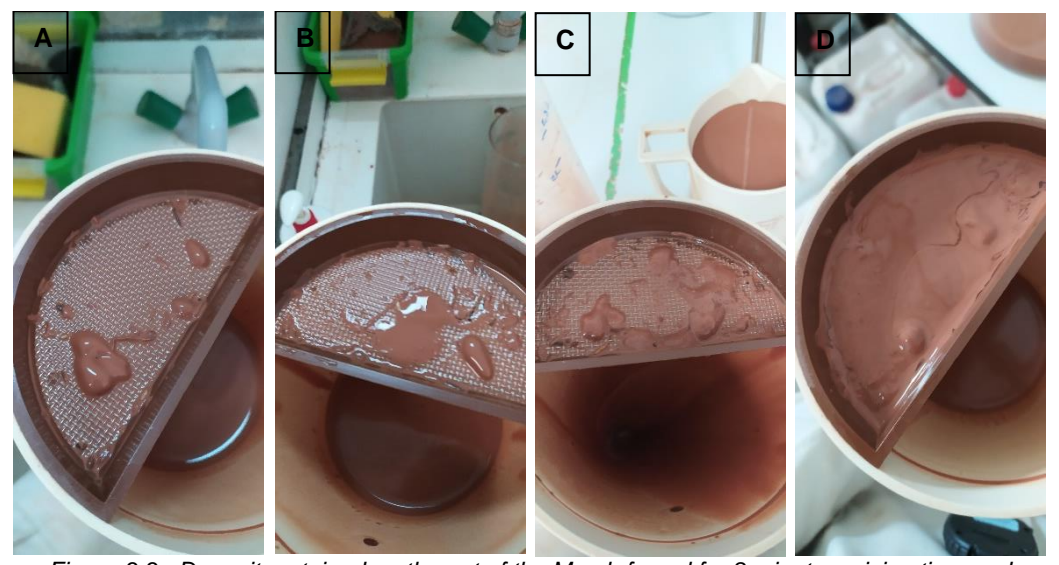


Figure 3.3 - Deposits retained on the net of the Marsh funnel for 8 minutes mixing time and different concentrations of $Al_2(SO_4)$: (A) - 5 mg/L, (B) - 50 mg/L, C - 200 mg/L, D - 600 mg/L

Figure 3.2 and Figure 3.3 represent the accumulation of clay agglomerates in the Marsh funnel nets and on the paddle at the end of the runs performed with a mixing time of 8 minutes. Clay accumulation increases as the coagulant concentration increases, as the destabilization of the suspensions is also enhanced. This way, the deposit at the bottom of the recipient may be

considered collectable for all coagulant concentrations although, it is visually more perceptible for 200 and 600 mg/L.

Table 3.2 – Initial densities, coagulant concentration, Marsh Viscosity gaps and final density of the runs performed at 16 minutes. ^{a)}Marsh gap is calculated from the difference between final and initial values. ^{b)}Final density gap is calculated from the difference between middle and bottom values.

Run	Zone	Concentration (mg/L)	Initial density (g/cm³)	Marsh Gap (s/quart) ^{a)}	Final density gap (g/cm³) ^{b)}	
11	Middle	5	1.1018	-1	0.0035	
Bottom			1.1175	-1	0.0033	
12	Middle	50	1.1015	1	0.0006	
12	Bottom		1.1129	l	0.0006	
13	Middle	200	1.1176	2	0.0047	
Bottom			1.1353	-2	0.0047	
1.4	Middle	600	1.1113	16	0.0005	
14	Bottom		1.1277	16	0.0005	

Table 3.2 represents the initial densities, Marsh viscosity gap and density gradient between middle and bottom for the selected runs performed for 16 minutes of mixing time at different concentrations of the coagulant (Al₂(SO₄)₃).

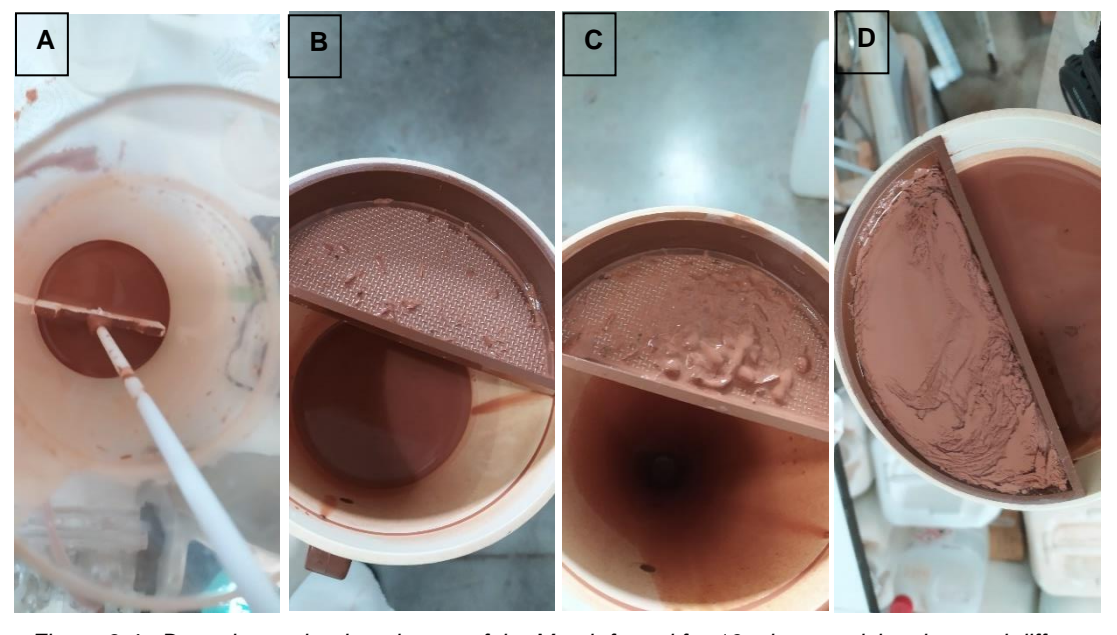


Figure 3.4 - Deposits retained on the net of the Marsh funnel for 16 minutes mixing time and different concentrations of $Al_2(SO_4)$: (A) – 5 mg/L, (B) – 50 mg/L, C – 200 mg/L, D – 600 mg/L

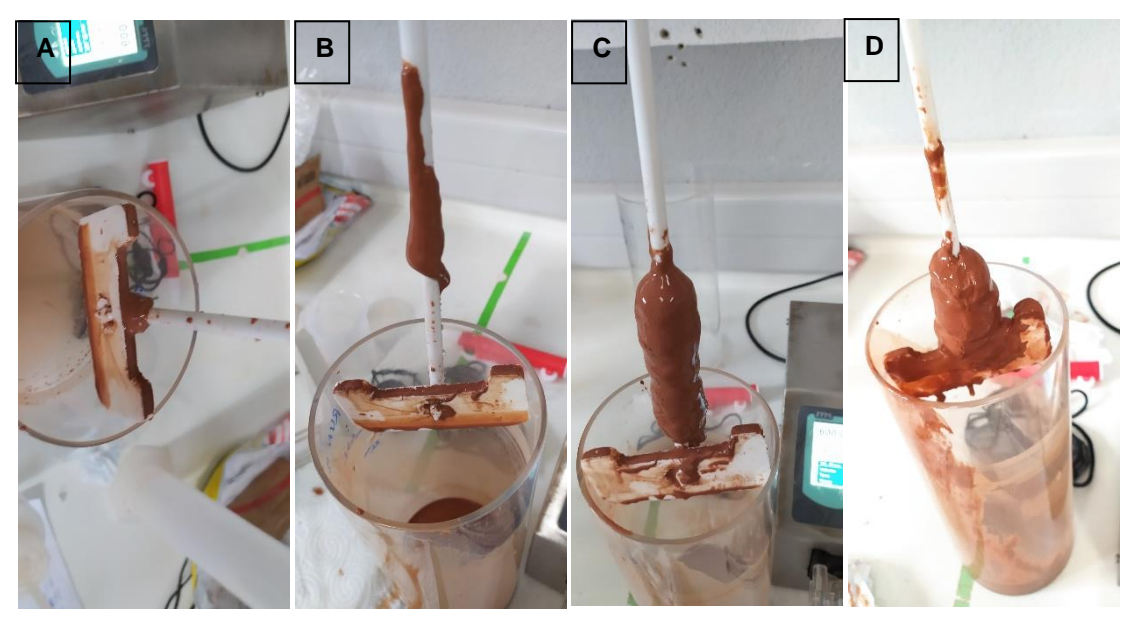


Figure 3.5 - Deposits on the blades for 16 minutes mixing time and different concentrations of $Al_2(SO_4)_3$. (A) - 5 mg/L, (B) - 50 mg/L, C- 200 mg/L, D- 600 mg/L

For the runs with a mixing time of 16 minutes, Marsh viscosity gap was lower than 5 s/quart and the final density gap between the bottom and middle of the column lower than 0.03g/cm³ for the four runs presented, meaning that the objectives related to these two points were accomplished.

Figure 3.4 and Figure 3.5 represent the accumulation of clay agglomerates in the Marsh funnel nets for the mixing time of 16 minutes. Similarly, to the runs performed with a mixing time of 8 minutes, the deposit at the bottom of the recipient may be considered collectable for all concentrations although it is visually more perceptible for 200 and 600 mg/L.

Table 3.3 – Initial densities, coagulant concentration, Marsh Viscosity gaps and final density of the runs performed at 24 minutes. ^{a)}Marsh gap is calculated from the difference between final and initial values. ^{b)}Final density gap is calculated from the difference between middle and bottom values.

Run	Zone	Concentration (mg/L)	Initial density (g/cm³)	Marsh Gap (s/quart) ^{a)}	Final density gap (g/cm³)b)
15	Middle	5	1.1095	0	0.0040
Bottom		5	1.1373	U	0.0048
16	Middle	50	1.1130	-10	0.0095
10	Bottom	50	1.1286		
17	Middle	200	1.1068	3	0.0019
17	Bottom	200	1.1202	3	0.0018
18	Middle	600	1.1182		0.0089
10	Bottom	600	1.1301	2	

Table 3.3 represents the initial densities, Marsh viscosity gap and density gradient between middle and bottom for the selected runs performed for 24 minutes of mixing time at different concentrations of the coagulant (Al₂(SO₄)₃).

For a mixing time of 24 minutes, Marsh viscosity gap is lower than 5 s/quart for all the runs with the exception of the run performed using 50 mg/L of Al₂(SO₄)₃ and the final density gap between the bottom and middle of the column is lower than 0.03 g/cm³ for the four runs presented, meaning that the objectives related to these two points were accomplished, with the one exception mentioned.



Figure 3.6 - Deposits retained on the net of the Marsh funnel for 24 minutes mixing time and different concentrations of $Al_2(SO_4)$: (A) - 5 mg/L, (B) - 50 mg/L, C - 200 mg/L, D - 600 mg/L

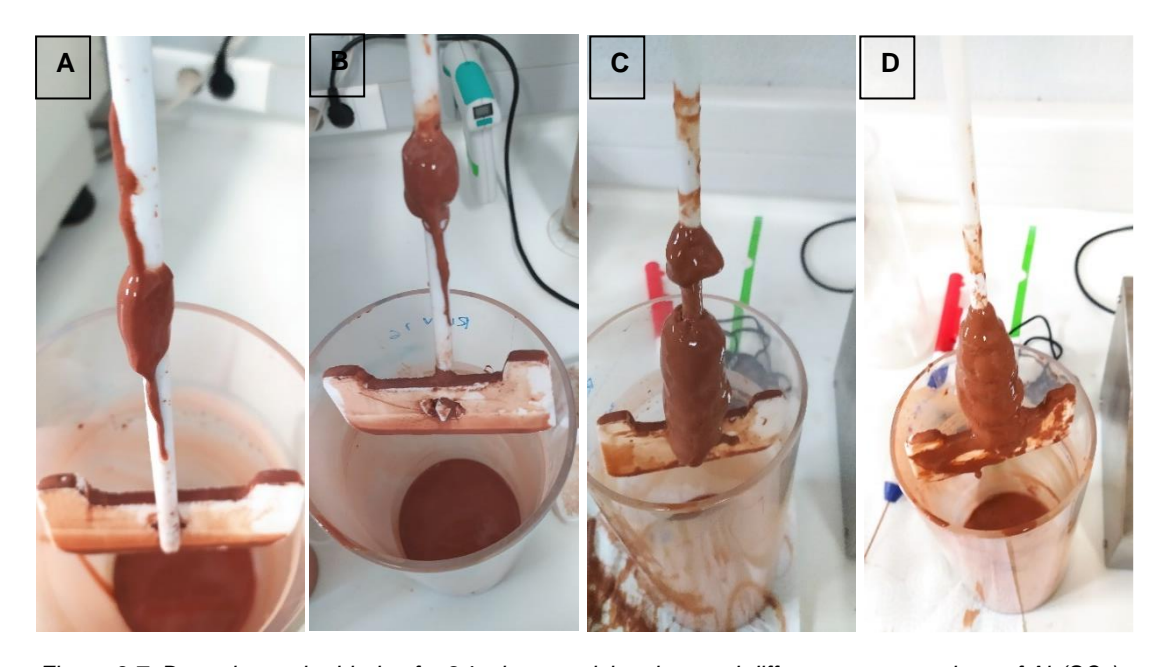


Figure 3.7 Deposits on the blades for 24 minutes mixing time and different concentrations of $Al_2(SO_4)_3$. (A) - 5 mg/L, (B) - 50 mg/L, (B) - 600 mg/L

Figure 3.6 and Figure 3.7 represent the accumulation of clay agglomerates in the Marsh funnel nets and paddle at the end of the runs performed with a mixing time of 24 minutes. Similarly, to the previous mixing times, the deposit at the bottom of the recipient may be considered collectable for all concentrations although it is visually more perceptible 200 and 600 mg/L.

Since the variation of mixing time had very little influence on DR and, for the coagulant concentration of 600 mg/L, where the highest DRs of 0.0069 g/cm³ and 0.0259 g/cm³ were observed, increasing mixing times did not decrease DR. Maintaining the mixing time at 8 minutes is the optimal condition as further studies are made. A study was then performed to further increase the coagulant concentration.

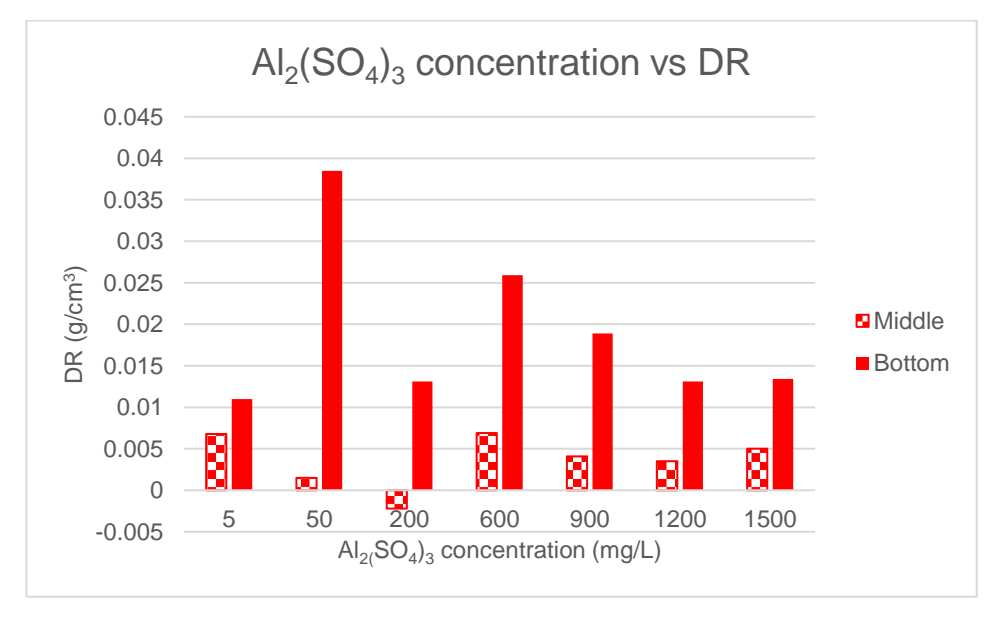


Figure 3.8 - Effect of the coagulant concentration on DR, for 8 minutes of mixing time

Figure 3.8 represents DR in function of the Al₂(SO₄)₃ for the concentration of 5, 50, 200, 600, 900, 1200, and 1500 mg/L. Fixed variables are mixing time (8 minutes), mixing speed (200 rpm), clay type (clay A from Terracota do Algarve) and polymer type (PolyMud).

For both middle and bottom samples, there is an increase of DR as the coagulant concentration increases, reaching a maximum value of $0.026g/cm^3$ for the bottom with 600 mg/L of $(Al_2(SO_4)_3)$. When coagulant concentration exceeds this value, DR decreases, reaching to values near 0.015 g/cm^3 for both 1200 and 1500 mg/L of coagulant. As previously mentioned, the bottom sample for 50 mg/L was considered an outlier, possibly due to incorrect use of the densimeter, and this way it was not considered comparable. This way, the optimal $Al_2(SO_4)_3$ concentration, for the conditions described above was found to be 600 mg/L,

This trend is in accordance with the work of most authors, as there is a consensus that the optimal coagulant concentration for each coagulation process depending on the conditions applied and the type of coagulant [142] [182].

For coagulant concentrations lower than the optimum concentration, the suspension will not destabilize enough to cause a noticeable impact, because the electrical double layer is not

compressed enough to allow the agglomeration of the clay particles. Otherwise, for coagulant concentrations higher than the optimum one, a charge reversal effect is verified. The electrical double layer is predominantly positively charged due to the excess of coagulant, which will cause the repulsion of the clay particles and the restabilization of the suspension, reflected by lower density decreases [183].

Table 3.4 – Initial densities, Marsh Viscosity gaps and final density of the runs performed at 8 minutes for the concentrations of 900, 1200 and 1500 mg/L. ^{a)}Marsh viscosity gap is calculated from the difference between final and initial values. ^{b)}Final density gap is calculated from the difference between middle and bottom density values after the coagulant effect. ^{c)}Impossible to measure, due to clogging of the Marsh funnel.

Run	Zone	Initial density (g/cm³)	Coagulant concentration (mg/L)	Marsh Gap (s/quart) ^{a)}	Final density gap between bottom and middle (g/cm³)b)	
51	Middle	1.1054	900	23	0.0004	
31	Bottom	1.1206	900	23	0.0004	
53	Middle	1.1057	4000		1200 52 0.001	0.0011
55	Bottom	1.1164	1200	52	0.0011	
55	Middle	1.1017	1500	I.M. ^{c)}	0.0015	
55	Bottom	1.1116	1300	1.101.9	0.0015	

Table 3.4 represents the initial densities, Marsh viscosity gap and density gradient between middle and bottom for the selected runs performed for 8 minutes of mixing time at different concentrations of the coagulant (Al₂(SO₄)₃).

As the coagulant concentration increased, the Marsh viscosity also increased due to the increase of floc distribution and size. When the concentration was set to 1500 mg/L, Marsh viscosity was impossible to measure due to the clogging of the Marsh funnel caused by an oversize of the flocs formed. Marsh viscosity does not decrease with concentrations of coagulant equal or above 900mg/L. The final density gap between the bottom and middle of the column is

lower than 0.03g/cm³ for the three runs presented, meaning that the objectives related to this point were accomplished.

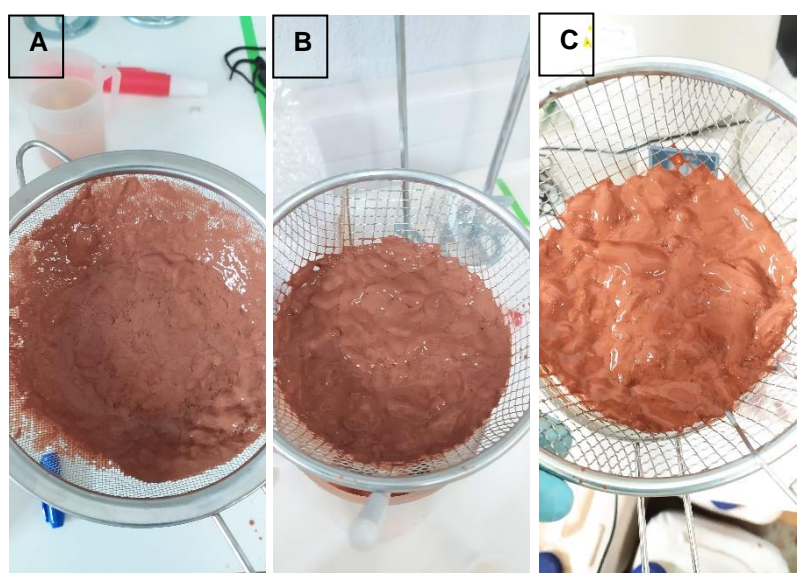


Figure 3.9 – Deposits retained in a sieve net for 8 minutes mixing time and different concentrations of $Al_2(SO_4)$: (A) – 900 mg/L, (B) – 1200 mg/L, C - 1500 mg/L

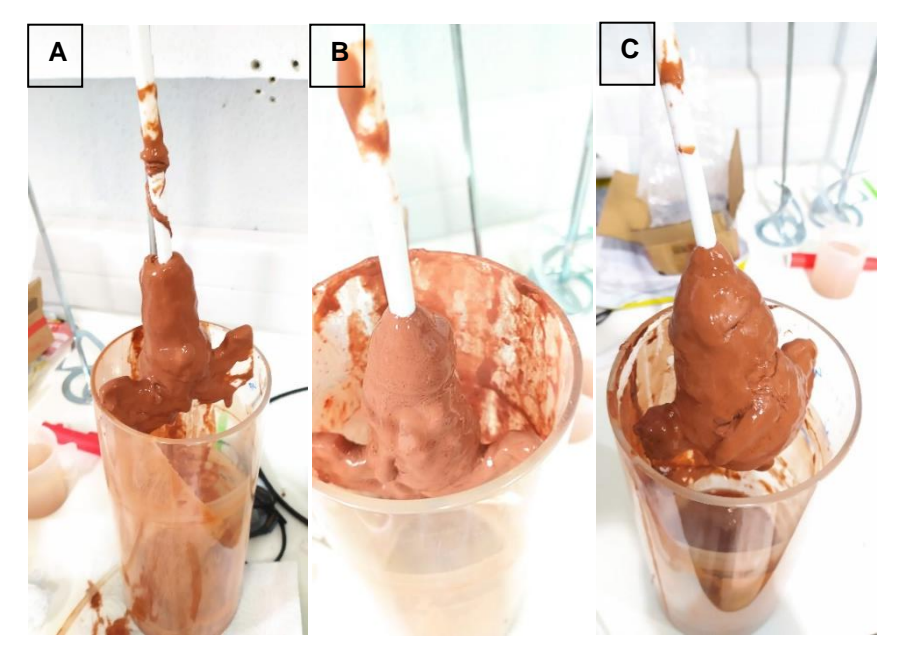


Figure 3.10 – Deposits on the blades for 8 minutes mixing time and different concentrations of $Al_2(SO_4)_3$. (A) – 900 mg/L, (B) – 1200 mg/L, C – 1500 mg/L

Figure 3.9 and Figure 3.10 represent the accumulation of clay agglomerates in sieve nets and paddle at the end of the runs performed with a mixing time of 8 minutes.

Clay accumulation increases with increasing coagulant concentration, as the destabilization of the suspensions is also enhanced. This way, the deposit at the bottom of the recipient may be considered collectable for all coagulant concentrations.

From the study of the mixing time, the major conclusion is that increasing the mixing time does not increase DR, contrarily it diminishes it mainly with 24 minutes of mixing time when compared to 8 and 16 minutes. Therefore, 8 minutes of mixing time will be maintained on further studies. With this mixing time, the DR objective of 0.02 g/cm³ was attained for the concentrations of 600 mg/L. It should be noted that for higher concentrations of coagulant - 200 mg/L and above, some leftover coagulant remained at the top of the solution, possibly reducing the coagulant's effectiveness. Therefore, the next studied variables will address the dispersion of the coagulant throughout the solution.

3.2 Influence of the coagulant dispersion on the density reduction

3.2.1 Study of the coagulant concentration and mixing speed

The purpose of this subsection is to study the influence of the coagulant concentration (5, 50, 200 and 600 mg/L) and mixing speed (200, 250, and 300 rpm) on DR (g/cm³), according to protocol 2.3.1. Fixed variables are mixing times (8 min), coagulant type (Al₂(SO₄)₃), clay type (clay A from Terracota do Algarve) and polymer type (PolyMud). Crossing these variables may lead to the optimal coagulant concentration and optimal mixing speed to attain the objectives proposed on **Error! Reference source not found.**

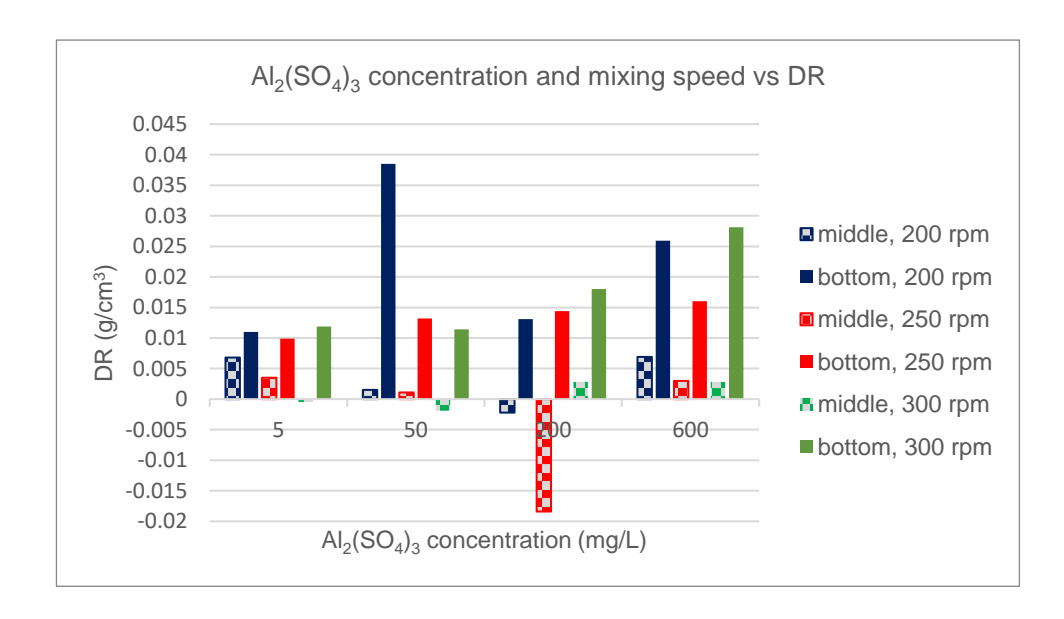


Figure 3.11 - Effect of Al₂(SO₄)₃ concentration and mixing speed on DR (8 minutes)

Figure 3.11 relates DR with the concentration of Al₂(SO₄)₃ and mixing speed.

It is possible to observe that DR in the middle samples is still very low compared to the bottom samples for all coagulant concentrations. For the middle zone, only the samples of the runs performed at 200 rpm (for the concentrations of 5 and 600 mg/L) surpass the value 0.005 g/cm³ for DR. In general, increasing the mixing speed to 250 rpm decreases DR for both middle and bottom samples. It should be noted that negative DR values represent density increases, such as the case of 50 mg/L at 24 minutes of mixing time and 200 mg/L at 8 and 16 minutes of mixing time. Meanwhile, for the bottom samples, when the mixing speed is increased from 250 to 300 rpm, DR decreases by less than 0.005 g/cm³ with the exception of 600 mg/L, where the decrease is of about 0.01 g/cm³ and for 200 mg/L, where there is a slight increase of DR lower than 0.005 g/cm³. For bottom samples, increasing the mixing speed to 300 rpm increases DR by less than 0.01 g/cm³ for all concentrations, except for 50 mg/L, where from 250 to 300 rpm, DR decreased. The first stage of DR of 0.02 g/cm³ is only achieved for the concentration of 600 mg/L at 200 and 300 rpm.

According to Ding et al., for magnesium hydroxide, increasing the mixing speed from 250 to 300 and 350 rpm reduced floc sizes but had little impact on the removal efficiency [153]. This goes in accordance with the experimental results, as smaller flocs tend to settle slower, therefore increasing local density in the middle while at the same time not contributing to an increase of DR in the bottom.

Table 3.5 - Initial densities, coagulant concentration, Marsh Viscosity gaps and final density of the runs performed at 250 rpm. ^{a)}Marsh viscosity gap is calculated from the difference between final and initial values. ^{b)}Final density gap is calculated from the difference between middle and bottom density values after the coagulant effect.

Run	Zone	Initial density (g/cm³)	Concentration (mg/L)	Marsh Gap (s/quart) ^{a)}	Final density gap (g/cm³) ^{b)}	
19	Middle	1.1069	5	-7	0.0015	
19	Bottom	1.1148	5	-1	0.0015	
20	Middle	1.0995	50	-3	0.0006	
20	Bottom	1.1110	50		0.0006	
21	Middle	1.0910	200	27	0.0007	
21	Bottom	1.1245	200	21	0.0007	
22	Middle	1.0987	600	56	0.0008	
22	Bottom	1.1109	000	50		

Table 3.5 represents the initial densities, Marsh viscosity gap and density gradient between middle and bottom for the selected runs performed at 250 rpm at different concentrations of the coagulant (Al₂(SO₄)₃)., to the remaining objectives defined. For a mixing speed of 250 rpm,

Marsh viscosity has a maximum decrease of 7s/quart for a coagulant concentration of 5 mg/L, two seconds higher than the objective defined of a maximum of 5s/quart. All remaining runs presented lower Marsh viscosity decreases or even exhibit final viscosities higher than the initial due to the flocs that passed through the net and caused an increase of this variable. The final density gap always lower than 0.03 g/cm³, meaning that the objectives related to these two points were accomplished, except for the gap on the Marsh viscosity for the concentration of 5 mg/L of coagulant, where the gap was 7 s/quart instead of the 5 s/quart.

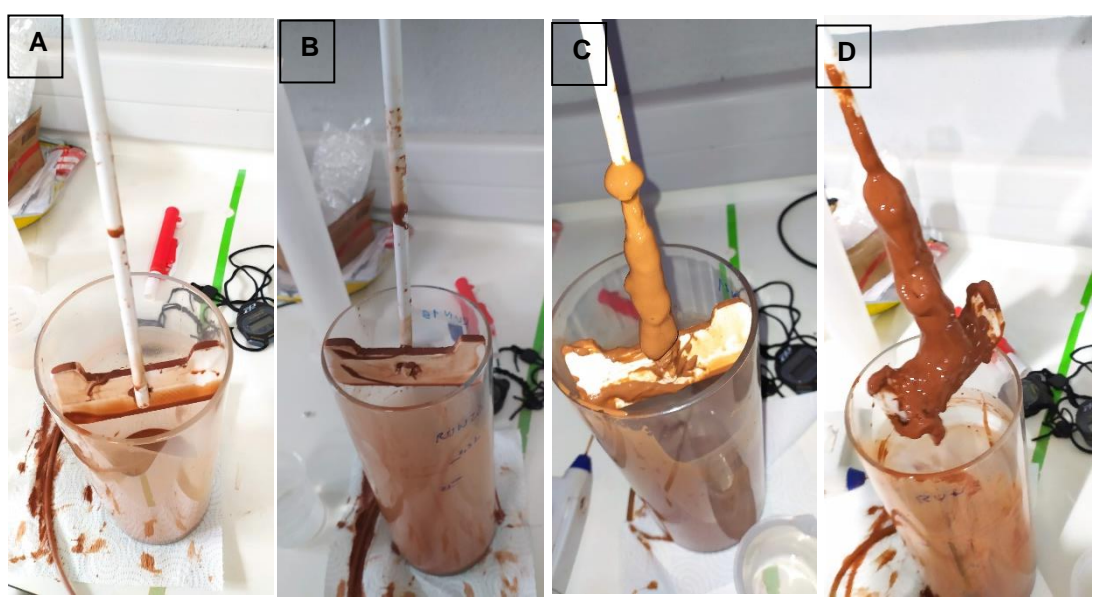


Figure 3.12 - Deposits on the blades for 250 rpm and different concentrations of $Al_2(SO_4)_3$. (A) – 5 mg/L, (B) – 50 mg/L, C – 200 mg/L, D – 600 mg/L

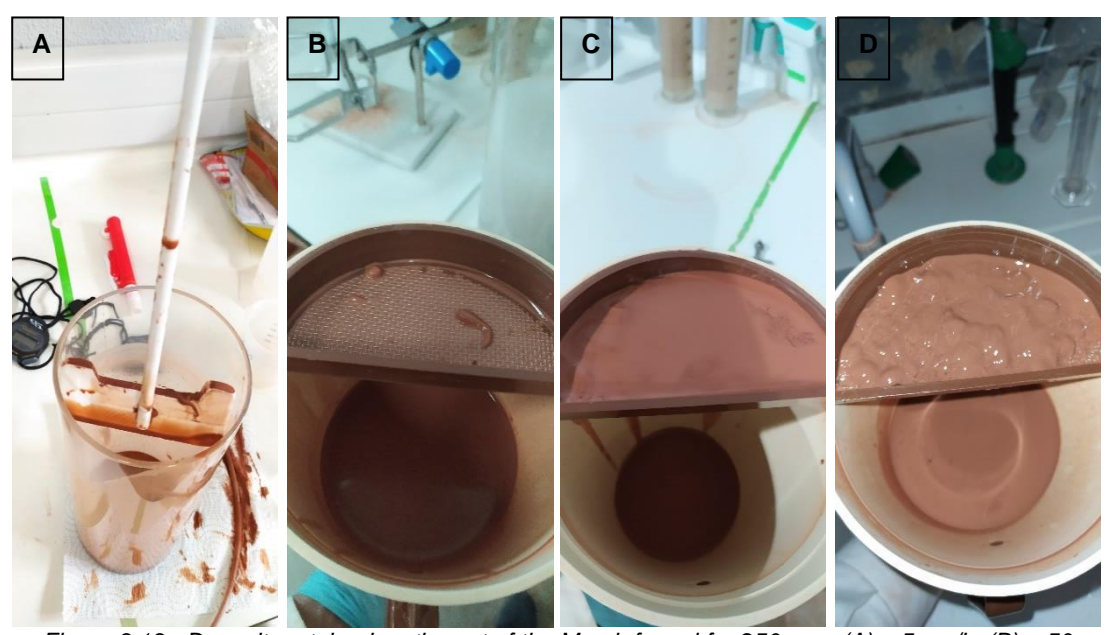


Figure 3.13 - Deposits retained on the net of the Marsh funnel for 250 rpm. (A) - 5 mg/L, (B) - 50 mg/L, C - 200 mg/L, D - 600 mg/L

Figure 3.12 and Figure 3.13 represent the accumulation of clay agglomerates in the Marsh funnel net and paddle at the end of the runs performed with a mixing rotation of 250 rpm.

The deposit at the bottom of the recipient may be considered collectable for all coagulant concentrations although it is visually more perceptible 200 and 600 mg/L.

Table 3.6 - Initial densities, coagulant concentration, Marsh Viscosity gaps and final density of the runs performed at 300 rpm. ^{a)}Marsh viscosity gap is calculated from the difference between final and initial values. ^{b)}Final density gap is calculated from the difference between middle and bottom density values after the coagulant effect. ^{c)}Impossible to measure, due to clogging of the Marsh funnel.

Run	Zone	Initial density (g/cm³)	Coagulant concentration (mg/L)	Marsh gap (s/quart) ^{a)}	Final density gap (g/cm³) ^{b)}
23	Middle	1.1101	5	10	0.0059
23	Bottom	1.1283	5	-12	0.0058
24	Middle	1.0964	50	-14	0.0033
24	Bottom	1.1130	50		
25	Middle	1.1032	200	11	0.0046
25	Bottom	1.1200	200	11	0.0016
26	Middle	1.1097	600	I.M.c)	0.0011
20	Bottom	1.1361	600	1.101.9	0.0011

Table 3.7 represents the initial densities, Marsh viscosity gap and density gradient between middle and bottom for the selected runs performed for 250 rpm at different concentrations of the coagulant (Al₂(SO₄)₃), to the remaining objectives defined.

For these runs, the objective concerning the final density gap lower than 0.03 g/cm³ was achieved, although Marsh viscosity gap was only accomplished for the run performed with 200 mg/L of coagulant.

For the coagulant concentrations of 5 and 50 mg/L, Marsh viscosities suffered a decrease higher than 5 s/quart, failing the Marsh viscosity objective. As previously mentioned, increasing the mixing speed reduces the floc sizes. There is the possibility that the high mixing speed of 300 rpm for long periods that can cause structural damage to the long polymer chains which is reflected in a decreasing of Marsh viscosity. For 600 mg/L, the numerous small flocs clogged the Marsh cone, and the measurement of this objective was impossible. In conclusion, only the concentration of 200 mg/L accomplished all objectives for these conditions.



Figure 3.15 - Deposits retained on the net of the Marsh funnel for 300 rpm. (A) - 5 mg/L, (B) - 50 mg/L, C- 200 mg/L, D- 600 mg/L

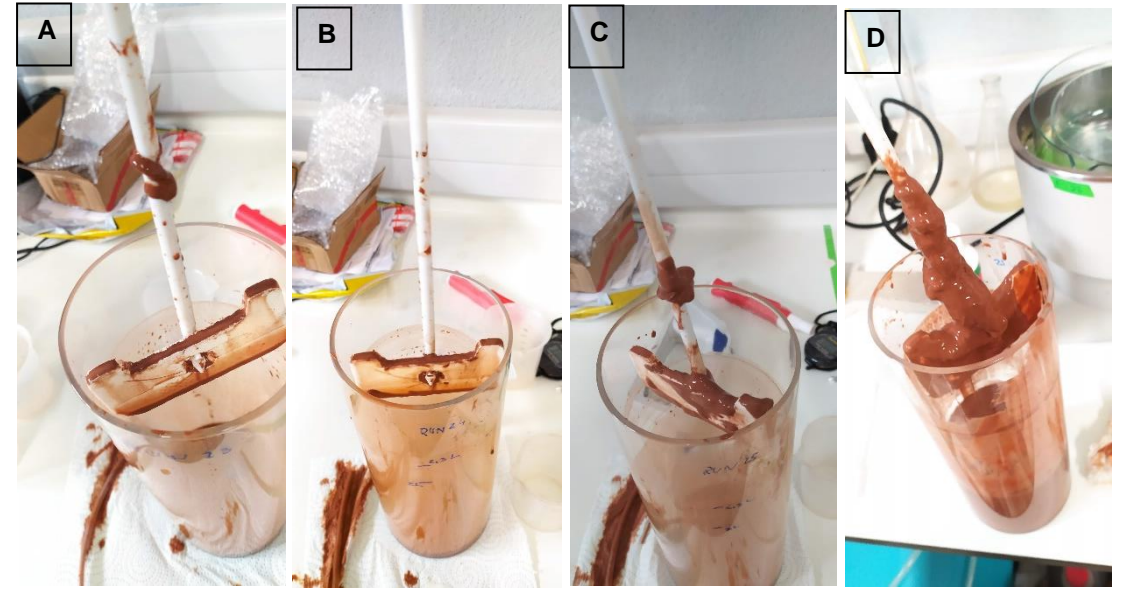


Figure 3.14 - Deposits on the blades for 300 rpm and different concentrations of $Al_2(SO_4)_3$. (A) – 5 mg/L, (B) – 50 mg/L, C – 200 mg/L, D – 600 mg/L

Figure 3.14 and Figure 3.15 represent the accumulation of clay agglomerates in the Marsh funnel net and paddle at the end of the runs performed with the mixing speed of 300 rpm.

When comparing the deposits of the runs performed at 250 with the ones performed at 300 rpm (Figure 3.12 and Figure 3.14), it can be seen that the flocs get smaller with the increase of the mixing speed due to the reduction of the size of the flocs, a behavior also verified by Ding et al [153]. This is due to the shear caused by the increase of the mixing speed rupturing the flocs.

The deposit at the bottom of the recipient may be considered collectable for all coagulant concentrations although it is visually more perceptible 200 and 600 mg/L.

The aim of the study of mixing speed was to improve the dispersion of coagulant throughout the solution and to solve the unreacted coagulant issue. Although no unreacted coagulant was observed for 250 and 300 rpm, with higher mixing speeds formed flocs became smaller causing the clogging of the Marsh funnel net making the measurement of the Marsh viscosity impossible. In addition, there was not a significant improvement of DR by increasing mixing speed, and so the mixing speed of 200 rpm will be maintained. On the next chapter it will be explored coagulant dispersion alternatives through the variation of the agitator type.

3.2.2 Study of agitator type

The purpose of this subsection is to study the uniformity of the agitation on DR (g/cm³) by studying 8 different agitators ("P1" to "P8", Figure 2.3), using red colorant. This subsection should give information whether if the remaining unreacted coagulant on previous runs is due to the inefficient agitation or if another agitator is required. Fixed variables are agitation speed (200 rpm) and polymer type (PolyMud). For the purpose of clarity of the colorant path through the solution, no additives or clay were used.

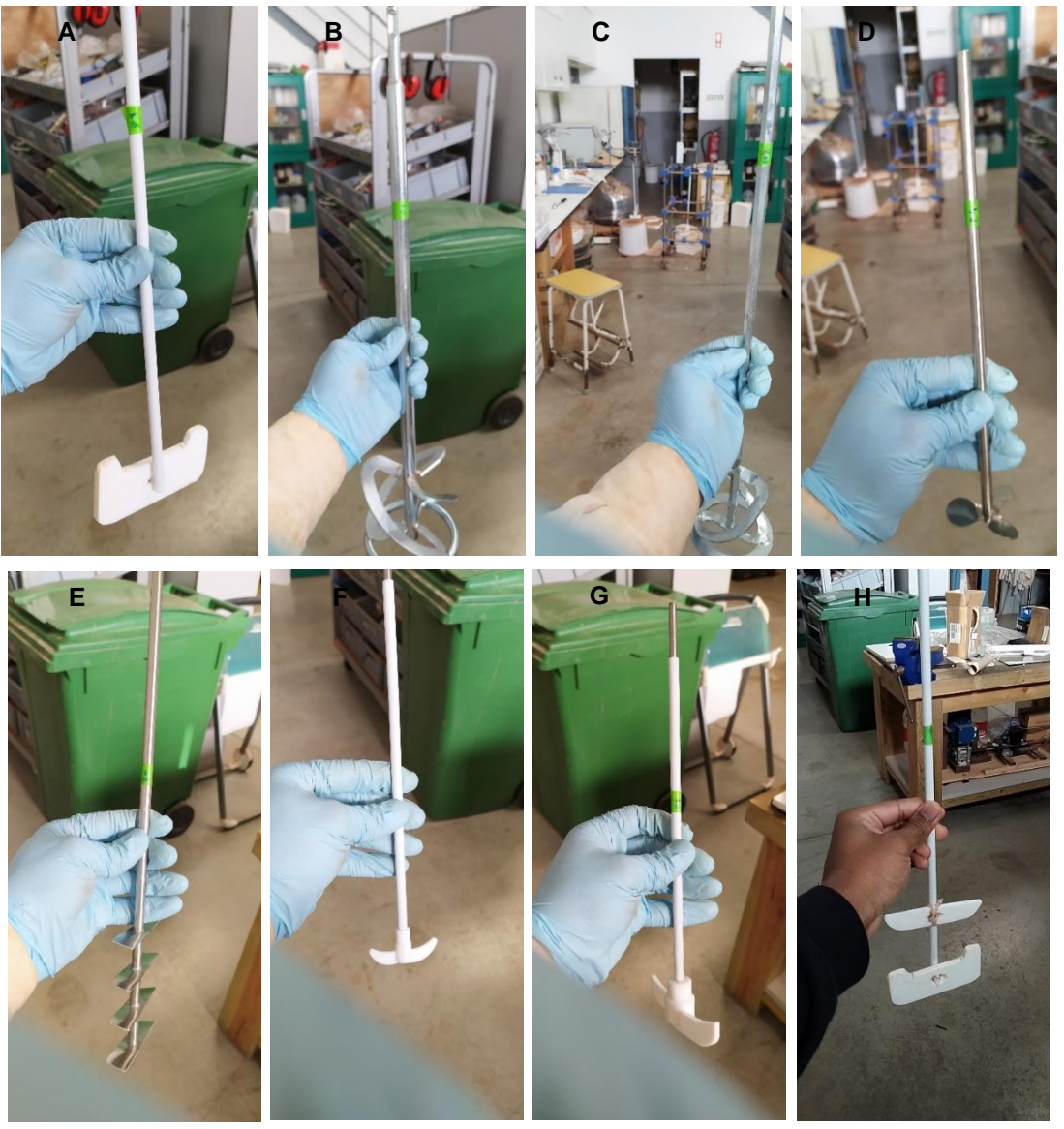


Figure 3.16 - (A) - Agitator "P1"; (B) - Agitator "P2"; (C) - Agitator "P3"; (D) - Agitator "P4"; (E) - Agitator "P5"; (F) – Agitator "P6"; (G) – Agitator "P7"; (H) – Agitator "P8".

As detailed on protocol 2.3.2, 8 agitators of different shapes were chosen to evaluate the behavior and uniformity of the colorant diffusion on the polymeric solution. Red colorant was slowly introduced at the top of the recipient and the process of colorant diffusion was recorded. Table 3.7 represents the time taken by each agitator to spread the colorant uniformly through the solution. Uniformization time represents the time it took for the solution to appear uniformly red, starting from the moment the first drop of colorant is introduced.

Table 3.7 - Time required for colorant uniformization with the different paddles tested.

Runs	Agitator	Uniformization time (s)
31	P1	20
32	P2	25
33	P3	30
34	P4	>90
35	P5	>90
36	P6	>90
37	P7	25
38	P8	25

The run performed with agitator "P1", the agitator used in previous studies, was the fastest at achieving uniformity (20seconds), while "P4", "P5", and "P6"" were the slowest, taking more than 90 seconds.

Agitator "P1" generated one of the strongest vortices, when compared to the remaining paddles, which may be the reason it was faster than the other agitators.

After the visual test, the influence of the agitation levels on DR was studied. For this study, clay and additive GPlus were used. Fixed variables are mixing time (8 min), $Al_2(SO_4)_3$ concentration (600 mg/L), clay type (clay A from Terracota do Algarve) and polymer type (PolyMud). This study should give information about the applicability of the colorant experiment. As detailed on protocol 2.3.2, the original agitator, "P1", was compared to its two-level modification, "P8" at 200 and 300 rpm.

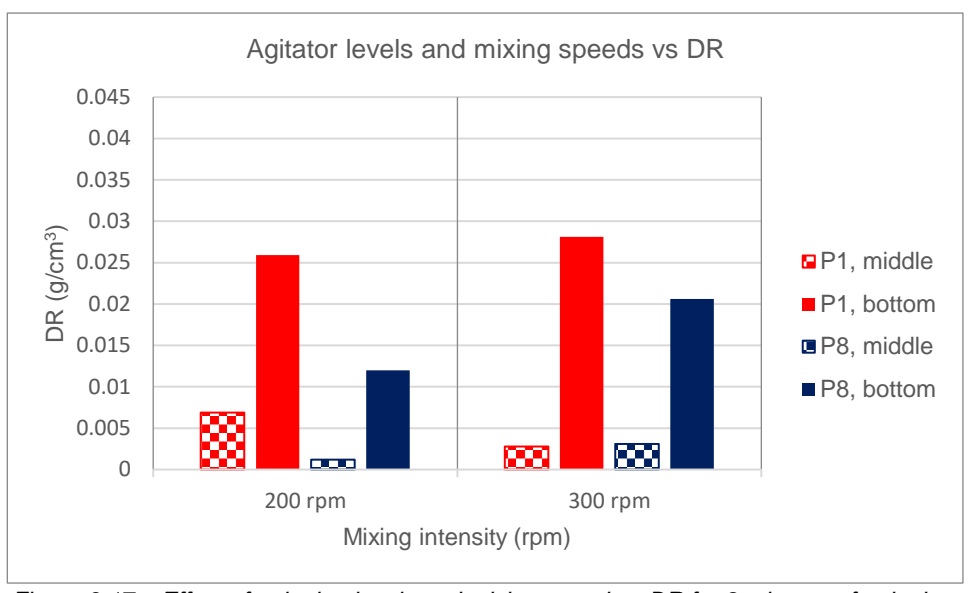


Figure 3.17 – Effect of agitation levels and mixing speed on DR for 8 minutes of agitation.

Figure 3.17 relates DR with the mixing speed and type of paddles. Generally, it is possible to observe that the runs performed with the single-level agitator provide a higher DR, for both middle and bottom samples. This goes in accordance with the visual results seen with red colorant, as agitator "P1" was the fastest agitator. The lowest DR for the runs performed with the two-level agitator may be due to the hindrance caused by the first level, causing the coagulant to react quickly with the clay in its vicinity.

Adding another level may have created another zone of accumulation – one at the middle and another at the bottom of the column, compared to only one zone for "P1". While the coagulant reacted heavily with the clay around the first level it did not react significantly with the clay further apart from the center, causing a reduction in the DR in the middle and a more significant reduction in the bottom, as less coagulant was available to react further down the recipient. A similar case occurred with the agitator "P5", a four-level agitator. In this case, the colorant, in 90 seconds, had mixed very thoroughly in the middle zone but had difficulty accessing the bottom of the column.

Table 3.8 - Initial densities, coagulant concentration, Marsh Viscosity gaps and final density of the runs performed using a single level agitator (8 and 26) and a two level agitator (39 and 40). ^{a)}Marsh viscosity gap is calculated from the difference between final and initial values. ^{b)}Final density gap is calculated from the difference between middle and bottom density values after the coagulant effect. ^{c)}Impossible to measure, due to clogging of the Marsh funnel.

Run	Agitator	Mixing speed (rpm)	Zone	Initial density (g/cm³)	Marsh Gap (s/quart) ^{a)}	Final density gap (g/cm³) ^{b)}
8		200	Middle	1.0974	6	0.0067
0	P1	200	Bottom	1.1231	0	
26		300	Middle	1.1097	I.M. ^{c)}	0.0011
20			Bottom	1.1361		
20		200	Middle	1.1052	27	0.0002
39	Do	200	Bottom	1.1162		
40	го	P8		1.1013	20	0.004
40		300	Bottom	1.1178	- 28	0.001

Table 3.8 represents the initial densities, Marsh viscosity gap and density gradient between middle and bottom for the selected runs performed for single level and two-level agitators at a fixed concentration of 600 mg/L of the coagulant (Al₂(SO₄)₃).,

For these runs, the objective concerning the final density gap lower than 0.03g/cm³ was achieved. As for the Marsh viscosity objective, it was accomplished for both speeds for the two-level agitator (P8) but it was not measurable for run performed at 300 rpm for the single level agitator. The increase of the Marsh viscosity, on runs 39 and 40, is due to the presence of the flocs in suspensions when the concentration of 600 mg/L of Al₂(SO₄)₃ is applied. The impossibility of measuring this value for the single-level agitator (run 26) may be due to a more uniform agitation that, as a consequence, translates to the formation of more and larger flocs that plug the Marsh funnel.



Figure 3.18 - Deposits retained on the net of the Marsh funnel for: (A) - single level agitator, 200 rpm; (B) - single level agitator, 300 rpm; (C) - two level agitator, 200 rpm; (D) – two level agitator, 300 rpm at 600 mg/L

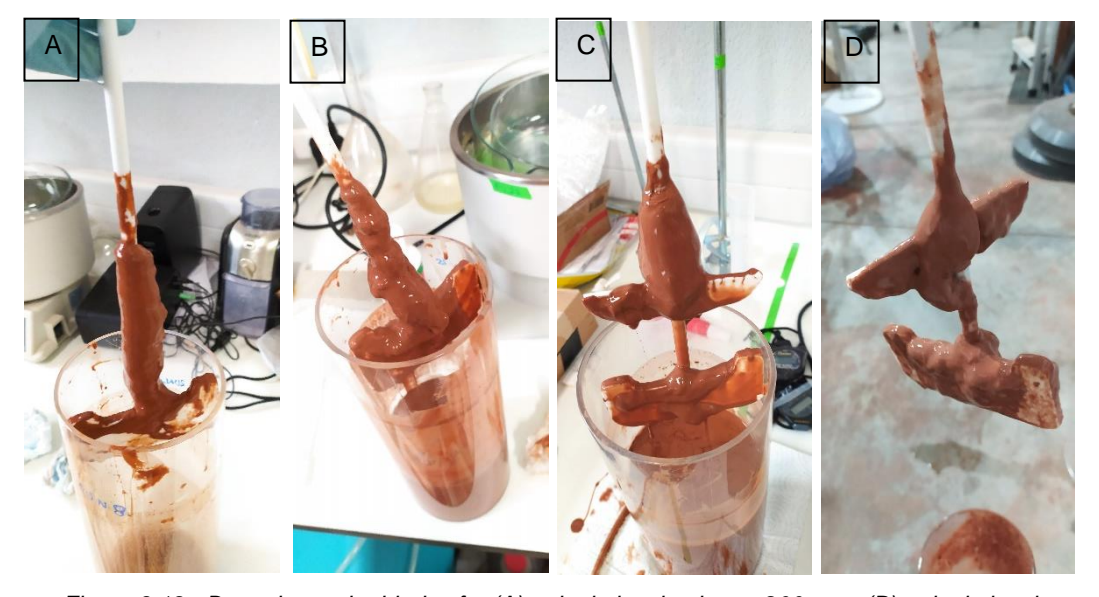


Figure 3.19 - Deposits on the blades for (A) - single level agitator, 200 rpm; (B) - single level agitator, 300 rpm; (C) - two level agitator, 200 rpm; (D) – two level agitator, 300 rpm at 600 mg/L

Figure 3.18 and Figure 3.19 represent the accumulation of clay agglomerates on the Marsh funnel nets. As the concentration was kept as 600 mg/L, no noticeable difference was observed between the deposits, as floc size did not vary amongst the experiences.

In conclusion, the use of a two level agitator (P8) did not solve the issue of the lower DR in the middle zone, when compared to the bottom zone and had a lower DR than the single level agitator. In this manner, alternative methods will be studied to prevent the problem of the unreacted coagulant, while maintaining or increasing DR.

3.2.3 Study of coagulant introduction method

The purpose of this subsection is to study the influence of the coagulant introduction method (external and internal) accordingly to protocol 2.3.1. Fixed variables are coagulant type (Al₂(SO₄)₃), mixing time (8 min), mixing speed (200 rpm), clay type (clay A from Terracota do Algarve) and polymer type (PolyMud). Studying this variable may lead to the optimal introduction method to improve the coagulant dispersion in the solution.

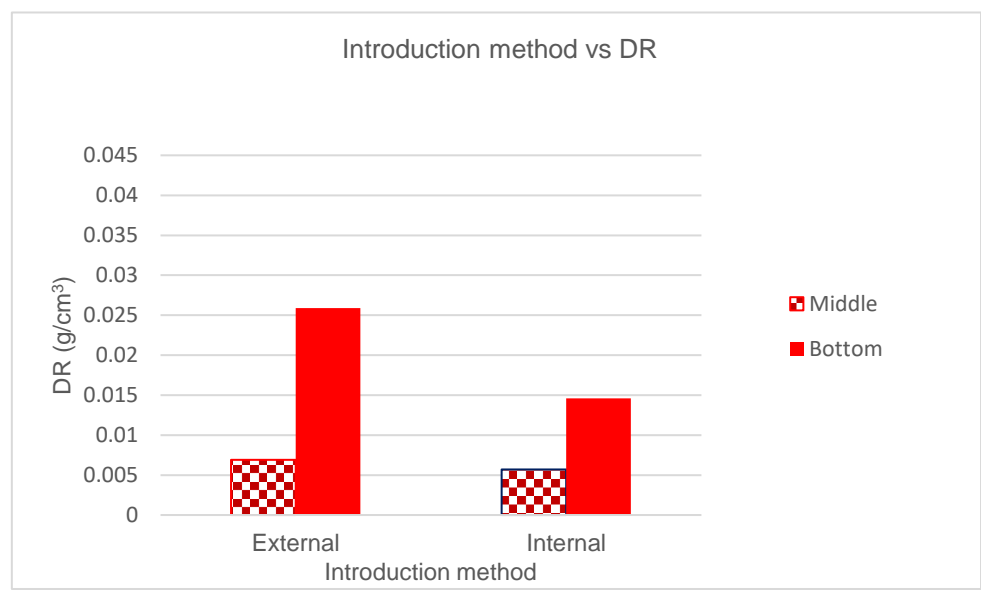


Figure 3.20 - Effect of the coagulant introduction method on DR

Figure 3.20 shows DR when introducing the coagulant externally, at the top of the column, and introducing internally with the assistance of a peristaltic pump.

The runs using external introduction yielded the highest DR than the ones using internal introduction method with a difference of slightly over 0.001 g/cm³ for the middle samples, which represents a difference of 17% and 0.011 g/cm³ for the bottom zone, which represents a difference of 43%.

The external introduction method is generally more accurate, as the peristaltic pump may have had an associated error due to the coagulant that may have not been cleared out from the tube when attempting to avoid air inside the solution.

Table 3.9 - Initial densities, coagulant concentration, Marsh Viscosity gaps and final density of the runs performed with external introduction and internal introduction. ^{a)}Marsh gap is calculated from the difference between final and initial values. ^{b)}Final density gap is calculated from the difference between middle and bottom values.

Run	Introduction type	Zone	Initial density (g/cm³)	Marsh Gap (s/quart) ^{a)}	Final density gap (g/cm³)b)	
0	External	Middle	1.0974	6	0.0007	
0	8 External	Bottom	1.1231	0	0.0067	
5 4	latera el	Middle	1.1011	47	0.0000	
54	Internal	Bottom	1.1103	17	0.0003	

Table 3.9 represents the initial densities, Marsh viscosity gap and density gradient between middle and bottom for the selected runs performed with external and internal introduction of coagulant at a fixed concentration of 600 mg/L of the coagulant (Al₂(SO₄)₃), to the remaining objectives defined on **Error! Reference source not found.**

For both introduction types, the Marsh viscosity gap had an increase of 6 and 17 s/quart and the final density gap was lower than 0.03 g/cm³, which are in line with the objectives.



Figure 3.21 - Deposits retained on the net of the Marsh funnel and in the sieve for: (A) - external introduction; (B) - internal introduction

Figure 3.21 represents the accumulation of clay agglomerates on the Marsh funnel nets. As the concentration was kept as 600 mg/L, no noticeable difference was observed between the deposits, as this is the most important factor contributing to the floc size and this did not vary amongst the experiences.

Thus, the external introduction method will be maintained since DR was higher for this experiment and does not require additional equipment.

From this study, no further improvement on the dispersion of the coagulant throughout the solution was possible. The optimal conditions remain 600 mg/L of Al₂(SO₄)₃, for 8 minutes of mixing time and 200 rpm of speed, using the "P1" agitator, with an external introduction of the coagulant. Therefore, for the next chapter, other coagulants will be tested to increase DR and the initial density of the solutions will be increased to be in line with this objective.

3.3 Influence of the increase of the solution's initial density and coagulant types on density reduction

In previous chapters, the initial densities were not fulfilling the objective proposed on **Error! Reference source not found.**, as they were lower than 1.14 g/cm³. For the following runs, the clay amount was increased from 750g (equivalent to 250 g/L) to 900g (equivalent to 300 g/L) to have initial densities within 1.14-1.16 g/cm³.

3.3.1 Study of the solution's initial density and coagulant types

The purpose of this subsection is to study the influence of increasing the solution's initial density and the coagulant type (Al₂(SO₄)₃, FeSO₄, Polyferric sulfate (PFS), and (NH₄)₂SO₄) on DR (g/cm³), according to protocol2.3.1. Fixed variables are mixing times (8 min), mixing speed (250 rpm), clay type (clay A from Terracota do Algarve) and polymer type (PolyMud). Crossing these variables may lead to the optimal coagulant type to attain the objectives proposed on **Error! Reference source not found.**

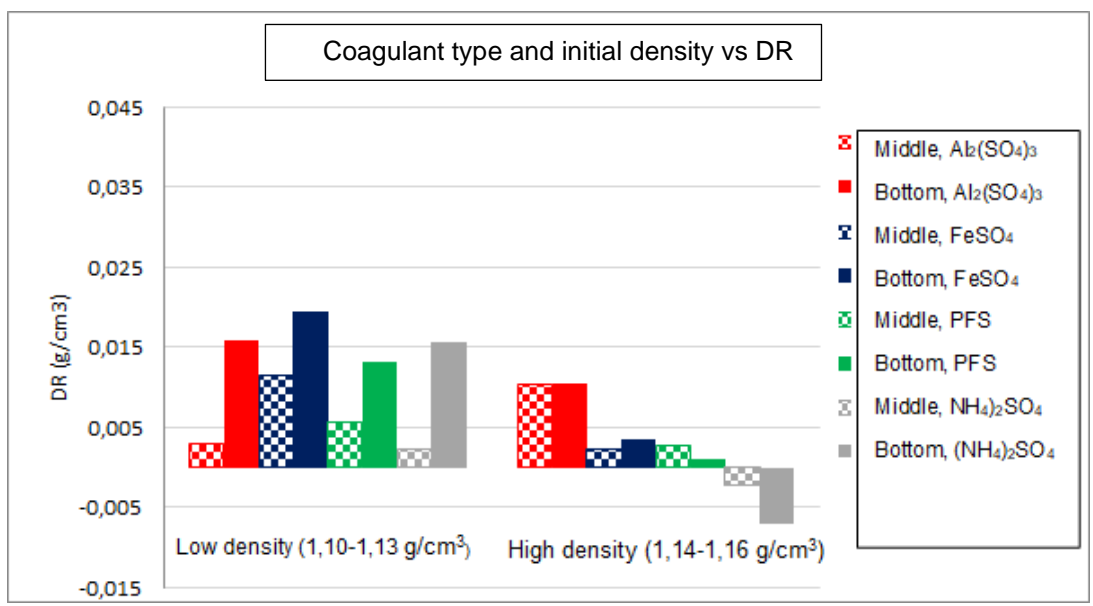


Figure 3.22 - Effect of coagulant type on DR at 8 min, 250 rpm at different initial densities.

Figure 3.22 represents DR obtained when using aluminum sulfate (Al₂(SO₄)₃), ferrous sulfate (FeSO₄), polyferric sulfate (PFS) and ammonium sulfate ((NH₄)₂SO₄) at initial densities between 1.10-1.13 g/cm³ (low density) and initial densities between 1.14-1.16 g/cm³ (high density).

For the runs performed with lower initial densities (1.10-1.13 g/cm³), it is possible to analyze that while all coagulants perform very close to each other at the bottom (DRs between 0.015 and 0.02g/cm³), the variation is more significant for the middle samples (0.01 g/cm³ gap between the highest (FeSO₄) and lowest value (NH₄)₂SO₄)). In this manner, the FeSO₄ run shows the highest DR at both middle and bottom of the column.

For the runs performed with higher initial densities (1.14-1.16g/cm³), Al₂(SO₄)₃ was the highest performing coagulant, with a DR of 0.01 g/cm³, while the other coagulants produced a DR below 0.005 g/cm³.

As far as DR per coagulant type, higher valency coagulants are typically more effective than the lower valency ones [92] [184]. However, solubility of each coagulant is also different and dependent on pH, as coagulants are more effective when the solubility of their hydrolyzed products is at the lowest point. Iron coagulants are less soluble than aluminum coagulants at pH greater than 5 [87]. In this manner, the results do not go in accordance with the literature and the expected order for DR, according to the coagulant valency would be PFS > $Al_2(SO_4)_3 > FeSO_4 > (NH_4)_2SO_4$. However, for all experiments, initial pH is between 10-11 and iron coagulants are less soluble at higher pH than aluminum coagulants compromising its performance. Nonetheless, it would be expected for the PFS runs to produce a higher DR than the FeSO₄ runs since the former has a higher valency than the latter. A possibility of the lower

DR for PFS runs compared to FeSO₄ may be the difficulty of the former to approach the clay particles, knowing that these are suspended by a high molecular weight anionic polymer. FeSO₄, a smaller molecule may not experience such diffusional constraints.

DR was higher for the low initial density experiments (1.10-1.13 g/cm³) than for the high initial density experiments (1.14-1.16 g/cm³).

Baghvand et al. (2010) conducted experiments for aluminum sulfate and ferric chloride, and they determined that higher doses of coagulant was required when turbidity was increased [185]. Increasing the initial density decreases DR when the same coagulant concentrations are applied. This suggests that increasing DR increases the amount of coagulant necessary to neutralize the additional clay particles, which is analogous to the findings of Baghvand et al.

A possible explanation for the smaller difference in DR between the middle and bottom samples, when the initial density is higher, may be the increase of particles available to react with the coagulant in the middle zone when the density is increased, since this does not occur for the higher density experiments. It is possible that more of the coagulant introduced reacted with the solution uniformly, as the unreacted coagulant at the top was no longer observed.

Table 3.10 - Initial densities, coagulant concentration, Marsh Viscosity gaps and final density of the runs performed with Al₂(SO₄)₃, FeSO₄, PFS and (NH4)₂SO₄ at densities below and within the objective range.

a) Marsh viscosity gap is calculated from the difference between final and initial values. b) Final density gap is calculated from the difference between middle and bottom density values after the coagulant effect.

c) Impossible to measure, due to clogging of the Marsh funnel.

Run	Coagulant	Zone	Initial density range (g/cm³)	Coagulant concentration (mg/L)	Marsh Gap (s/quart) ^{a)}	Final density gap (g/cm³) ^{b)}
22	Al ₂ (SO ₄) ₃	Middle			56	0.0008
22	Al2(3O4)3	Bottom			50	0.0008
27	FeSO ₄	Middle			57	0.0035
21	Fe3O ₄	Bottom	1.1000-		57	0.0035
28	PFS (NH ₄) ₂ SO ₄	Middle	1.1300		I.M.c)	0.0043
20		Bottom		600	1.1017	0.0043
29		Middle			31	0.0004
29		Bottom			31	0.0004
57	۸۱۰(۵۵۰)۰	Middle		000	-14	0.0008
57	Al2(3O4)3	Al ₂ (SO ₄) ₃ Bottom		-14	0.0008	
65	FeSO ₄	Middle			-23	0.0063
05	PFS	Bottom	1.1400-		-23	0.0003
66		Middle	1.1600		-25	0.0032
00		Bottom			-20	0.0032
67	(NILL.)-CO	Middle			16	0.0016
67	(NH ₄) ₂ SO ₄	Bottom			-16	0.0016

Table 3.10 represents the initial densities, Marsh viscosity gap and density gradient between middle and bottom for the selected runs performed with the different coagulant types.

At low initial densities (1.10-1.13 g/cm³), all runs fulfilled the Marsh viscosity gap when they were measurable. With PFS, at low initial densities, the Marsh viscosity was impossible to measure since the flocs produced clogged the Marsh funnel net, possible due to the larger polymeric structure facilitating the formation of large ferric hydroxides that can bind to several clay particles simultaneously-At higher initial densities (1.14-1.16 g/cm³), the objective of initial densities between 1.15-1.20 g/cm³ is accomplished, however, for none of these runs Marsh viscosity gaps objective was accomplished.

Marsh viscosity was lower for higher densities, which was not expected, as more clay in suspension would mean a higher viscosity. It is possible that switching the filtration method from the Marsh net to the sieves may have influenced the Marsh viscosity value, as the sieves have smaller openings.

It is also possible that increasing the concentration of suspended clay facilitates the aggregation effect of the coagulant, as a higher concentration means a higher number of particles per unit of volume, thus increasing the chance of collision and aggregation. This causes a negative collateral effect of coagulating, along with the clay, the PolyMud polymer that provides viscosity to the solution, thus the viscosity decreases.

For the runs at lower initial densities (1.10-1.13 g/cm³), the order of the viscosities was FeSO₄>Al₂(SO₄)₃>(NH₄)₂SO₄. The expected result would be for Al₂(SO₄)₃ run to produce more flocs that would in turn increase the Marsh viscosity, based on its valency and the effect it has on the compression of the double layer. For higher densities (1.14-1.16 g/cm³), the order of the Marsh viscosity gaps was Al₂(SO₄)₃>(NH₄)₂SO₄>FeSO₄>PFS (lower is better in this case, as a negative gap represents a higher reduction, which in turn represents a negative impact on the objective). Due to the secondary effect of PolyMud being dragged with the clay, the expected result would be (NH₄)₂SO₄>Al₂(SO₄)₃>FeSO₄> PFS, as explained previously, due to the larger sieve used to filter flocs or due to increasing the initial density also increases the particles available to react with the coagulant and the likelihood of PolyMud being dragged, and consequently decrease the viscosity of the solution.

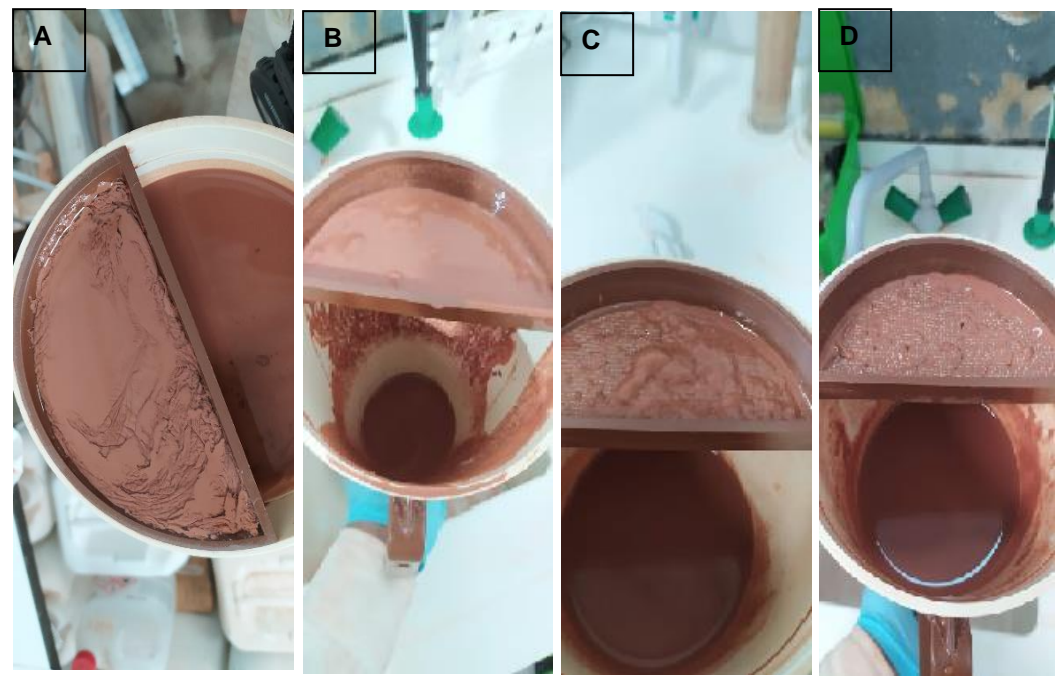


Figure 3.23 - Deposits retained on the net of the Marsh funnel for $(A) - Al_2(SO_4)_3$; (B) - PFS; $(C) - FeSO_4$; $(D) - (NH_4)_2SO_4$ for initial densities of 1.10-1.13 g/cm³

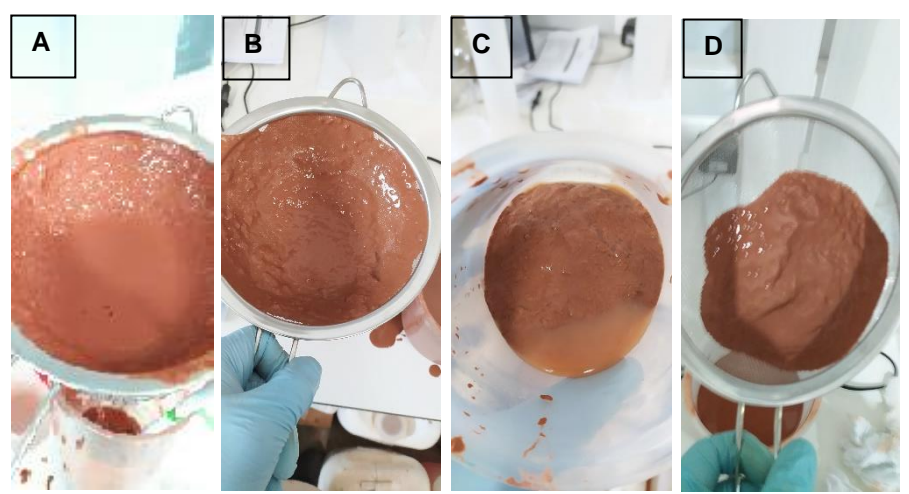


Figure 3.24 - Deposits for (A) $-Al_2(SO_4)_3$; (B) - PFS; (C) $-FeSO_4$; (D) $-(NH_4)_2SO_4$ for an initial density of 1.14-1.16 g/cm³

Figure 3. and Figure 3. represent the accumulation of clay agglomerates on the Marsh funnel nets at lower initial densities (1.10-1.13 g/cm³) and on the filter sieves at higher initial densities (1.14-1.16 g/cm³), respectively. At lower densities, even though the concentration was kept at 600 mg/L, there was a noticeable difference in the floc sizes amongst the four coagulants, as shown on the nets, Higher valence coagulants such as Al₂(SO₄)₃ and PFS blocked the net but FeSO₄ and (NH₄)₂SO₄ showed a smaller accumulation. Increasing the valence of coagulants increases the compression of the electrical double layer and promotes aggregation, as described on subchapter 1.2.2.

At higher initial densities (1.14-1.16 g/cm³), the difference between the deposits of the different coagulants is less noticeable although all coagulants produced recoverable deposits. (NH₄)₂SO₄ produced the smallest amount, as expected from its lower valency. More deposits were observed at the sieve nets for higher initial densities of 1.14-1.16 g/cm³ than for lower densities of 1.10-1.13 g/cm³, as more clay in suspension may correlate to more, bigger agglomerates when these particles are neutralized.

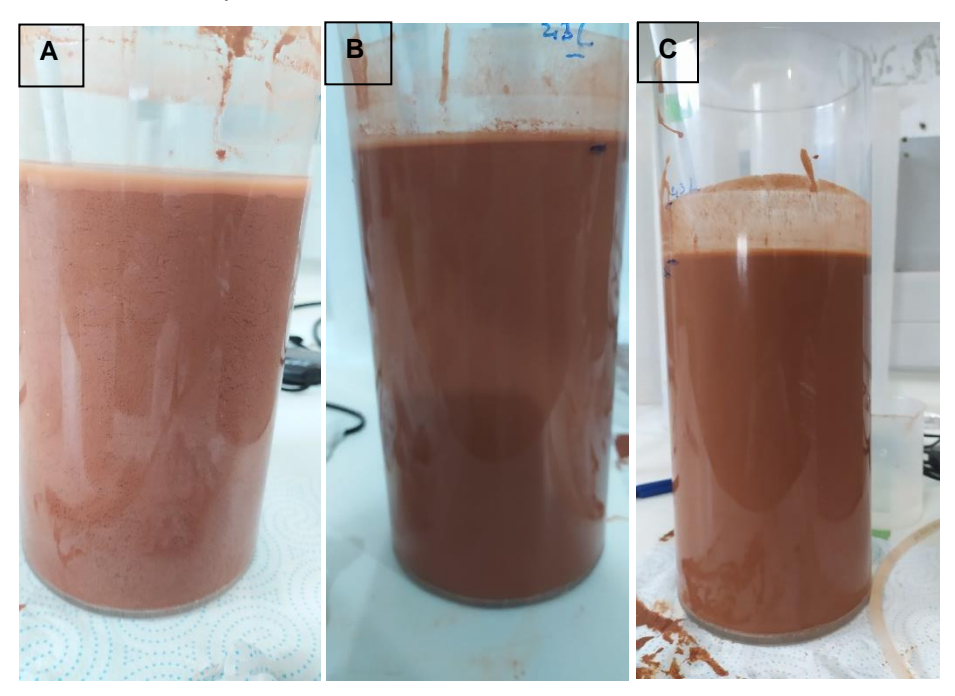


Figure 3.25 - Side view of the solutions treated with: (A) - PFS, (B) - FeSO₄, (C) - $(NH_4)_2SO_4$ for initial densities of 1.14-1.16 g/cm³

Figure 3.25 represents the photos of the solutions treated with PFS, FeSO₄ and (NH₄)₂SO₄ at densities between 1.14-1.16 g/cm³ taken to observe visual differences between the solutions.

From these pictures it is possible to observe that the solution where (NH₄)₂SO₄ was added has the least visual effect (most homogeneity) while the run performed with PFS shows some heterogeneity in the solution. This is possibly due to the polymerization of ferric hydroxides in its constitution. This reaction is carried out in acidic conditions, generally using H₂SO₄, where ferrous sulfate is oxidized to ferric sulfate using an oxidizing agent. Then, when the amount of sulfuric acid is limited, the hydroxide ion replaces the sulfate ion, creating a ferric hydroxide, and the polymerization occurs. The detailed reaction can be seen on the work of Zouboudis et al (2008) [186]. This pre-hydrolized structure combined with a higher molecular weight than the other inorganic coagulants promote adsorption with clay and PolyMud in solution. In consequence, larger and more visible flocs are formed. While the solution with FeSO₄ does not yet show any heterogeneity throughout the middle and bottom of the column, it has a larger section of clean fluid at the top of the column compared to the run where (NH₄)₂SO₄ was added but smaller when compared to PFS. This may be visual evidence of the effect of the valency

increase. However, the flocs are uniformly separated throughout the solutions, as seen on the PFS solution, possibly indicating that these are not settling out.

While $Al_2(SO_4)_3$ is still optimal, as it produced the highest DR at both zones at densities that fulfilled the objective (1.14-1.16 g/cm³), the heterogeneity of the PFS solution will be explored in the next subsection, to compare the visual differences between $Al_2(SO_4)_3$ and PFS using different concentrations.

3.3.2 Study of the coagulant types and concentration

The purpose of this subsection is to study the influence of the coagulant type (Al₂(SO₄)₃ and Polyferric sulfate (PFS)) and their concentrations (200, 600, 1000, and 1500mg/L) on DR (g/cm³) at initial densities between 1.14-1.16 g/cm³, following protocol 2.3.1. As mentioned in the previous chapter, the visual aspect of the runs performed with PFS created an interest in the behavior of this coagulant if the concentration were to be varied, as it began to produce a small strip of clean fluid at the top of the solution and some signs of heterogeneity in the solution. Fixed variables are mixing time (8 min), mixing speed (200 rpm), clay type (clay A from Terracota do Algarve) and polymer type (PolyMud). Crossing these variables may lead to the optimal coagulant type and optimal concentration to attain the objectives proposed on **Error! Reference source not found.**

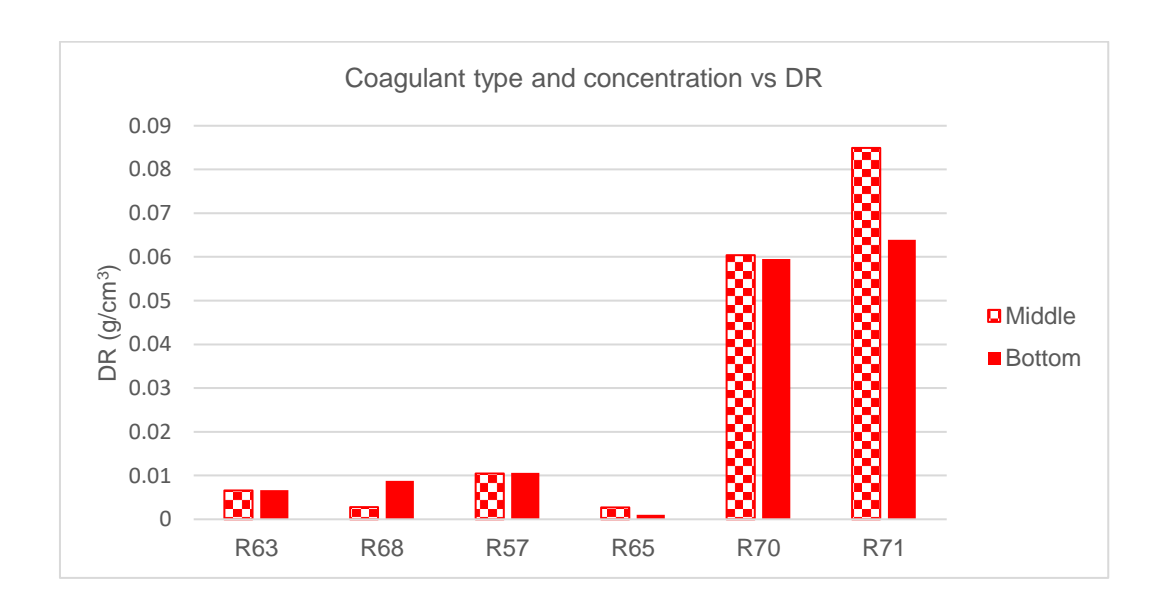


Figure 3.23 – Effect of Al₂(SO₄)₃ and PFS concentration on DR

Figure 3.23 represents the behavior of DR on the runs with the coagulants $Al_2(SO_4)_3$ and PFS, at the concentrations of 200, 600 and 1000

Table 3.11 - Coagulants and concentrations for the runs shown in Figure 4.26

Run	Coagulant	Coagulant concentration (mg/L)	
63	Al ₂ (SO ₄) ₃	200	
68	PFS	200	
57	Al ₂ (SO ₄) ₃	600	
67	PFS	600	
70	Al ₂ (SO ₄) ₃	1000	
71	PFS		

For the runs performed with the concentrations of 200mg/L and 600mg/L (see Figure 3.23), both coagulants presented DR equal or lower than 0.01g/cm³, thus very low. With the increase of coagulants concentration to 1000mg/L, the DR for both coagulants raised to values near 0.06g/cm³ (more than six times higher), with the exception of the middle sample of PFS run, where DR was about 0.08g/cm³.

The same comparison was also performed at a higher concentration of 1500 mg/L, which produced different results. Fixed variables are mixing times (8 min), mixing speed (200 rpm) and polymer type (PolyMud) and coagulant concentration (1500 mg/L)

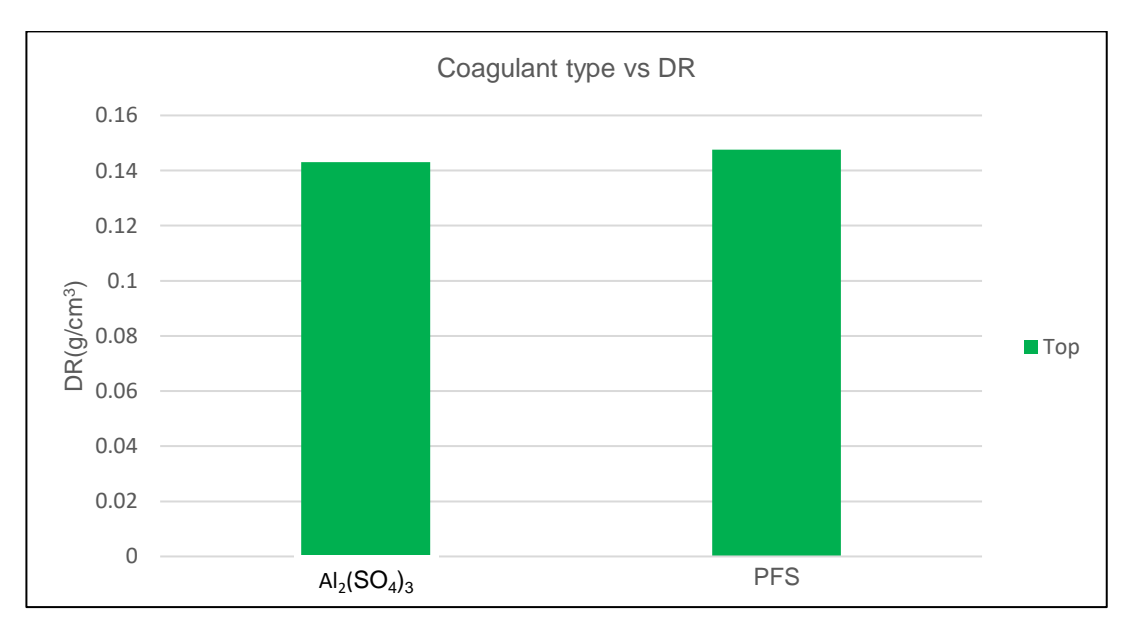


Figure 3.24 - Effect of coagulant type on DR

Figure 3.27 represents the comparison of $Al_2(SO_4)_3$ and PFS when they were applied at the concentration of 1500 mg/L.

When the coagulant concentration was increased to 1500 mg/L, on for both runs clean strip of fluid was formed on the top of the columns. The final density in this area was compared to the initial density in the middle, as at this point, the initial density at the top was not measured. This clean strip has a DR of 0.14g/cm³, thus higher than the higher DR on the objective of 0.12g/cm³. In addition, density was only measurable at the top of the columns, due to the large flocs present on the remaining solution clogging the nets, making it impossible to measure either density on the other areas or the Marsh viscosity.

The high DR obtained for the runs performed with the concentration of 1500 mg/L can be explained by an occurrence known as "sweep floc", where a coagulant, in concentrations above the restabilization zone, form metal hydroxides that consequently form larger, insoluble flocs that trap the clay particles and decrease the settling time, hence the nearly complete removal of clay [187]. While these flocs are larger, they still did not settle out of the solution, as they were suspended as dispersed throughout the solution below the clean fluid strip.

From the visual results observed from chapter 3.3.1 and from the results obtained from the present chapter, an analysis was made using photos to evaluate the evolution of the aspect of the solution when increasing the concentration.



Figure 3.25 – Side by side comparison of solutions treated with $Al_2(SO_4)_3$ at: (A) – 200 mg/L; (B) - 1000 mg/L; (C) – 1500 mg/L and PFS at (D) – 200 mg/L; (E) – 1000 mg/L; (F) – 1500 mg/L

Figure 3.28 represents the solutions treated with $Al_2(SO_4)_3$ and PFS at different concentrations.

At the coagulant concentrations of 200 mg/L, both solutions remain homogeneous, possibly due to the insufficient amount of coagulant. When the concentration was increased to 1000 mg/L, a strip of cleaner fluid was observed at the top of the solutions, although the density was not measured in this zone. This indicates that at this zone, the solution is destabilized and there was settling of clay even though these solutions are heterogeneous, with visible flocs in the middle

and bottom zones due to the increased concentration of coagulant, there was not a total coagulation of the column, which indicates that the stability of the column was not compromised. At 1500 mg/L of Al₂(SO₄)₃, the clean fluid section on the top of the fluids is bigger, and the flocs are more visible, but they are still evenly distributed below the strip. For this concentration, however, the total flocculation observed in the column increases the likelihood that the stability of the column was affected, and that this concentration is unviable for real-world use. Both coagulants produced nearly identical results amongst all concentrations.

In conclusion, both solutions are visually similar, thus, from DR and the visual results, it cannot be said that either coagulant is preferred. In addition, starting from the coagulant concentration of 1000 mg/L, a strip of clean fluid was observed, and its size increased as the concentration of coagulant also increased.

Table 3.12 - Initial densities, coagulant concentration, Marsh Viscosity gaps and final density of the runs performed with Al₂(SO₄)₃ and PFS. ^{a)}Marsh gap is calculated from the difference between final and initial values. ^{b)}Final density gap is calculated from the difference between middle and bottom values. ^{c)}Impossible to calculate due to inability to draw samples. ^{d)}Not measured.

Run	Coagulant	Zone	Initial density (g/cm³)	Coagulant concentrati on (mg/L)	Marsh Gap (s/quart) ^{a)}	Final density gap (g/cm³) ^{b)}
63	M-(SO.)-	Middle	1.1592		-7	0.0013
03	Al ₂ (SO ₄) ₃	Bottom	1.1606	200	-7	0.0013
68	PFS	Middle	1.1526	200	-18	0.0009
00	PFS	Bottom	1.1595		-10	0.0009
57	AL(CO.)	Middle	1.1607		-14	0.0008
57	Al ₂ (SO ₄) ₃	Bottom	1.1600	600	-14	0.0006
67	67 PFS	Middle	1.1595	600	-16	0.0016
67		Bottom	1.1623			0.0010
70	AL(CO.)	Middle	1.1489	1000		
70	Al ₂ (SO ₄) ₃	Bottom	1.1509			
71	PFS	Middle	1.1614		1000	
/ 1	PFS	Bottom	1.1639			
		Тор	NM ^{d)}		1.0 c)	1 C c)
58	Al ₂ (SO ₄) ₃	Middle	1.1490		I.C.c)	I.C.º)
		Bottom	1.1516	1500	4500	
		Тор	NM ^{d)}			
69	PFS	Middle	1.1515			
		Bottom	1.1525			

Table 3.12 represents the initial densities, Marsh viscosity gap and density gradient between middle and bottom for the selected runs performed with Al₂(SO₄)₃ and PFS, which are to be compared to the remaining objectives.

Marsh viscosity was only measurable for the coagulant concentrations of 200 and 600 mg/L, although they did not attain the objective. This reduction of the Marsh viscosity may be attributed to the coagulation of the polymer PolyMud, reducing the viscosity of the solution. Marsh viscosities are further reduced compared to previous studies due to the use of the sieves to improve the time taken to filter out the flocs to enable the measure of the Marsh viscosity. The nets in these sieves are smaller than those of the Marsh cones that were being used until this point (although having a larger surface area available), reducing the flocs that would pass and increase the Marsh viscosity. Even when the values are measurable, they do not accomplish the objective proposed on **Error! Reference source not found.**. The density gap of the runs performed with 200 and 600mg/L of coagulants are within the objective of 0.03 g/cm³.

For the runs performed with 100 and 1500mg/L of coagulants (Al₂(SO₄)₃ and PFS, the flocs in solution were considerably harder to filter and the measurement of both Marsh viscosity and density on the bottom of the columns was impossible to measure.

A possible solution for the measurement of the Marsh viscosity for higher coagulant concentrations would be to use a higher surface area filter that would be able to filter out the flocs, even with partial blockage on some zones.

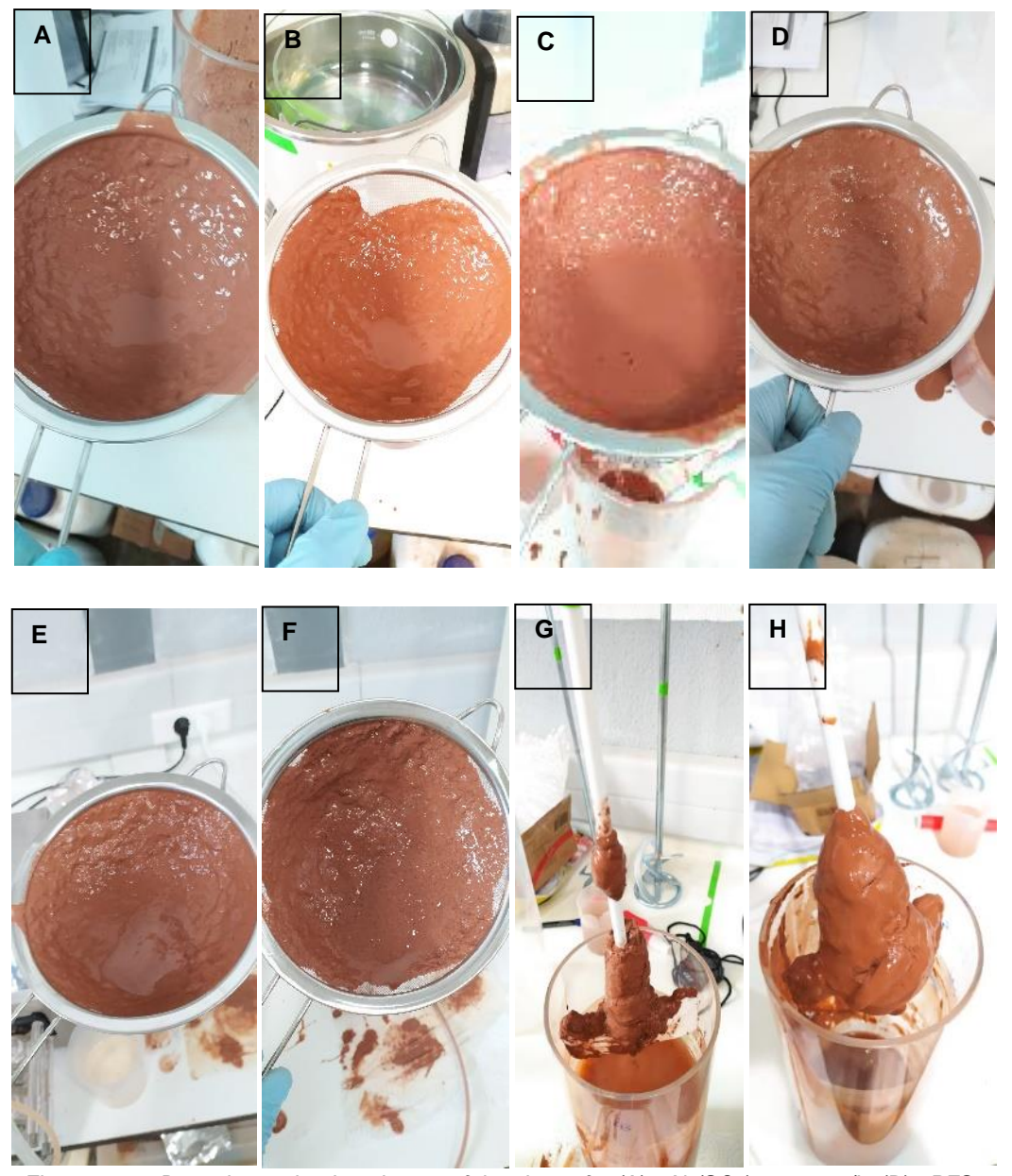


Figure 3.26 - Deposits retained on the net of the sieves for (A) - $Al_2(SO_4)_3$, 200 mg/L; (B) - PFS, 200 mg/L; (C) - $Al_2(SO_4)_3$, 600 mg/L; (D) - PFS, 600 mg/L; (E) - $Al_2(SO_4)_3$, 1000 mg/L; (F) - PFS, 1000 mg/L; and on the agitator blades for: (G) - $Al_2(SO_4)_3$, 1500 mg/L; (H) - PFS, 1500 mg/L

Figure 3.29 represents the deposits retained in sieves and in the blades of the agitators for the solutions treated with Al₂(SO₄)₃ and PFS at different concentrations.

All concentrations produced recoverable deposits that were more pronounced at the concentration of 1500 mg/L. There was only an observable difference between both coagulants at the concentration of 1500 mg/L, where with PFS was produced more deposit around the blades than with $Al_2(SO_4)_3$.

In conclusion, no significant difference is observable between the two coagulants in terms of the visual aspect of the solutions. With the increase of both coagulants from 600mg/L to 1000

mg/L the DR values hit the second objective of DR equal to $0.06~g/cm^3$ for the run where Al₂(SO₄)₃ is used and $0.09~g/cm^3$ for the run where PFS is used. Al₂(SO₄)₃ is still the optimal coagulant since the Marsh viscosity values are higher for this coagulant when they are measurable. However, Marsh viscosities were not within the objective for any of the concentrations of coagulant tested. Density gaps were lower than $0.03~g/cm^3$ when measurable. Flocs were still distributed mostly throughout the solution and not settling, with comparatively small amounts recovered at the sieves and blades of the agitators. As such, for the next studies, Al₂(SO₄)₃ will be maintained as the coagulant and new methods to increase the settling speed of flocs will be explored.

3.4 Study of the use of flocculants

For this chapter, a new approach will be used to increase the floc size and settling speed, flocculants will be added after the addition of coagulants or alone.

3.4.1 Study of flocculant type

The purpose of this subsection is to study the influence of the flocculant type on DR. Flocculants will be added after the coagulant (Al₂(SO₄)₃), following protocol 2.3.32.3.3. Flocculants studied were the cationic polymer Microbond (quaternary ammonium polymer), 6610 (cationic polyacrylamide) and Telsun 5153 (anionic polyacrylamide). Fixed variables are coagulant type (Al₂(SO₄)₃), coagulant concentration (600 mg/L), flocculant concentration (75 mg/L), mixing times (8 min), clay type (clay A from Terracota do Algarve) and mixing speed (200 rpm). This study may lead to the acceleration of the settling time and an increase of DR.

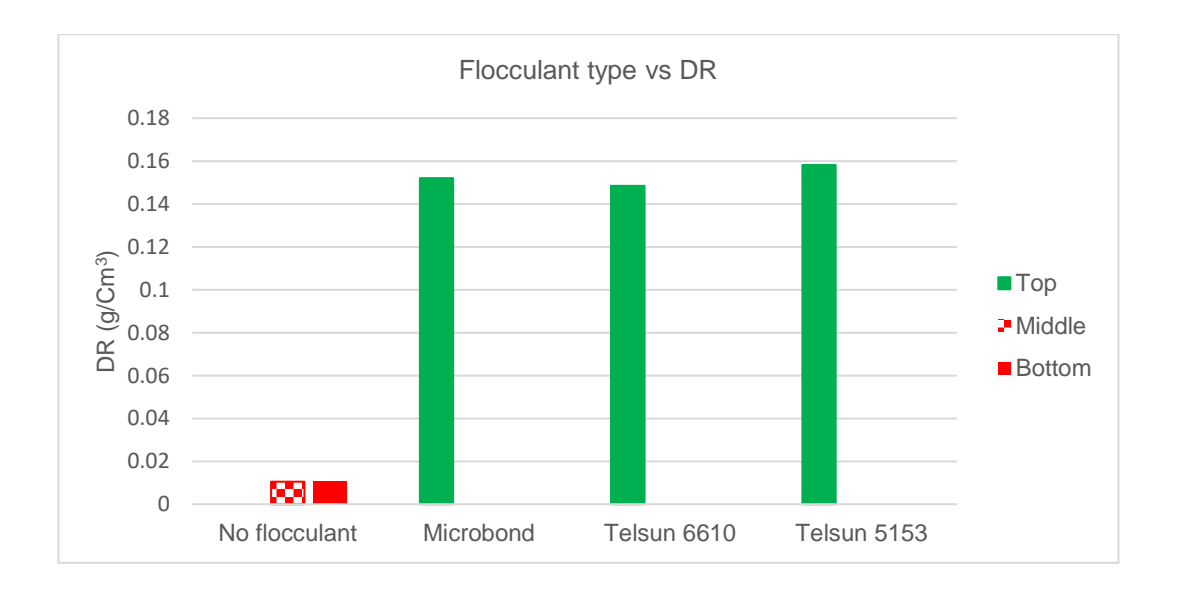


Figure 3.27 - Effect of flocculant type on DR

Figure 3.27 represents DR when $Al_2(SO_4)_3$ is used solely (no flocculant) and when coupled with three flocculants: two cationic (Microbond and 6610) and one anionic (Telsun 5153).

When no flocculant is used, DR is 0.0069 g/cm³ at the middle and 0.0259 g/cm³ at the bottom area. DR increased to the range of 0.15 and 0.16 g/cm³ for any of the runs where flocculants were combined with the coagulant Al₂(SO₄)₃. From the three flocculants, DR values are very similar, yet superior to the maximum established by the objective, as detailed on **Error! Reference source not found.**

As the objective of this subsection is to promote and accelerate the settling speed of the flocs, the visual aspect of the columns will be analyzed without completely removing the clay from the solution and creating clean sections.

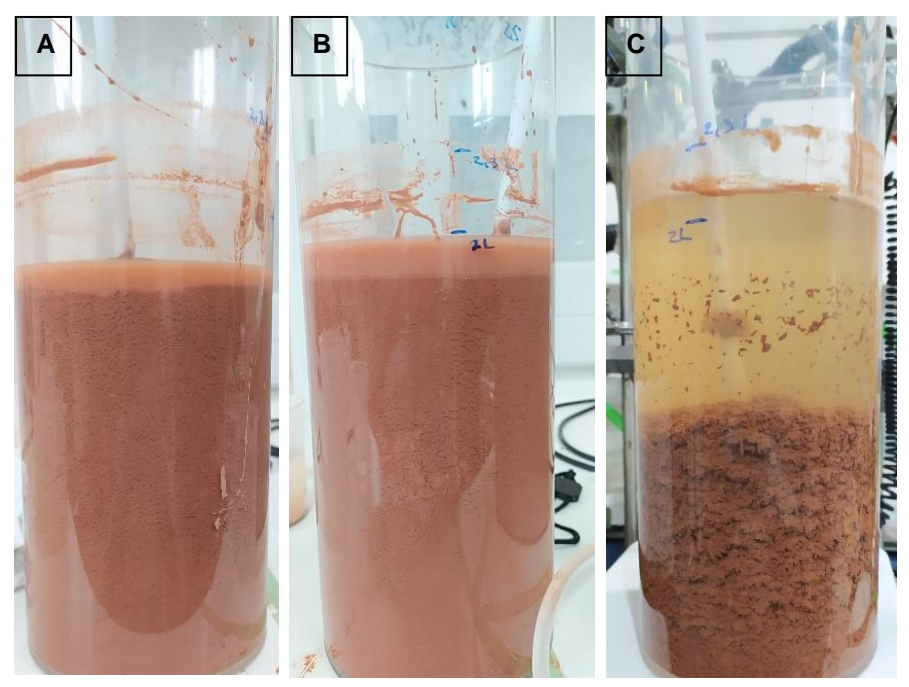


Figure 3.28 - Side view of the solutions treated with the coagulant $Al_2(SO_4)_3$ and -(A) - Microbond; 6610 - (B) -; Telsun 5153 - (C).

Figure 3.31 represents the aspect of the solutions after being treated with Microbond, 6610 and Telsun 5153.

Table 3.13 - Clean strip heights for the solutions presented on Figure 3.31

Run	Clean strip height (cm)	Clean strip height (%)
72	1.5	5
73	1.8	6.2
74	10.4	35.7

Table 3.13 represents the clean strip heights for the solutions treated with $Al_2(SO_4)_3$ combined with Microbond, 6610 and Telsun 5513, respectively, after 30 minutes of rest.

From the analysis of Figure 3.31 and Table 3.13, it is possible to observe that the first two solutions (with Microbond (A) and 6610 (B) polymers, both cationic flocculants) show a small section of clean fluid (5 and 6.2% of the column total height, respectively), while the third has a much higher zone (35.7% of the column height). In the latter, treated with the anionic flocculant Nonionic 5153, the flocs are also more compacted than the ones created on the solution treated with the cationic flocculants. At these concentrations of coagulant and flocculant, the clay is completely removed from the suspension, as a DR of 0.14-0.16 g/cm³ from solutions with initial densities of 1.14-1.16 g/cm³ brings the densities close to that of the PolyMud solution, coupled with the visual clues from the pictures. As seen on chapter 3.3.2, such high DR results, combined with an heavily flocculated column raises concerns about the stability of the column, which in turn makes the applications of Telsun 5153, in particular, in such concentration.

The solutions were put in rest overnight to evaluate if the settling continued post experiment.

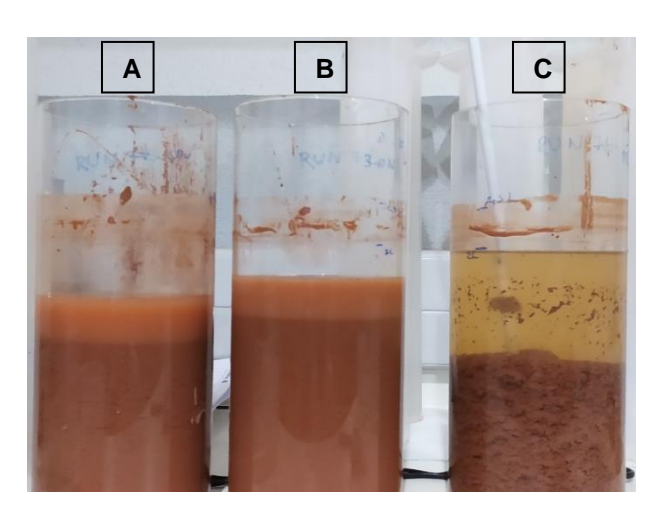


Figure 3.29 - Side view of the solutions treated with (A) - Microbond; (B) – 6610; (C) – Telsun 5153 after overnight.

Figure 3.32 represents the solutions treated with Microbond, 6610 and Telsun 5153 in the morning after the test, approximately 18 hours later, for the purpose of evaluating if the flocs continued to settle.

Table 3.14 - Clean strip heights for the solutions on Figure 3.31 30 minutes and 18 hours after their completion

Runs	Clean strip height (cm)	Clean strip height (%)	Overnight clean strip height (cm)	Overnight clean strip height (%)
72	1.5	5	3.2	10.8
73	1.8	6.2	3	10.3
74	10.4	35.7	10.5	36.5

Table 3.14 represents the clean strip heights for the solutions treated with $Al_2(SO_4)_3$ combined with Microbond, 6610 and Telsun 5513 30 minutes after the introduction of flocculant and overnight (18 hours after the test).

For the runs using Microbond and 6610, the clean strips increased in size, with an increase of 1.7 and 1.2 cm for Microbond and 6610, respectively. However, for the Telsun 5153 solution, the clean section remains almost identical when compared to the section formed after the 30 minutes rest.

This means that the Telsun 5153 flocs, as they were larger, required less time to reach the bottom of the solution, while for Microbond and 6610 runs, the smaller flocs took longer to reach the bottom, hence the height difference increasing for these two solutions.

Some authors claim that using coagulants combined with cationic flocculants reduces the dose of primary coagulant, while maintaining a high removal rate (>98%). Essentially the cationic flocculant acts as a secondary coagulant. Otherwise, the anionic flocculant will bridge the cationic flocs through electrostatic attraction [166]. Mahmudabadi et al. (2018) conducted experiments using PAC as primary coagulant and determined that anionic coagulant aids performed better than cationic or non-ionic [167]. The results obtained are in accordance with the literature mentioned above, as the solutions treated with cationic flocculants produced a clean strip like the Al₂(SO₄)₃ concentration of 1000 mg/L, as seen on previous chapter (3.3.2). When the anionic flocculant (Nonionic 5153) was used, the clean strip was higher and more transparent, DR was higher, and the flocs were visible from the exterior. When compared to the coagulant-only run, all runs using coagulant and flocculant produced the clean strip, indicating that the clay removal process (coagulation, flocculation and settling) is more efficient, while applying the same concentration of coagulant. This is due to the possibility that anionic flocculants can form bigger and heavier flocs because of the electrostatic attractions between

the polymer chains, that have a negative net charge, and the coagulant flocs, that are positively charged. For Microbond and CPAM (cationic polyacrylamides, such as 6610), it is possible that an excess of positive charges formed less consistent flocs due to repulsion between the positively charged polyacrylamides and the likewise positively charged flocs. The extent of flocculation (apparent floc size, and compression) may also have been inferior due to the dual function of these coagulant aids acting as both coagulant and flocculant, possibly reducing the effectiveness of each one. No difference was observable between Microbond and 6610, neither for DR results nor the clean solution heights.

Table 3.15 - Initial densities, coagulant concentration, Marsh Viscosity gaps and final density of the runs performed with Al₂(SO₄)₃ and when combined with Microbond, 6610 and Telsun 5153. ^{a)}Marsh gap is calculated from the difference between final and initial values. ^{b)}Final density gap is calculated from the difference between middle and bottom values. ^{c)}Impossible to measure, due to clogging of the Marsh funnel. ^{d)}Impossible to calculate

Run	Coagulant/ flocculant	Zone	Initial density (g/cm³)	Coagulant/ flocculant concentration (mg/L)	Marsh gap (s/quart) ^{a)}	Final density gap (g/cm³) ^{b)}
57	Al ₂ (SO ₄) ₃	Middle	1.1607	600/0	14	0.0481
57	A12(3O4)3	Bottom	1.1600	000/0	14	0.0401
72	Al ₂ (SO ₄) ₃ /		1.1566			
12	Microbond	Bottom	1.1630			
73	Al ₂ (SO ₄) ₃ /		1.1558	000/75	I.M.c)	I.C. ^{d)}
73	6610	Bottom	1.1580	600/75	1.101.	1.0.37
74	Al ₂ (SO ₄) ₃ /	Middle	1.1601			
/4	5153	Bottom	1.1604			

Table 3.15 represents the initial densities. Marsh viscosity gap and density gradient between middle and bottom for the selected runs performed with Al₂(SO₄)₃ solely and when combined with Microbond, 6610 and Telsun 5153, which are to be compared to the remaining objectives.

Initial densities were within the objective range of 1.15-1.20 g/cm³.

Marsh viscosity was not measurable for the runs which were performed with flocculant, due to the larger flocs in solution making the measurement impossible, especially for the Telsun 5153 solution and the density gap was impossible to calculate due to the inability to draw samples. Thus, the Brookfield viscosity was used to assess the loss of viscosity of the solution once Marsh viscosity was not measurable. The Brookfield viscometer measures viscosity by correlating the torque required to rotate a spindle at constant speed while immersed in the sample fluid to the viscous drag, and thus to the viscosity of the fluid [188].

Table 3.16 – Initial and final Brookfield viscosity for the selected runs performed using performed with Al₂(SO₄)₃ and when combined with Microbond, 6610 and Telsun 5153. ^{a)}Impossible to measure due to the inability to draw samples. ^{b)}Not measured

Run	Coagulant/flocculant	Zone	Initial Brookfield (cP)	Final Brookfield (cP)
	PolyMud (control)	-	74.64	74.64
57	AL (SQ.)	Middle	818.4	730.8
57	Al ₂ (SO ₄) ₃	Bottom	859.2	783.6
		Тор	N.M. ^{b)}	11.04
72	Al ₂ (SO ₄) ₃ /Microbond	Middle	1659	1017
		Bottom	1608	1062
		Тор	N.M. ^{b)}	15.38
73	Al ₂ (SO ₄) ₃ /6610	Middle	1323	I.M. ^{a)}
		Bottom	1560	I.M.*
		Тор	N.M. ^{b)}	14.04
74	Al ₂ (SO ₄) ₃ /Telsun 5153	Middle	1554	I.M. ^{a)}
		Bottom	1674	I.M. ^{a)}

Table 3.16 represents the Brookfield viscosity for the runs performed with $Al_2(SO_4)_3$ with and without the use of flocculants.

The aim of this study is to maintain the Brookfield viscosity at a value as high as the one obtained by PolyMud solution

The top sections were then compared to the PolyMud solution to correlate viscosity gap. For this zone, all solutions had a Brookfield viscosity lower viscosity than the one from the polymeric solution of PolyMud, 6610 solution had the highest value of 15.38 cP and Microbond solution having the lowest value of 11.01 cP. The reduction of the Brookfield viscosity can be correlated to the loss of the suspended PolyMud molecules in the solution and the loss of the tridimensional structure that this polymer creates. A possible cause of this may be the indiscriminate action of the coagulant on negatively charged particles in the solution and the subsequent flocculation of the neutralized particles.

Although Telsun 5153 run produces bigger and heavier flocs that settle effectively, its final viscosity is lower than that of PolyMud, thus the latter is being coagulated and flocculated alongside the clay.

In sum, when any of the flocculants tested are added in the amount of 75 mg/L, coupled with 600 mg/L of Al₂(SO₄)₃ clean strips are formed where the clay settles out, meaning that the clay is completely removed. The highest Brookfield viscosity achieved for these clean strips was 15.38 cP for the run performed with 6610. Even though the 6610 run yielded the highest Brookfield viscosity, the difference is minimal between all the flocculants used. DR was similar amongst all three flocculants tested and is superior to the maximum objective of 0.12 g/cm³. therefore none of the flocculants optimizes this objective, once the fluid is completely cleaned on the top of the column which does not meet the objective of having a controlled cleaning of the column. The difference between these runs was the clean fluid height, which was superior for the TelSun 5153 run. However, none of these runs are viable, as the complete flocculation of the column compromises the stability of the column. In sequence of this findings, Telsun 5153 will be explored as it settled the flocs more effectively, as seen from the visual analysis from the photos taken 30 minutes and in the next morning., and it will be compared to other anionic flocculant types with varying properties to diminish DR, maintain the viscosity of the solution and the stability of the column.

3.4.2 Study of density charge and molecular weight of anionic polyacrylamides used as flocculants

The purpose of this subsection is to study the influence of the charge density and molecular weight of anionic polyacrylamides on DR (g/cm³), following protocol 2.3.3. Fixed variables are coagulant type (Al₂(SO₄)₃), coagulant concentration (150 mg/L), flocculant concentration (150 mg/L), mixing times (8 min), clay type (Clay A from Terracota do Algarve) and mixing speed (200 rpm). This study may lead to the acceleration of the settling time and an increase of DR, while maintaining the viscosity of the clean fluid.

Table 3.17 - Molecular weights and charge densities of the anionic flocculants tested.

Flocculant	Molecular Weight (MDa)	Charge Density (%)
Telsun 5153	15.5	12.6
9233	15-17	4-8
Telsun N23	10.1	2.8
Flonex 934	4.54	15

Table 3.17 represents the comparison of the molecular weights and charge densities of the anionic flocculants used for this study.

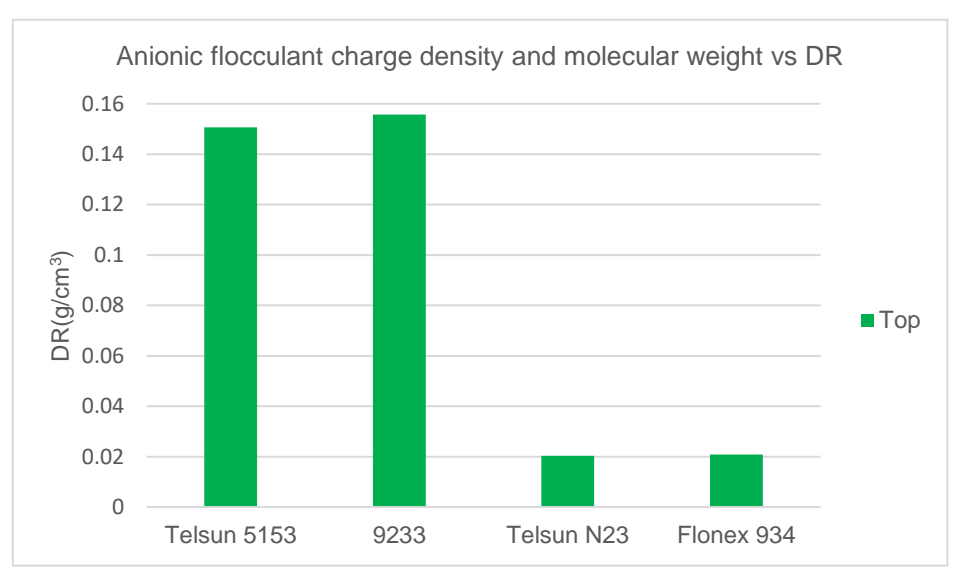


Figure 3.30 – Effect of charge density and molecular weightof anionic flocculants (Telsun 5153, 9233, Telsun N23 and Flonex 934)

Figure 3.33 represents the DR obtained when the coagulant Al₂(SO₄)₃ was combined with four anionic flocculants: Telsun 5153, 9233, Telsun N23 and Flonex 934.

Similar to the results in chapter 3.4.1, density was only measurable at the top. For the runs performed with Telsun 5153 and 9233, DR values at the top were 0.1506 g/cm³ and 0.1557 g/cm³, respectively, representing the total removal of clay. For Telsun N23 and Flonex 934 were 0.0203 g/cm³ and 0.0208 g/cm³, respectively. Both Telsun 5153 and 9233 surpass the maximum DR of 0.12 g/cm³, while Telsun N23 and Flonex 934 reach the first objective range of 0.02 g/cm³.

Runs performed with the flocculants with highest molecular weights (9233 and Telsun 5153) had the highest DRs (superior to 0.15 g/cm³). 9233 and Telsun 5153 have charge densities of 4-8% and 12.8%, and molecular weights of 15-17 and 15.5 MDa, respectively. Even though Telsun 5153 has a higher charge density than 9233 and both flocculants having similar molecular weights, DR for both runs employing these flocculants was nearly identical. It is possible that for these ranges of DR where there is nearly complete flocculation, the charge density is not a contributing factor but the molecular weight. From the comparison between 9233 and Telsun N23, two polymers with low charge densities (2.8 for N23 and 4-8 for 9233), it is also possible to assume that the molecular weight is the decisive factor, as the run with the higher molecular weight polymer, 9233, produced a far higher DR. High molecular weight polymers perform well due to polymer bridging, being one of the main flocculation mechanisms, and this mechanism occurs even on non-ionic polymers. The same comparison can be made with Telsun 5153 and Telsun N23, two polymers with similar charge densities, but different molecular weights as well. The run using Telsun 5153 also produced a higher DR.

As DR values do not fully represent the difference between the runs using Telsun 5153 and 9233 and between Telsun N23 and Flonex 934, a visual approach was taken.

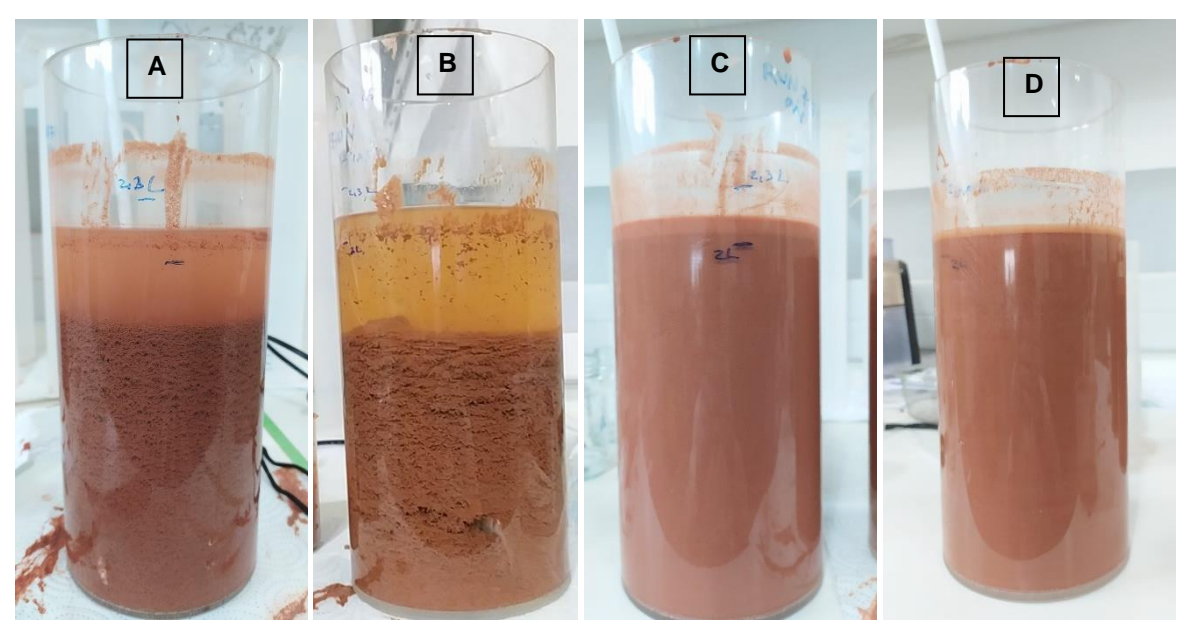


Figure 3.31 - Side view of the solutions treated with (A) – Telsun 5153; (B) – 9233; (C) – Telsun N23; (D) – Flonex 934

Figure 3.34 represents the visual results of the solutions treated with Telsun 5153, 9233, Telsun N23 and Flonex 934.

For the runs performed with Telsun 5153 and 9233 a very different aspect than of Telsun N23 and Flonex 934 is observable. In the first two solutions, a strip of clean fluid is observed at the top, while in the last two, the solution remained mostly homogeneous from the side view. As described above, the anionic polyacrylamides with higher molecular weight, Telsun 5153 and 9233, generated a wide strip of clean fluid, while Telsun N23 and Flonex 934 had low molecular weights, which in turn did not generate clean strips of fluid

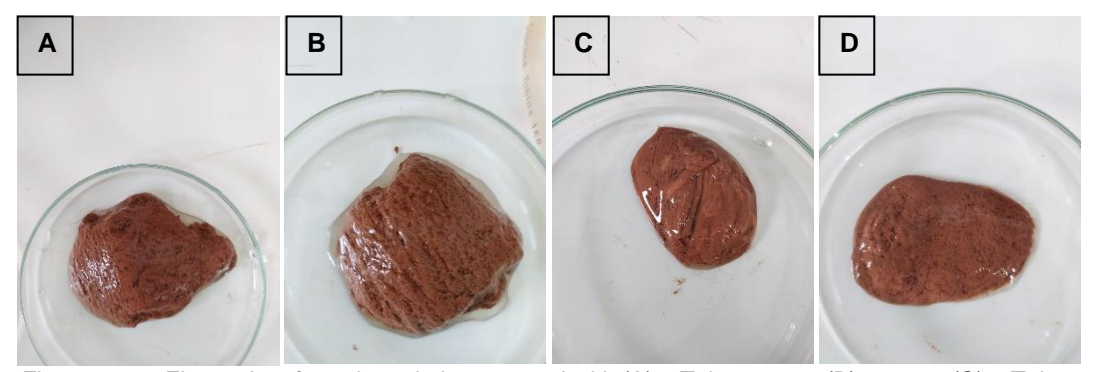


Figure 3.32 - Flocs taken from the solutions treated with (A) – Telsun 5153; (B) – 9233; (C) – Telsun N23; (D) – Flonex 934

Figure 3.35 represents the flocs removed from the solutions overnight.

9233 and Telsun 5153 runs produced the most visually perceptive, compact and cohesive flocs, while Telsun N23 and Flonex 934 runs produced flocs that were smaller, less compact, less cohesive and more liquid. As previously said, the molecular weight plays a very important role in polymer bridging which is responsible for the higher consistency of flocs.

Marsh viscosities of these four runs were impossible to measure due to the blockage of the nets and, consequently, density gradients were not calculated. Thus, the Brookfield viscosities of the solutions that generated the clean strip were analyzed.

Table 3.18 - Initial and final Brookfield viscosity for the selected runs performed using performed with Al₂(SO₄)₃ when combined with Telsun 5153, 9233, Telsun N23 and Flonex 934. ^{a)}Impossible to measure due to the impossibility of drawing samples

Run	Coagulant/ flocculant	Zone	Coagulant/flocculant concentration (mg/L)	Initial Brookfield (cP)	Final Brookfield (cP)	
-	PolyMud (control)	-	-	74.64	74.64	
		Тор		1650	26.46	
83	Al ₂ (SO ₄) ₃ / Telsun 5153	Middle		1599	I.M. ^{a)}	
	T Clour O TOO	Bottom		1635	I.IVI. ^a /	
		Тор		1899	37.32	
87	87 Al ₂ (SO ₄) ₃ / 9233	Middle	150/150	1980	I.M. ^{a)}	
		Bottom		2016	1.IVI. [©])	
		Тор	130/130	1509	25.32	
89	Al ₂ (SO ₄) ₃ / Telsun N23	Middle		1554	I.M. ^{a)}	
	10.001111420	Bottom		1638	1.IVI. [©])	
		Тор		1710	30.36	
90	90 Al ₂ (SO ₄) ₃ / Flonex 934		Middle		1737	I.M. ^{a)}
		Bottom		1836	I.IVI. [~] /	

Table 3.18 represents the Brookfield viscosity for the runs performed with Al₂(SO₄)₃ combined with different anionic flocculants.

Brookfield viscosity of the top sections of these four runs were compared to the Brookfield viscosity of PolyMud run. This comparison is useful, as the goal of this section is still to maximize the Brookfield viscosity of the clean fluid sections as a secondary objective, while the primary goal is the controlled DR. The Telsun 5153 run produced a value of 26.26 cP, 48.18 cP lower thanthe Telsun 5156 solution. For the 9233 run, the Brookfield viscosity was 11.14 cP higher than the Telsun 5153 solution. It can be inferred that from the difference between Brookfield values between Telsun 5153 and 9233 that both flocculants assist in the coagulation of clay simultaneously to the coagulation of PolyMud. The remaining unreacted flocculant relaces the original PolyMud in solution. The run performed with 9233 had a higher viscosity due to the higher molecular weight of this flocculant. When this flocculant remains in solution, increases the Brookfield viscosity of the solution higher than Telsun 5153.

Changing from Telsun 5153 to 9233 did not move DR closer to the objective of 0.12 g/cm³. In fact, DR remained mostly similar, however the solution was more transparent, which indicates that 9233 removed more clay than Telsun 5153, which may further compromise the stability the column, making this system unviable for use.

3.4.3 Study of the coagulant and flocculant concentration on DR

The purpose of this subsection is to study the influence of the coagulant $(Al_2(SO_4)_3)$ and flocculant (Telsun 5153) concentrations on the density reduction, following protocol 2.3.3. Fixed variables are coagulant type $(Al_2(SO_4)_3)$, flocculant type (5153) mixing time (8 min), clay type (clay A from Terracota do Algarve) and mixing speed (200 rpm). This study may lead to the acceleration of the settling time and an increase of DR, while maintaining the viscosity of the clean fluid.

For this study, mean and median values of DR were calculated from the three zones: top, middle, and bottom to reduce the variability of the measurements and their respective errors produced by the filtration of the samples and human error on the selection of the samples of each zone. This method will in turn simplify the values for easier comprehension.

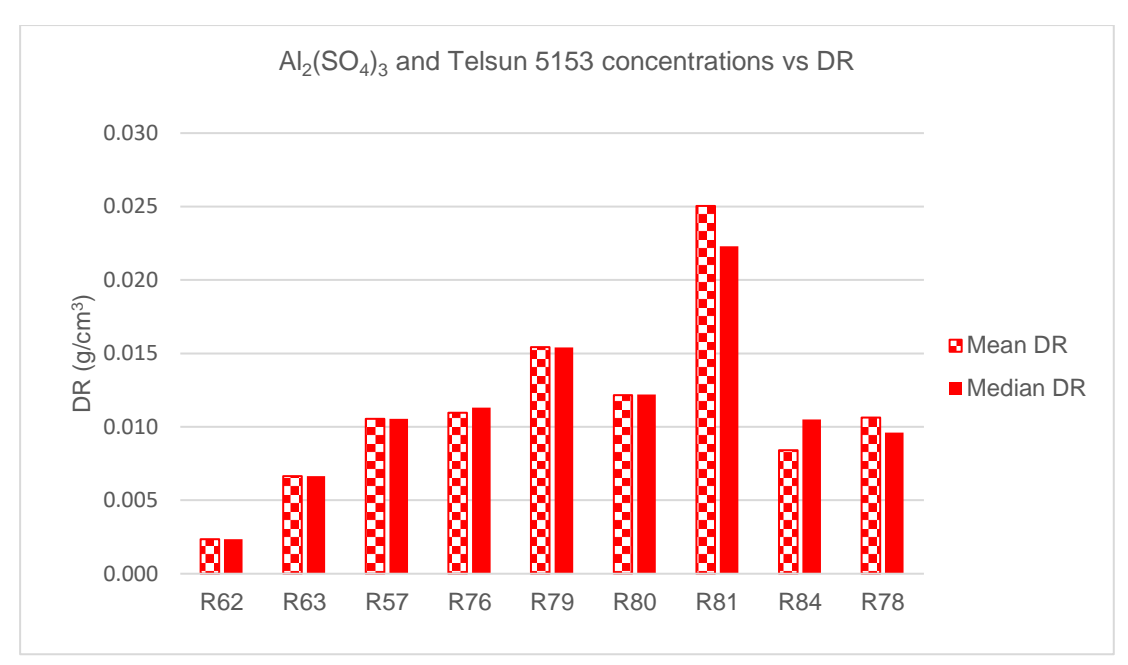


Figure 3.33 – Effect of different concentrations of Al₂(SO₄)₃ and Telsun 5153 on DR

Figure 3.36 represents the influence of the concentrations of coagulant $Al_2(SO_4)_3$ and flocculant Telsun 5153 on DR.

Table 3.19 - Coagulant and flocculant concentrations for the runs shown on Figure 3.36

Run	Coagulant concentration (mg/L)	Flocculant concentration (mg/L)
62	100	0
63	200	0
57	600	0
76	50	75
79	100	37.5
80	150	37.5
81	150	75
84	175	37.5
78	200	15

Table 3.19 represents the runs where Al₂(SO₄)₃ was used in combination with TelSun 5153 at different concentrations where no clean fluid was observed.

From Figure 3.36 it is possible to observe that the mean and median values are quite close to each other, which means that both adequately represent the behavior of the column as a

whole. When the coagulant is used without flocculant, DR does not reach the first objective of 0.02 g/cm³. However, for the same concentrations, when flocculant was used in combination with the coagulant, higher DR was achieved even though up until 150 mg/L of coagulant and 75 mg/L of flocculant, DR is still inferior to 0.02 g/cm³. For example, when 100 mg/L of coagulant is introduced, DR increased from -0.0001 g/cm³ to 0.0164 g/cm³ (increase of 0.01 g/cm³ in DR is observed when 37.5 mg/L of Telsun 5153 is used in conjunction). For 200 mg/L of coagulant, an initial amount of 15 mg/L increases DR marginally. Thus, the DR objective of 0.02 g/cm³ is for the runs using concentrations of 50/75, 100/37.5 150/37.5 and 150/75 mg/L of coagulant/flocculant.

Onen and Gocer (2018) performed experiments using FeCl₃ and Al₂(SO₄)₃ with anionic coagulant aids on the settling of bentonite suspensions, achieving removal rates over 90% [189]. The anionic coagulant had a molecular weight between 5-15 MDa and a high charge density of 50-60%. They determined that anionic flocculant yielded a sedimentation percentage that increased as the flocculant concentration increased, when used between 2.5 and 15 mg/L. The results obtained for this study are in accordance with the literature experiments, as the tendency observed on the current work follows the same tendency observed by Onen et al. The charge density was also considerably higher, although from the current work, it did not have any influence on DR. Like in the study of Haydar et al. [166], the high removal may have been a low concentration of clay. This concentration was of 2.5% solid ratio, while in the present work, a solid ratio of 45% is being used, which may explain such difference is removal rates with such difference in concentrations.

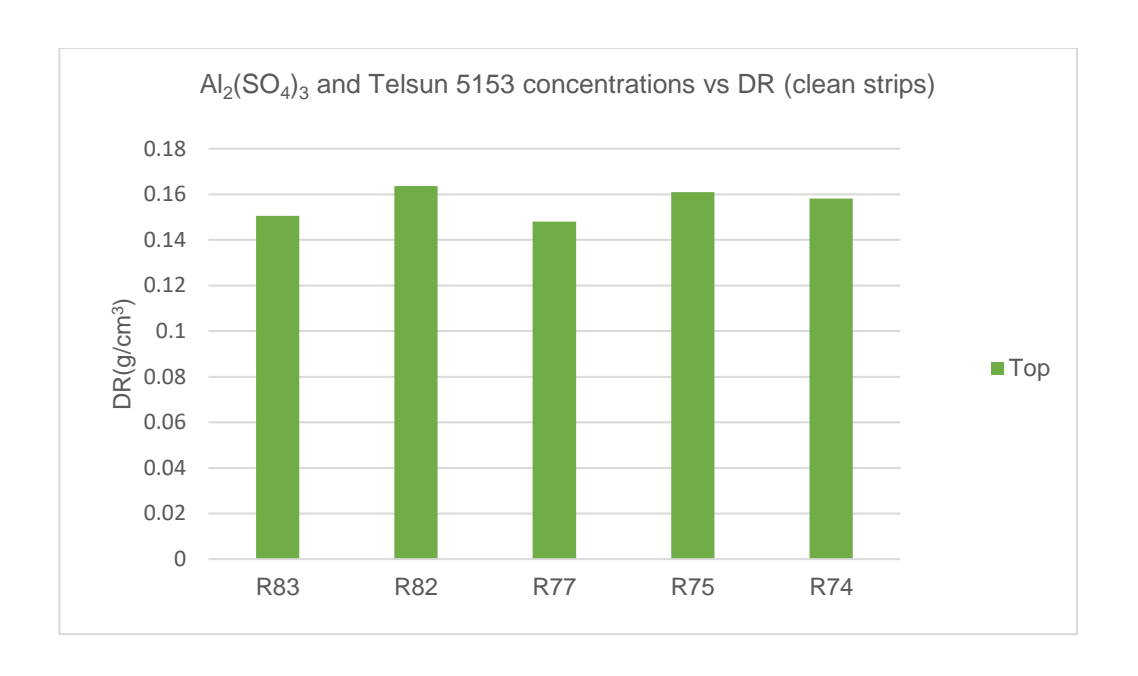


Figure 3.34 - Effect of Al₂(SO₄)₃ and Telsun 5153 concentrations on DR

Figure 3.34 represents the influence of the concentrations of coagulant $Al_2(SO_4)_3$ and flocculant Telsun 5153 on DR when the solution was fully cleaned.

Table 3.20 - Coagulant and flocculant concentrations for the runs shown on Figure 3.34

Run	Coagulant concentration	Flocculant concentration (mg/L)
83	150	150
82	150	300
77	200	37.5
75	200	75
74	600	75

Figure 3.34 represents the influence of the concentrations of coagulant Al2(SO4)₃ and flocculant Telsun 5153 on DR when the solution was fully cleaned.

Table 3.20 represents the coagulant and flocculant concentrations for the runs shown on Figure 3.36.

For the runs using the coagulant concentrations of 150 mg/L and 200 mg/L, increasing the concentration flocculant from 75 to 150 mg/L and from 15 to 37.5 mg/L increased DR by 0.14 g/cm³ and 0.15 g/cm³, respectively. Increasing the concentration of coagulant reduced the

concentration of flocculant necessary to reach the boundary zone. For 150 mg/L of coagulant, the concentration of flocculant necessary was 4 times higher than for 200 mg/L.

Some authors have conducted experiments with coagulant and flocculant systems. Haydar et. al conducted experiments with tannery wastewaters [166]. They concluded that the turbidity was gradually reduced as the coagulant concentration was increased. The highest rate of removal (99.4%) was achieved using 160 mg/L of Al₂(SO₄)₃ and 5 mg/L of an anionic flocculant, which was characterized by having 16% charge density and 15 MDa. Results are in accordance with this study, as even though the flocculant used is similar to Telsun 5153 - 16% charge density compared to 12.6% of Telsun 5153 and 15 MDa compared to 15.5 Mda of Telsun 5153. Even though the suspended particles had a different nature and structure than clays, they were also negatively charged colloids and the same trend was observed when the coagulant concentration was increased. It is possible that the zeta potential of the solution is further reduced below the optimal range of -30 to 30 mV, requiring higher doses of coagulant and flocculant to achieve higher rates of removal [190].

For the concentrations of 150 mg/L of $Al_2(SO_4)_3$ and 150 mg/L of Telsun 5153, 150 mg/L of $Al_2(SO_4)_3$ and 300 mg/L of Telsun 5153, 200 mg/L of $Al_2(SO_4)_3$ and 37.5 mg/L of Telsun 5153 and 600mg/L of $Al_2(SO_4)_3$ and 75 mg/L of Telsun 5153, the DR of 0.12 g/cm³ overachieved by at least 0.04 g/cm³.

It is possible that a certain amount of coagulant is necessary to compress the electrical double layer, neutralize the clay particles and consequently destabilize the solution, forming flocs. Increasing the concentration of coagulant further promotes aggregation and reduces the amount of flocculant necessary to bridge together the clay agglomerations formed by the coagulant.

Thus, the conditions necessary to reach this boundary zone, which makes the column unfeasible due to the total flocculation of the column and the complete removal of clay, were with 150/150 mg/L 200/75 mg/L and 600/75 mg/L of coagulant/flocculant, respectively.

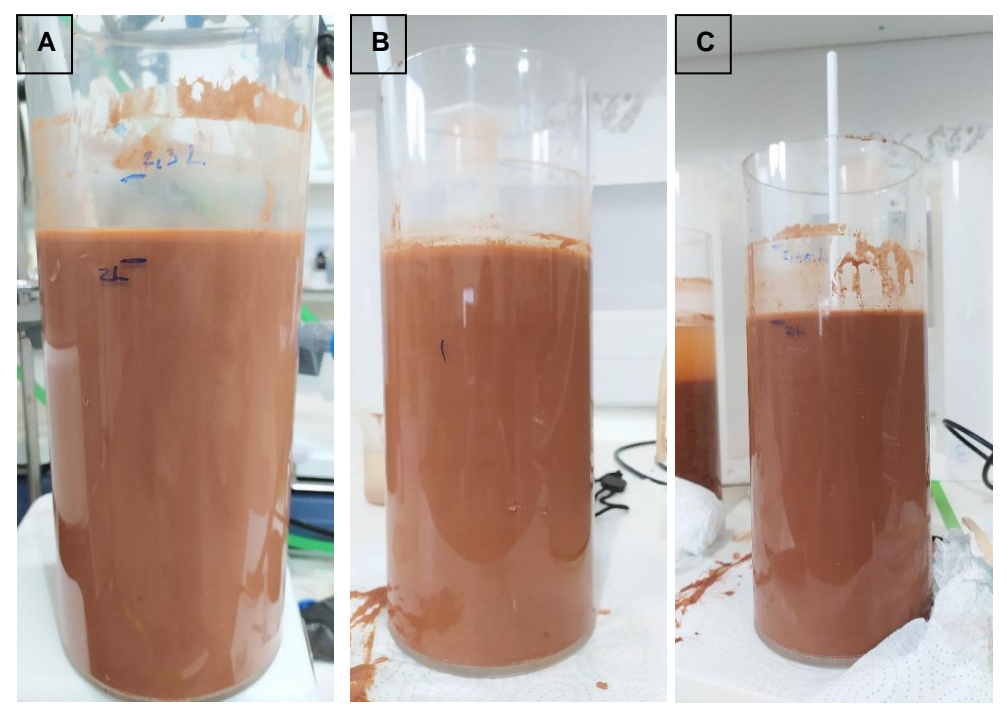


Figure 3.38 - Side view of the solutions treated with $Al_2(SO_4)_3$ and Telsun 5153 at : (A) - 50/75 mg/L; (B) - 100/37.5 mg/L and (C) - 175/37.5 mg/L

Figure 3. represents the visual aspect of the solutions treated with $Al_2(SO_4)_3$ and Telsun 5153 at different concentrations.

The solutions remained homogeneous and as such, at these concentrations, the boundary zone is not reached.

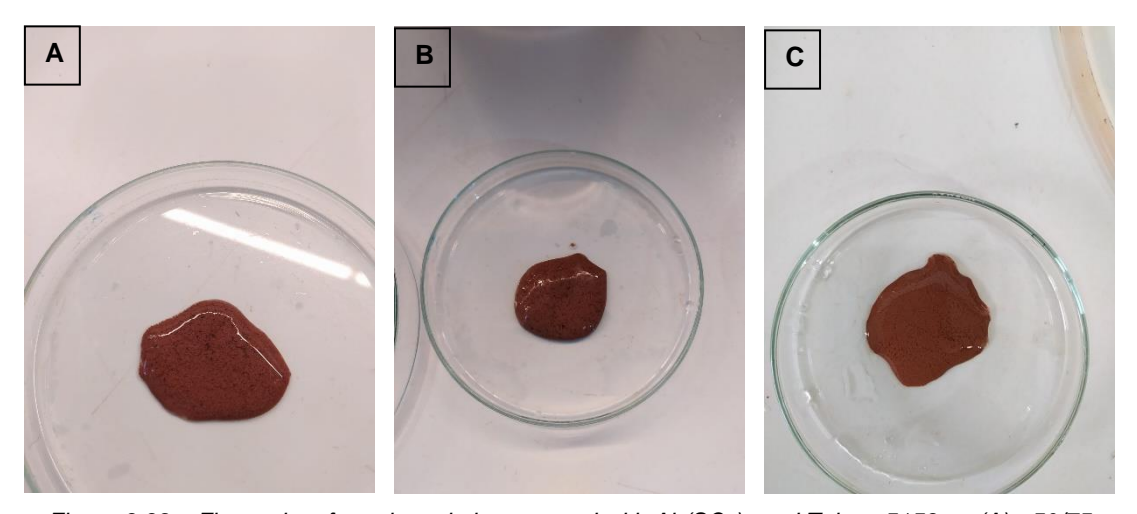


Figure 3.39 – Flocs taken from the solutions treated with $Al_2(SO_4)_3$ and Telsun 5153 at: (A) - 50/75 mg/L; (B) - 100/37.5 mg/L and (C) - 175/37.5 mg/L

Figure 3. represents a sample of the flocs formed removed from the solutions overnight.

The flocs were of very low consistency, as expected from the exterior aspect of the solutions.

Table 3.21 - Clean fluid height of the solutions treated with $Al_2(SO_4)_3$ and Telsun 5153 at: (A) - 50/75 mg/L; (B) - 100/37.5 mg/L and (C) - 175/37.5 mg/L

Run	Coagulant/ flocculant	Coagulant/ flocculant concentration (mg/L)	Clean fluid height (cm)	Clean fluid height (%)
76	VI-(80.)- /	50/75	3.5	18%
79	Al ₂ (SO ₄) ₃ / Telsun	100/37.5	5	25%
84	5153	175/37.5	1.5	8%

Table 3.21 represents the clean fluid height of the solutions treated with 50/100/175 mg/L of coagulant and 75/37.5/37.5 mg/L of flocculant.

Clean fluid heights did not show any trend.

It is possible that the negative charge of the clays is not completely neutralized by the coagulant or at least not "screened" (see chapter 1.2.2.1.1) to allow the flocculant to adsorb effectively to the clay and coagulant aggregate. It is possible that the compression of the double layer is not enough to allow the aggregation of the clays. The residual negative charge may have created electrostatic repulsions between the clays and the flocculant, reducing in turn the effectiveness of the flocculant as well.

Thus, the coagulant concentration was increased for further observations.

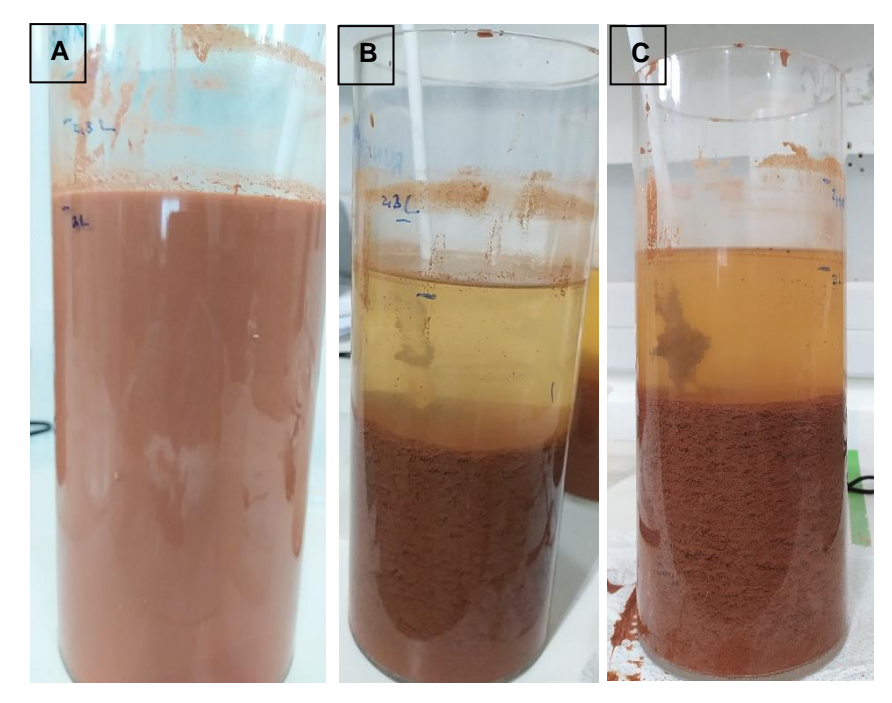


Figure 3.40 - Side view of the solutions treated with $Al_2(SO_4)_3$ at 200 mg/L and Telsun 5153 at (A) - 15 mg/L; (B) - 37.5 mg/L; (C) - 75 mg/L

Figure 3. represents the aspect of the solutions treated with $Al_2(SO_4)_3$, maintained at 200 mg/L and Telsun 5153 at 15, 37.5 and 75 mg/L.

Increasing the concentration of coagulant from 175 mg/L to 200 mg/L may have screened the negative charge of the clay and increased the electrostatic attraction of the anionic polymer to the clay surrounded by the coagulant. In turn, increasing the flocculant concentration while the coagulant concentration is maintained at 200 mg/L, hits the boundary zone, where a noticeable height of clean fluid is observed for the runs using concentrations of Telsun 5153 upwards of 37.5mg/L. Only for the flocculant concentration of 15 mg/L that the stability of the column is not possibly compromised, since for the other solutions, the column cannot be used for further construction in real-world scenarios.

A B C

Figure 3.41 - Flocs taken from the solutions treated with $Al_2(SO_4)_3$ at 200 mg/L with Telsun 5153 at (A) - 15 mg/l; (B) - 37.5 mg/L and (C) - 75 mg/L

Figure 3. represents the flocs formed by the solutions treated with 200 mg/L of $Al_2(SO_4)_3$ and concentrations of Telsun 5153 between 15 and 75 mg/L.

No flocs were formed for 15 mg/L, while for the higher concentrations of flocculant, consistent flocs were formed. These observations are in line with the exterior aspect of the solutions, as the flocculant concentration of 15 mg/L showed no effect.

Table 3.22 - Clean fluid height of the solutions treated with $Al_2(SO_4)_3$ at 200 mg/L with Telsun 5153 at (A) - 15 mg/l; (B) - 37.5 mg/L and (C) - 75 mg/L

Run	Coagulant/ flocculant	Coagulant/ flocculant concentration (mg/L)	Clean fluid height (cm)	Clean fluid height (%)
78	Al ₂ (SO ₄) ₃ / Telsun 5153	200/15	1.0	5%
77		200/37.5	8.5	43%
75		200/75	9.0	45%

Table 3.22 represents the clean fluid height of the solutions treated with 200 mg/L of coagulant and 15/37.5/75 mg/L of flocculant.

Increasing the flocculant concentration from 15 mg/L to 37.5 mg/L increased the clean fluid height drastically by 7.5 cm, but doubling again the flocculant concentration only increased the clean fluid height by another 0.5 cm. It is possible that the flocs may have been saturated with flocculant in the concentrations between 37.5 and 75 mg/L and that may have caused them to be unavailable to adsorption.

But as the complete removal of clay is not the objective, the concentration of coagulant was reduced to 150 mg/L and the flocculant concentration was manipulated to move closer to the controlled coagulation/flocculation system.

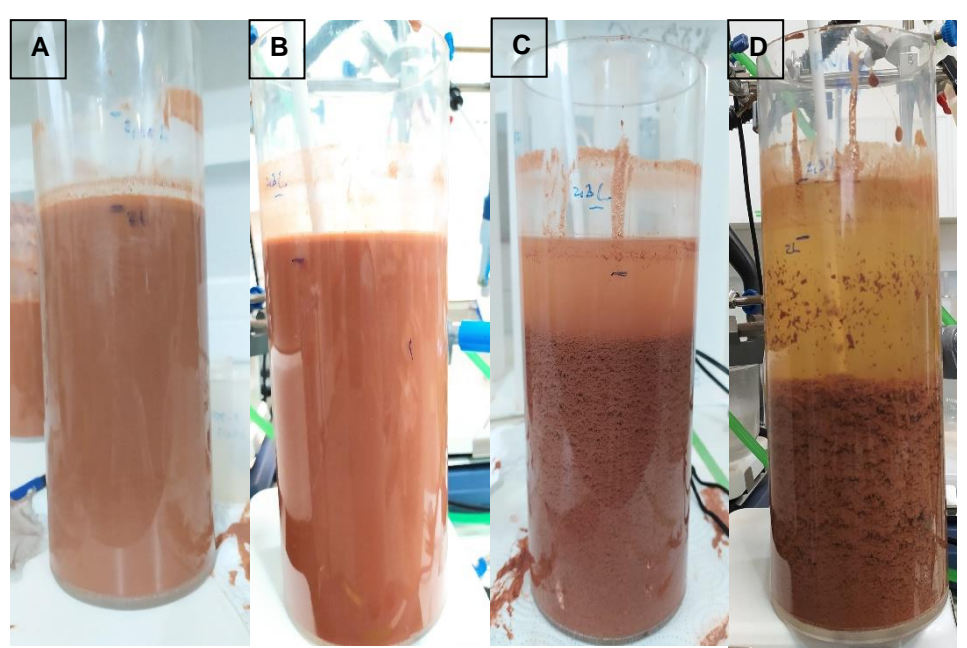


Figure 3.42 - Side view of the solutions treated with $Al_2(SO_4)_3$ at $1\overline{50}$ mg/L with Telsun 5153 at (A) - 37.5 mg/l; (B) - 75 mg/L; (C) - 150 mg/L and (D) - 300 mg/L

Figure 3. represents the solutions treated with $Al_2(SO_4)_3$ and 5153 when the concentration of the former was maintained at 150 mg/L.

For the runs using concentrations of 37.5 and 75 mg/L of Telsun 5153, the aspect of the solution remains homogeneous, but increasing this to 150 and 300 mg/L produced very different results. In these last two cases, a strip of clean fluid is observed at the top of the solutions, which heights increase as the concentration of 5153 increases. For the concentrations of 150 and 300 mg/L of flocculant, the stability of the column may be at risk due to the flocs and the clean strip formed, and this column may not be used for further construction in real-world cases.

These heights are in accordance with the visual aspect of the solutions. Increasing both the concentrations of coagulant and floculant increased the height of clean fluid.

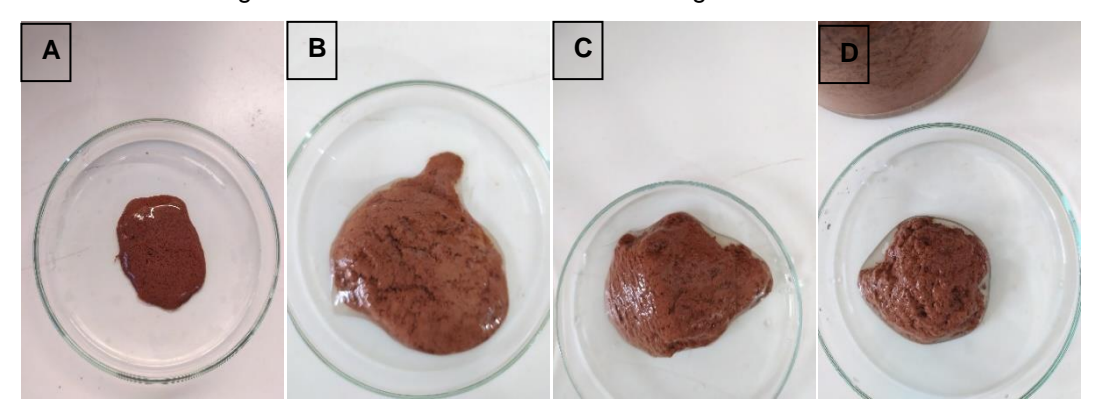


Figure 3.43 – Flocs taken from the solutions treated with $Al_2(SO_4)_3$ at 150 mg/L with Telsun 5153 at (A) - 37.5 mg/l; (B) - 75 mg/L; (C) – 150 mg/L and (D) – 300 mg/L

Figure 3. represents the flocs formed by the solutions treated with 150 mg/L $Al_2(SO_4)_3$ and concentrations of Telsun 5153 between 37.5 and 300 mg/L.

Increasing the flocculant concentration increases the consistency of the flocs. These tend to agglomerate closer and have a more solid look.

Table 3.23 - Clean fluid height of the solutions treated with $Al_2(SO_4)_3$ at 150 mg/L with Telsun 5153 at (A) - 37.5 mg/l; (B) - 75 mg/L; (C) - 150 mg/L and (D) - 300 mg/L

Run	Coagulant/ flocculant	Coagulant/ flocculant concentration (mg/L)	Clean fluid height (cm)	Clean fluid height (%)
80		150/37.5	4.0	20%
81	Al ₂ (SO ₄) ₃ / Telsun	150/75	5.5	28%
83	5153	150/150	10.0	50%
82		150/300	12.5	63%

Table 3.23 represents the clean fluid height of the solutions treated with 150 mg/L of coagulant and 37.5/75/150/300 mg/L of flocculant.

Increasing the concentration of flocculant increased the clean fluid height, as a higher concentration of flocculant may have promoted the bridging between molecules of flocculant and consequently, the formation of larger flocs that settled quicker. The highest increase in height

(4.5 cm) was observed between the concentrations where the boundary zone was observed. Increasing the concentration of flocculant below and above this boundary zone produced a significantly lower height increase (1.5 and 2.5 cm, respectively). It is possible that below these concentrations, the flocculant was not present in concentrations high enough to form flocs large enough to settle quickly and above these concentrations, the flocs may have been saturated with flocculant, preventing these from adsorbing onto the flocs.

Table 3.24 - Initial densities, coagulant concentration, Marsh Viscosity gaps and final density of the runs performed with Al₂(SO₄)₃ combined with Telsun 5153. ^{a)}Marsh gap is calculated from the difference between final and initial values. ^{b)}Final density gap is calculated from the difference between middle and bottom values. ^{c)}Impossible to measure, due to clogging of the Marsh funnel. ^{d)}Impossible to calculate due to the inability to draw samples. ^{e)}Not measured

Run	Coagulant/ flocculant	Zone	Initial density (g/cm³)	Coagulant/ flocculant concentration (mg/L)	Marsh gap (s/quart) ^{a)}	Final density gap (g/cm³) ^{b)}
		Тор	N.M.e)			
62		Middle	1.1566	100/0	5	0.0015
		Bottom	1.1618			
		Тор	N.M.e)			
63	Al ₂ (SO ₄) ₃	Middle	1.1592	200/0	-9	0.0001
		Bottom	1.1606			
		Тор	N.M.e)			
57		Middle	1.1607	600/0	-14	0.0008
		Bottom	1.1600			
		Тор	1.1529			
76		Middle	1.1543	50/75	-15	0.0010
		Bottom	1.1546			
		Тор	1.1572		I.M.°)	0.0028
79	Al ₂ (SO ₄) ₃ /	Middle	1.1551	100/37.5		
		Bottom	1.1570			
		Тор	1.1482	150/37.5 150/75		
80		Middle	1.1497			0.0059
		Bottom	1.1543			
		Тор	1.1614			
81		Middle	1.1604			0.0009
		Bottom	1.1680			
	Telsun	Тор	1.1524	150/150		
83	5153	Middle	1.1561			
		Bottom	1.1654			1 C q)
		Тор	1.1654			I.C. ^{d)}
82		Middle	1.1653	150/300		
		Bottom	1.1655			
		Тор	1.1607			
84		Middle	1.1619	175/37.5		0.0054
		Bottom	1.1609			
		Тор	1.1560	200/15		
78		Middle	1.1570			0.0011
		Bottom	1.1601			
77		Тор	1.1497	200/37.5		I.C.d)

	Middle	1.1530		
	Bottom	1.1567		
	Тор	1.1625		
75	Middle	1.1635	200/75	
	Bottom	1.1648		

Table 3.24 represents the initial densities, Marsh viscosity gap and density gradient between middle and bottom for the selected runs performed with Al₂(SO₄)₃ solely and when combined with Telsun 5153, which are to be compared to the remaining objectives.

Marsh viscosity was impossible to measure above the concentration of 50 mg/L of coagulant and 75 mg/L of flocculant due to the blockage of the nets and, density gradients were not calculated because of the inability of removing samples from the middle and bottom zones. For the run using the concentration of 50/75 mg/L, the Marsh viscosity gap was of 15 s/quart, 10 s/quart higher than the objective. While the coagulant concentration was low, it is possible that most of the coagulant that attached to the PolyMud in solution, was aggregated into flocs and settled out of the solution, reducing considerably the Marsh viscosity of the solution. The zone gaps were always within the objective of 0.03 g/cm³ when they were measurable. To evaluate the loss of viscosity of the remaining solutions, the Brookfield viscosities of the solutions that generated the clean strip were analyzed.

Table 3.25 - Initial and final Brookfield viscosity for the selected runs performed using performed with Al₂(SO₄)₃ when combined with Telsun 5153. ^{a)}Impossible to measure due to the inability to take samples. ^{b)}Not measured

Run	Coagulant/ flocculant	Zone	Coagulant concentration (mg/L)	Flocculant concentration (mg/L)	Initial Brookfiel d (cP)	Final Brookfiel d (cP)
-	PolyMud (control)	-	-	-	74.64	74.64
		Тор		150	1650	26.46
83		Middle	150		1599	I.M. ^{a)}
		Bottom			1635	
	Al ₂ (SO ₄) ₃ / Telsun 5153	Тор	150	300	1761	29.52
82		Middle			1800	I.M. ^{a)}
		Bottom			1812	
		Тор	200	37.5	1257	19.92
77		Middle			1287	· I.M. ^{a)}
		Bottom			1311	
		Тор	200	75	1449	22.68
75		Middle			1677	I.M. ^{a)}
		Bottom			1818	I.IVI.
		Тор	600	75	NM b)	I.M. ^{a)}
74		Middle			1554	14.04
		Bottom			1674	I.M. ^{a)}

Table 3.25 represents the Brookfield viscosity for the runs performed with Al₂(SO₄)₃ combined with Telsun 5153.

The Brookfield viscosity of the solutions was compared to the PolyMud solution to evaluate the loss of viscosity. The apparent trend of the Brookfield viscosity is to decrease as the coagulant concentration increases and to increase as the flocculant concentration increased.

The lowest Brookfield value of 14.04 cP is obtained with the coagulant concentration of 600 mg/L, while the highest value of 29.52 cP is obtained with the coagulant concentration of 150 mg/L, Through direct comparison of the concentrations of 200 mg/L and 600 mg/L of coagulant, when 75 mg/L of flocculant is added, it can be observed that the lowest concentration of coagulant yielded a higher Brookfield viscosity value with 22.68 cP for the first concentration and 14.04 cP for the latter. Two possibilities exist to explain this phenomenon. The first is the direct coagulation of the PolyMud polymer in solution, reducing the viscosity. The second is the

screening of the negative charge of the clays that had not been coagulated and of the PolyMud, allowing the flocculant to also actuate on the latter.

For the runs applying concentrations of 150 mg/L and 200 mg/L of coagulant, increasing the concentration of flocculant increases the likelihood of unabsorbed high molecular weight anionic polymer in solution, which in turn increases the Brookfield viscosity of the solution through repulsion of these molecules and formation of tridimensional polymeric structures.

However, nor the density reductions or the aspect is controllable with these coagulant and flocculant concentrations, so other methods to control the dispersion of flocculant throughout the solution will be explored in the next chapter.

3.4.4 Study of the mixing speed and introduction method

The purpose of this subsection is to study the effect of the mixing speed and introduction types on the distribution of coagulant and flocculant throughout the solution. Fixed variables are coagulant type (Al₂(SO₄)₃), flocculant type (Telsun 5153), coagulant concentration (150 mg/L), flocculant concentration (150 mg/L), clay type (clay A from Terracota do Algarve) and mixing times (8 min). This study may lead to the controlled and non-uniform settling of flocs.

The mixing speed was fixed at 200 rpm before the introduction of flocculant to assure the formation of smaller flocs through the actuation of the coagulant and reduced to 20 rpm after the introduction of flocculant to reduce the dispersion in an attempt to control the flocculation. A run was also made at 200 rpm with internal introduction for comparison purposes. As described on protocol 2.3.3, after the introduction of coagulant, the mixing was performed for 3 minutes and then flocculant was introduced, and the agitation extended for another 4 minutes.

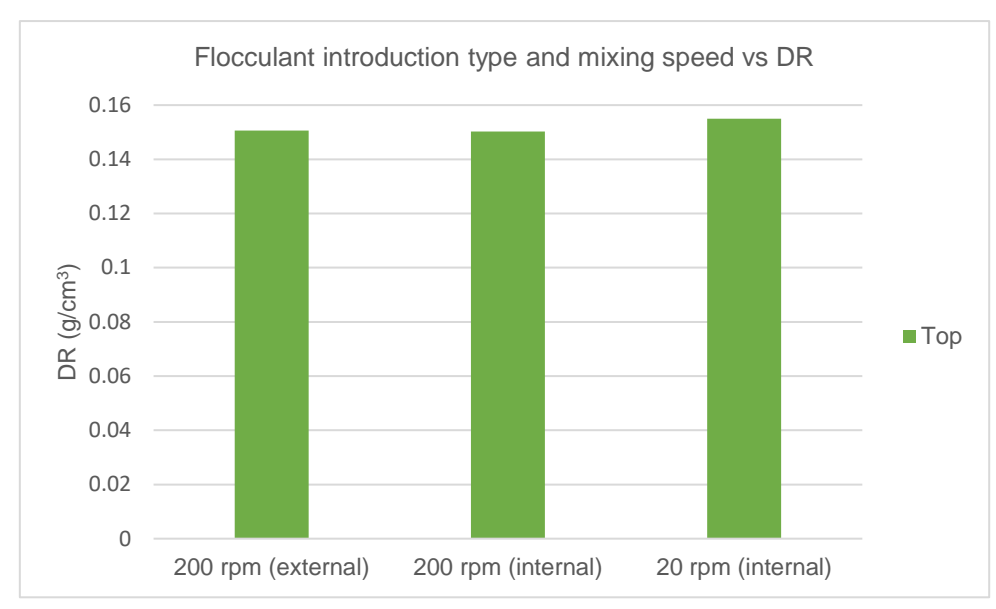


Figure 3.35 - Effect of the introduction type and mixing speed of the flocculant in DR

Figure 3.44 represents DR of the solutions when $Al_2(SO_4)_3$ was introduced previously to flocculant Telsun 5153. For comparison, a run was made at 200 rpm only varying the introduction type.

DR was still superior to the maximum value established by the objective (0.12 g/cm³). The difference between DR for the runs performed with internal and external introduction at 200 rpm was of 0.0004 g/cm³, which can be considered as almost identical. For the internal introduction runs at 20 rpm, it is very likely that the measured density was that of the flocculant, as due to the low intensity of the agitation, the flocculant would naturally rise in the column due to the density difference. In short, nor the internal addition at 200 rpm or the internal addition at 20 rpm created a significant variation in DR.

As DR does not clearly tell any case apart, a visual approach was taken to observe the results.

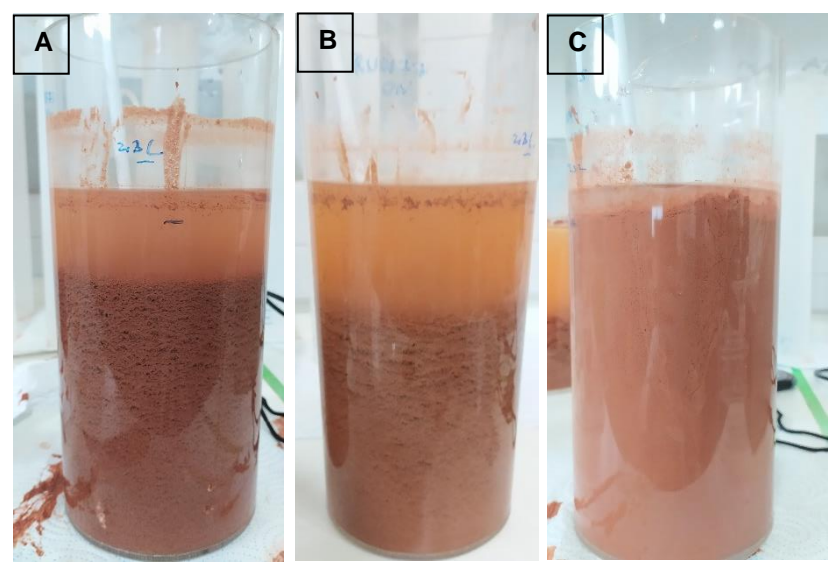


Figure 3.36 – Side view of the solutions treated with Al₂(SO₄)₃ and Telsun 5153 at 150 mg/L when introduced at: (A) – external introduction, 200 rpm; (B) – bottom, 200 rpm, and (C) – bottom, 20 rpm

Figure 3.45 represents the external aspect of the solutions treated with $Al_2(SO_4)_3$ and Telsun 5153, both at a concentration of 150 mg/L.

Solutions A and B are very similar to each other in appearance since the strips and the external aspect of the flocs produced are visually similar, while solution C, operated at 20 rpm after the introduction of flocculant, showed a very different aspect: the flocculant floated to the top due to the density difference and had limited interaction with the solution, as expected.

Table 3.26 - Introduction method and clean fluid height for the solutions treated with $Al_2(SO_4)_3$ and Telsun 5153

Run	Coagulant/ flocculant	Introduction method	Clean fluid height (cm)	Clean fluid height (%)
83		External	10	50%
86	Al ₂ (SO ₄) ₃ / Telsun 5153	Internal	10	50%
88		Internal, 20 rpm	3	15%

Table 3.26 represents the clean fluid heights for the solutions prepared previously.

When the introduction method was varied and the mixing speed was maintained, the clean fluid height did not change, as the flocculant still distributed evenly throughout the solution. When the introduction of flocculant was made internally and the mixing speed was reduced to 20 rpm, there was no clean strip, as the volume of liquid at the top corresponds to the flocculant that arose.

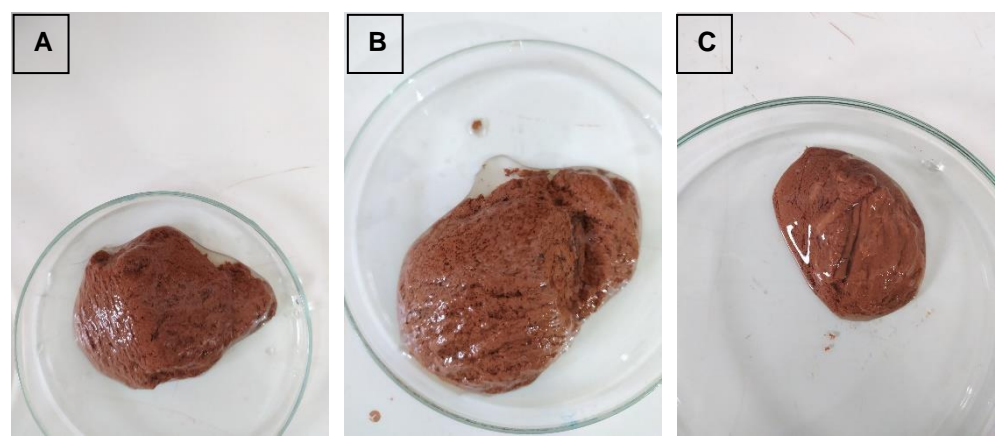


Figure 3.37 - Flocs taken from the solutions treated with $Al_2(SO_4)_3$ and Telsun 5153 at 150 mg/L when introduced at: (A) – top, 200 rpm; (B) – bottom, 200 rpm, and (C) – bottom, 20 rpm

Figure 3.46 represents the aspect of the flocs taken from the previous solutions. The floc consistency was very different for the solution C as well. Solutions A and B had very consistent flocs, matching the external aspect, while on the other hand, solution C had a very low consistency.

Taşdemir [165], in 2012, claims that rapid mixing and slow mixing serve two different purposes: rapid mixing distributes the flocculant uniformly and slow mixing promotes the enlargement of the smaller flocs without risking their breakage. However, for their work, rapid mixing was also used. They concluded that, as in coagulation, mixing speeds also influence the performance of the coagulation process. They tested slow mixing speeds of 10, 20, 30 and 40 rpm and concluded that 40 rpm was the slow mixing speed that generated the least amount of residual turbidity, while 20 rpm generated the highest. Results are in accordance, as when rapid mixing was used (200 rpm), flocs were of large dimensions and flocculation was uniformly distributed (not controlled) and when only slow mixing was used (20 rpm), the flocculant only reacted with the clay on its path upward and flocs did not form to the point that enlargement was possible.

Marsh viscosity and density gradients were impossible to measure due to the blockage of the nets. Thus, the Brookfield viscosities of the solutions that generated the clean strip were analyzed.

Table 3.27 - Initial and final Brookfield viscosity for the selected runs performed using performed with $Al_2(SO_4)_3$ when combined with Telsun 5153. ^{a)}Not measured due to the impossibility of drawing samples

Run	Coagulant/ flocculant	Zone	Introduction method	Mixing speed (rpm)	Initial Brookfield (cP)	Final Brookfield (cP)
-	PolyMud (control)	-	-	-	74.64	74.64
	Al ₂ (SO ₄) ₃ / Telsun 5153	Тор	External	200	1650	26.46
83		Middle			1599	N.M. ^{a)}
		Bottom			1635	IN.IVI.
	Al ₂ (SO ₄) ₃ / Telsun 5153	Тор	Internal		2013	37.80
86		Middle			1899	N.M. ^{a)}
		Bottom			1875	IN.IVI. ^{cs}
	Al ₂ (SO ₄) ₃ / Telsun 5153	Тор	Internal	20	2031	94.80
88		Middle			1731	1497
		Bottom			1773	1524

Table 3.27 represents the Brookfield viscosity measured of the solutions.

The Brookfield viscosity presents the lowest value (26.46 cP) when the flocculant is introduced externally. The internal introduction of flocculant (run 86) at 200 rpm also yielded a higher Brookfield viscosity value, as it may have assisted in the dispersion of the viscous, low-density solution, which would otherwise have caused diffusion issues when introduced externally. The Brookfield viscosity was at the highest when the mixing speed was set to 20 rpm before the introduction of flocculant. This viscosity may correspond to the viscosity of the Telsun 5153 solution, as, previously mentioned, this fluid came atop of the solution without completely reacting with the solution, due to the slow mixing speed reducing the dispersion and the difference between the density of the polymeric clay solution and the Telsun 5153 solution.

Overall, the reduction of the mixing speed does not accomplish its purpose of limiting the flocculant reaction with the solution to move to a more controlled reduction of density, as the majority of the flocculant did not react with the solution.

The attempts to control DR and maintain the viscosity of the solution were continued by varying the concentration of Al₂(SO₄)₃ and Telsun 5153. No progress was made, as boundary regions were observed where the solution either remained homogeneous or total flocculation of clay and PolyMud polymer was observed, which considerably decreased the Brookfield viscosity of the solution. Introducing the flocculant internally and reducing the mixing speed overshot the reduction of the dispersion of flocculant to attempt a non-uniform flocculation to control DR. More

studies should be made to attain this goal using a mixing speed higher than 20 rpm and lower than 200 rpm. No optimal conditions were achieved for this study, as for 200 rpm using internal and external introduction, the stability of the column was compromised by the complete flocculation of the solution. For 20 rpm using internal introduction, flocculant was observed at the top of the column, yet its application had no effect on the solution.

3.5 Influence of clay type

Due to clay stock rupture, the purpose of this subsection is to confirm the validity of the following runs. A comparison was made between the previously used clay supplied by Terracota do Algarve (clay A) and the currently used clay type supplied by MCS (clay B), according to protocol 2.3.1. Fixed conditions are mixing speed (200 rpm), mixing time (8 minutes), coagulant type (Al₂(SO₄)₃) and flocculant type (Microbond).

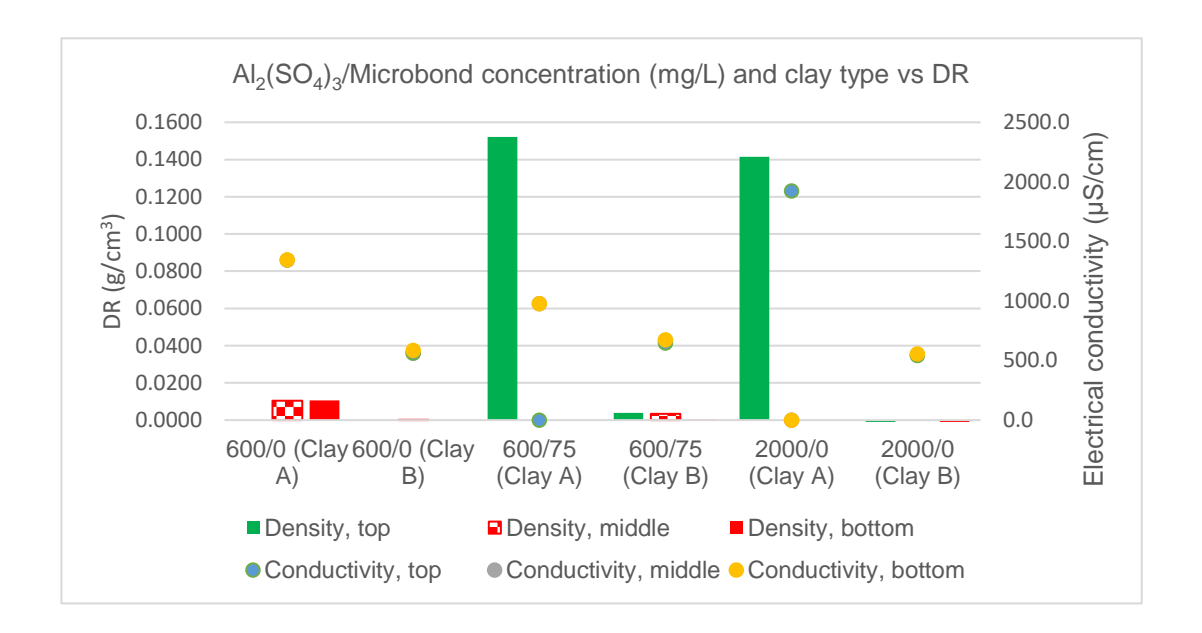


Figure 3.38 - Effect of Al₂(SO₄)₃ concentration, clay type, and Microbond concentration for 8 minutes and 200 rpm

Figure 3.38 represents the comparison of both clays when Al₂(SO₄)₃ is applied at 600 mg/L and 2000 mg/L with and without the addition of Microbond at 75 mg/L.

From the analysis of Figure 3.38, when Al₂(SO₄)₃ is used solely at the concentration of 600 mg/L, DR obtained by the run using clay A is 0.0106 and 0.0105 g/cm³ for middle and bottom areas, respectively and by approximately 0.01 g/cm³ to nearly null for the run where clay B was used. The same effect is observed at the concentration of 2000 mg/L of coagulant: DR decreased from 0.1415 g/cm³ with clay A to nearly null values with clay B. As seen on chapter 3.4.1, when Microbond was added, the DR from the runs using Clay A increased substantially

to 0.1521 g/cm³, which is over 0.15 g/cm³ is higher than clay B, which suggests that the charge neutralization in clay B was less effective.

Electrical conductivity was measured as a method to compare the availability for each clay to exchange ions. The runs using Clay A had an electrical conductivity of 1340 and 1344 μ S/cm, more than double of clay B's conductivity. Electrical conductivity for the Al₂(SO₄)₃/Microbond system was 977 μ S/cm for the middle zone for clay A, compared to 666 μ S/cm for clay B. Although the objective of this section is to compare clays, none of the runs performed on clay B fulfill any DR objective.

Zhang et al. [183] conducted trials using ferric chloride (FeCl₃) on bentonite and kaolinite, two common clay minerals. They claimed that higher doses of FeCl₃ were needed for bentonite, as this mineral has a higher negative charge than kaolinite. Tombácz and Szekeres [191] related the swellability of bentonite to its stability in aqueous systems. The results obtained in this study are in accordance with the present work. Onen and Göcer [189] studied coagulation-flocculation phenomena on Na-bentonites and Ca-bentonites. For Na-bentonites, the electrical conductivity was lower due its higher swelling and water holding capability.

It is possible that the clay B is a bentonite, due to its lower electrical conductivity, possibly due to the lower number of free ions in solution than the Clay A and higher swelling capability. Probably more negatively charged, clay B may require more coagulant to compress the electrical double layer, and consequently lower DR.

Table 3.28 - Initial densities, coagulant concentration, Marsh Viscosity gaps and final density gaps of the runs performed with Al₂(SO₄)₃. ^{a)}Marsh gap is calculated from the difference between initial and final values. ^{b)}Density gap is calculated from the difference between middle and bottom values. ^{c)}Impossible to measure due to blockage of the Marsh funnel net. ^{d)}Impossible to calculate. ^{e)}Not measured

Run	Zone	Initial density (g/cm³)	Coagulant concentration (mg/L)	Clay	Flocculant concentration (mg/L)	Marsh gap (s/quart) ^{a)}	Final density gap (g/cm³) ^{b)}
57	Middle	1.1607	600	^	0	4.4	0.0000
57	Bottom	1.1600	600	Α	0	-14	0.0008
	Тор	1.1605		В	0	-2	0.001
97	Middle	1.1611	600				
	Bottom	1.1617					
	Тор	-	600	А	75	I.M. ^{c)}	I.C. ^{d)}
72	Middle	1.1566					
	Bottom	1.1630					
	Тор	1.1561	600	В	75	8	0.0039
96	Middle	1.1569					
	Bottom	1.1576					
	Тор	1.1452	2000	А	0	I.M. ^{c)}	I.C. ^{d)}
59	Middle	1.1481					
	Bottom	N.M. ^{e)}					
108	Тор	1.1503	2000	В	0	I.M.c)	0.0017
	Middle	1.1523					
	Bottom	1.1522					

Table 3.28 represents the initial densities, Marsh Viscosity gaps and final density gaps of the runs performed with $Al_2(SO_4)_3$ at the concentrations of 600 mg/L and 200 mg/L, Microbond at 0 and 75 mg/L and clay types A and B.

All runs fulfill the objectives of having initial densities between 1.15-1.20 g/cm³ and creating a final density gap lower than 0.03 g/cm³, apart for runs 59 and 72, where this value was not possible to calculate. For the Marsh viscosity, only clay B clay without Microbond (run 97) fulfills the objective.

As seen on previous studies in this work, the application of coagulants generally reduces the Marsh viscosity. Therefore, the unchanging value obtained on run 97, may have been a consequence of insufficient concentration of coagulant that did not generate flocs in the solution, contrarily to the verified on the run 57. The increase in the final Marsh viscosity, when compared to the initial value observed in run 96 can be explained by the possibility of the formation of flocs that could not settle due to the small size, while still significant to cause drag throughout the

Marsh cone. Marsh viscosity was not possible to measure when 75 mg/L of Microbond was added to 600 mg/L of coagulant, since as adding long chain polymers into the solution increases the viscosity of the solution, making this measurement impossible. It was also not possible for 2000 mg/L of coagulant, as more flocs were formed which clogged the Marsh funnel.

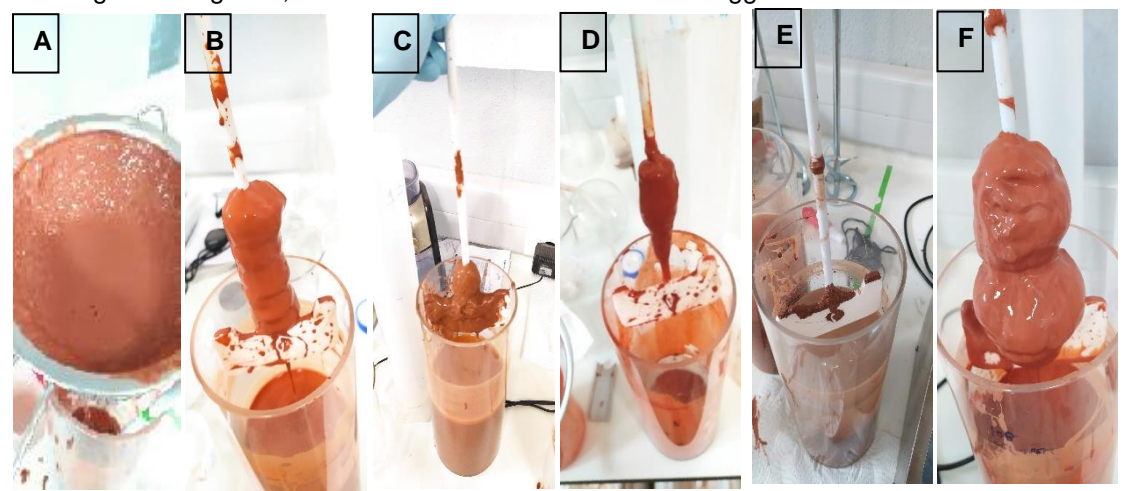


Figure 3.39 - Deposits on the nets and blades for (A) - Al₂(SO₄)₃, 600 mg/L (clay A); (B) - Al₂(SO₄)₃, 600 mg/L (clay B); (C) - Al₂(SO₄)₃ + Microbond, 600/75 mg/L (clay A); (D) - Al₂(SO₄)₃ + Microbond, 600/75 mg/L (clay B); (E) - Al₂(SO₄)₃, 2000 mg/L (clay A); (F) - Al₂(SO₄)₃, 2000 mg/L (clay B);

Figure 3.48 represents the deposits on the blades and nets for the solutions presented previously.

Only small amount of the deposits is collectable for all solutions, except 2000 mg/L with clay A. For this solution, no deposit was collectable, as even though the clay settled out of the solution, none remained on the blades.

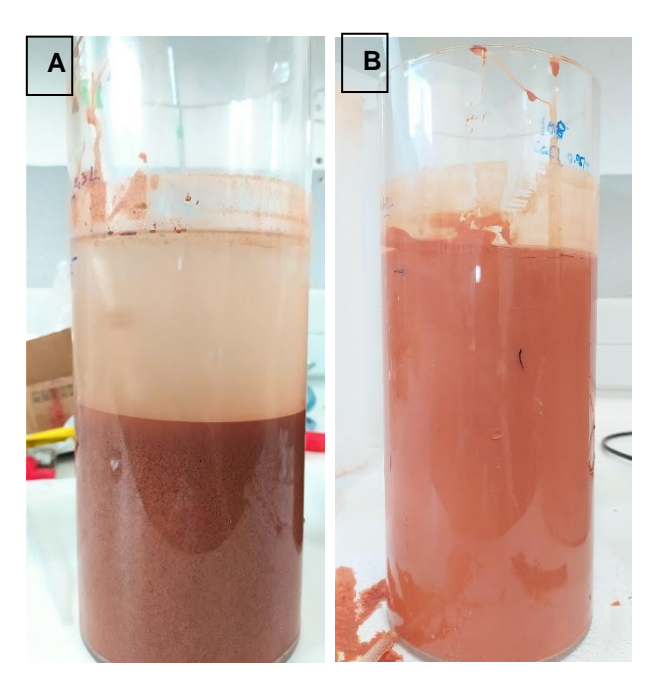


Figure 3.40 - Side view of the solutions treated with 2000 mg/L of Al₂(SO₄)₃ on: (A) - clay A; (B) - clay B

Figure 3.49 represents the aspect of the solutions treated with 2000 mg/L using clay A and clay B.

Furthermore, for 2000 mg/L, a noticeable difference in the external aspect is observed. For clay A, a large strip of clean fluid is formed, while for clay B, no strip is formed. This means that the electrical double layer was effectively compressed for clay A and that the stability of the column may be compromised. For clay B, the suspension remained stable and the repulsion between clays remains the dominant force, due to the lack of impact on DR, which hints that the charge neutralization was not effective.

For the next comparison study, Al₂(SO₄)₃ was combined with Telsun 5153 and both were applied on solutions containing the two clay types at different speeds, according to protocol 2.3.3. Fixed variables are mixing time (8 minutes), coagulant type (Al₂(SO₄)₃), flocculant type (Telsun 5153) and coagulant and flocculant concentration (150/150 mg/L) and clay type (clay B from MCS). The intent of this study is to compare the effect of the first concentration of coagulant and flocculant that completely cleaned the solution on both clays, the effect of the flocculation in high concentrations of polymer and the effect of reducing the mixing speed.

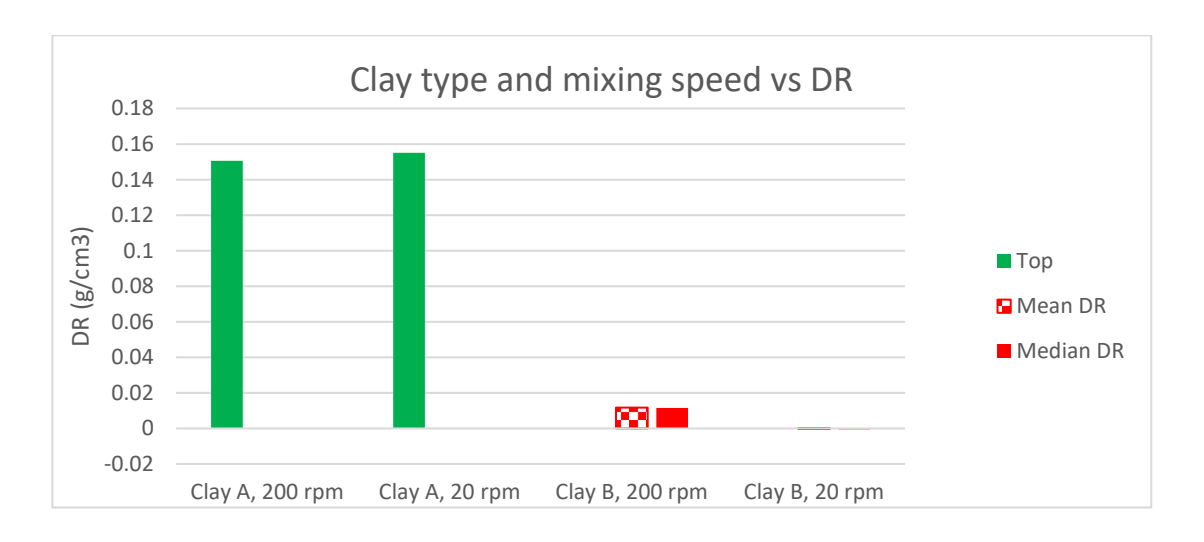


Figure 3.41 – Effect of clay types and mixing speeds on DR

Figure 3.41 represents the comparison of Al₂(SO₄)₃ with Telsun 5153 for clay A and clay B at different mixing speeds (200 and 20 rpm).

Samples were only taken from the top of the solutions tested on clay A due to the extent of the flocculation impairing the extraction of samples from other regions. On clay B, since it was possible to extract samples for every region, the mean and median of the values was then applied for examination.

From the analysis of the graph, it is possible to observe that DR decreases significantly for the run using 200 rpm on clay B. The run where the mixing speed was decreased to 20 rpm generated a slight but negligible DR decrease.

As seen previously in the literature results, bentonite requires a higher amount of coagulant for effective charge neutralization to occur, and the results obtained confirm that.

If the charge neutralization does not happen correctly, then the anionic flocculant cannot effectively form larger, faster settling flocs through electrostatic attractions, resulting in a lower DR.

Table 3.29 - Initial densities, concentrations, Marsh and final density gaps and Brookfield viscosities for the runs performed with Al₂(SO₄)₃₂ at different mixing speeds, for clay A and clay B. ^{a)}Marsh gap is calculated from the initial and final values. ^{b)}Final density gap is calculated from the difference between middle and bottom values. ^{c)}Impossible to measure due to blockage of the Marsh funnel net. ^{d)}Impossible to calculate. ^{e)}Not measured.

Run	Zone	Intial density (g/cm³)	Clay type	Mixing speed (rpm)	Marsh gap (s/quart) ^{a)}	Initial Brookfield (cP)	Final Brookfield (cP)	Final density gap (g/cm³) ^{b)}
	Тор	1.1524				1650	26.46	
83	Middle	1.1561		200		1599	N.M. ^{e)}	
	Bottom	1.1654	А		1.04.6)	1635	N.M. ^{e)}	10 4
88	Тор	1.1558		20	· I.M. ^{c)}	2031	94.8	0.0011
	Middle	1.156				1731	1497	
	Bottom	1.158				1773	1524	
	Тор	1.151			8	434	700.7	
95	Middle	1.1524		200		438	711.1	
	Bottom	1.1523				434	727.2	
	Тор	1.1482	В			446.8	424.8	0.0001
98	Middle	1.149		20	I.M. ^{c)}	448.8	439.2	
	Bottom	1.1504				456	450	

Table 3.29 represents the Initial densities, concentrations, Marsh and final density gaps and Brookfield viscosities for the runs performed with Al₂(SO₄)₃ and Telsun 5153 at different mixing speeds.

Initial densities were within the objective of 1.15-1.20 g/cm³. Final density gaps were lower than 0.03 g/cm³ when they were possible to calculate.

Marsh viscosity gap was only possible to calculate for the run using Clay B, at 200 rpm and it was lower than 5 s/quart. This increase of Marsh viscosity observed for this run was due to the introduction of a high molecular weight polymer that increases the viscosity of the solution, exacerbated by the possibility that PolyMud was not coagulated when the charge neutralization was ineffective. The impossibility of measuring the Marsh viscosity for clay A was due to the complete flocculation that occurred at 200 rpm and the partial flocculation that occurred at 20 rpm, which destabilized the solution locally. For clay B, Brookfield viscosity was used then to assess the solutions.

Initial Brookfield viscosities of the runs performed with clay A were nearly 4 times higher than those of clay B. This may be due to the possibility of the higher negative charges on clay B allowing this clay to form more uniform and more dispersed suspensions, resulting in a lower viscous drag. After the addition of Al₂(SO₄)₃ and Telsun 5153, Brookfield viscosities increased significantly from around 430 cP to approximately 700 cP in all zones for the run using Clay B at 200 rpm, due to the homogeneous dispersion of the flocculant increasing the viscosity of the column. No difference was observed for the run using Clay B at 20 rpm. It is possible that the flocculant did not interact with the solution at all due to the low mixing speed, hence the similarity of the Brookfield viscosities, coupled with the DR result. For clay A, at 200 rpm, the uniform distribution of flocculant caused a different effect than of the clay B due to the different properties of these clays causing the clay B to remain negatively charged, thus reducing the effectiveness of the anionic flocculant. The Brookfield viscosity was not measurable however for the 200 rpm run on clay B due to the complete flocculation and destabilization of the column, caused by the charge neutralization followed by the agglomeration of the flocs by the flocculant. As seen on chapter 3.4.4, on this clay, reducing the mixing speed caused the flocculant to rise to the top,

achieving in this manner a higher viscosity than the solution using 200 rpm, since the viscosity measured for the former mixing speed was of the flocculant that rose.

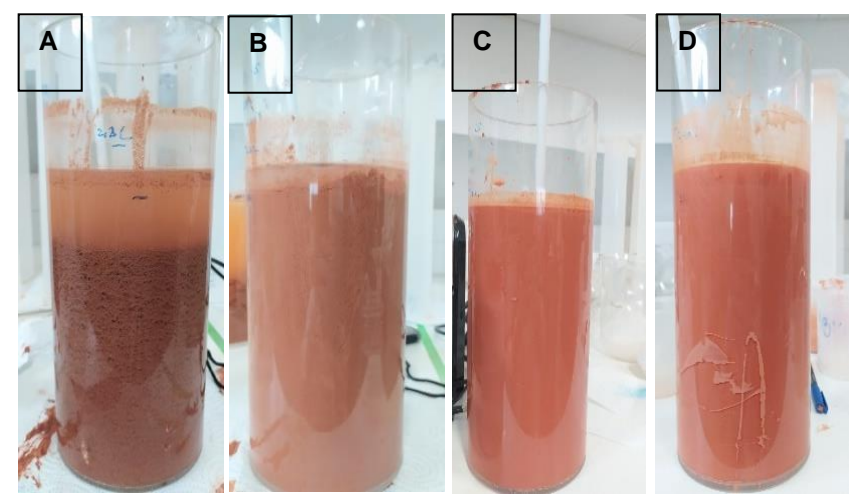


Figure 3.42 – Al₂(SO₄)₃ + Telsun 5153 at :(A) – Clay A (200 rpm); (B) –Clay A (20 rpm), 20 rpm (Terracota); (C) –Clay B (200 rom); (D) – Clay B (20 rpm)

Figure 3.51 represents the photos taken from the solutions treated with $Al_2(SO_4)_3$ in combination with $Al_2(SO_4)_3$ at different mixing speeds for both clays.

Photos A and B, from Figure 3.51 using Clay A were the only ones that produced any visual results. For solution A, large, fast settling flocs were observed, while for solution B, small, localized flocs were observed, although only in the ascending path of the flocculant solution. For the remaining solutions, no visual impact is observed, which reflects the DR results.

As previously mentioned, bentonite solutions have a higher negative charge, thus, more coagulant is required to compress the electrical double layer. For Clay A, even introducing 150 mg/L of coagulant is enough to form flocs that increase in size when flocculant is added. For clay B, since the coagulant concentration is not enough to neutralize the electrical double layer, adding anionic flocculant does not affect the solution, as no flocs are formed.

In conclusion, the clay type is an important factor in the coagulation due to their intrinsic properties that affect the stability of the solution, and consequently the coagulation process, such as the compression of the double layer. Furthermore, the systems that compromised the stability of the column on clay A, such as 600 mg/L of $Al_2(SO_4)_3 + 75 \text{ mg/L}$ of Microbond and 2000 mg/L of $Al_2(SO_4)_3$ no longer form the clean strips of fluid that cause this effect on clay B. Even though the column remained stable, DR values achieved for this clay did not accomplish any objectives.

For the next study, different combinations of coagulants and flocculants will be tested on clay B to increase DR.

3.6 Study of different coagulants and flocculants and their combinations

The purpose of this subsection is to compare the different combinations of coagulants and flocculants on the new clay B to attain a controlled density reduction, according to protocol 2.3.3. Fixed variables are coagulant and flocculant concentration (150 mg/L), clay type (clay B from MCS) and mixing times (8 min) and coagulant type (Al₂(SO₄)₃). Study variables is flocculant type (TelSun 5153 and Microbond). For this study, mean and median values of DR were calculated, as previously mentioned, to reduce the variability of the experiments, reduce the human error associated and in turn, simplify the results.

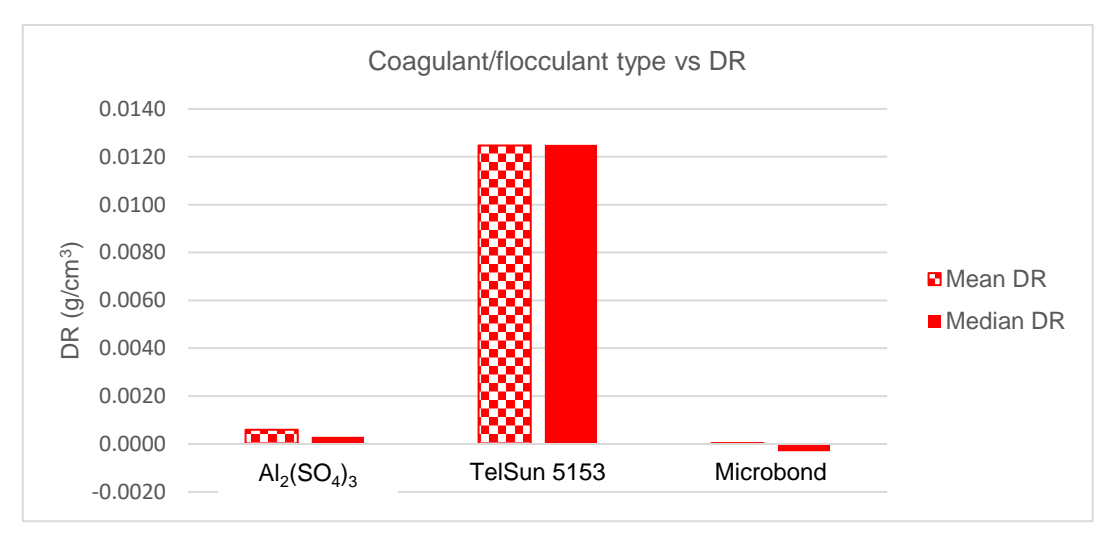


Figure 3.43 – Effect of $Al_2(SO_4)_3$, 5153 and Microbond at 150 mg/L

Figure 3.52 represents the comparison of $Al_2(SO_4)_3$ with anionic flocculant Telsun 5153 and cationic flocculant Microbond.

For the run where Al₂(SO₄)₃ was applied, mean DR value was 0.0006 g/cm³, nearly identical to the median DR value of 0.0003 g/cm³. For the Microbond run, the mean and median DR values were 0 and -0.0003 g/cm³, respectively. So, for both Microbond and Al₂(SO₄)₃ runs, DR values were practically null. The Telsun 5153 run produced mean and median DR values of 0.0116 g/cm³ and 0.0115 g/cm³, respectively. Thus, none of the runs performed achieve any DR objectives.

Generally, when cationic flocculants are used, these bind to clays through electrostatic attraction and form flocs through charge neutralization. When anionic flocculants bind to clays, these require a cationic ion to form a bridge between the anionic clay and the anionic polymer [192].

As seen previously, it is a possibility that the zeta potential of bentonite clays is more negative, thus requiring more cationic charge to neutralize these clays, hence the low DR from Al₂(SO₄)₃

and Microbond runs. Meanwhile, since the solution has a high concentration of NaOH to have a basic pH (10-11), the Na⁺ ions in solution may facilitate the approximation of anionic Telsun 5153 to the ionized clays at this pH range even though electrostatic repulsion plays a role.

Once Telsun 5153 obtained the highest DR, even though it was lower than the objective, for the next study, other coagulants were combined with this flocculant and compared amongst each other according to protocol 2.3.3. Fixed variables are mixing time (8 minutes), mixing speed (200 rpm), coagulant concentration (150 mg/L), clay type (clay B from MCS), flocculant type (TelSun 5153) and flocculant concentration (150 mg/L). Study variables are coagulant type (Al₂(SO₄)₃, FeSO₄, and PFS).

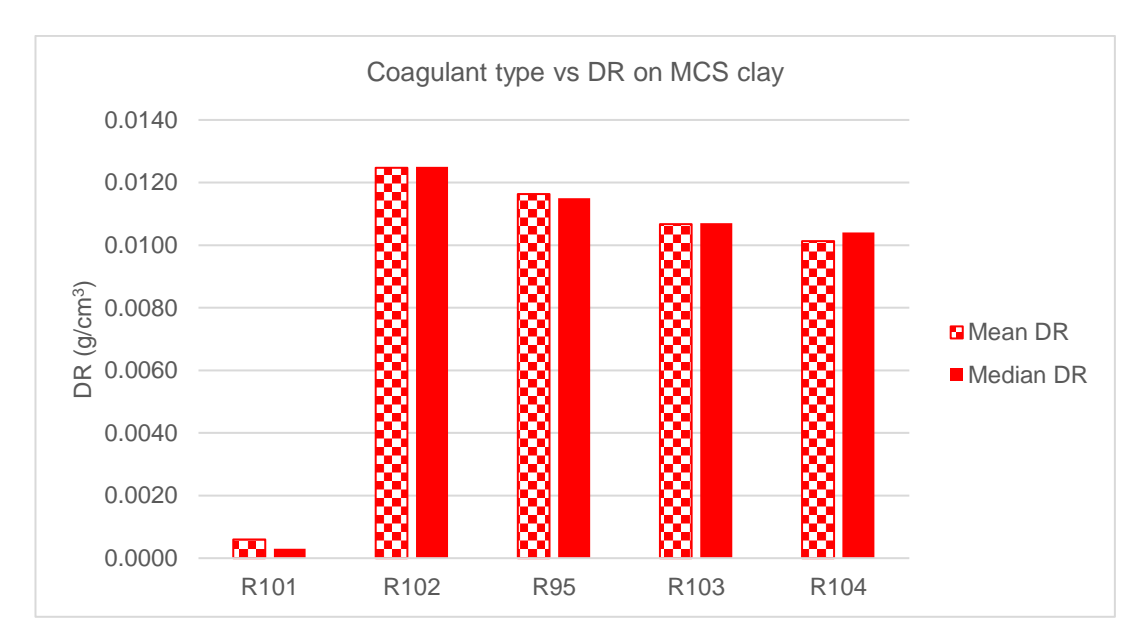


Figure 3.44 – Effect of Al₂(SO₄)₃, PFS and FeSO₄ combined with Telsun 5153 on DR

Figure 3.53 represents the comparison of three coagulants when used with Telsun 5153 at the concentration of 150 mg/L.

Table 3.30 - Coagulants and flocculants for the runs performed on Figure 3.53

Run	Coagulant	Flocculant	
101	Al ₂ (SO ₄) ₃	-	
102	-	Telsun 5153	
95	Al ₂ (SO4) ₃	Telsun 5153	
103	PFS	Telsun 5153	
104	FeSO ₄	Telsun 5153	

Table 3.30 represents the coagulants and flocculants used on the runs shown on Figure 3.53.

From the analysis of the graph, it is possible to observe that DR does not see significant change for any of the other coagulants tested along with Telsun 5153. For the combination of coagulant and flocculant, independently of the coagulant used, DR had mean and median values between 0.0101 and 0.0116 g/cm³, respectively, thus, very similar very low and did not reach the lowest DR objective When these values are compared to the Al₂(SO₄)₃ run without Telsun 5153 and vice-versa, it is obvious that Telsun 5153 had a much larger influence than Al₂(SO₄)₃. Nonetheless, none of the DR objectives were achieved.

As described in the previous Figure 3.52 discussion, the coagulants had a very low influence on the charge neutralization, due to the high negative charge of bentonite suspensions, and instead, DR was achieved mainly due to the electrolytes in solution providing a bridge that allowed for the Telsun 5153 to bond to the clays.

Table 3.31 – Initial densities, concentrations, Marsh and final density gaps for the runs performed with different coagulant types combined with Telsun 5153. ^{a)}Marsh gap is calculated from the initial and final values. ^{b)}Final density gap is calculated from the difference between middle and bottom values. ^{c)}Impossible to measure due to blockage of the Marsh funnel net

Run	Zone	Initial density (g/cm³)	Coagulant/ flocculant	Coagulant/ flocculant concentration (mg/L)	Marsh gap (s/quart) ^{a)}	Final density gap (g/cm³) ^{b)}
	Тор	1.1624				
102	Middle	1.1630	Telsun 5153		12	0.0005
	Bottom	1.164				
	Тор	1.1551		450/0		
101	Middle	1.1562	Al ₂ (SO ₄) ₃	150/0	0	0.0001
	Bottom	1.1574				
	Тор	1.1612				
99	Middle	1.1620	Microbond		1	0.0008
	Bottom	1.1638				
	Тор	1.1510	AL (00) (8	0.0011
95	Middle	1.1524	Al ₂ (SO ₄) ₃ / Telsun 5153			
	Bottom	1.1523	10,00110100			
	Тор	1.1644		450/450		
103	Middle	1.1651	PFS/Telsun 5153	150/150	I.M.c)	0.0002
	Bottom	1.1653	0100			
	Тор	1.1640				
104	Middle	1.1657	FeSO ₄ /Telsun 5153		5	0.0004
	Bottom	1.1668	0100			

Table 3.31 represents the initial densities, Marsh Viscosity gaps and final density gaps of the runs performed with Al₂(SO₄)₃, PFS and FeSO₄ with Telsun 5153

All runs fulfill the objectives of having initial densities between 1.15-1.20 g/cm³ and creating a final density gap lower than 0.03 g/cm³. For the Marsh viscosity, all runs fulfilled this objective when it was measurable.

It is likely that simultaneously to the reduced effect of the coagulant for the reasons mentioned previously, the high molecular weight polymer Telsun 5153 is affecting the solution's viscosity, hence the general trend of the increase of the Marsh viscosity whenever this polymer was applied.

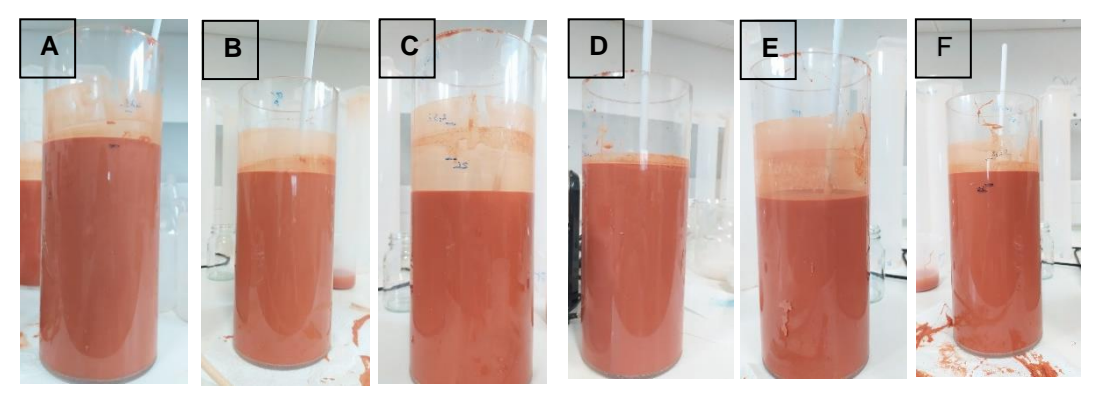


Figure 3.45- Side view of the runs performed with (A) – Microbond; (B) - $Al_2(SO_4)_3$; (C) – Telsun 5153; (D) – $Al_2(SO_4)_3$ + Telsun 5153; (E) – PFS + Telsun 5153; (F) – FeSO4 + Telsun 5153

Figure 3.54 represents the visual aspect of the solutions prepared above.

All solutions remained homogeneous, and no effect is observable. This may be due to charge neutralization being insufficient for the positively charged Al₂(SO₄)₃ and Microbond and the weak interactions between Na⁺ ions and clay being insufficient to form flocs large enough to settle effectively.

In conclusion, the charge of the coagulation/flocculation agent is also important, as charge neutralization is not the only form of coagulation, however, none of these agents were able to impact the solutions DR, possibly due to the very negative zeta potential of the solution. The charge neutralization must occur for the electrical double layer to be compressed effectively, and consequently promote aggregation. Charge screening was slightly more effective than charge neutralization, possibly due to the sodium ions in solution. Since these ions can also promote aggregation, as seen on chapter 1.2.2, for the next chapter, calcium and sodium salts will be

used to control the coagulation process through the reduction of the valency of the salts, in order to have a higher margin for control.

3.7 Study of calcium and sodium salts

The purpose of this subsection is to study the influence of the cation valency on the visual impact of coagulation using calcium and sodium salts and indirectly increase the electrical conductivity due to the presence of these salts in solution, according to protocol 2.3.1. Fixed variables are mixing time (8 minutes), clay type (clay B from MCS) and mixing speed (200 rpm).

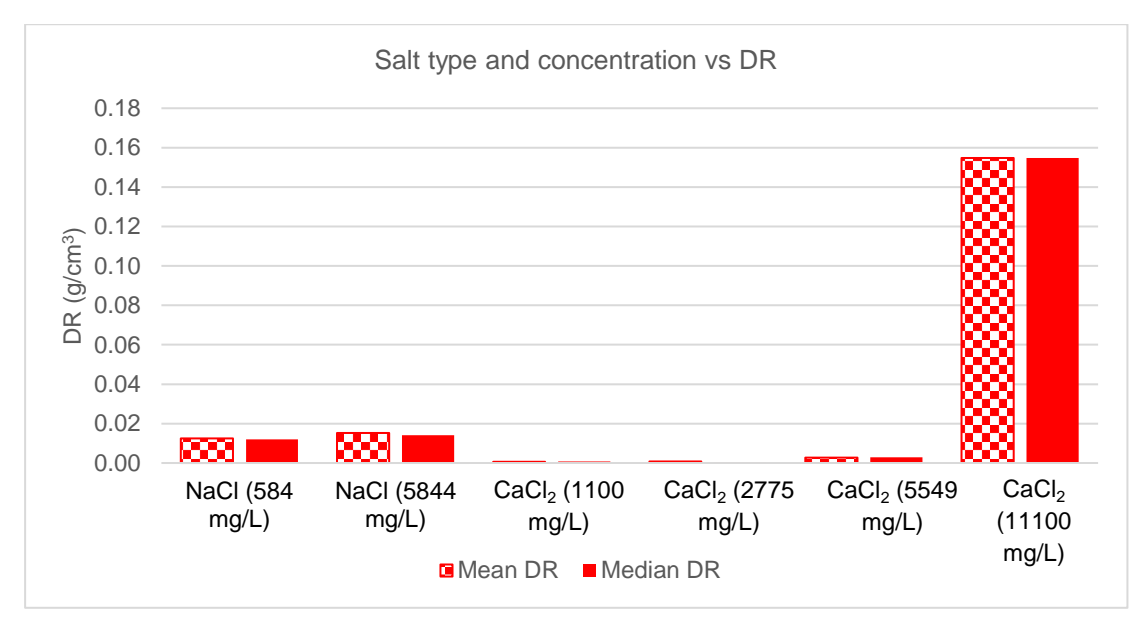


Figure 3.46 - Effect of NaCl and CaCl2 at different concentrations with clay B on DR

Figure 3.55 represents the DR when NaCl was used in concentrations of 584 and 5844 mg/L (corresponding to 0.01 and 0.1M) and CaCl₂ in the concentrations of 1110, 2775, 5549 and 11100 mg/L (corresponding to the concentrations of 0.01, 0.025, 0.05 and 0.1M).

DR reached a mean value of 0.0124 g/cm³ and a median value of 0.0120 g/cm³ for the run where 584 mg/L of NaCl were applied and a maximum of 0.0154 g/cm³ for the run using a concentration of 5844 mg/L of NaCl on the bottom area. For CaCl₂ runs, DR was minimal below 11100 mg/L, and slightly increased mean value to 0.0028 g/cm³ at the concentration of 5549 mg/L. At 11100 mg/L, a sharp increase is observed, and DR at the top reaches the value of 0.1548 g/cm³. Thus, DR for 0.02 g/cm³ is achieved for NaCl, while no DR results are achieved for 11100 mg/L,

Niriella and Carnahan (2006) [193] conducted studies on bentonite using salts and measured the zeta potential of the solutions. In 0.001M and 0.01M NaCl solutions, the zeta potential did not change. Fil et al. (2014) [194] conducted studies on montmorillonite clays using monovalent,

divalent and trivalent salts. Increasing the valency of the salts increased the zeta potential towards less negative values.

Such results are in accordance with the present work, as for the runs using concentrations of 0.01 and 0.1M of NaCl, the low DR values can be indirectly compared to the zeta potential results – since no change was observed at these concentrations, it could be assumed that the zeta potential was not in optimal range for coagulation.

It is possible that coagulation using NaCl requires a higher concentration than the ones used due to the monovalent nature of the Na⁺ ion, while for CaCl₂, the highest concentration, which was vastly superior to the highest NaCl concentration, was enough to completely clean the solution, destabilize the column and compromise its stability. The behavior of NaCl at the concentration of 11100 mg/L is unknown. The inversion of behavior is typical when salts are used. When low concentrations are applied, low DR values are achieved and for the concentration of 11100 mg/L of CaCl₂ and the column is destabilized.

Table 3.32 - Initial densities, coagulant concentrations, initial and final brookfield values and final density gaps for the solutions treated with NaCl and CaCl₂. ^{a)}Density gap is calculated from the difference between middle and bottom values ^{b)}Impossible to measure due to inability to collect samples.

^{c)}Impossible to calculate

Run	Zone	Initial density (g/cm³)	Salt	Salt concentration (mg/L)	Initial Brookfield (cP)	Final Brookfield (cP)	Final density gap (g/cm³)a)
	Тор	1.1424			417.6	4776	
111	Middle	1.1429	NaCl	584	427.2	5664	0.0013
	Bottom	1.1441			427.2	5334	
	Тор	1.1542			352.8	3196	
112	Middle	1.1562	NaCl	5844	357.6	3840	0.0023
	Bottom	1.1579			356.4	3138	
	Тор	1.1512	CaCl ₂	1110	484.8	441.6	0.0011
106	Middle	1.1517			480.0	452.0	
	Bottom	1.1520			472.8	420.0	
	Тор	1.1533			392.4	351.6	
109	Middle	1.1542	CaCl ₂	2775	400.8	352.8	0.0008
	Bottom	1.1551			399.6	351.6	
	Тор	1.1589			398.4	300.0	
107	Middle	1.1603	CaCl ₂	5549	402.0	303.6	0.0007
	Bottom	1.1605			396.0	309.6	1
	Тор	1.1574			402.0	2.2	
105	Middle	1.1577	CaCl ₂	11100	404.4	L D A b)	I.C. ^{c)}
	Bottom	1.1590			405.6	I.M. ^{b)}	

Table 3.32 represents the initial densities, salt concentrations, initial and final Brookfield viscosity values. This last variable was measured due to the difficulty of measuring the Marsh viscosity of the solutions and will be used to indirectly evaluate the change of viscosity of the solutions.

All runs fulfill the objectives of having initial densities between 1.15-1.20 g/cm³ and creating a final density gap lower than 0.03 g/cm³, except for run 105, where the latter was not possible to calculate. Brookfield viscosity tends to decrease as salt concentration is increased, as expected, since as seen on previous chapters, increasing the coagulant (or salt) concentration produces a side effect of coagulating PolyMud along with the clay. At the top, Brookfield viscosity is significantly lower for the CaCl₂ treated solutions, especially at the top for the CaCl₂ concentration of 11100 mg/L since as explained previously, the higher valency and the bridging effect may be causing a collateral coagulation of the PolyMud.

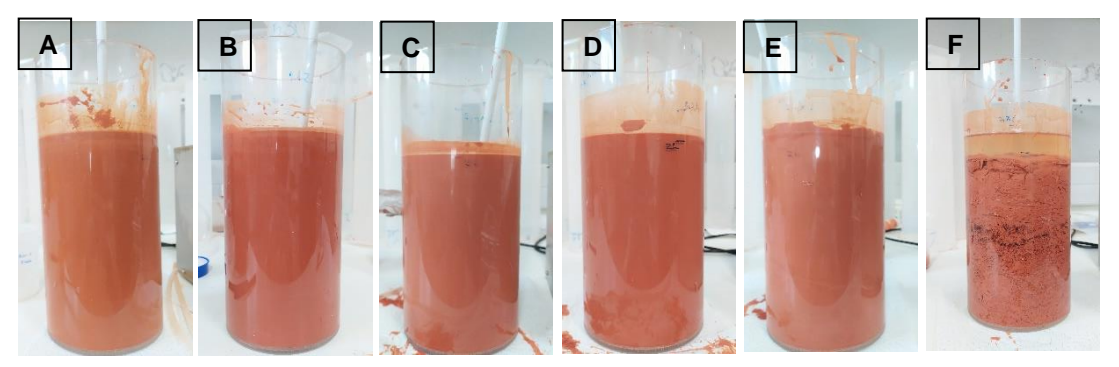


Figure 3.47 - Side view of the solutions treated with (A) – NaCl, 584 mg/L; (B) – NaCl, 5844 mg/L; (C) – CaCl₂, 1110 mg/L; (D) – CaCl₂, 2775; (E) – CaCl₂, 5549 mg/L; (F) – CaCl₂, 11100 mg/L

Figure 3.56 represents the visual aspect of the solutions treated with NaCl and CaCl₂ at different concentrations.

For NaCl solutions, no impact was observable. For CaCl₂ solutions, up to the concentration of 5549 mg/L, no impact is observable again, although, at the concentration of 11100 mg/L, the solution is heavily flocculated and a strip of clean fluid was formed, meaning that the stability of the column may be compromised. This also means that the latter concentration is unviable.

For the run using the latter concentration of CaCl₂, the concentration of Ca²⁺ ions in solution may have been sufficient to compress the electrical double layer enough to promote coagulation,

In conclusion, even though NaCl runs produced DR results within the objective, it could not produce a visual impact on the solution. Runs using CaCl₂ did not achieve any DR objective for any concentration, as for the runs using concentrations below 11100 mg/L, DR did not achieve 0.02 g/cm³, and for the former concentration, the column became inoperable. This hints that the action of the divalent CaCl₂, particularly the bridging effect that it can cause between two clay particles, not controllable. The results also hint that there is a margin to explore NaCl for later studies. In this manner, the dispersant used to suspend the clay will be reduced to reduce the amount of coagulant required.

3.8 Study of the reduction of dispersant

The purpose of this subsection is to study the effect of the reduction of anionic sodium polyacrylate-based dispersant, GPlus, to increase the DR, according to protocol 2.3.1. GPlus is of the family of sodium polyacrylates. These are anionic polymers traditionally used as dispersants., which increase the stability of the suspensions an its been used to achieve to initial density required. Fixed variables are clay type (clay B from MCS) and mixing time (8min). This study may lead to the reduction of coagulant/flocculant necessary to achieve coagulation/flocculation by reducing the initial concentration of GPlus, thus reducing the stability of the initial solution.

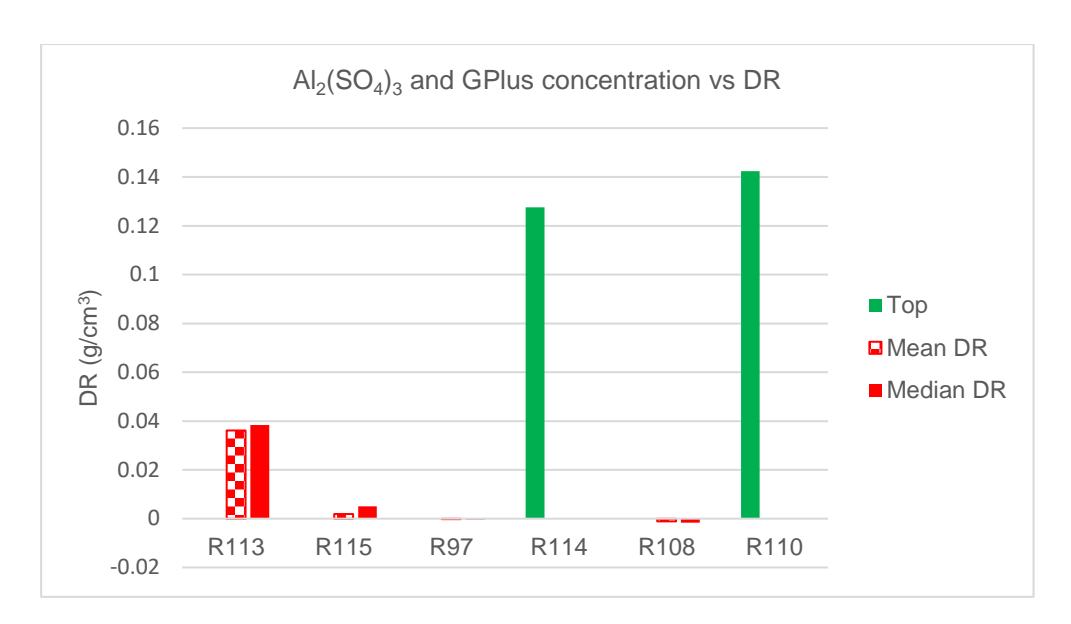


Figure 3.57 - Effect of Al₂(SO₄)₃ concentration on clay B at 0 and 1.5 mL/L of GPlus Figure 3. represents DR in function of Al₂(SO₄)₃ at GPlus concentrations of 0 and 1.5 mL/L.

Table 3.34 - Coagulant (Al₂(SO₄)₃) and GPlus concentrations for the runs performed

Runs	Coagulant concentration (mg/L)	GPlus concentration (mL/L)
113	0	0
115	300	0
97	600	1.5
114	600	0
108	2000	1.5
110	2000	0

In general, DR is practically null for the runs using Al₂(SO₄)₃ concentrations of 600 and 2000 mg/L, when GPlus is applied. For the former, mean and median values are -0.0002 and -0.0003 g/cm³, respectively. For the latter, mean and median values are -0.0012 and -0.0017 g/cm³, respectively. DR increases when GPlus is removed. However, for the run using 300 mg/L without GPlus, DR is still below the objective of 0.02 g/cm³. For the runs performed with the Al₂(SO₄)₃ concentration of 600 mg/L, this increase is of 0.1278 g/cm³ and for the Al₂(SO₄)₃ concentration of 2000 mg/L, this increase is 0.1435 g/cm³. None of the runs performed attain any DR objective.

Ersoy et al. [195] conducted experiments on kaolinites slurries in the presence of dispersants. They concluded that zeta potential became more negative when dispersants were used, and these stabilized the suspensions through electrostatic repulse. This is in accordance with the

results in this work, as the solutions without GPlus achieved a higher DR, which can be indirectly related to the ease of destabilization of the suspensions.

In conclusion, removing GPlus removes anionic charges from the system, reducing the barrier for coagulation and promoting the compression of the electrical double layers, however this also increases the likelihood of cleaning the solution completely, which is not the goal.

Table 3.33 - Initial densities, coagulant concentrations, initial and final brookfield values and final density gaps for the solutions treated with Al₂(SO₄)₃ with and without GPlus. ^{a)}Density gap is calculated from the difference between middle and bottom values. ^{b)}Impossible to measure due to inability to collect samples. ^{c)}Impossible to calculate

Run	Zone	Initial density (g/cm³)	Coagulant concentration (mg/L)	GPlus concentration (mL/L)	Initial Brookfield (cP)	Final Brookfield (cP)	Final density gap (g/cm³)ª
	Тор	1.1549			436.8	367.2	
113	Middle	1.1605	0	0	544.8	518.4	0.0174
	Bottom	1.1612			667.2	589.2	
	Тор	1.1290	300	0	680.4	483.6	
115	Middle	1.1303			698.4	483.6	0.0045
	Bottom	1.1329			760.8	667.2	
	Тор	1.1605	600	1.5	410.4	393.6	0.0010
97	Middle	1.1611			408.0	397.2	
	Bottom	1.1617			411.6	385.2	
	Тор	1.1293			775.2	29.8	
144	Middle	1.1369	600	0	796.8	129.6	I.C.c)
	Bottom	1.1382			825.6	I.M. ^{b)}	
	Тор	1.1503			435.6	396.0	
108	Middle	1.1523	2000	1.5	445.2	411.6	0.0017
	Bottom	1.1522			450.0	412.8	
	Тор	1.1424			652.8	1.44	
110	Middle	1.1556	2000	0	519.6	I.M. ^{b)}	I.C.c)
	Bottom	1.1560			612.0	1.IVI.~ ⁷	

Table 3.33 represents the initial densities, $Al_2(SO_4)_3$ concentration, initial and final Brookfield viscosity values. This last variable was measured due to the impossibility of measuring the Marsh viscosity, particularly for the concentrations of 600, when GPlus is removed and 2000 mg/L, using both concentrations of GPlus.

Initial densities were within the objective of 1.15-1.20 g/cm³ for all runs except for the coagulant concentrations of 300 and 600 mg/L without GPlus, since the removal of this additive

reduces the overall negative charges, which reduces the repulsion between clays and consequently, reduces the stability of the system. Final density gaps created were lower than the objective of 0.03 g/cm³ when they were possible to calculate.

Brookfield viscosities decrease after the application of coagulant, with steeper reductions when GPlus is not present in the system and as the coagulant concentration is increased, as expected.

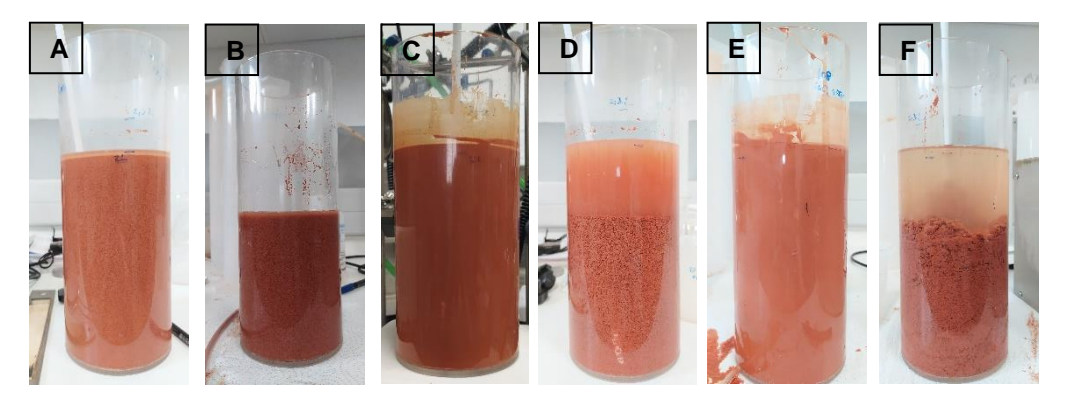


Figure 3.48 – Side view of the solutions treated with $Al_2(SO_4)_3$ at: (A) – 0 mg/L (no GPlus); (B) – 300 mg/L (no GPlus); (C) – 600 mg/L; (D) – 600 mg/L (no GPlus); (E) – 2000 mg/L; (F) – 2000 mg/L (no GPlus)

Figure 3.58 represents the visual aspect of the solutions treated with Al₂(SO₄)₃ at different concentrations with and without the presence of GPlus.

In the solutions where GPlus was present, no visual effect was observed for any concentration. When GPlus was removed, a clean fluid section was observed for the concentrations of 600 and 2000 mg/L, meaning that the clay is nearly completely removed. This also means that the stability of the column may have been compromised and that the concentrations of 600 mg/L and 2000 mg/L without GPlus are unviable. Furthermore, elimination GPlus from the system is undesirable, as the viable concentration zone is smaller, as lower concentrations of coagulant completely clean the solution, compared to the concentration of 1.5 mL/L of GPlus.

For the next study, other coagulants were tested without GPlus. Fixed variables are mixing time (8 minutes), mixing speed (200 rpm) and coagulant concentration (300 mg/L), according to protocol 2.3.3. Study variable is coagulant type (Al₂(SO₄)₃, PFS and AO410).

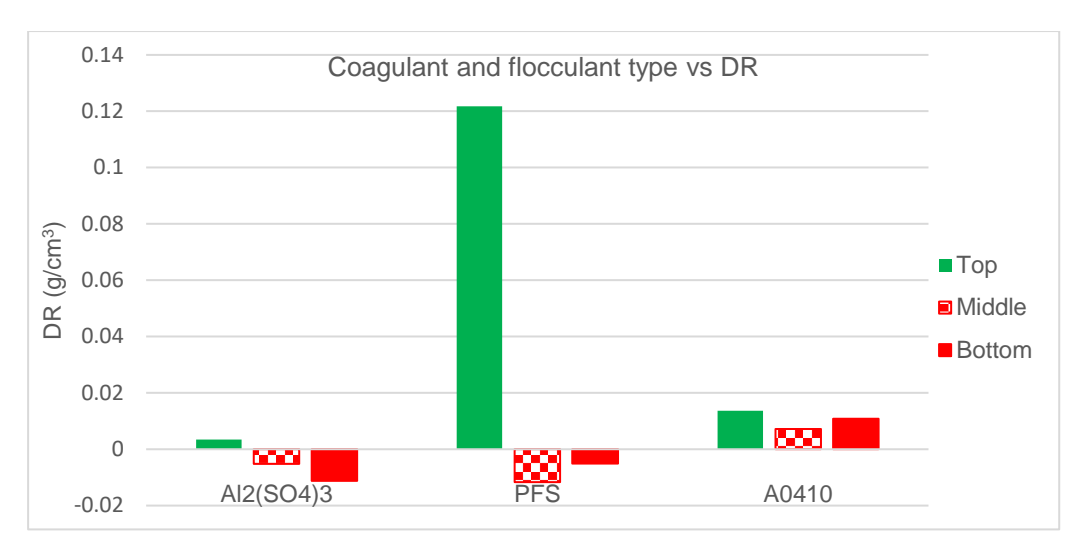


Figure 3.49 – Effect of coagulant and flocculant type on DR at the concentration of 0 mL/L of GPlus

Figure 3.59 represents DR in function of coagulant ($Al_2(SO_4)_3$ and PFS) and flocculant type (A0410) at 300 mg/L when GPlus is removed.

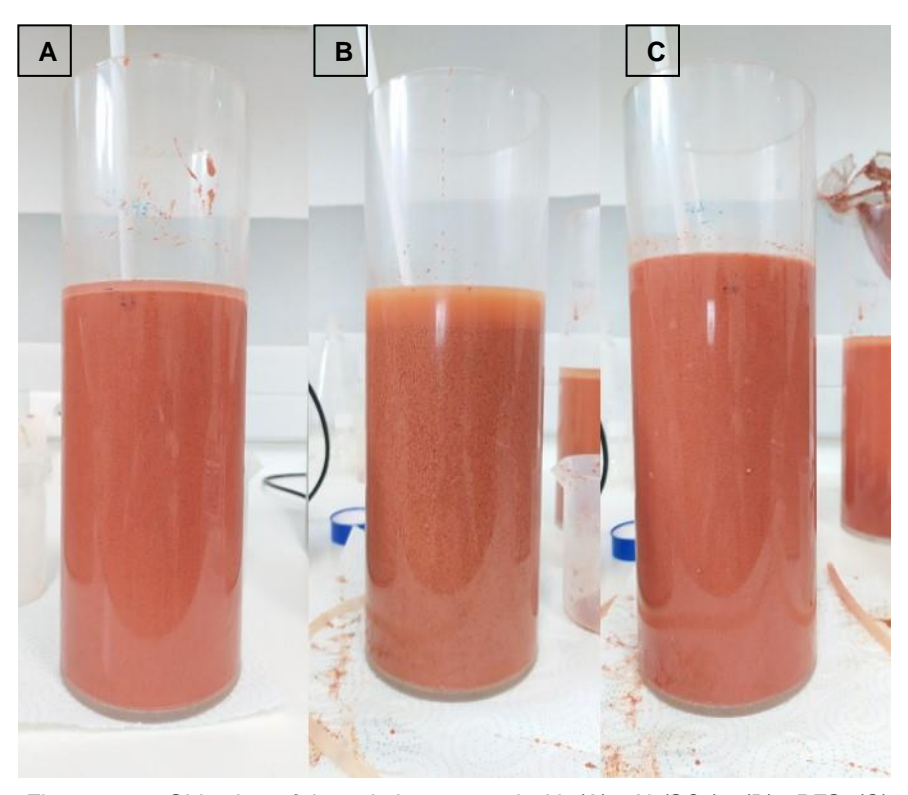


Figure 3.50 - Side view of the solutions treated with (A) - Al₂(SO₄)₃; (B) - PFS; (C) - A0410

Figure 3.60 represents the visual aspect of the solutions treated with $Al_2(SO_4)_3$, PFS and A0410 at the concentrations of 300 mg/L.

For the $Al_2(SO_4)_3$ run, DR values for top, middle, and bottom were -0.0034 g/cm³, -0.0052 g/cm³ and -0.0112 g/cm³, respectively. For the run performed with FPS, DR values for top,

middle and bottom zones were 0.1218 g/cm³, -0.117 g/cm³ and -0.0051 g/cm³, respectively. For the A0410 run, DR values for top, middle, and bottom zones were 0.0137 g/cm³, 0.0072 g/cm³ and 0.0108 g/cm³. The run performed with PFS attained the highest DR value amongst the solutions tested, as the suspended clay settled quickly at the top. No DR objective was achieved.

As seen on chapter 3.3.2, the polymerized ferric hydroxides contained in the structure of PFS may have an added effect on the adsorption on clays, and consequently on the coagulation when compared to Al₂(SO₄)₃, which relies almost totally on charge neutralization. A0410 had a superior DR than Al₂(SO₄)₃ possibly due to the volume added, as preparing very concentrated stock polymer solutions creates diffusion problems adding the possibility that a dilution effect may have occurred. This can also be inferred due to the higher DR combined with the homogeneity of the column and the lack of clean strip, hinting that it is possible that flocs may not have formed, and the dilution is the predominant effect.

The visual aspect is also more pronounced at the top for the PFS solution. It indicates heavier flocs and a more destabilized solution

Table 3.34 - Initial densities, concentrations, initial and final Brookfield viscosities and final density gaps for the runs performed with Al₂(SO₄)₃, PFS and AO410. ^{a)}Density gap is calculated from the difference between middle and bottom values. ^{b)}Impossible to calculate due to inability to collect samples.

Run	Zone	Initial density (g/cm³)	Coagulant/flocculant	Initial Brookfield (cP)	Final Brookfield (cP)	Final density gap (g/cm³)a)
	Тор	1.1270		774	872.2	
143	Middle	1.1275	A0410	806.4	855.6	0.0004
	Bottom	1.1307		770.4	898.8	
141	Тор	1.1326		759.6	550.8	
	Middle	1.1277	Al ₂ (SO ₄) ₃	802.8	674.4	0.0053
	Bottom	1.1270		822	649.2	
	Тор	1.1236		602.4	62.88	
142	Middle	1.1275	PFS	646.8	182.4	I.C. ^{b)}
	Bottom	1.1368		746.4	214.8	

Table 3.34 represents Initial densities, concentrations, initial and final Brookfield viscosities for the runs performed with Al₂(SO₄)₃, PFS and A0410.

Initial densities were not within the objective range of 1.15-1.20 g/cm³ due to the reduction of the dispersant leading to the loss of stability of the suspensions and consequent settling of the

clay before the experiment. Density gaps created for A04010 and Al₂(SO₄)₃ runs were lower than the objective of 0.03 g/cm³.

Brookfield viscosities increased for A0410 solution due to the addition of a large volume of high molecular weight polymer, as expected. For Al₂(SO₄)₃ and PFS, Brookfield viscosities decreased, with the latter producing a more pronounced decrease, as expected from the DR results.

In conclusion, DR objectives were not achieved for any run tested. Runs using Al₂(SO₄)₃ and A0410 generated practically no effect on the solutions, while the run using PFS generated a clean strip of fluid, combined a noticeable coagulation, making the use of PFS unviable. It is likely that the removal of GPlus is the main cause of this effect.

For the next study, cationic flocculants were combined with NaCl to attempt to use the former to create flocs after the action of NaCl on the aggregation of the clays, according to protocol 2.3.3. Fixed variables are mixing time (8 minutes), mixing speed (200 rpm), Gplus concentration (0.5 mL/L), salt type (NaCl), salt concentration (5844 mg/L), clay type (clay B from MCS) and flocculant concentration (50 mg/L).

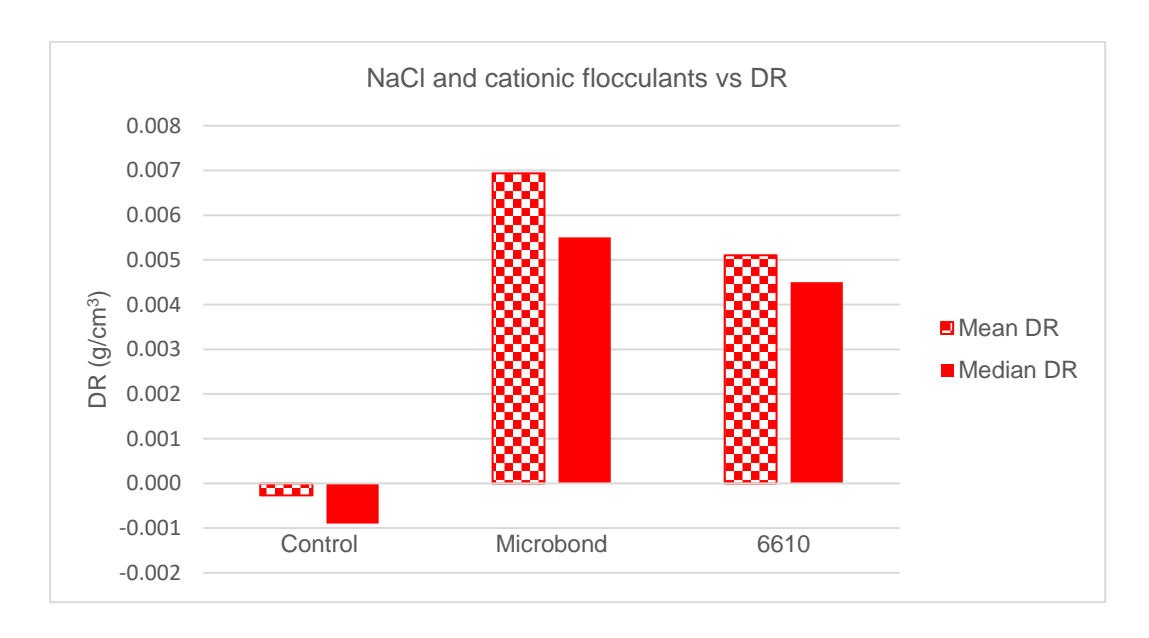


Figure 3.61 – Effect of NaCl with cationic flocculants a 5844/50 mg/L and 0.5 mL/L of GPlus

Figure 3. represents DR when NaCl is used in combination with either Microbond or 6610, where NaCl is applied at 5844 mg/L and the flocculants at concentration of 50 mg/L. Control run was performed without the addition of any product.

Both runs using Microbond and 6610 present values higher than the control run, meaning they might have had some effect on DR compared to the natural settling. The run performed

with Microbond produced mean and median DR values of 0.0069 g/cm³ and 0.0055 g/cm³, respectively. The run performed with 6610 produced mean and median DR of 0.0051 g/cm³ and -0.0045 g/cm³, respectively. Overall, the Microbond run had a very similar DR value to 6610. No DR objective was achieved for any combination tested.

Wilkinson et al. (2018) [196] tested the flocculation of bentonites under different pH ranges using a cationic polyacrylamide. Cationic polyacrylamides are polyacrylamides where the functional group (COOH) is substituted by cationic functional groups, generally amines.

Both Microbond and 6610 are cationic flocculants, however, they have different functional groups, which are differently affected by pH. It is possible that Microbond, being a quarternary ammonium, is less affected by pH than 6610, able be to maintain a higher positive charge in higher pH ranges (>10) and consequently attain a marginally higher DR value.

Table 3.35 - Initial densities, concentrations, initial and final Brookfield viscosities and final density gaps for the runs performed with NaCl combined with Microbond and 6610. ^{a)}Density gap is calculated from the difference between middle and bottom values.

Run	Zone	Initial density (g/cm³)	Flocculant	Initial Brookfield (cP)	Final Brookfield (cP)	Final density gap (g/cm³)a)
131	Тор	1.1483		4686	4936	0.0005
	Middle	1.1481	Control	5046	5046	
	Bottom	1.1556		5526	5526	
	Тор	1.1400		2418	4512	0.0088
R116	Middle	1.1433	Microbond	2643	4782	
	Bottom	1.1480		4773	4920	
	Тор	1.1257		3048	>6000	
R117	Middle	1.1309	6610	3324	>6000	0.0005
	Bottom	1.1386		3678	>6000	

Table 3.35 represents the initial densities, concentrations, initial and final Brookfield viscosities for the runs performed with NaCl with Microbond and 6610.

Initial densities were not within the objective of 1.15-1.20 g/cm³, due to the reduction of dispersant GPlus. This reduction causes in turn the reduction of negative charges in the solution, which stabilize the clay particles and keep them in suspension.

Brookfield viscosities increased significantly for both runs, especially for the combination of NaCl with 6610. This combination may have caused a higher increase due to the higher molecular weight of the 6610 polymer increasing the overall viscosity of the solution.

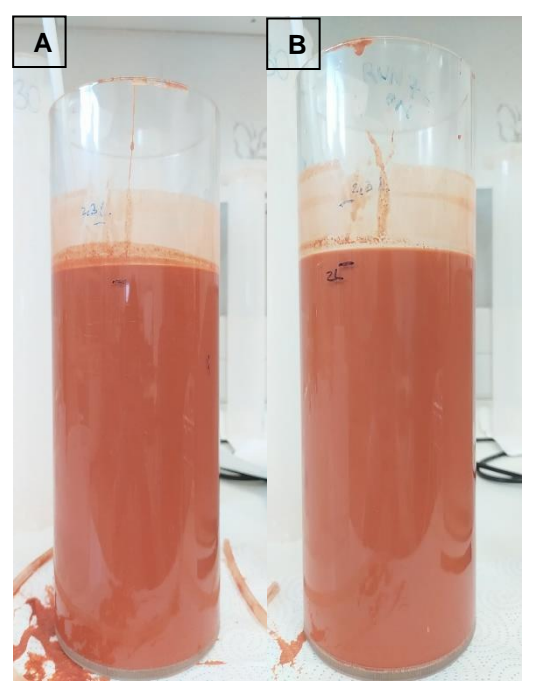


Figure 3.51 – Side view of the solutions treated with (A) – NaCl + Microbond and (B) – NaCl + 6610

Figure 3.62 represents the visual aspect of the solutions treated with NaCl combined with Microbond and 6610.

No visual change was observed for any of the solutions, as expected from the low DR results.

In conclusion, the reduction of dispersant is an effective method to reduce the amount of coagulant/flocculant required for charge neutralization. However, cleaning the solution is not yet controllable and, therefore, non-ionic polymers will be tested in the next section and compared to cationic polymers.

3.9 Study of nonionic and cationic polymers as flocculants and their solution pH

3.9.1 Study of the use of cationic polymer 6605

The purpose of this subsection is to find alternatives to coagulants by testing cationic flocculant 6605 and its interaction with HCl, according to protocol 2.3.4. Fixed variables are mixing time (8 minutes), flocculant type (6605), clay type (clay B from MCS) and mixing speed (300/50 – fast and slow mixing). Study variable is HCl concentration (0 and 2.1 mM)

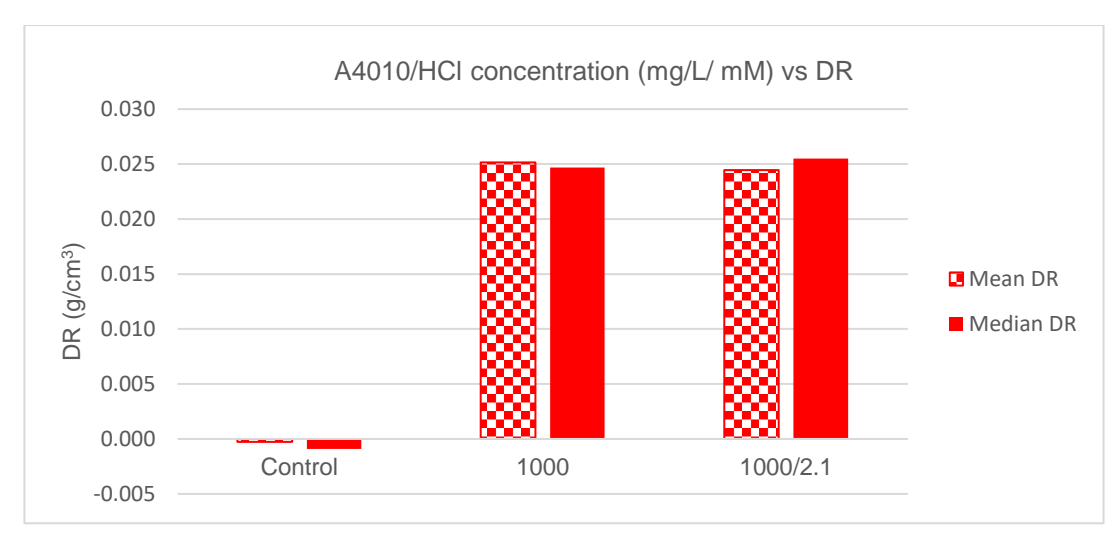


Figure 3.52 - Effect of HCl concentration combined with 6605 on DR

Figure 3.63 represents DR in function of the concentration of 6605 and HC

Runs performed produced DR values significantly higher than the control run, which means that 6605 reduced DR further than natural settling, which is the phenomenon observed for the control run. For the runs performed at the concentration of 1000 mg/L, adding 2.1 mM of HCl had minimal DR gains when compared to the run performed without this acid: mean and median DR went from 0.0252 and 0.0247 g/cm³ to 0.0283 and 0.0269 g/cm³ These results indicate that adding HCl had no influence on DR. Nonetheless, DR is achieved for the objective of 0.02 g/cm³ for both runs.

In 2018, Seo et al. [197]conducted experiments using a cationic polyacylamide on calcium carbonate and state that, by increasing pH from 7 to 9, a decrease of of adsorption rate andfloc size is observed as the polymer is hydrolyzed. They explained that this is due to the increase of negative charges in the polymeric structure causing the polymer to adopt a stretched conformation, which leads to reduced bridging flocculation.

Results are not in accordance with the findings of Seo et al., as adding HCI decreases the solution's pH, which is the reverse effect the work of Seo et al.. It should be expected for DR to increase when HCI is added, as the protons may increase the positive charge of 6605. However, reducing the pH by HCI addition caused practically no effect on DR.

Flocculant concentration was then increased to 2000 mg/L. Fixed variables are mixing time (8 minutes), flocculant type (6605), clay type (clay B from MCS) and mixing speed (300/50 – fast and slow mixing). Study variable is HCl concentration (0 and 4.2 mM)

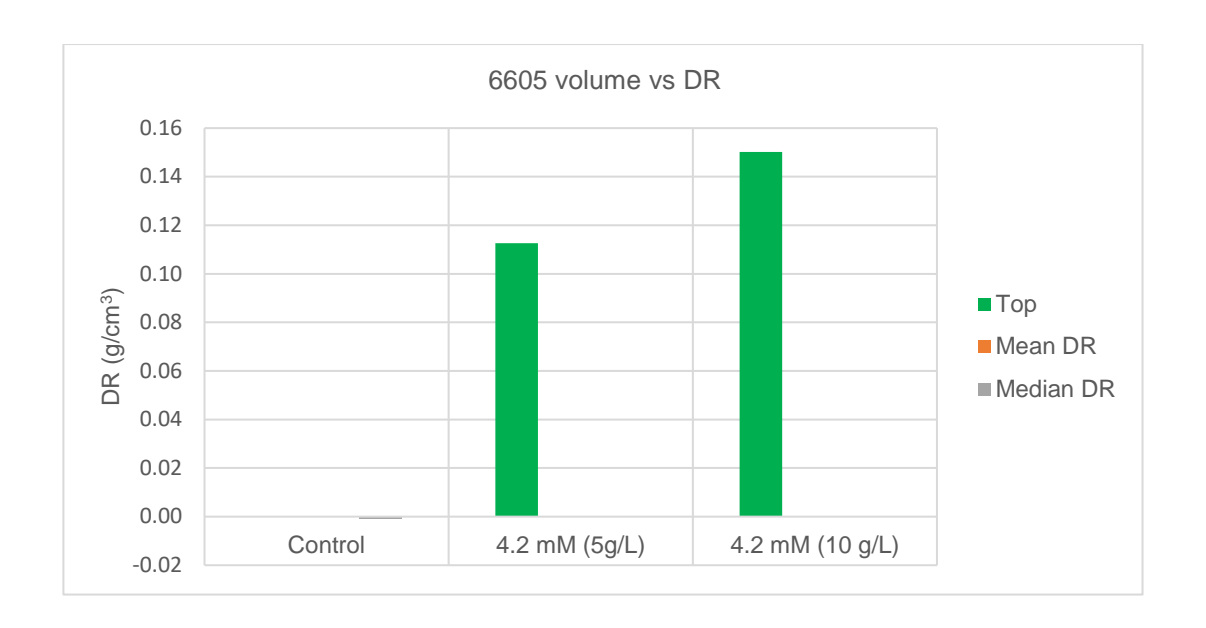


Figure 3.64 - Effect of 6605 volume on DR

Figure 3. represents the runs performed at 2000 mg/L with 4.2 mM of HCl at different volumes.

Flocculant concentration was then increased to 2000 mg/L, and DR at the top was 0.1126 g/cm³. Results are in accordance with the study performed on chapter 3.4.3, where increasing the concentration of flocculant also increased DR.

The volume of solution required for a 5 g/L solution was now 800 mL. Thus, another run was made for a 2000 mg/L run using a 10 g/L stock polymer solution. DR increased by 0.0376 g/cm³ for the 10 g/L stock solution, even though the volume for this solution was halved to 400 mL. Since the run using half the volume of solution achieved higher DR, it cannot be assumed that dilution is occurring. No DR objective was achieved for the concentrations of 6610 and HCl applied.

Table 3.36 - Initial densities, flocculant concentration, HCl volumes, initial and final Brookfield viscosities, initial and final pH values and final density gaps for the runs performed with Telsun 66 and HCl. ^{a)}Density gap is calculated from the difference between middle and bottom values. ^{b)}Impossible to measure due to inability to collect samples. ^{c)}Impossible to calculate

Run	Zone	Initial density (g/cm³)	Flocculant concentration (mg/L)	HCI concentration (mM)	Initial Brookfield (cP)	Final Brookfiel d (cP)	Final density gap (g/cm³)
	Тор	1.1483			4686	4936	
131	Middle	1.1481	0 (control)	0	5046	5046	0.0011
	Bottom	1.1556			5526	5622	
	Тор	1.1486		0	5634	3780	
129	Middle	1.1434	1000		5832	3792	0.0010
	Bottom	1.1503			5976	4416	
	Тор	1.1423		2.1	>6000	5232	0.0015
127	Middle	1.1485	1000		5942	5484	
	Bottom	1.1582			>6000	5784	
	Тор	1.1122			2520	6.0	
126	Middle	1.1350	2000	4.2 (5 g/L)	3414	, a a b)	
	Bottom	1.1780			4668	I.M. ^{b)}	1 C C)
	Тор	1.1515	2000 mg/L /		>6000	19.5	I.C. ^{c)}
130	Middle	1.1511	4.2 mMH Cl (10 g/L)	4.2 (10 g/L)	>6000	I.M. ^{b)}	
	Bottom	1.1534			>6000		

Table 3.36 represents the initial densities, flocculant and acid concentrations, initial and final Brookfield viscosities and final pH of the runs performed with 6605 and HCl.

Initial densities were within the objective of 1.15-1.20 g/cm³ for all runs except for 126. Density gaps between middle and bottom accomplished the objective of 0.03 g/cm³ when they were possible to calculate.

Increasing HCI concentration from 0 to 2.1 mM increased the final Brookfield viscosity, however, increasing the 6605 concentration past 1000 mg/L decreased the Brookfield viscosity significantly due to the complete cleaning of the solution in the top area.

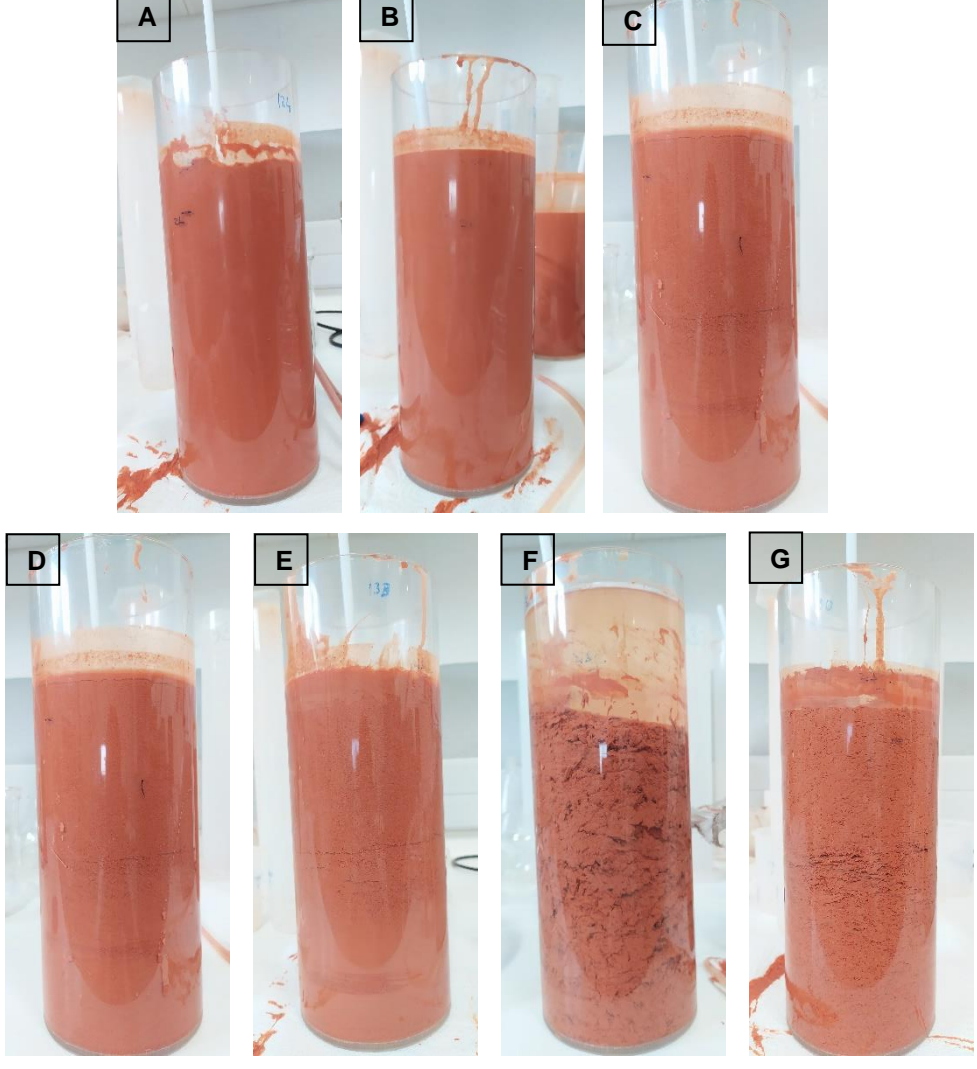


Figure 3.65 - Side view of the solutions treated with 6605 at: (A) - 1000 mg/L; (B) - 1000 mg/L / 2.1mM HCl; (C) - 1200 mg/L: (D) - 1200 mg/L / 2.5 mM HCl; (E) - 1500 mg/L; (F) - 2000 mg/L / 4.2 mM HCl (5 g/L); (G) - 2000 mg/L + 4.2 mM HCl (10g/L)

Figure 3. represents the visual aspect of the solutions treated with 6605 at different concentrations and different volumes of HCI.

Increasing the HCl concentration from 0 to 2.1 mM mL at 1000 mg/L of 6605 did not produce any visual results, however increasing the flocculant concentration produced different visual results. The cutoff point where the top solution is cleaned is 2000 mg/L. The 5 mg/L stock solution created a higher clean solution height due to the volume of the solution added being twice of that of the 10 g/L. The 6605/HCl concentrations of 2000 mg/L/4.2 mM completely flocculated the column and generated clean strips of fluid, possibly compromising the stability of the column, and thus can be considered as unviable.

It is possible that increasing the concentration of 6605 increased the charge neutralization effect, increases the effect of the electrical double layer compression, allowing for the flocculation of the solution and settling of the clay.

Since the application of cationic flocculants does not lead to the control of DR, the next chapter will focus on the application of non-ionic flocculants in an attempt to explore other effects other than electrostatic attractions.

3.9.2 Study of the use of non-ionic polymers

The purpose of this subsection is to study the effect of non-ionic polymers according to protocol 2.3.4. Fixed variables are mixing time (8 min), mixing speed (300/50 rpm), GPlus concentration (0.5 mL/L) flocculant type (Nonionic 513) and clay type (clay B from MCS). Study variable is HCl concentration (0 and 0.4 mM). This study may lead to the flocculation through weaker physical interactions instead of electrostatic interactions in to control DR.

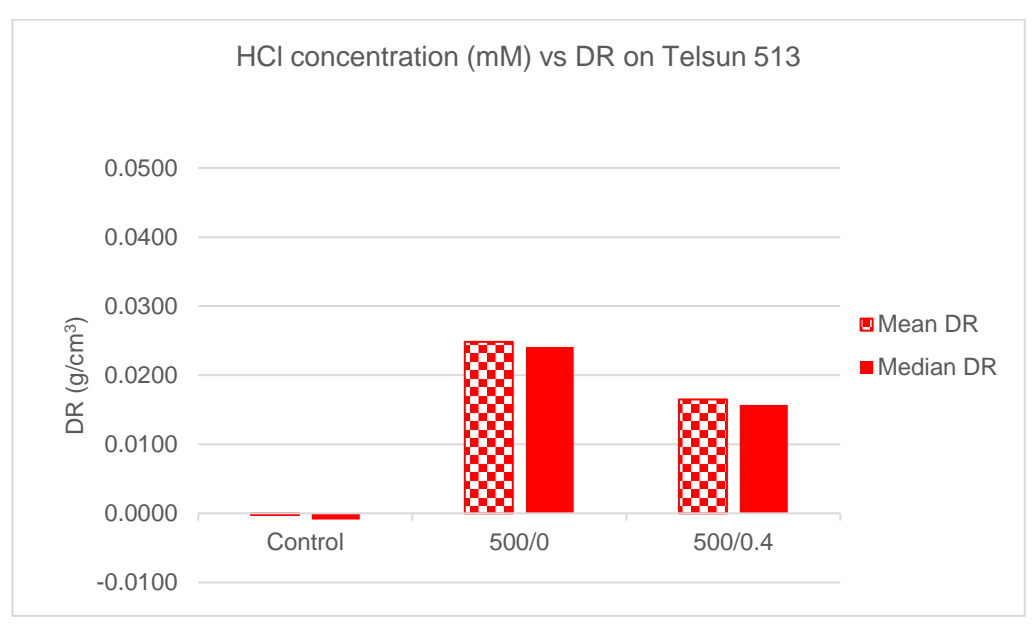


Figure 3.53 – Effect of HCl concentration with Nonionic 513 on DR

Figure 3.66 represents DR when non-ionic polymer Nonionic 513 is used with and without HCl at 0 and 0.4 mM

Table 3.37 - Molecular weight and charge density of the flocculants used

Flocculant	Molecular Weight (MDa)	Charge Density (%)
Nonionic 513	10-15	0.5-1

Table 3.37 represents the molecular weight of the flocculant tested, denominated Nonionic 513.

For the run without HCI, the mean DR value achieved was 0.0248 g/cm³ and the median DR value was 0.0241 g/cm³. When 1 mL of HCI was previously added to the Nonionic 513 solution, mean DR was reduced to 0.0165 g/cm³ and median DR was 0.0157 g/cm³. Results achieve the 0.02 g/cm³ objective for the Nonionic 513 run without HCI.

Flocculants are non-ionic if their charge density is lower than 3% [198]. These polymers generally tend to interact with clays through polymer bridging instead of electrostatic attraction.

HCl addition reduced the DR, possibly due to the compression of the polymer chains. As seen on chapter 1.2.2.1.1, non-ionic polymers bind to clays through their dehydration, creating a favorable reaction through enthalpy changes. This phenomenon depends on the size and conformation of the flocculant, as it is only dependent on the surface area available for adsorption. Thus, the addition of HCl, reduces the contact area of the polymer, thus making the adsorption less favorable.

Table 3.38 - Initial densities, initial and final Brookfield viscosity values for the runs performed. ^{a)}Density gap is calculated from the difference between middle and bottom values.

Run	Zone	Initial density (g/cm³)	Flocculant	HCI concentration (mM)	Initial Brookfield (cP)	Final Brookfield (cP)	Final density gap (g/cm³)a)
	Тор	1.1483		O [4686	4936	
131	Middle	1.1481	0 (Control)		5046	5046	0.0008
	Bottom	1.1556			5526	5622	
	Тор	1.1460		0	5058	5724	0.0051
118	Middle	1.149	Nonionic 513		5412	>6000	
	Bottom	1.1533			5754	5904	
	Тор	1.1442			502	4904	
119	Middle	1.1450	Nonionic 513	0.4	501	>6000	0.0021
	Bottom	1.1498			499	>6000	

Table 3.38 represents the initial densities, initial and final Brookfield viscosities for the runs performed using 500 mg/L of flocculant.

For the Brookfield viscosities, an overall increase is observed when A0410. Values represented as ">6000" represent in turn measurements that were situated above the limits of

the spindle LV-01. Thus, values cannot be compared between the HCl concentrations of 0 and 0.4 mM.

Initial densities were within the objective of 1.15-1.20 g/cm³ and all final density gaps created are lower than 0.03 g/cm³

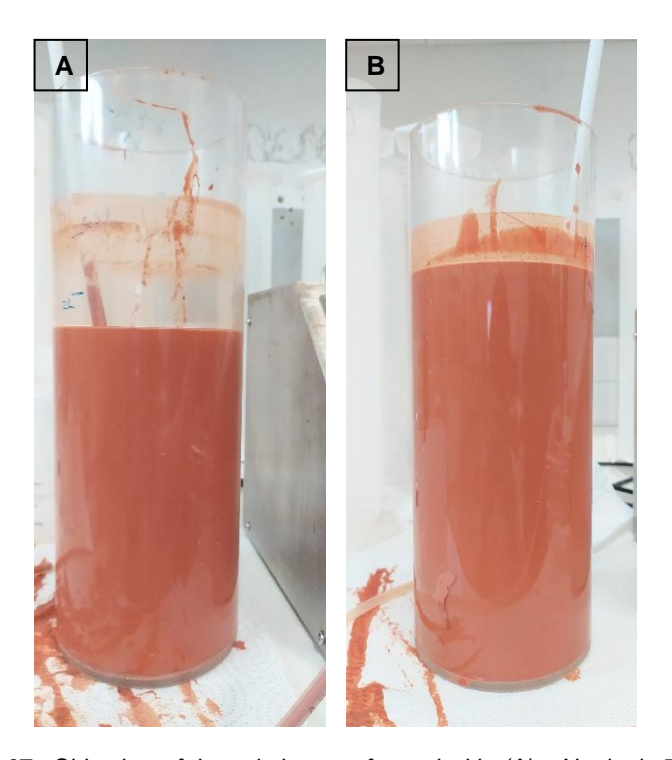


Figure 3.67 - Side view of the solutions performed with: (A) – Nonionic 513; (B) – Nonionic 513 with 0.4 mM of HCl

Figure 3.67 represents the visual aspect of the solutions treated with Nonionic 513 with and without HCI.

None of the solutions presented any visual impact. This may be due to the weak flocs created by the weaker hydrogen bonds responsible for the polymer bridging phenomena being easily broken by high shear rates caused by the agitation at 300 rpm.

In conclusion, the run using HCl concentration of 0.4 mM produced a lower DR than the run without HCl. It is uncertain if this reduction is caused by the addition of HCl or due to measurement errors, as the difference was minimal. However, the run where HCl was applied did accomplish the DR objective of 0.02 g/cm³.

Since the polymer used had a low charge density of 0.5-1%, the influence of HCl may not have been noticeable, as there may not be enough ionizable COOH groups to notice the influence of HCl. Thus, for further studies, HCl will be studied with other polymers with different charge densities. These polymers should have a slightly higher charge density to evaluate the

effect of HCl. Fixed variables are mixing time (8 minutes), mixing speed (300/50 rpm – fast/slow mixing), flocculant type (A0410), flocculant concentration (1000 mg/L). Study variable is HCl concentration (0-6.6 mM)

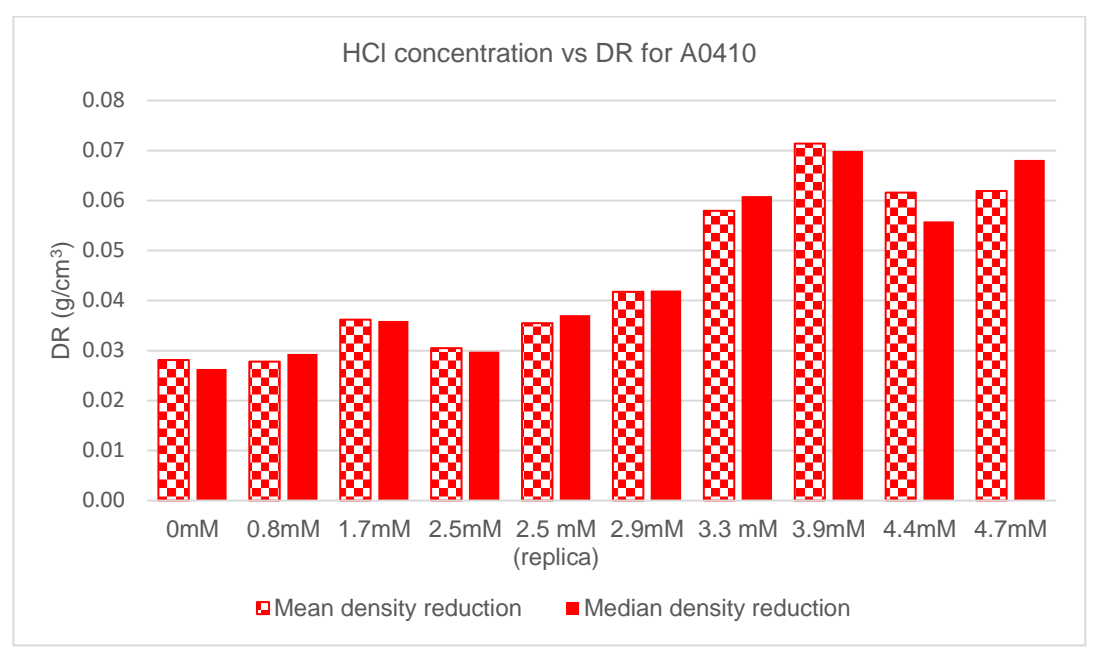


Figure 3.54 – Effect of HCl concentration on DR in conjunction with A0410

Figure 3.68 represents DR in function of HCl concentration (0-4.7 mM).

In general, increasing HCl concentration increased mean and median DR. First DR objective of 0.02 g/cm³ is achieved for all runs, independently if HCl is applied or not. The runs using 0 and 0.8 mM of HCl achieved the 0.02 g/cm³ objective and the runs using 3.3, 4.4 and 4.7 mM of HCl achieved the 0.06 g/cm³ DR objective. Highest mean and median DR were 0.0714 g/cm³ and 0.0699 g/cm³, respectively, and were observed for the run where 3.9 mM of HCl were applied. Increasing HCl concentration past 3.9 mM reduced mean and median DR.

As seen on chapter 1.2.2.1.1, non-ionic flocculants are generally insensitive to pH due to their lack of charge.

However, A0410 has 5% charge density, which may increase its sensitivity to pH. Therefore, two possible scenarios may be in place: the first is the possibility that adding HCl assists in the protonation of the polymer chains. These chains may create some electrostatic attraction to the deprotonated, highly negative bentonite sheets at pH range 10-11. The second is the increase of the zeta potential of the solution by simultaneously protonating the bentonite sheets, which in turn, promotes flocculation.

The concentration of HCl was further increased to increase DR and evaluate the impact of the concentration of HCl on the stability of the column. Fixed variables are mixing time (8 minutes), mixing speed (300/50 rpm - fast/slow mixing), flocculant type (A0410), flocculant concentration (1000 mg/L). Study variable is HCl concentration (5 mM and 6 mM)

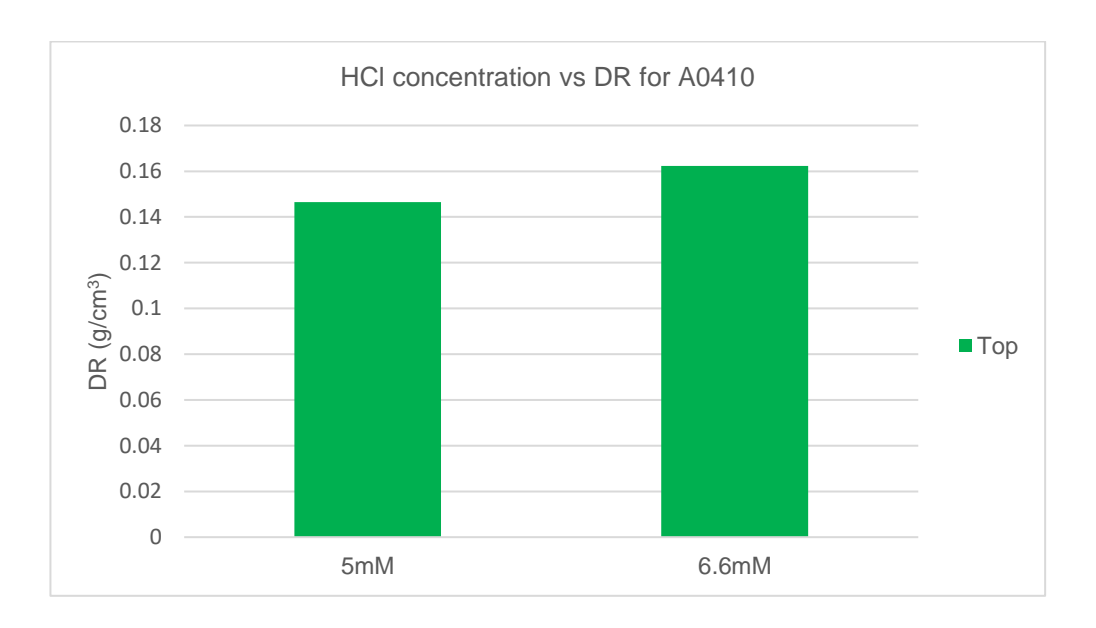


Figure 3.55 - Effect of HCl concentration on DR in conjunction with A0410 for 5 mM and 6.6 mM of HCl Figure 3.55 represents DR in function of HCl concentration (5 mM and 6.6 mM).

For the concentrations of 5 and 6.6 mM of HCl, DR attained was 0.1465 g/cm³ and 0.1623 g/cm³, respectively. These DR values do not accomplish any DR objective.

Table 3.39 - Initial densities, flocculant concentration, initial and final Brookfield viscosities for the runs performed. ^{a)}Density gap is calculated from the difference between middle and bottom values. ^{b)}Impossible to measure. ^{c)}Impossible to calculate due to the inability to draw samples

Run	Zone	Initial density (g/cm³)	HCI concentration (mM)	Spindle	Initial Brookfield (cP)	Final Brookfield (cP)	Final density gap (g/cm³) ^{a)}
	Тор	1.1535			>6000	>6000	
120	Middle	1.1554	0	LV-01	>6000	>6000	0.002
	Bottom	1.1661			>6000	>6000	
	Тор	1.1217			2634	>6000	
121	Middle	1.1321	0.8	LV-01	3012	>6000	0.0013
	Bottom	1.1403		- 	4306	>6000	
	Тор	1.1439			5514	>6000	
122	Middle	1.1457	1.7	LV-01	5760	>6000	0.0113
	Bottom	1.1509			>6000	>6000	
	Тор	1.1443			5238	>6000	
136	Middle	1.1456	2.5	LV-01	5574	>6000	0.0112
	Bottom	1.1493			5808	>6000	
	Тор	1.1615		LV-03	55320	292800	0.0064
152	Middle	1.1644	2.5 (replica)		47160	>300000	
	Bottom	1.1628			49866	292800	
	Тор	1.1582			39540	270600	0.0001
153	Middle	1.1529	2.9	LV-03	38820	275700	
	Bottom	1.1598			38700	278700	
	Тор	1.1476		LV-03	5136	>6000	0.0211
140	Middle	1.1487	3.3		5946	>6000	
	Bottom	1.1540			>6000	>6000	
	Тор	1.1597			48360	202500	
154	Middle	1.1623	3.9	LV-03	42540	200400	0.0099
	Bottom	1.1643			40800	276000	
	Тор	1.1532			42720	286500	
155	Middle	1.1530	4.4	LV-03	35400	261900	0.0021
	Bottom	1.1531			34800	269400	
	Тор	1.158			15600	6300	
158	Middle	1.1604	4.7	LV-03	23760	745280	0.0183
	Bottom	1.1624			17340	766800	
	Тор	1.1466			48720		
151	Middle	1.1593	5	LV-03	38580	I.M. ^{b)}	
	Bottom	1.1481			37020		1 C c)
	Тор	1.1597			52320		I.C.c)
R50	Middle	1.1601	6.6	LV-03	51480		
	Bottom	1.1612			48240		

Table 3.39 represents the initial densities, flocculant and acid concentration, initial and final Brookfield viscosities for the runs performed with A0410 and HCI.

Initial densities were within objective for all runs except for run 121. This may be due to the reduction of the GPlus reducing in turn the stability of the suspension due to the reduction of negative charges in the system,

Initial Brookfield viscosities for the runs using the concentrations of 2.5 mM, 3.9 mM, 4.4 mM, 5 mM and 6.6 mM were nearly an order of magnitude higher than the viscosities measured for other runs. It is possible that this was due to the ambient temperature difference. This effect will be explored in a future chapter.

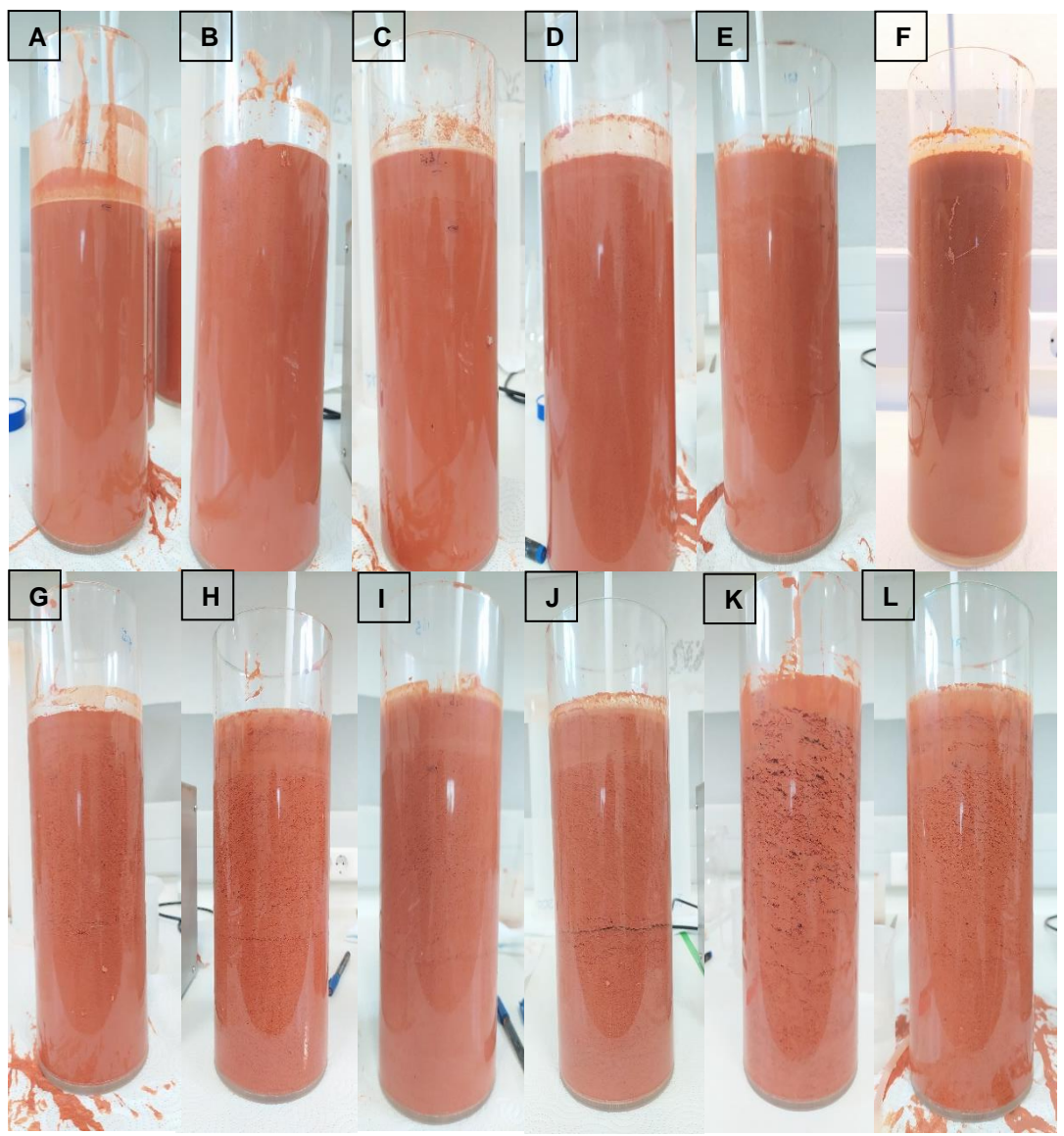


Figure 3.70 - Side view of the solutions treated with A0410 at 100 mg/L and HCl at: (A) - 0 mM; (B) - 0.8 mM; (C) - 1.7 mM; (D) - 2.5 mM; (E) - 2.5 mM; (F) - 2.9 mM; (G) - 3.3 mM; (H) - 3.9 mM; (I) - 4.4 mM; (I) - 4.7 mM; (I) - 5 mM; (I) - 6.6 mM

Figure 3.70 represents the visual aspect of the solutions treated with A0410 and HCl.

Adding increased amounts of HCI creates slightly more apparent flocs. As the HCI concentration is increased, the solutions show a unique effect seen so far: three distinct areas – the first is the original introduction area, also where the distribution of the flocculant was the least efficient, hence no flocs formed. The second area is the middle area, where the flocs are more visible. The third and final area is the bottom, where some flocs can be seen, but are not very evident. It is possible that the shear from the agitation caused the breakage of the flocs in this section.

In conclusion, increasing the HCl concentration when the concentration of A0410 was fixed at 1000 mg/L increased DR in general. As the HCl concentration was increased, more flocs are observed throughout the column, with distinct areas formed. The HCl concentrations above 5 mM generate clean strips of fluid, which, when combined with the complete flocculation of the column, may compromise the stability of the column. Thus, the concentrations of 5 mM and 6.6 mM are unviable for use.

For the next study, the concentration of A0410 was tested, to determine if its effect was similar to the addition of HCl and if the current concentration of polymer is optimal, according to protocol 2.3.4. Fixed variables are mixing time (8 minutes), HCl concentration (2.5 mM), flocculant type (A0410) and mixing speed (300/50 rpm) and clay type (clay B from MCS). Study variable is A0410 concentration (250, 800, 1000 and 1500 mg/L).

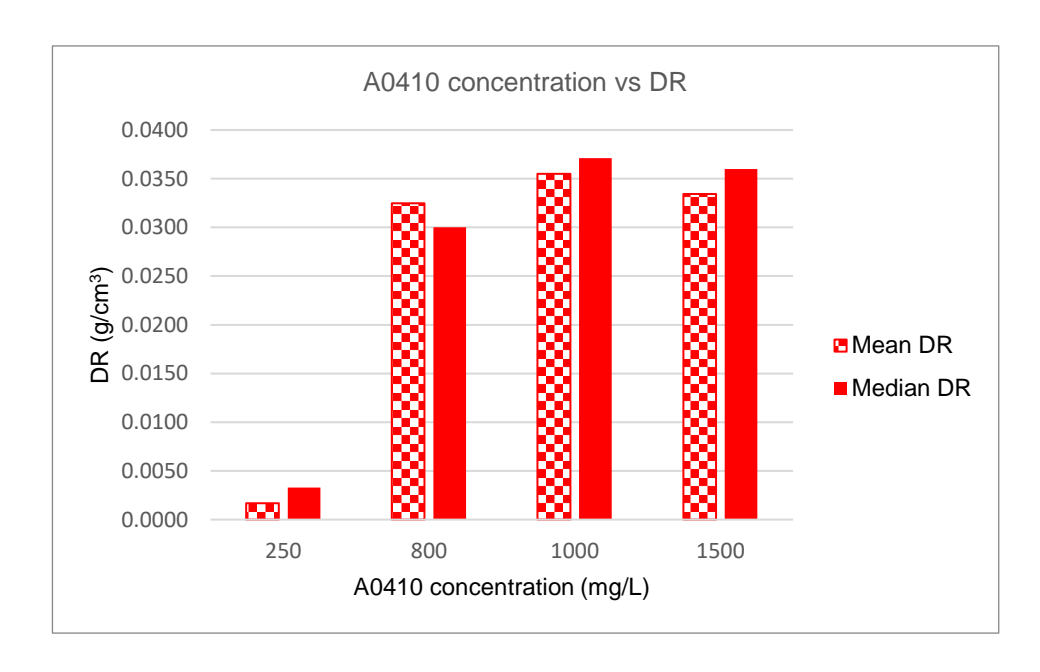


Figure 3.56 - Effect of A0410 concentration on DR

Figure 3.56 represents DR in function of A0410 concentration.

Increasing A0410 concentration yielded a significant DR increase of nearly 0.03 g/cm³ between the run using 250 mg/L and the run using 800 mg/L of A0410. Between the run using the concentration of 800 mg/L and the run using the concentration of 1000 mg/L, the increase was minimal. From the run using 1000 mg/L to the run using 1500 mg/L there was a decrease in DR. No DR objective was achieved.

Gregory (1993) [41], described the main mechanisms of adsorption for long chain, non-ionic and charged flocculants. These flocculants generally adsorb through polymer bridging, where a single chain can adsorb into multiple clay particles simultaneously. This effect has an optimal

dose of flocculant: too low of an amount leads to insufficient polymer to bind clays together and an overdose of polymer leads to restabilization of the suspension, caused by steric repulsion.

Results are in accordance with the results of Gregory, as for the run performed with the concentration of 250 mg/L, there may have been insufficient polymer to flocculate the suspension. The optimal concentration was achieved for the run with the concentration of 1000 mg/L. Steric repulsion was then observed for the run using the concentration of 1500 mg/L.

Table 3.40 - Initial densities, flocculant concentrations, initial and final Brookfield values and final density gaps for the runs performed. ^aDensity gap is calculated from the difference between middle and bottom values.

Run	Zone	Initial density (g/cm³)	Flocculant concentration (mg/L)	Spindle	Initial Brookfield (cP)	Final Brookfield (cP)	Final density gap (g/cm³) ^{a)}
149	Тор	1.1434	250	LV-03	39660	180300	0.0031
	Middle	1.1520			32700	135600	
	Bottom	1.1530			33300	181500	
159	Тор	1.1576	800		44340	1037000	0.0082
	Middle	1.1570			46680	765600	
	Bottom	1.1595			39300	978000	
152	Тор	1.1615	1000		55320	292800	0.0064
	Middle	1.1644			47160	>300000	
	Bottom	1.1628			49866	292800	
137	Тор	1.1457	1500	LV-01	4308	>6000	0.0030
	Middle	1.1472			4452	>6000	
	Bottom	1.1492			5740	>6000	

Table 3.40 represents the initial densities, flocculant concentrations, initial and final Brookfield values and final density gaps for the runs performed with A0410 with 2.5 mM of HCl.

Initial densities were within the objective range of 1.15-1.20 g/cm³ for all runs and density gaps created were lower than 0.03 g/cm³.

Initial and final Brookfield viscosities still remained considerably higher for the runs using 250, 800 and 1000 mg/L., as these runs were performed at a later date than the run performed at 1500 mg/L, opening up the possibility that this increase in Brookfield viscosity may be due to the different batch of clay bags, due to equipment calibration errors occurred due to the incorrect spindle used or due to the ambient temperature variation between the dates when the runs where such differences were observed.

In conclusion, varying the concentration of A0410 decreased DR. No DR objectives were achieved for any of the concentrations tested, and, as such, the concentration of 1000 mg/L should be kept, as for this concentration, through the adjustment of HCl concentration, other DR objectives were hit. For the run using A0410 concentration of 1000 mg/L and 2.5 mM of HCl, Marsh viscosity was not measurable, initial densities were within the objective, the deposit was not collectable.

Thus, for the next chapter, the temperature of the solution will be tested to verify its influence on the Brookfield values, as for water-based solutions, the viscosity is influenced the temperature.

3.9.3 Influence of the solution temperature

The purpose of this subsection is to determine the influence of the solution temperature on its Brookfield viscosity and on DR, according to protocol 2.3.4. Fixed variables are mixing time (8 minutes), mixing speed (300/50 rpm), clay type (clay B from MCS), flocculant type (A0410), flocculant concentration (1000 mg/L) and HCl concentration (2.5 mM). Study variable is solution temperature (room temperature ≈21°C and controlled temperature ≈16°C).

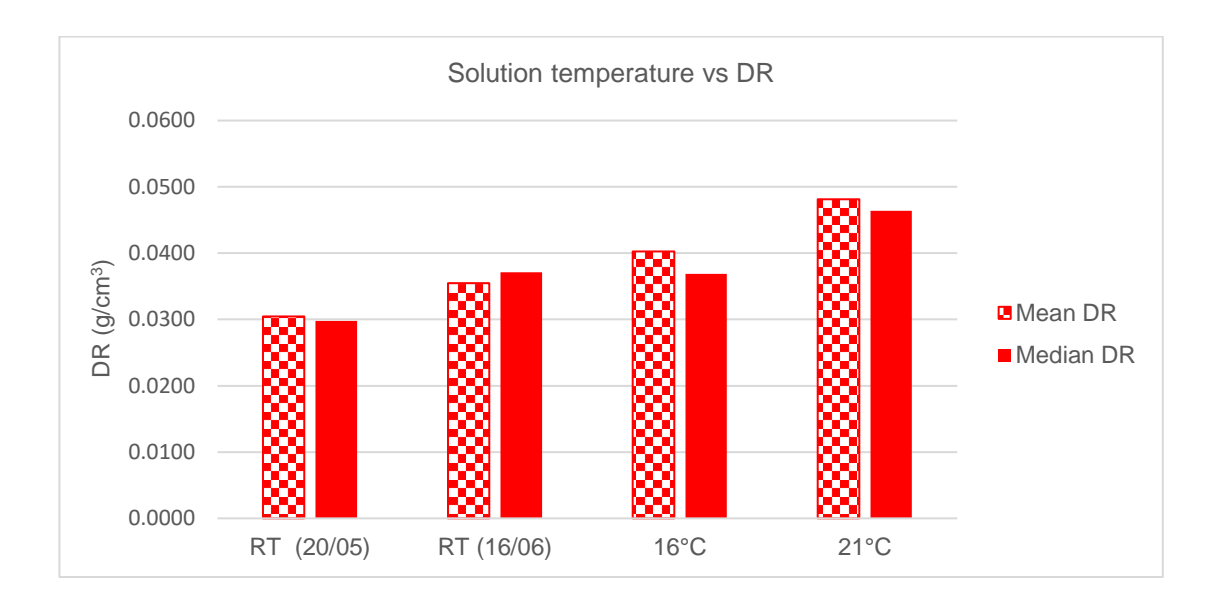


Figure 3.57 - Effect of solution temperature on DR

Figure 3.57 represents DR in function of the solution temperature.

Two solutions at room temperature were kept as reference. From the figure, it is possible to observe that an increment of DR is observed for the run at 16°C to the run at 21°C. However, an increase was also observed for both runs at room temperature where the exact temperature is unknown. Thus, no influence from temperature was observed.

Table 3.41 - Initial densities, Brookfield viscosities and final zone gaps for the runs performed. ^aDensity gap is calculated from the difference between middle and bottom values.

Run	Zone	Initial density (g/cm³)	Spindle	Initial Brookfield (cP)	Final Brookfield (cP)	Final density gap (g/cm³)ai
	Тор	1.1443		5238	>6000	
RT (20/05)	Middle	1.1456	LV-01	5574	>6000	0.0112
	Bottom	1.1493		5808	>6000	
	Тор	1.1615		55320	292800	
RT (16/06)	Middle	1.1644		47160	>300000	0.0064
	Bottom	1.1628		49866	292800	
	Тор	1.1555		48900	273000	
16°C	Middle	1.1583	LV-03	43140	298300	0.0062
	Bottom	1.1626		52200	427800	
	Тор	1.1491		31500	628800	
RT (21/06)	Middle	1.1537		48360	728400	0.0037
	Bottom	1.1634		37320	885600	

Table 3.41 represents the initial densities, flocculant concentrations, initial and final Brookfield values and final density gaps for the runs performed with A0410 with 2.5 mM of HCl.

Initial densities were within the objective range of 1.15-1.20 g/cm³ for all runs and density gaps created were lower than 0.03 g/cm³.

Initial Brookfield viscosities from the controlled temperature runs at room temperature was still an order of magnitude higher than the room temperature run performed at 20/05. Maintaining the solution at 16°C did not reduce the Brookfield viscosity, meaning that this effect is not caused by the temperature.

It is a possibility that the abrupt increase in the Brookfield viscosities is caused by the miscalibration caused by the change of spindles, as different spindles experience different drag, affecting the Brookfield viscosity values. However, a difference of a magnitude of values might

not be explainable by the spindles alone. To study this effect, a control run was performed using the spindles LV-02 and LV-03 for the measurement of initial Brookfield values.

Table 3.42 - Initial densities, spindles and initial Brookfield values for the control run performed for confirmation

Run	Zone	Initial density (g/cm³)	Spindle	Initial Brookfield (cP)
	Тор	1.1597		52320
	Middle	1.1601	LV-02	51480
150	Bottom	1.1612		48240
	Тор	1.1597		81300
	Middle	1.1601	LV-03	66600
	Bttom	1.1612		69000

Table 3.42 represents the control run performed with spindles LV-02 and LV-03.

It is possible to observe that the initial Brookfield viscosities increased in general. This is probably due to the different shape of the spindles, which causes them to experience different viscous drags in the same solution. However, these results do not explain an increase of nearly tenfold. It might be to an external factor such as a difference in clay grades or grinding existent in different batches, resulting in different properties, such as particle size, which may not be observable. Human error may be an explanation as well.

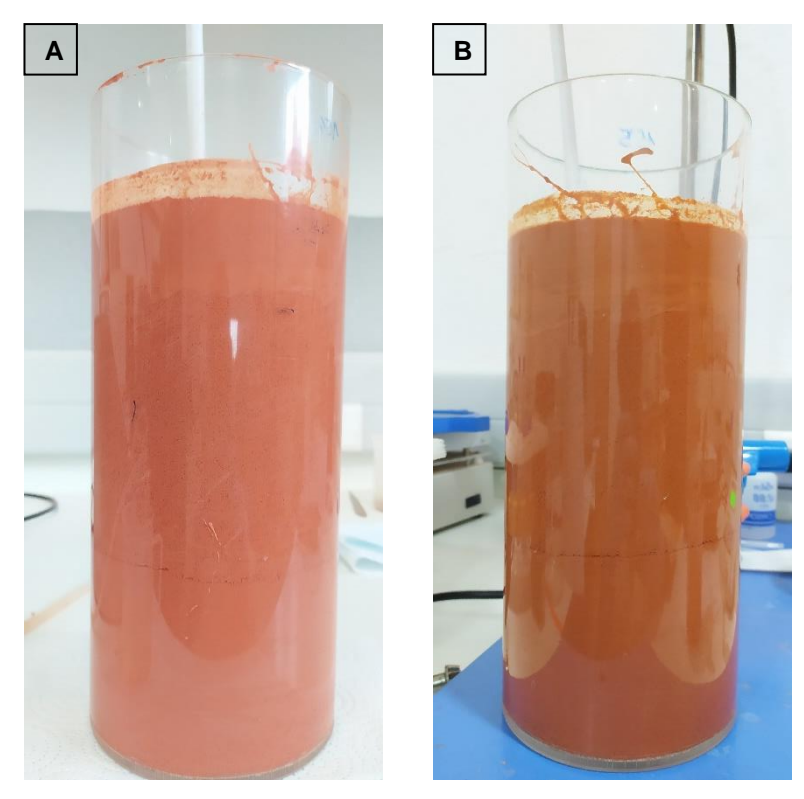


Figure 3.73 - Side view of the solutions treated with A0140 at 1000 mg/L and 2.5 mM of HCl at: (A) - Room temperature; (B) – Controlled temperature (16°C)

Figure 3. represents the aspect of the solutions treated with A0140 at room temperature and at the controlled temperature of 16°C.

No difference can be observed from both solutions.

In conclusion, no influence from the solution temperature was observed, either on DR or on the Brookfield viscosities. Moving forward, a different approach will be used to attain a controlled DR. Clay/sand mixtures will be used to simulate more accurately real-world conditions and to achieve higher, more controlled DR through the settling of sand particles.

3.9.4 Use of clay/sand solutions

The purpose of this subsection is to add sand to the clay suspension to simulate real-world conditions and generate higher DR by settling denser sand particles, according to protocol2.3.5. Fixed variables are mixing time (8 minutes), mixing speed (300/50 rpm), clay type (clay B from MCS) sand concentration (100 g/L), flocculant type (A0410) and flocculant concentration (1000 mg/L). Study variable Is HCI concentration (0, 0.8 and 2.5 mM).

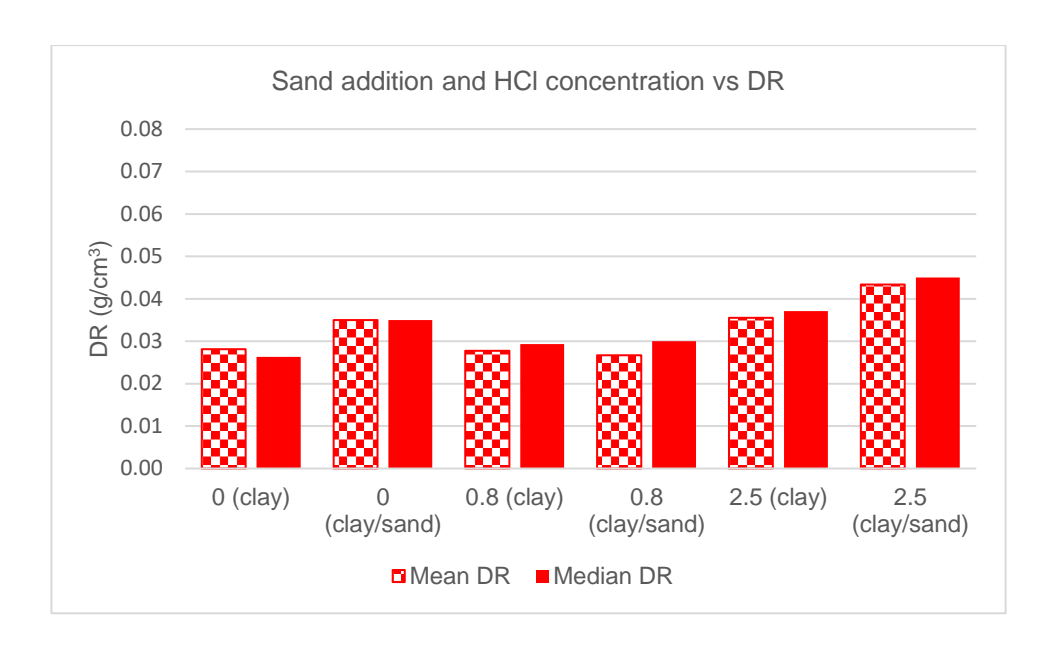


Figure 3.74 - Effect of sand addition and HCl concentration on DR

Figure 3. represents DR when sand is added at 300 mg/L and when HCl is applied at 0, 0.8 and 2.5 mM.

For the run where no HCl was applied and for the run where 2.5 mM of HCl was applied, a minimal increase in DR was produced. For the first, this increase was 0.0069 g/cm³ for the mean and 0.0087 g/cm³ for the median. For the latter, the increase was 0.0078 g/cm³ for the mean and 0.0079 g/cm³ for the median. For the run performed with 0.8 mM, DR was nearly identical, with differences of 0.0008 g/cm³ and 0.0007 g/cm³ for the mean and median value, respectively).

As seen on chapter 1.3.1.2, the settling speed of a particle depends on its diameter and its density, amongst other factors. Sand particles are larger and denser than clay particles and less electrically charged. Therefore, its suspension mechanism is mainly physical by integrating in tridimensional structures formed by clay particles and PolyMud.

The close resemblance of DR results between clay-only and clay/sand mixtures may be due to the settling of sand particles being conditioned by the settling of the clay particles. If the clay does not settle, the incorporated sand may not settle either.

Table 3.43 - Initial densities, HCl concentrations, Brookfield viscosities and final density gaps for the runs performed with A410 at 1000 mg/L with 0-2.5mM HCl on clay/sand mix. ^{a)}Density gap is calculated between the difference between the middle and the bottom values.

Run	Zone	Initial density (g/cm³)	HCI concentration (mM)	Soil type	Spindle	Initial Brookfiel d(cP)	Final Brookfield (cP)	Final densit y gap (g/cm³	
	Тор	1.1535				>6000	>6000		
120	Middle	1.1554	0			>6000	>6000	0.0020	
	Bottom	1.1661		LV-01	I \/-01	>6000	>6000		
	Тор	1.1217			LV-01	2634	>6000		
121	Middle	1.1321	0.8	clay		3012	>6000	0.0013	
	Bottom	1.1403				4306	>6000		
	Тор	1.1615				55320	292800		
152	Middle	ddle 1.1644 2.5	2.5	2.5		LV-03	47160	>300000	0.0064
	Bottom	1.1628				49866	292800		
	Тор	1.2100				109800	294600		
160	Middle	1.2200	0			73200	585600	0.0050	
	Bottom	1.2200				79200	274800		
	Тор	1.2000		Olav./		63000	937200		
161	Middle	1.2100	0.8 (clay/sand)	Clay/ sand	LV-04	56400	853200	0.0100	
	Bottom	1.2200		oana		59100	763800		
	Тор	1.2100				151200	1968000		
162	Middle	1.2200	2.5 (clay/sand)			153600	1626000	0.0100	
	Bottom	1.2150				152400	1566000		

Table 3.43 represents the Initial densities, HCl concentrations, Brookfield viscosities and final density gaps for the runs performed with A0410 and HCl on clay/sand mix.

Initial densities are within the objective of 1.15-1.20 g/cm³ for the clay-only runs. For clay/sand runs, the initial densities are above this objective. Final density gaps created by all runs are lower than 0.03 g/cm³

Both initial and final Brookfield viscosities are considerably higher for the sand/clay runs, as adding larger sand particles that incorporate in the tridimensional polymer/clay structure increases considerably the viscous drag experienced by the spindle.



Figure 3.75 - Side view of the solutions treated with 1000 mg/L of A0410 and HCl at: (A) - 0mM; (B) - 0.8mM; (C) - 2.5 mM

Figure 3.75 represents the aspect of the solutions treated with 1000 mg/L of A0410 and HCI at the concentrations of 0-2.5 mM.

All solutions present the formation of three zones: the top zone where no flocs are formed, the middle zone where there is floc formation, and the bottom zone where there is floc formation followed by destruction caused by agitation. However, no difference is observable amongst the three solutions.

The middle zone suggests that the flocs are still suspended in the solution, even after the addition of sand, which is denser than clay [199]. This hints at the possibility that the sand/clay flocs do not settle.

In conclusion, adding sand to the clay mixture did not influence DR positively, as the settling of sand is influenced by the settling of clay, as the former is incorporated in the latter when the suspension is formed.

For the next study, using the clay/sand mixture, the volume of solution of A0410 + HCl was varied to test the influence of the dilution of the column, according to protocol 2.3.5. Fixed

variables are mixing time (8 minutes), mixing speed (300/50 rpm), clay type (clay B from MCS), sand concentration (100 g/L) flocculant type (A0410), flocculant concentration (1000 mg/L) and HCI concentration (2.5 mM). The variable under study is the volume of HCI solution (0.2, 0.4, 0.67 and 1L).

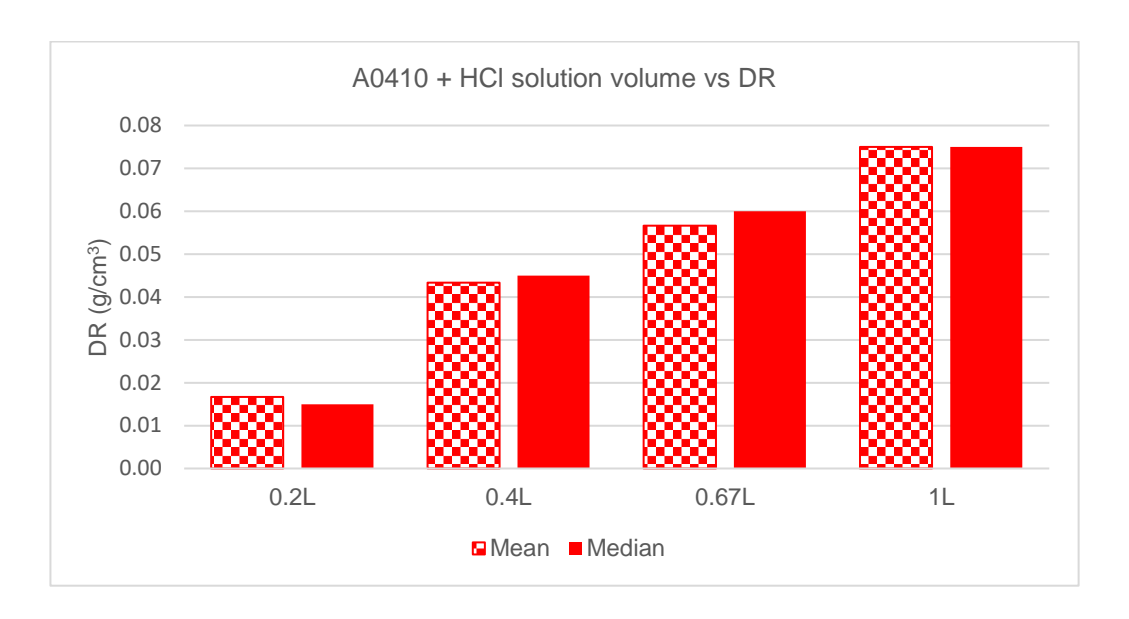


Figure 3.58 - Effect of A0410 + HCl solution volume on DR

Figure 3.58 represents DR in function of the total A0140 and HCl solution volume.

The trend is for DR to increase as the HCl solution volume also increases. An increase of 0.0583 g/cm³ for the mean and 0.0600 g/cm³ for the median was observed between the run using 0.2L of solution and the run using 1L solution. For further analysis this graph was represented as a dispersion. If the tendency of DR is linear, then it can be assumed that DR is a function of the A4010 solution volume.

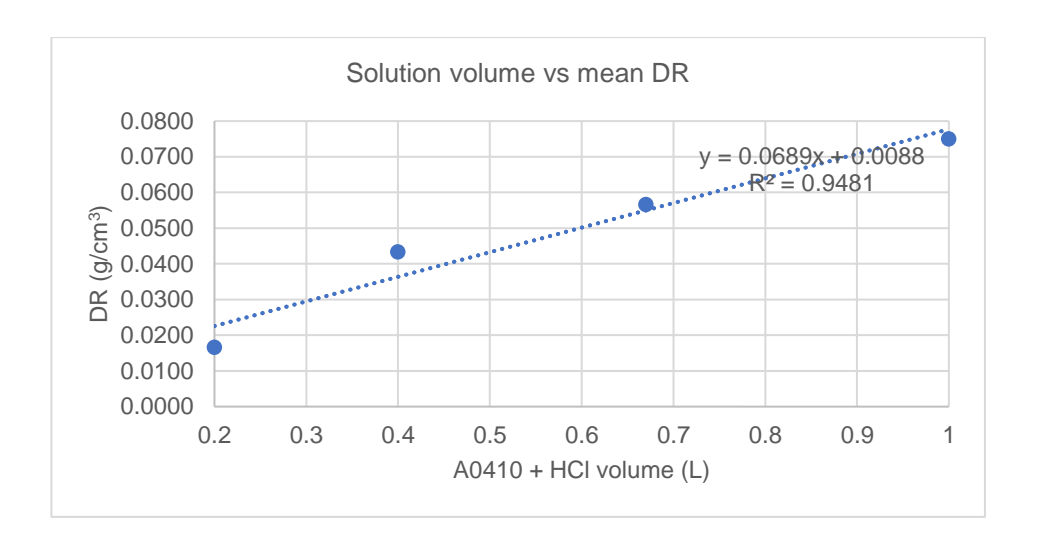


Figure 3.59 - Effect of A0410 + HCl solution volume on mean DR

Figure 3.59 represents the DR in function of the total A0140 and HCl solution volume as a dispersion.

The tendency suggests that DR was linear when the volume of A0410 increased. This suggests that, as expected, a dilution effect is occurring, since the flocculant and HCl concentrations were maintained, adding more volume of low density A0410 solution (density equivalent to water) decreased the overall density of the column.

Table 3.44 - Initial densities, solution volumes, Brookfield viscosities and final density gaps for the runs performed with A0410 and HCl on clay/sand mixture. ^{a)}Density gap is calculated from the difference between middle and bottom values.

Run	Zone	Initial density (g/cm³)	Solution volume (L)	Spindle	Initial Brookfield (cP)	Final Brookfield (cP)	Final density gap (g/cm³) ^{a)}
	Тор	1.200			52800	2214000	
165	Middle	1.210	0.20		42600	2394000	0.01
	Bottom	1.210			43200	2340000	
	Тор	1.210			151200	1968000	
162	Middle	1.220	0.40		153600	1626000	0.01
	Bottom	1.215			152400	1566000	
	Тор	1.210		LV-04	105600	3432000	
164	Middle	1.210	0.67		82800	2382000	0
	Bottom	1.220			87600	1920000	
	Тор	1.210			128500	978000	
163	Middle	1.210	1.00		133200	690000	0.01
	Bottom	1.210			91200	924000	

Table 3.44 represents the Initial densities, solution volumes, Brookfield viscosities and final density gaps for the runs performed with 1000 mg/L A0410 and 2.5mM HCl on clay/sand mixture.

Initial densities were not within the objective range of 1.15-1.20 g/cm³. All density gaps created were lower than 0.03 g/cm³.

For the final Brookfield viscosities, the apparent trend is a decrease when the solution volume is increased, except for the run where 0.67L was used.

The reduction of Brookfield viscosity may be a consequence of the decrease of the viscous drag. This decrease can be explained by the dilution, as the A0410 and HCl solution has a considerably lower viscosity than the clay/sand solution.

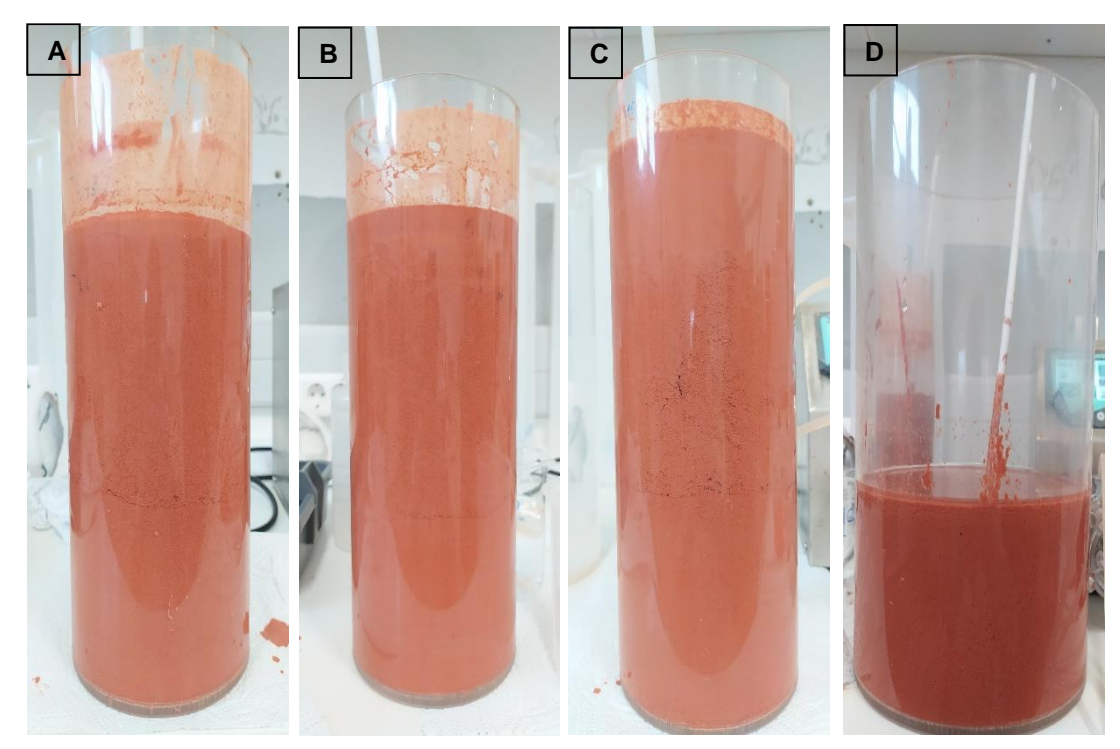


Figure 3.78 - Side view of the solutions treated with A0410 at 1000 mg/L and HCl at 2.5mM and at the volumes of: (A) - 0.2L; (B) - 0.4 L; (C) - 0.67L; (D) - 1L

Figure 3.78 represents the aspect of the solutions treated with A0410 at 1000 mg/L and HCl at 2.5mM and at the volumes of 0.2, 0.4, 0.67 and 1L.

No difference is observable between the runs performed with 0.2 to 0.67L. However, the run performed with a 1L solution showed a thin layer of clean fluid. The clean fluid observed in the last solution is due to the increase of water content. The interstitial water progressively travelled to the top of the column.

In conclusion DR values did achieve the objective of 0.06 g/cm³, however this was only for the run performed with a volume of 0.67L. The purpose of this work is to reduce the density of the solution by settling particles, which adding water does not achieve. Furthermore, it is a possibility that, when using a larger volume of clay/sand mixture, the influence of the dilution becomes less prevalent and adding more volume becomes inefficient and unviable, as adding water may compromise the stability of the column, as it greatly affects the viscosity of the system and the clay/sand suspension.

Overall, DR was not controllable when adding sand, as these particles were integrated in the tridimensional structure formed by the clay and the base polymer PolyMud. Increasing the volume A0410/HCl solution increased DR, but due to the dilution of the column. For both cases, initial densities were above the objective of 1.15-1.20 g/cm³, due to the addition of sand. Marsh

viscosities were not measurable, density gaps created were lower than 0.03 g/cm³ and deposits were not recoverable, as the flocs did not settle.

The exceptional suspension capability of clay B, partially due to its higher negative charge, conditioned the results, due to the flocs also being suspended. However, such a system is not representative of real-world applications, as soils tend to be more varied, instead of pure clay systems or binary clay/sand systems, hence the results may be skewed towards the most extreme case. Performing tests on soils with different textures (different percentages of clay, silts and sands) should provide more accurate real-world insight of whether or not the systems are able to effectively form and settle flocs and reduce the density of the solutions in a controlled fashion, as clays tend to form the most stable suspensions out of the three textures described.

For these soils, the systems which fulfilled the most objectives or accomplished a higher number of DR objectives, such Al₂(SO₄)₃, PFS and A0410+HCl should be tested.

4. Conclusions

The aim of this work was to find a product or formulation capable of decrease the density of soil containing solutions, in a controlled way.

Throughout the development of this work, it was verified that for the results varied significantly for two clay types used. For Clay A, the density reductions of 0.02 g/cm³, 0.06 g/cm³ and 0.09 g/cm³ were attained using the coagulants Al₂(SO₄)₃ and PFS. Runs using Al₂(SO₄)₃ achieved the first and second intervals at the concentration of 600 mg/L and 1000 mg/L, respectively and runs using PFS achieved the third using a concentration of 1000 mg/L as well. Optimal mixing speed was 200 rpm and increasing it had a negative effect on DR. Varying mixing times, using alternative coagulants, agitators and introduction methods did not impact any objective positively. No system achieved simultaneously the DR and Marsh viscosity objective for this clay and when the density gaps between the middle and bottom were measurable, they were lower than 0.03 g/cm³. For this same clay, flocs formed were observed in suspension and, to address this issue, flocculants were introduced. For this system, the density reduction of 0.02 g/cm³ was achieved. The coagulant/flocculant system attained a density reduction of 0.02 g/cm3 using Al₂(SO₄)₃ with Telsun 5153 at the concentrations of 50/75, 100/37.5 150/37.5 and 150/75 mg/L. Al₂(SO₄)₃ with Telsun N23 and Al₂(SO₄)₃ with Flonex 934 also achieved this interval at the concentrations of 150 mg/L of coagulant and 150 mg/L of flocculant. For the coagulant/flocculant system, reducing the agitation speed, introduction methods or using alternative flocculants did not impact any objective positively. A boundary zone was observed where the concentrations of coagulant and flocculant either did not form clean strips and did not cause any visual impact or caused this clean section, where the fluid remaining had viscosities close to that of water, thus, the stability of the solution may have been compromised.

Tests were also run on clay B and this clay behaved differently than the clay A. The same systems that caused clean strips on clay A did not have the same effect on clay B, possibly due to their structural differences.

For clay B, the density reduction of 0.02 g/cm³ was attained for the following system: Telsun 5153 with Al₂(SO₄)₃, FeSO₄ and PFS at the concentration of 150 mg/L of each, with a mixing speed of 200 rpm for 8 minutes. Marsh viscosity was only measurable for the Telsun 5153, Al₂(SO₄)₃/Telsun 5153 and FeSO₄/Telsun 5153 runs, where this objective was accomplished. The density gap between middle and bottom was always lower than 0.03 g/cm³. For this same clay, a density reduction of 0.06 g/cm³ was also attained for the AO₄10/HCl system at the concentration of 1000 mg/L of AO₄10 and concentrations of HCl of 3.3-4.7 mM. Initial densities were within 1.15-1.20 g/cm³, Marsh viscosities were not measurable, the density gaps between the bottom and middle were lower than 0.03 g/cm³.

Deposits were not collectable for clay B, as it formed more stable suspensions that prevented flocs from settling.

Reducing the concentration of anionic dispersant from 1.5 mL/L to 0.5 mL/L facilitated the action of coagulants and flocculants without compromising the initial densities and removing the dispersant increased the variability of the system even for control runs.

For future studies, tests should be performed on soils with different compositions (different percentages of clay, silts and sands) and these should provide more accurate real-world insight of whether or not the systems are able to effectively form and settle flocs and reduce the density of the solutions in a controlled manner, as clays tend to form the most stable suspensions out of the three compositions described. Relatively to the systems tested, the use of flocculants opens more pathways than the use of coagulants, since flocculants have more controllable properties that leads to the controlled density reduction, such as the molecular weight, charge and charge density.

5. References

- [1] H.-Y. Fang, "Preface," in *Foundation Engineering Handbook*, Chapman & Hall, 1991, p. xv.
- [2] H.-Y. Fang, "Soil Stabilization and Grouting," in *Foundation Engineering Handbook*, Chapman & Hall, 1991, pp. 317-369.
- [3] N. Latifi, A. S. A. Rashid, S. Siddiqua and M. Z. A. Majid, "Measurement," *Strength measurement and textural characteristics of tropical residual soil stabilized with liquid polymer*, pp. 46-54, 10 Maio 2016.
- [4] H. F. Winterkorn and S. Pamukcu, "Soil Stabilization and Grouting," in *Foundation Engineering Handbook*, 1991, pp. 317-378.
- [5] E. R. Graber, P. Fine and G. J. Levy, "Soil Stabilization in Semiarid and Arid Land Agriculture," *Journal of Materials in Civil Engineering*, vol. 18, no. 2, pp. 190-205, 2006.
- [6] M. E. Zeynali, "Mechanical and psysico-chemical aspects of wellbore stability during drilling operations," *Journal of Petroleum Science and Engineering*, Vols. 82-83, pp. 120-124, 2012.
- [7] P. Skalle, "Keeping the wellbore stable," in *Support fluids Manual*, Ventus Publishing, 2012, pp. 95-117.
- [8] K. Hussein and K. Al-soudany, "Improving geotechnical properties of clayey soil using polymer material," *MATEC Web of Conferences*, vol. 162, no. 01002, 2018.
- [9] F. H. Chen, Foundations on Expansive Soils, New York, NY: Elsevier, 1975.
- [10] Zumrawi, M. M. E., A. O. Abdelmarouf and A. E. A. Gameil, "Damages of Buildings on Expansive Soils: Diagnosis and Avoidance," *International Journal of Multidisciplinary and Scientific Emerging Research*, vol. 6, no. 2, pp. 108-116, 2017.
- [11] B. R. Cristopher, P.E., C. Schwartz and R. Boudreau, "Geotechnical Aspects of Pavements Reference Manual," U.S. Department of Transportation, Washington, D.C., 2006.
- [12] S. A. Jefferis, Y. Ouyang, P. Wiltcher, T. Suckling and C. Lam, "The On-Site Management of Polymer Support Fluids for the Construction of Drilled Shafts and Diaphragm Walls," in *Grouting*, Honolulu, Hawaii, 2017.

- [13] C. Lam, S. Jefferis and V. Troughton, "Polymer Systems for fluid support excavations," in *Geotechnical issues in construction: short paper series and 2nd conference*, London, 2011.
- [14] Texas Shaft Inc., "Texas Shaft Inc.," 2015. [Online]. Available: http://texas-shafts.com/education/methods/#wetshaft. [Accessed 21 October 2020].
- [15] EFFC, Guide to Support Fluids for Deep Foundations, 2019.
- [16] Amoco Production Company, "Support fluids Manual," 2007.
- [17] S. Kumar, R. Jain, P. Chaudhary and V. Mahto, "Development of Inhibitive Water Based Support fluid System with Synthesized Graft Copolymer for Reactive Indian Shale Formation," in *Kumar, S., Jain, R., Chaudhary, P., & Mahto, V. (2017). Development of Inhibitive Water Based Support fluid System with SySPE Oil and Gas India Conference and Exhibition*, Mumbai, India, 2017.
- [18] N. J. Alderman, D. R. Babu, T. L. Hughes and G. C. Maitland, "The Rheological Properties of Water-Based Support fluids," *Specialty Chemicals*, vol. 9, no. 5, pp. 314-326, 1989.
- [19] Fann Instrument Company, "Marsh Funnel Viscometer," [Online]. Available: https://www.fann.com/fann/products/oil-well-cement-testing/viscosity/marsh-funnel.html?nodeld=3_leveltwo_7&pageld=Products. [Accessed 03 10 2021].
- [20] S. Chemwotei, "GEOTHERMAL SUPPORT FLUIDS," Grensásvegur, Reykjavik, Iceland, 2011.
- [21] T. N. Ofei, "Effect of Yield Power Law Fluid Rheological Properties on Cuttings Transport in Eccentric Horizontal Narrow Annulus," *Journal of Fluids*, vol. 2016, p. 10, 2016.
- [22] A. Tehrani, "Behaviour of Suspensions and Emulsions in Support fluids," *Annual Transactions of the Nordic Rheology Society*, vol. 15, 2007.
- [23] S. V. Mohan, S. Varjani and A. Pandey, Microbial Electrochemical Technology, Elsevier, 2018.
- [24] H. Gamal, S. Elkatatny, S. Basfar and A. Al-Majed, "Effect of pH on Rheological and Filtration Properties of Water-Based Support fluid Based on Bentonite," *Sustainability*, vol. 11, no. 23, p. 6714, 2019.
- [25] Amoco Production Company, "Drilled Shafts Manual," 2010.
- [26] F. Fuping, A. Chi, Y. Fahao, C. Zhihua, F. Sen and X. Haisu, "The Effects of Density Difference on Displacement Interface in Eccentric Annulus During Horizontal Well Cementing," *The Open Petroleum Engineering Journal*, vol. 6, pp. 79-87, 2013.

- [27] D. L. Carbajal, W. Shumway and R. G. Ezell, "Inhibitive water-based support fluid system and method for drilling sands and other water-sensitive formations". United States Patent 7,825,072 B2, 2 November 2010.
- [28] G. J. Goodhue and M. M. Holmes, "Polymeric Earth Support Fluid Compositions and Method For Their Use". World Patent 96/23849, 8 August 1996.
- [29] R. R. Weil and N. C. Brady, "Soil Architecture and Physical Properties," in *The Nature and Properties of Soils*, London, Pearson, 2017, pp. 148-205.
- [30] K. Brown and J. Lemon, "Cations and Cation Exchange Capacity," Ghost Media, 2021. [Online]. Available: http://www.soilquality.org.au/factsheets/cation-exchange-capacity. [Accessed 04 March 2021].
- [31] L. Meozzi, "Relation between turbidity and suspended material at different soils, scales and phosphorus levels, Msc Thesis," 2011. [Online]. Available: https://stud.epsilon.slu.se/3629/1/Meozzi_I_111121.pdf. [Accessed 26 02 2021].
- [32] A. Hanousse, G. Ghassan, G. Ruban, B. Tassin, B. J. Lemaire and C. Joannis, "Relationship between turbidity and total suspended solids concentration within a combined sewer system," *Water Science and Technology,* vol. 64, no. 12, pp. 2445-2452, 2011.
- [33] B. Theng, "Chapter 1. The Clay Minerals," in *Developments in soil science* 9, Netherlands, Elsevier, 1979, pp. 3-36.
- [34] J. O. Rawson, "Physicochemical Studies of Clay Polymer Interactions, PhD Thesis," Sheffield Hallam University, United Kingdom, 1995.
- [35] E. Partheniades, "Chapter 2 The Mineralogy and the Physicochemical Properties of Cohesive Sediments," in *Cohesive Sediments in Open Channels: Properties, Transport and Applications*, MA, Butterworth-Heineman, 2009, pp. 11-45.
- [36] M. Ishiguro and L. K. Koopal, "Surfactant adsorption to soil components and soils," *Advances in colloid and interface science*, vol. 231, pp. 59-102, 2016.
- [37] I. Odom, "Smectite clay minerals: properties and uses," *Phil. Trans. R. Soc. Land*, vol. 311, pp. 391- 409, 1984.
- [38] K. Huang, P. Rowe and C. e. a. Chi, "Cation-controlled wetting properties of vermiculite membranes and its promise for fouling resistant oil—water separation," *Nature Communications*, vol. 11, no. 1097, 2020.
- [39] A. Alvarez, "Sepiolite: Properties and Uses," in *Palygorskite Sepiolite:* Occurrences, Genesis and Uses, Elsevier, 1984, pp. 253-287.
- [40] W. L. Haden and I. Schwint, "ATTAPULGITE: ITS PROPERTIES AND APPLICATIONS," in *Industrial & Engineering Chemistry*, ACS Publications, 1967, pp. 58-69.

- [41] J. Gregory, "The role of colloid interactions in solid-liquid separation," *Water Science Tech.*, vol. 27, no. 10, pp. 1-17, 1993.
- [42] E. Partheniades, "Chapter 3 Forces between Clay Particles and the Process of Flocculation," in *Cohesive Sediments in Open Channels: Properties, Transport and Applications*, Oxford, Butterworth-Heinemann, 2009, pp. 47-88.
- [43] Y. Liang, N. Hilal, P. Langston and V. Starov, "Interaction forces between colloidal particles in liquid: Theory and experiment," *Advances in Colloid and Interface Science*, Vols. 134-135, pp. 151-166, 2007.
- [44] M. Gouy, "Sur la constitution de la charge électrique à la surface d'un électrolyte," J. Phys. Theor. Appl., vol. 9, no. 1, pp. 457-468, 1910.
- [45] D. L. Chapman, "A contribution to the theory of electrocapillarity," *The London, Edinburgh, and Dublin Philosophical Magazine and Journal of Science,* vol. 25, no. 141, pp. 475-481, 1913.
- [46] O. Stern, "The theory of the electrolytic double shift," *Z Elektrochem,* vol. 30, pp. 508-516, 1924.
- [47] P. F. Luckham and S. Rossi, "The Colloidal and Rheological Properties of Bentonite Suspensions," Advances in Colloid and Interface Science, vol. 82, pp. 43-92, 1999.
- [48] C. C. Tester, S. Aloni, B. Gilbert and J. F. Banfield, "Short- and Long-Range Attractive Forces That Influence the Structure of Montmorillonite Osmotic Hydrates," Langmuir: the ACS journal of surfaces and colloids, vol. 32, no. 46, 2016.
- [49] Z. R. Patwary, "Clay Fluid Interactions in Montmorillonite Swelling Clays A Molecular Dynamics and Experimental Study, M.S. thesis," March 2012. [Online]. Available: https://library.ndsu.edu/ir/bitstream/handle/10365/26757/Clay%20Fluid%20Interactions%20in%20Montmorillonite%20Swelling%20Clays%20A%20Molecular%20Dynamics%20and%20Experimental%20Study.pdf?sequence=1. [Accessed 23 October 2020].
- [50] J. Pietri and J. Clark, "Chemistry LibreTexts Hydrogen Bonding," LibreTexts, 22
 August 2020. [Online]. Available:
 https://chem.libretexts.org/Bookshelves/Physical_and_Theoretical_Chemistry_Textb
 ook_Maps/Supplemental_Modules_(Physical_and_Theoretical_Chemistry)/Physical
 _Properties_of_Matter/Atomic_and_Molecular_Properties/Intermolecular_Forces/Sp
 ecific_Interactions/Hy. [Accessed 19 October 2020].
- [51] F. L. Leite, C. C. Bueno, A. L. Da Róz, E. C. Ziemath and O. N. Oliveira Jr., "Theoretical Models for Surface Forces and Adhesion and Their Measurement Using

- Atomic Force Microscopy," *International Journal of Molecular Sciences,* vol. 13, pp. 12773-12856, 2012.
- [52] J. Lim, "Controlling Clay Behaviour in Suspension: Developing a New Paradigm for the Minerals Industry, PhD thesis," *The University of Melbourne*, April 2011.
- [53] J. H. Lu, L. Wu and J. Letey, "Effects of Soil and Water Properties on Anionic Polyacrylamide Sorption," Soil Science Society of America, vol. 66, no. 2, pp. 578-584, 2002.
- [54] "Carnegie Mellon University," [Online]. Available: https://www.cmu.edu/gelfand/lgc-educational-media/polymers/natural-synthetic-polymers/index.html. [Accessed 14 October 2020].
- [55] T. F. R. Alves, M. Morsink, F. Batain, M. V. Chaud, T. Almeida, D. A. Fernandes, C. F. da Silva, E. B. Souto and P. Severino, "Applications of Natural, Semi-Synthetic, and Synthetic Polymers in Cosmetic Formulations," *Cosmetics*, vol. 7, no. 75, 2020.
- [56] M. Kim and C. Cha, "Modulation of functional pendant chains within poly(ethylene glycol) hydrogels for refined control of protein release," *Scientific Reports*, vol. 8, no. 4315, 2018.
- [57] S. Devereux, "Well Programing," in *Practical Well Planning and Drilling Manual*, United States of America, PennWell, 1998, pp. 121-310.
- [58] S. Burchill, P. L. Hall, R. Harrison, M. H. Hayes, J. I. Langford, W. R. Livingston, R. J. Smedley, D. K. Ross and J. J. Tuck, "SMECTITE-POLYMER INTERACTIONS IN AQUEOUS SYSTEMS," *Clay Minerals*, vol. 18, pp. 373-397, 1983.
- [59] S. Banerjee, Z. R. Abdulsattar, K. Agim and R. H. Lane, "Mechanism of polymer adsorption on shale surfaces: Effect of polymer type and presence of monovalent and divalent salts," *Petroleum*, vol. 3, pp. 384-390, 2017.
- [60] P. Somasundaran, T. W. Healy and D. W. Fuerstenau, "The Aggregation of Colloidal Alumina Dispersions by Adsorbed Surfactant Ions," *Journal of Colloid and Interface Science*, vol. 22, no. 6, pp. 599-605, 1966.
- [61] E. Pefferkorn, L. Nabzar and R. Varoqui, "Polyacrylamide Na-kaolinite interactions: Effect of electrolyte concentration on polymer adsorption," *Colloid & Polymer Science*, vol. 265, no. 10, pp. 889-896, 1987.
- [62] B. Gu and H. E. Doner, "THE INTERACTION OF POLYSACCHARIDES WITH SILVER HILL ILLITE," *Clays and Clay Minerals*, vol. 40, no. 2, pp. 151-156, 1992.
- [63] M. Ben-Hur, M. Malik, J. Letey and U. Mingelgrin, "Adsorption of polymers on clays as affected by clay charge and structure, polymer properties, and water quality," *Soil Science*, vol. 153, no. 5, pp. 349-356, 1992.

- [64] A. Jacquet, D. L. Geatches, S. J. Clark and H. C. Greenwell, "Understanding Cationic Polymer Adsorption on Mineral Surfaces: Kaolinite in Cement Aggregates," *Minerals*, vol. 8, no. 4, pp. 130-151, 2018.
- [65] B. K. Theng, "CLAY-POLYMER INTERACTIONS: SUMMARY AND PERSPECTIVES," *Clays and Clay Minerals*, vol. 30, no. 1, pp. 1-10, 1982.
- [66] L. T. Lee, R. Rahbari, J. Lecourtier and G. Chauveteau, "Adsorption of Polyacrylamides on the Different Faces of Kaolinites," *Journal of Colloid and Interface Science*, vol. 147, no. 2, pp. 351-357, 1991.
- [67] H. Heller and R. Keren, "Anionic Polyacrylamide Polymers Effect on Rheological Behavior of Sodium-Montmorillonite Suspensions," *Soil Science Society of America Journal*, vol. 66, no. 1, pp. 19-25, 2002.
- [68] B. J. Lee and M. A. Schlautman, "Effects of Polymer Molecular Weight on Adsorption and Flocculation in Aqueous Kaolinite Suspensions Dosed with Nonionic Polyacrylamides," Water, vol. 7, pp. 5896-5909, 2015.
- [69] G. Durand-Pina, F. Lafuma and R. Audebert, "Flocculation and adsorption properties of cationic polyelectrolytes toward Na-montmorillonite dilute suspensions," *Journal of Colloid and Interface Science*, vol. 119, no. 2, pp. 474-480, 1987.
- [70] N. Schamp and J. Huylebroek, "Adsorption of polymers on clays," *Journal of Polymer Science: Polymer Symposia*, vol. 42, no. 2, pp. 553-562, 1973.
- [71] P. Espinasse and B. Siffert, "Acetamide and Polyacrylamide Adsorption onto Clays: Influence of the Exchance Caton and the Salinity of the Medium," *Clays and Clay Miner*, vol. 27, no. 4, pp. 279-284, 1979.
- [72] R. B. Seymour and C. J. E. Carraher, "Mechanical Properties of Polymers," in *Structure--Property Relationships in Polymers*, New York, NY, Plenum Press, 1984, pp. 57-72.
- [73] X. Zhao, K. Urano and S. Ogasawara, "Adsorption of polyethylene glycol from aqueous solution on montmorillonite," *Colloid & Polymer Science*, vol. 267, no. 10, pp. 899-906, 1989.
- [74] O. M. Sadek, W. K. Mekhemer, F. F. Assaad and B. A. Mostafa, "Adsorption of poly (4-sodium styrene sulfonate) on kaolinite clays," *Journal of Applied Polymer Science*, vol. 100, no. 3, p. 1712–1719, 2006.
- [75] W. Heller and T. L. Pugh, ""Steric" Stabilization of Colloidal Solutions by Adsorption of Flexible Macromolecules," *Journal of Polymer Science*, vol. 47, no. 149, pp. 203-217, 1960.
- [76] J. Schubert and M. Chanana, "Coating Matters: Review on Colloidal Stability of Nanoparticles with Biocompatible Coatings in Biological Media, Living Cells and Organisms," *Current Medicinal Chemistry*, vol. 25, no. 35, pp. 4553-4586, 2018.

- [77] W. Heller and T. L. Pugh, "Steric stabilization of colloidal solutions by adsorption of flexible macromolecules," *Journal of Polymer Science*, vol. 47, no. 149, pp. 203-217, 1960.
- [78] A. A. Zaman, "Effect of polyethylene oxide on viscosity of dispersions of charged silica particles: interplay between rheology, adsorption, and surface charge," *Colloid & Polymer Science*, vol. 278, no. 12, pp. 1187-1197, 2000.
- [79] R. Hogg, "Bridging flocculation by polymers," *Powder and Particle Journal*, no. 30, pp. 3-14, 2013.
- [80] Y. Adachi, A. Kobayashi and M. Kobayashi, "Structure of Colloidal Flocs in relation to the Dynamic Properties of Unstable Suspension," *International Journal of Polymer Science*, vol. 2012, 2012.
- [81] M. Kamibayashi, H. Ogura and Y. Otsubo, "Viscosity behavior of silica suspensions flocculated by associating polymers," *Journal of Colloid and Interface Science*, vol. 290, no. 2, pp. 592-597, 2005.
- [82] K. Sutherland, Filters and Filtration Handbook, Elsevier, 2008.
- [83] K. Sutherland, "Types of filter," in *Filters and Flltration Handbook*, Elsevier, 2008, pp. 97-207.
- [84] R. L. Sloan, K. W. Smith and H. D. Smith Jr, "Viscosity control and filtration of well fluids". 2010 Patent US7736521B2, 15 June 200.
- [85] D. Verdoes and H. Visscher, "Method and device for separating metals and/or metal alloys of different melting points". United States Patent 6224648B1, 1 May 2001.
- [86] E. Ortega-Rivas, "Separation Techniques for Solids and Suspensions," in *Non-thermal Food Engineering Operations*, New York, NY, Springer Science, 2012, pp. 131-197.
- [87] D. D. Ratnayaka, M. J. Brandt and J. Michael, "Storage, Clarification and Chemical Treatment," in *Twort's Water Supply*, Oxford, Butterworth-Heinemann, 2009, pp. 267-314.
- [88] Environmental Protection Agency, "Screens," Combined Sewer Overflow Technology Fact Sheet, September 1999.
- [89] Y. Wen, "Solid-liquid separation vibration sieve device". China Patent CN102380253B, 26 March 2014.
- [90] A. Gupta and D. S. Yan, "Screening," in *Mineral Processing Design and Operations: An introduction*, Oxford, Elsevier, 2016, pp. 357-419.
- [91] KMI Zeolite, "Mesh to Micron Conversion chart," 2018. [Online]. Available: https://www.kmizeolite.com/mesh-chart/. [Accessed 25 October 2020].

- [92] S. Moran, "Chapter 4: Engineering science of water treatment units," in *An applied Guide to Water and Effluent Treatment Plant Design*, Elsevier, 2018, pp. 39-51.
- [93] N. Coote, C. Carrol and N. P. Leavins, "Processing," *Deep Bed Filtration in the Sugar Industry*, pp. 732-741, 1986.
- [94] S. Ray, B. Miligan and N. Keegan, "Measurement of filtration performance, filtration theory and practical applications of ceramic foam filters," in *9th Australasian Conference and Exhibition*, 2005.
- [95] G. Crini, "Advantages and disadvantages of techniques used for wastewater treatment," *Environmental Chemistry Letters*, vol. 17, no. 1, pp. 145-155, 2019.
- [96] Environmental Protection Agency, "Filtration," *WATER TREATMENT MANUALS*, 1995.
- [97] J. H. Jhaveri and Z. Murthy, "A comprehensive review on anti-fouling nanocomposite membranes for pressure driven membrane separation processes," *Desalination*, vol. 379, pp. 137-154, 2016.
- [98] E. Drioli and L. Giorno, Comprehensive Membrane Science and Engineering, Oxford: Elsevier, 2010.
- [99] E. O. Ezugbe and S. Rathilal, "Membrane Technologies in Wastewater Treatment: A review," *Membranes*, vol. 10, no. 5, p. 89, 2020.
- [100] D. D. Ratnayaka, M. J. Brandt and M. K. Johnson, "Water Filtration Granular Media Filtration," in *Twort's Water Supply*, 6^a ed., Elsevier, 2009, pp. 315-347.
- [101] M. A. Abdel-Fatah, "Nanofiltration systems and applications in wastewater treatment: Review article," Ain Shams Engineering Journal, vol. 9, pp. 3077-3092, 2018.
- [102] F. N. Kemmer, "Membrane Separation," in *The Nalco Water Handbook*, McGraw-Hill, 1998, pp. 15.1-15.20.
- [103] K. Scott, "Microfiltration," in *Handbook of industrial membranes*, Elsevier, 1995, pp. 373-429.
- [104] Synder Filtration, "Synder Filtration," [Online]. Available: https://synderfiltration.com/applications/industries/food-beverage/gelatin-production/. [Accessed 10 October 2020].
- [105] H. C. Van Der Horst and J. H. Hanemaaijer, "Cross-flow Microfiltration in the Food Industry. State of the Art," *Desalination*, vol. 77, pp. 235-258, 1990.
- [106] A. F. Ismail and P. S. Goh, "Microfiltration Membrane," in *Encyclopedia of Polymeric Nanomaterials*, Springer-Verlag, 2015, pp. 1250-1255.

- [107] X. Li, L. Jiang and H. Li, "Application of Ultrafiltration Technology in Water Treatment," *IOP Conference Series: Earth and Environment Science*, vol. 186, no. 012009, 2018.
- [108] A.-S. Jönsson and G. Trägårdh, "Ultrafiltration Applications," *Desalination*, vol. 77, pp. 135-179, 1990.
- [109] D. Yordanov, "Preliminary study of the efficiency of ultrafiltration treatment of poultry slaughterhouse wastewater," *Bulgarian Journal of Agricultural Science*, vol. 16, no. 6, pp. 700-704, 2010.
- [110] B. Z. Gönder, S. Arayici and B. Hulusi, "Advanced treatment of pulp and paper mill wastewater by nanofiltration process: Effects of operating conditions and membrane fouling," *Separation and Purification Technology*, vol. 76, pp. 292-302, 2011.
- [111] T. Y. Cath, A. E. Childress and M. Elimelech, "Forward osmosis: Principles, applications, and recent developments," *Journal of Membrane Science*, vol. 281, pp. 70-87, 2006.
- [112] L. Jiang, Y. Tu, X. Li and H. Li, "Application of reverse osmosis in purifying drinking water," in *International Conference on Energy Materials and Environment Engineering (ICEMEE 2018)*, Malaysia, 2018.
- [113] A. C. Mecha, "Applications of Reverse and Forward Osmosis Processes in Wastewater Treatment: Evaluation of Membrane Fouling," in *Osmotically Driven Membrane Processes - Approach, Development and Current Status*, IntechOpen, 2018, pp. 235-254.
- [114] F. Concha A., "Sedimentation of Particulate Systems," in *Solid-Liquid Separation* in the Mining Industry, London, Switzerland, 2014, pp. 43-95.
- [115] A. K. Coker, "Chapter 6 Mechanical Separation," in *Ludwig's Applied Process Design for Chemical and Petrochemical Plants*, United States of America, Elsevier, 2007, pp. 371-444.
- [116] F. N. Kemmer, "Solids/Liquids Separation," in *Nalco Water Handbook*, United States of America, McGraw-Hill, 1988, pp. 9.1-9.59.
- [117] World Health Organization, "Managing water in the home," World Health Organization, Geneva, 2002.
- [118] W. Leung, "Introduction," in *Centrifugal Separations in Biotechnology*, United Kingdom, Elsevier Science, 2007, pp. 1-36.
- [119] S. O. Majekoudunmi, "A Review on Centrifugation in the Pharmaceutical Industry," *American Journal of Biomedical Engineering*, vol. 5, no. 2, pp. 67-78, 2015.

- [120] Alfa Laval, "Decanter Centrifuge," [Online]. Available: https://www.alfalaval.com/globalassets/documents/industries/pulp-and-paper/pcd00002en.pdf. [Accessed 21 October 2020].
- [121] R. Schnause, "Method and device for centrifuging viscous fluids". World Patent 1999011379A1, 11 March 1999.
- [122] S.-A. Marthinusse, Y.-F. Chang, B. Balakin and A. C. Hoffman, "Removal of particles from highly viscous liquids with hydrocyclones," *Chemical Engineering Science*, vol. 108, pp. 169-175, 2014.
- [123] E. Ortega-Rivas and S. Perez-Vega, "Solid-liquid separations in the food industry: operating aspects and relevant applications," *Journal of Food and Nutrition Research*, vol. 50, no. 2, pp. 86-105, 2011.
- [124] X.-m. Ye and Y.-x. Guo, "Solid-Liquid Separation Technology in Contaminated Soil Leaching," in *2nd International Conference on Applied Mechanics, Electronics and Mechanics Engineering*, Beijing, 2017.
- [125] R. Packam and W. Richards, "Water clarification by flotation," *Technical Paper Tp.* 87, p. 35, November 1972.
- [126] N. K. Shammas and G. F. Bennet, "Fundamentals of Wastewater Flotation," in *Handbook of Environmental Engineering*, vol. 12, New York, NY, Springer Science, 2010, pp. 1-48.
- [127] J. Haarhoff and J. K. Edzwald, "Adapting dissolved air flotation for the clarification of seawater," *Desalination*, vol. 311, pp. 90-94, 2013.
- [128] A. Luszczkiewicz, P. Karwowski, A. Muszer and J. Drzymala, "Separation of copper flotation concentrates into density fractions by means of polytungstate aqueous solution," in E3S Web of Conferences, 2016.
- [129] A. Vidyadhar and R. Singh, "Froth Flotation and its Application to Concentration of Low Grade Iron Ores," in *Processing of Iron Ore*, India, NML, 2007, pp. 103-114.
- [130] Y. Otsubo and M. Horigome, "Effect of surfactant adsorption on the rheology of suspensions flocculated by associating polymers," *Korea-Australia Rheology Journal*, vol. 15, no. 4, pp. 179-185, 2003.
- [131] T. Zabel, "The Advantages of Dissolved-air Flotation for Water Treatment," American Water Works Association, vol. 77, no. 5, pp. 42-46, 1985.
- [132] L. K. Wang, N. K. Shammas, W. A. Selke and D. B. Aulenbach, Handbook of Environmental Engineering, vol. 12, New York, NY: Springer Science, 2010.
- [133] M. Delon and R. Wajsfelner, "CLARIFICATION METHOD FOR GRAPE MUST AND THE MUST THUS OBTAINED". U.S. Patent 4,994,290, 19 February 1991.

- [134] Environmental Protection Agency, "Gravity Separation," in *Process Design Manual for Suspended Solids Removal*, United States of America, 1975, pp. 7.1-7.40.
- [135] V. V. Ranade and V. M. Bhandari, "Advanced Phiysico-Chemical Methods of Treatment of Wastewaters," in *Industrial Wastewater Treatment, Recycling and Reuse*, United Kingdom, Butterworth-Heimemann, 2014, pp. 81-140.
- [136] F. N. Kemmer, "Adsorption," in *The Nalco Water Handbook*, United States of America, McGraw-Hill, 1988, pp. 17.1-17.13.
- [137] N. K. Amin, "Removal of reactive dye from aqueous solutions by adsorption onto activated carbons prepared from sugarcane bagasse pith," *Desalination*, vol. 223, pp. 152-161, 2008.
- [138] M. K. Amosa, M. S. Jami, M. F. Alkatib, T. Tajari, D. N. Jimat and R. U. Owolabi, "Turbidity and suspended solids removal from high strength wastewater using high surface area adsorbent: Mechanistic pathway and statistical analysis," *Cogent Engineering*, pp. 1-18, 09 March 2016.
- [139] H. Small, F. L. Saunders and J. Solc, "Hydrodynamic Chromatrography: A New Approach to Particle Size Analysis," *Advances in Colloid end interface Science*, vol. 6, pp. 237-266, 1976.
- [140] A. M. Striegel, "Hydrodynamic chromatography: Packed columns, multiple detectors, and microcapillaries," *Analytical and Bioanalytical Chemistry*, vol. 402, no. 1, pp. 77-81, 2011.
- [141] F. N. Kemmer, "Coagulation and Flocculation," in *The Nalco Water Handbook*, United States of America, McGraw-Hill, 1988, pp. 8.3-8.23.
- [142] J. Bratby, Coagulation and Flocculation With An Emphasis On Water and Wastewater Treatment, England: Uplands Press Ltd., 1980.
- [143] E. S. Tarleton and R. J. Wakeman, "Pretreatment of suspensions," in *Solid/Liquid Separation: Equipment Selection and Process Design*, Oxford, United Kingdom, Butterworth-Heineman, 2007, pp. 126-151.
- [144] H. Wei, B. Gao, J. Ren, A. Li and H. Yang, "Coagulation/flocculation in dewatering of sludge: A review," *Water Research*, vol. 143, pp. 608-631, 2018.
- [145] M. Jang, H. Lee and Y. Shim, "Rapid removal of fine particles from mine water using sequential processes of coagulation and flocculation," *Environmental technology*, vol. 31, no. 4, pp. 423-432, 2010.
- [146] H. Katja and S. Mika, "Flocculation in Paper and Pulp Mill Sludge Process," Research Journal Of Chemistry And Environment, vol. 11, no. 3, pp. 96-103, 2007.
- [147] H. U. Zeidler, "Process and aparatus for treating support fluid". Canada Patent CA2867496A1, 28 August 2014.

- [148] P. Leopold and S. D. Freese, "A simple guide to the chemistry, selection and use of chemicals for water and wastewater treatment," *WRC Report NO. TT 405/09*, pp. 1-136, July 2009.
- [149] V. Önen, M. Göçer and H. A. Taner, "Effect of coagulants and flocculants on dewatering of kaolin suspensions," *OHU J. Eng. Sci*, vol. 7, no. 1, pp. 297-305, 2018.
- [150] State of Oregon, "Operations: Coagulation," Oregon.
- [151] O. P. Sahu and P. K. Chaudhari, "Review on Chemical treatment of Industrial Waste Water," *J. Appl. Sci. Environ. Manage.*, vol. 17, no. 2, pp. 241-257, 2013.
- [152] I. G. Bantcheva, "Study on the factors affecting coagulation and flocculation in treatment of industrial effluents," *Transactions on Ecology and the Environment*, vol. 48, pp. 155-162, 2001.
- [153] Y. Ding, J. Zhao, L. Wei, W. Li and Y. Chi, "Effects of Mixing Conditions on Floc Properties in Magnesium Hydroxide Continuous Coagulation Process," *Applied Sciences*, vol. 973, no. 9, 2019.
- [154] W.-z. Yu, J. Gregory, L. Campos and G. Li, "The role of mixing conditions on floc growth, breakage and re-growth," *Chemical Engineering Journal*, vol. 171, no. 2, pp. 425-430, 2011.
- [155] Z. Zhang, D. Liu, D. Hu, D. Li, X. Ren, Y. Cheng and Z. Luan, "Effects of Slow-Mixing on the Coagulation Performance of Polyaluminum Chloride (PACI)," *Chinese Journal of Chemical Engineering*, vol. 21, no. 3, pp. 318-323, 2013.
- [156] E. K. Tetteh and S. Rathilal, "Application of Organic Coagulants in Water and Wastewater Treatment," 3 April 2019. [Online]. Available: https://www.intechopen.com/books/organic-polymers/application-of-organic-coagulants-in-water-and-wastewater-treatment. [Accessed 17 February 2021].
- [157] A. D. Zand and H. Hoveidi, "Comparing Aluminium Sulfate and Poly-Aluminium Chloride (PAC) Performance in Turbidity Removal from Synthetic Water," *Journal of Applied Biotechnology Reports*, vol. 2, no. 3, pp. 287-292, 2015.
- [158] F. Concha A., "Flocculation," in *Particle Aggregation by Coagulation and Flocculation*, Springer, Switzerland, 2014, pp. 143-172.
- [159] T. Lindström and G. Glad-Nordmark, "Network Flocculation and Fractionation of Latex Particles by Means of a Polyethyleneoxide-Phenolformaldehyde Resin Complex," *Journal of Colloid and Interface Science*, vol. 97, no. 1, pp. 62-67, 1984.
- [160] J. Gregory and S. Barany, "Adsorption and flocculation by polymers and polymer mixtures," *Advances in Colloid and Interface Science*, vol. 169, pp. 1-12, 2011.

- [161] T. T. Teng, S. S. Wong and L. W. Low, "Coagulation–Flocculation Method for the Treatment of Pulp and Paper Mill Wastewater," in *The Role of Colloidal Systems in Environmental Protection*, Elsevier, 2014, pp. 239-259.
- [162] A. K. Verma, R. R. Dash and P. Bhunia, "A review on chemical coagulation/flocculation technologies for removal of colour from textile wastewaters," *Journal of Environmental Management*, vol. 93, pp. 154-168, 2012.
- [163] S. Peng, G. Jiang, X. Li, L. Yang, F. Liu and Y. He, "Flocculation of submicron particles in water-based support fluids by CMC-g-DMDAAC," *Journal of Petroleum Science and Engineering*, vol. 162, pp. 55-62, 2018.
- [164] M. S. Nasser and A. E. James, "The effect of polyacrylamide charge density and molecular weight on the flocculation and sedimentation behaviour of kaolinite suspensions," Separation and Purification Technology, vol. 52, no. 2, pp. 241-252, 2006.
- [165] T. Taşdemir and A. Taşdemir, "Effect of Mixing Conditions on Flocculation," in XIIIth International Mineral Processing Symposium, Turkey, 2012.
- [166] S. Haydar and J. A. Aziz, "Coagulation-flocculation studies of tannery wastewater using combination of alum with cationic and anionic polymers," *Journal of Hazardous Materials*, vol. 168, no. 2-3, pp. 1035-1040, 2009.
- [167] T. Z. Mahmudabadi, A. A. Ebrahimi, H. Eslami, M. Mokhtari, M. H. Salmani, M. T. Ghaneian, M. Mohamadzadeh and M. Pakdaman, "Optimization and economic evaluation of modified coagulation-flocculation process for enhanced treatment of ceramic-tile industry wastewater," *Zarei Mahmudabadi et al. AMB Expr*, vol. 8, no. 172, pp. 1-12, 2018.
- [168] W. Bai, L. Kong and A. Guo, "Effects of physical properties on electrical conductivity of compacted lateritic soil," *Journal of Rock Mechanics and Geotechnical Engineering*, vol. 5, no. 5, pp. 406-411, 2013.
- [169] J. B. Culkin, "Method and apparatus for electrofiltration". Europe Patent 0,202,934, 21 05 1986.
- [170] E. S. Tarleton, "The Role Of Field-Assisted Techniques in Solid/Liquid Separation," Filtration & Separation, pp. 246-238, May/June 1992.
- [171] G. Tchillingarian, "Possible utilization of electrophoretic phenomenon for separation of fine sediments into grades," *Journal of Sedimentary Petrology*, vol. 22, no. 1, pp. 29-32, 1952.
- [172] A. K. Mostafazadeh, M. Zolfaghari and P. Drogui, "Electrofiltration technique for water and wastewater treatment and bio-products management: A review," *Journal of Water Process Engineering*, 2016.

- [173] W. Pigman, F. M. Patton and D. Platt, "The Effect of "Viscosity" on the Electrophoretic Mobilities of the Components of Synovial Fluids and Blood Serums," ARCHIVES OF BIOCHEMISTRY AND BIOPHYSICS, vol. 69, pp. 334-345, 1957.
- [174] N. S. Zaidi, J. Sohaili, K. Muda and M. Sillanpää, "Magnetic Field Application and its Potential in Water and Wastewater Treatment Systems," *Separation & Purification Reviews*, vol. 43, no. 3, pp. 206-240, 2014.
- [175] A. Yadollahpour, S. Rashidi, Z. Ghotbeddin, M. Jalilifar and Z. Rezaee, "Electromagnetic Fields for the Treatments of Wastewater: A Review of Applications and Future Opportunities," *Journal of Pure and Applied Microbiology*, vol. 8, no. 5, pp. 3711-3719, 2014.
- [176] S. Hibayashi, F. Mishima, Y. Akiyama and S. Nishijima, "Study on High Gradient Magnetic Separation for Selective Removal of Impurity From Highly Viscous Fluid," *IEEE TRANSACTIONS ON APPLIED SUPERCONDUCTIVITY*, vol. 21, no. 3, pp. 2055-2058, 2011.
- [177] M. Bekker, J. P. Meyer, L. Pretorius and D. F. van der Merwe, "Separation of solid-liquid suspensions with ultrasonic accoustic energy," Wat. Res., vol. 31, no. 10, pp. 2543-2549, 1997.
- [178] T. Leong, "Ultrasonic Separation of Food Materials," in *Handbook of Ultrasonics* and *Sonochemistry*, Singapore, Springer Science, 2015, pp. 1-21.
- [179] N. A. H. Fetyan and T. M. S. Attia, "Water purification using ultrasound waves: application and challenges," *Arab Journal of Basic and Applied Sciences*, vol. 27, no. 1, pp. 194-207, 2020.
- [180] D. M. Bates and W. Bagnall, "Viscosity reduction". World Patent 2010/012032 A1, 29 July 2009.
- [181] M. A. A. Hassan, T. P. Li and Z. Z. Noor, "COAGULATION AND FLOCCULATION TREATMENT OF WASTEWATER IN TEXTILE INDUSTRY USING CHITOSAN," *Journal of Chemical and Natural Resources Engineering*, vol. 4, no. 1, pp. 43-53.
- [182] V. Saritha, N. Srinivas and S. Vuppala, "Analysis and optimization of coagulation and flocculation process," *Applied Water Science*, vol. 7, pp. 451-460, 2017.
- [183] Y. Zhang, F. Nakamura, Y. Sakamoto and K. Nishida, "Coagulation Behaviors and Coagulant Dosage Control of Kaolin and Bentonite Suspensions," *Environmental Engineering Research*, vol. 39, 2002.
- [184] H. A. Aziz, S. Alias, F. Assari and M. N. Adlan, "The use of alum, ferric chloride and ferrous sulfate as coagulants in removing suspended solids, colour and COD from semi-aerobic landfill leachate at controlled pH," *Waste Management & Research*, vol. 25, no. 6, pp. 556-565, 2007.

- [185] A. Baghvand, A. D. Zand, N. Mehrdadi and A. Karbassi, "Optimizing Coagulation Process for Low to High Turbidity Waters Using Aluminum and Iron Salts," *American Journal of Environmental Sciences*, vol. 6, no. 5, pp. 442-448, 2010.
- [186] A. I. Zouboulis, P. A. Moussas and F. Vasilakou, "Polyferric sulphate: Preparation, characterisation and application in coagulation experiments," *Journal of Hazardous Materials*, vol. 155, pp. 459-468, 2008.
- [187] D. Ghernaout and B. Ghernaout, "Sweep flocculation as a second form of charge neutralization a review," *Desalination and Water Treatment*, vol. 44, pp. 15-28, 2012.
- [188] Anderen Ltd., "Brookfield Viscometers," Anderen Ltd., 2017. [Online]. Available: http://www.ceramictestingequipment.co.uk/. [Accessed 15 02 2021].
- [189] V. Onen and M. Gocer, "The effect of single and combined coagulation/flocculation methods on the sedimentation behavior and conductivity of bentonite suspensions with different swelling potentials," *Particulate Science and Technology*, vol. 37, no. 7, pp. 823-830, 2019.
- [190] E. Joseph and G. Singhvi, "Chapter 4 Multifunctional nanocrystals for cancer therapy: a potential nanocarrier," in *Nanomaterials for Drug Delivery and Therapy*, William Andrew, 2019, pp. 91-116.
- [191] E. Tombácz and M. Szekeres, "Surface charge heterogeneity of kaolinite in aqueous suspension," *Applied Clay Science*, vol. 34, pp. 105-124, 2006.
- [192] A. Shakeel, Z. Safar, M. Ibanez, L. von Passen and C. Chassagne, "Flocculation of Clay Suspensions by Anionic and Cationic Polyelectrolytes: A Systematic Analysis," *Minerals*, vol. 999, no. 10, p. 24, 2020.
- [193] D. Niriella and R. P. Carnahan, "Comparison Study of Zeta Potential Values of Bentonite in," *Journal of Dispersion Science and Technology,* vol. 27, p. 123–131, 2006.
- [194] B. A. Fil, C. Özmetin and M. Korkmaz, "Characterization and electrokinetic properties of montmorillonite," *Bulgarian Chemical Communications*, vol. 46, no. 2, pp. 258-263, 2014.
- [195] B. Ersoy, A. Evcin, T. Uygunoglu, Z. B. Akdemir, W. Brostow and J. Warmund, "Zeta Potential–Viscosity Relationship in Kaolinite Slurry in the Presence of Dispersants," *Arabian Journal for Science and Engineering*, vol. 39, pp. 5451-5457, 2014.
- [196] N. Wilkinson, A. Metaxas, C. Quinney, S. Wickramaratne, T. M. Reineke and C. S. Dutcher, "pH dependence of bentonite aggregate size and morphology on polymerclay flocculation," *Colloids and Surfaces A*, vol. 537, pp. 281-286, 2018.

- [197] D. Seo, K. Oh, W. Im and H. L. Lee, "Hydrolysis of Cationic Polyacrylamide and its Effect on Flocculation of Ground Calcium Carbonate," *BioResources*, vol. 13, no. 3, pp. 5303-5318, 2018.
- [198] G. Craciun, D. Ighigeanu and M. D. Stelescu, "Synthesis and Characterization of Poly(Acrylamide-Co-Acrylic Acid) Flocculant Obtained by Electron Beam Irradiation," *Materials Researc*, vol. 18, no. 5, pp. 984-993, 2015.
- [199] K. Brown, "Fact Sheets: Bulk Density Measurement," Ghost Media Writing Services, 2021. [Online]. Available: http://soilquality.org.au/factsheets/bulk-density-measurement. [Accessed 06 08 2021].
- [200] H.-Y. Fang, Foundation Engineering Handbook, 1991.
- [201] R. R. Weil and N. C. Brady, "Soil Architecture and Physical Properties," in *The Nature and Properties of Soils*, London, Pearson, 2017, pp. 148-205.
- [202] T. Stutzmann and B. Siffert, "Contribution to adsorption mechanism of acetamide and polyacrylamide on to clays," *Clays and Clay Minerals*, vol. 25, pp. 392-406, 1977.
- [203] R. A. Arterburn, "The Sizing And Selection of Hydrocyclones," 2001.
- [204] K. Miller, "Electric double layer," 9 December 2011. [Online]. Available: http://soft-matter.seas.harvard.edu/index.php/Electric_double_layer. [Accessed 14 October 2020].
- [205] S. Marchuk, "The Dynamics of Potassium in some Australian soils, PhD Thesis," The University of Adelaide, 2015.
- [206] J. Cadera and P. Cote, "Use of polymer as flocculation aid in membrane filtration". World Patent 2004/031083 A1, 15 April 2004.
- [207] E. A. López-Maldonaldo, M. T. Oropeza-Guzmán and A. Ochoa-Terán, "Improving the Efficiency of a Coagulation-Flocculation Wastewater Treatment of the Semiconductor Industry through Zeta Potential Measurements," *Journal of Chemistry*, vol. 2014, pp. 1-10, 2014.
- [208] A. S. Michaels, "Aggregation of Suspensions by Polyelectrolytes," *Industrial & Engineering Chemistry*, vol. 56, no. 7, pp. 1485-1490, 1954.

6. Appendix

Appendix 1 - Runs performed on protocol 2.3.1

Run	Coagulant concentration (mg/L)	Agitation time (min)	Mixing speed (rpm)	Introduction method	Coagulant	Initial density (g/cm³)	Clay added (g)
7	50						
8	600						
9	5	8	200				750
10	200						
11	5			External			
12	50						
13	200	16			Al ₂ (SO ₄) ₃		
14	600					1.10-1.13	
15	5		1				
16	50	0.4					
17	200	24					
18	600						
19	5						
20	50		050				
21	200	8	250				
22	600						

23	5						
24	50						
25	200		300				
26							
54			200	Internal			
27					FeSO ₄		
28	000				PFS		
29	600	250		(NH4) ₂ SO ₄			
57					Al ₂ (SO ₄) ₃		
65					FeSO ₄		
66					PFS		
67					(NH ₄) ₂ SO ₄		
63	200			External	Al ₂ (SO ₄) ₃		
68	200				PFS		
57	600				Al ₂ (SO ₄) ₃	1.14-1.16	900
65	600				PFS	1.14-1.10	900
70	1000		200		Al ₂ (SO ₄) ₃		
71	1000		200		PFS		
58	4500				Al ₂ (SO ₄) ₃		
69	1500				PFS		
106	1110				CaCl		
109	2775				CaCl ₂		

107	5549
105	111000
111	584
112	5844
113	0
115	300
144	600
110	2000

Appendix 2 - Runs performed on protocol 2.3.3

Run	Coagulant	Flocculant	Coagulant concentration (mg/L)	Flocculant concentration (mg/L)	Introduction method	Flocculant mixing speed (rpm)
72	Al ₂ (SO ₄) ₃	Microbond	600	75		
73		6610				
74		Telsun 5153				
76			50	75		
79			100	37.5	External	200
80			150	37.5		
81				75		
82				300		
83				150		

84			175	37.5		
78			200	15		
77				37.5		
75				75		
83			150	150		
87		9233				
89		Telsun N23				
90		Flonex 934				
86		Telsun 5153			Internal	
88						20
102	-	Telsun 5153	-	150		
101	Al ₂ (SO ₄) ₃		150	-		
99	-	Microbond	-	150		
95	Al ₂ (SO ₄) ₃	Telsun 5153	150	150		
103	PFS	Telsun 5153	150	150	External	200
143	-	A0410	-	-		
141	Al ₂ (SO ₄) ₃	-	300	-		
142	PFS	-	300	-		
111	NaCl	-	584	-		
112			5844			
116		Microbond		50		

117		6610				
-----	--	------	--	--	--	--

Appendix 3 - Runs performed on protocol 2.3.4

Run	Flocculant	Flocculant concentration (mg/L)	HCI concentration (mM)	Solution volume (L)	Solution temperature (°C)
129		1000	0	0.4	
127	6605	1000	2.1	0.4	-
126	6005	4.2 0.8		0.8	
130		2000	4.2	0.4	
118	Nonionic	500	0	0.2	
119	513	500	0.4	0.2	Rta
120			0		
121			0.8		
122			1.7		
136 152			2.5		
153	A0410	1000	2.9	0.4	
140	710110		3.3	.	
154	-		3.9		
155					
158			4.7		
151			5		

150		6.6	
149	250		
159	500	2.5	
152	800		
137	1500		
156			16
157			21

Appendix 4 - Runs performed on protocol 2.3.5

Run	HCI concentration (mM)	Solution volme (mL)
160	0	
161	0.8	400
162		
163	2.5	200
164	2.5	670
165		1000

Appendix 5 – Input variables (Coagulant concentration and initial density) and output variables (final density, Brookfield viscosities, Marsh viscosities, pH, conductivities, DR, Marsh gaps and initial and final density gaps) for the runs performed with Al₂(SO₄)₃, with a mixing speed of 200 rpm, for 8 minutes on Clay A clay

Run	Coagulant concentration	Zone	De	nsity (g/cm	³)		kfield ity (cP)	Marsh	viscosity ((s/quart)	p⊦	I		uctivity 6/cm)	DR
Kuli	(mg/L)	Zone	Initial	Final	Final gap	Initial	Final	Initial	Final	Gap	Initial	Final	Initial	Final	(g/cm³)
9	5	Middle	1.1018	1.0958	0.0034	45.06	43.32	71	69	-2	9.92	9.94	1251	1263	0.006
9	5	Bottom	1.1175	1.0992		47.34	49.86	71	09		9.93	9.90	1267	1275	0.0183
7		Middle	1.1125	1.1110	0.012	48.06	43.44	72	67	-5	10.13	10.16	1366	1386	0.0015
/	7 50	Bottom	1.1375	1.0990		50.34	45.48	12	67		10.25	10.20	1374	1389	0.0385
10	200	Middle	1.1114	1.0766	0.0566	50.82	46.02	62	63	1	-	9.97	N.M.	1417	0.0348
10	10 200	Bottom	1.2766	1.0200		253.5	44.1	02	03		N.M.	10.07	N.M.*	1411	0.2566
	8 600 -	Middle	1.0974	1.0905	0.0067	45.5	43.44	62	68	6	10.31	9.72	1366	1425	0.0069
0	8 600	Bottom	1.1231	1.0972		47.76	45.48	02	00		10.32	9.92	1360	1434	0.0259

Appendix 6 - Input variables (Coagulant concentration and initial density) and output variables (final density, Brookfield viscosities, Marsh viscosities, pH, conductivities, DR, Marsh gaps and initial and final density gaps) for the runs performed with Al₂(SO₄)₃, with a mixing speed of 200 rpm, for 16 minutes on Clay A clay

Run	Coagulant concentrati	Zone	D	ensity (g/cr	m3)	viso	okfield cosity cP)	Marsh	viscosity	(s/quart)	р	Н	condu (µS/	•	DR
	on (mg/L)		Initial	Final	Gap	Initia I	Final	Initial	Final	Gap	Initial	Final	Initial	Final	(g/cm3)
11	5	Middle	1.1018	1.1001	0.0035	39.4 2	44.1	69	68	-1	10.29	10.16	1236	1248	0.0017
11	Bot	Bottom	1.1175	1.1036	0.0035	45.7 8	45.36	69	00	-1	10.40	10.36	1237	1253	0.0139
12		Middle	1.1015	1.1005	0.0006	46.3 8	44.88	79	80	1	10.28	10.36	1263	1272	0.001
12	12 50	Bottom	1.1129	1.1011	0.0006	48.0 6	46.26	79	60	ı	10.44	10.36	1260	1277	0.0118
12	200	Middle	1.1176	1.1151	0.0047	96.8 4	101.2	90	88	-2	10.14	10.09	1299	1347	0.0025
13	13 200	Bottom	1.1353	1.1198	0.0047	105. 6	176.6	90	00	-2	10.17	10.08	1301	1343	0.0155
		Middle	1.1113	1.1061		125	156.8				10.30	9.92	1310	1386	0.0052
14	14 600	Bottom	1.1277	1.1066	0.0005	126. 6	533.4	90	106	16	10.30	9.83	1300	1389	0.0211

Appendix 7 - Input variables (Coagulant concentration and initial density) and output variables (final density, Brookfield viscosities, Marsh viscosities, pH, conductivities, DR, Marsh gaps and initial and final density gaps) for the runs performed with Al₂(SO₄)₃, with a mixing speed of 200 rpm, for 24 minutes on Clay A clay

Run	Zone	Coagulant concentration	Den	sity (g/d	cm³)	Brool viscosi			sh visco (s/quart)	•	р	Н		uctivity /cm)	DR (g/cm³)
		(mg/L)	Initial	Final	Gap	Initial	Final	Initial	Final	Gap	Initial	Final	Initial	Final	(g/ciii [*])
15	Middle	5	1.1095	1.1090	0.0048	37.5	48.06	88	88	0	10.28	10.08	1235	1283	0.0005
15	Bottom	3	1.1373	1.1138	0.0046	51.78	51.56	00	00	U	10.31	10.32	1255	1287	0.0235
16	Middle	50	1.1130	1.1127	0.0095	55.8	80.4	99	89	10	10.18	10.12	1216	1237	0.0003
16	Bottom	50	1.1286	1.1222	0.0095	95.28	92.4	99	69	-10	10.13	10.10	1217	1235	0.0064
17	Middle	200	1.1068	1.1070	0.0018	72.96	75.24	85	88	3	10.42	10.34	1283	1313	0.0002
	Bottom		1.1202	1.1088		87.36	84				10.47	10.41	1276	1316	0.0114
10	Middle	600	1.1182	1.1087	0.0010	77.52	514.2	95	07	2	10.35	9.69	1282	1436	0.0095
18	Bottom	600	1.1301	1.1106	0.0019	84.24	693.6	95	97	2	10.42	5.35	1281	1432	0.0195

Appendix 8 - Input variables (Coagulant concentration and initial density) and output variables (final density, Brookfield viscosities, Marsh viscosities, pH, conductivities, DR, Marsh gaps and initial and final density gaps) for the runs performed with Al₂(SO₄)₃, with a mixing speed of 250 rpm, for 8 minutes on Clay A clay.

Run	Zone	Coagulant concentration	Den	sity (g/d	cm³)	Broo viscos			sh visco (s/quart)		р	Н	conductiv	vity (µS/cm)	
		(mg/L)	Initial	Final	Gap	Initial	Final	Initial	Final	Gap	Initial	Final	Initial	Final	(g/cm³)
19	Middle	5	1.1069	1.1034	0.0015	65.04	62.4	88	81	-7	10.44	10.48	1270	1268	0.0035
19	Bottom	5	1.1148	1.1049	0.0013	70.68	65.76	00	01	-7	10.48	10.48	1259	1274	0.0099
20	Middle	50	1.0995	1.0984		57	55.08	82	79	-3	10.52	10.45	1226	1232	0.0011
20	Bottom	50	1.1110	1.0978	0.0006	60.24	57	02	79	?	10.50	10.47	1226	1258	0.0132
21	Middle	200	1.0910	1.1094	0.0007	84.36	92.88	93	120	27	10.37	10.22	1253	1308	- 0.0184
	Bottom	200	1.1245	1.1101		89.4	106.9				10.39	10.22	1252	1209	0.0144
22	Middle		1.0987	1.0957	0.0008	72.48	112.4	97	153	56	10.50	9.90	1245	1365	0.003
22	Bottom		1.1109	1.0949	0.0006	71.4	553.2	97	103	90	10.51	9.71	1236	1400	0.016

Appendix 9 - Input variables (Coagulant concentration and initial density) and output variables (final density, Brookfield viscosities, Marsh viscosities, pH, conductivities, DR, Marsh gaps and initial and final density gaps) for the runs performed with Al₂(SO₄)₃, with a mixing speed of 300 rpm, for 8 minutes on Clay A clay. ^{a)}Impossible to measure

Run	Zone	Coagulant concentration	Den	sity (g/c	m³)		kfield ity (cP)		sh visco: (s/quart)	sity	р	Н	conductivi	ty (µS/cm)	DR
		(mg/L)	Initial	Final	Gap	Initial	Final	Initial	Final	Gap	Initial	Final	Initial	Final	(g/cm ³)
23	Middle	5	1.1101	1.1106	0.0058	70.32	67.32	116	104	-12	10.36	10.38	1273	1276	- 0.0005
	Bottom		1.1283	1.1164		84.96	76.68				10.40	10.36	1268	1281	0.0119
24	Middle	50	1.0964	1.0983	0.0033	66.96	60.12	114	100	-14	10.40	10.38	1304	1327	- 0.0019
	Bottom	50	1.1130	1.1016		67.2	64.8				10.40	10.35	1301	1324	0.0114
25	Middle	200	1.1032	1.1004	0.0016	68.52	88.32	109	120	11	10.38	10.03	1299	1357	0.0028
25	Bottom	200	1.1200	1.1020	0.0016	72	110.8	109	120	11	10.43	10.04	1286	1253	0.018
26	Middle	600	1.1097	1.1069	0.0011	80.28	775.2	105	I.M. ^{a)}	I.M. ^{a)}	10.33	9.57	1314	1501	0.0028
20	26 Middle Bottom	600	1.1361	1.1080	0.0011	85.68	820.8	105	1.IVI. ^a)	i.ivi. ^a	10.47	9.04	1304	1488	0.0281

Appendix 10 - Input variables (Coagulant concentration and initial density) and output variables (final density, Brookfield viscosities, Marsh viscosityies, pH, conductivities, DR, Marsh gaps and initial and final density gaps) for the runs performed with Al₂(SO₄)₃, with a mixing speed of 200 rpm, for 8 minutes on Clay A clay. ^{a)}Impossible to measure

Run	Zone	Coagulant concentratio	Den	sity (g/d	cm³)		kfield ity (cP)	Marsh viscosi	ty (s/q	uart)	рH	I		uctivity /cm)	DR
		n (mg/L)	Initial	Final	Gap	Initial	Final	Initial	Final	Gap	Initial	Final	Initial	Final	(g/cm³)
E4	Middle	000	1.1054	0.0004	1.1013	73.92	88.56	80	102	22	10.65	10.41	1113	1163	0.0041
51	Bottom	900	1.1206	0.0004	1.1017	75.96	109.3	- 80	103	23	10.64	10.37	1112	1186	0.0189
50	Middle	4000	1.1057	0.0044	1.1022	63.6	90.36	77	400		10.55	10.33	1098	1177	0.0035
53	Bottom	1200	1.1164	0.0011	1.1033	69.24	195.6	- 77	129	52	10.66	10.22	1106	1193	0.0131
EE	Middle	1500	1.1017	0.0015	1.0967	72.24	405.6	76	LMa)	LMa)	10.52	10.01	1148	1212	0.005
55	55 Bottom	1500	1.1116	0.0015	1.0982	77.52	549.6	76	I.IVI. ^α	I.M.a)	10.58	9.97	1144	1218	0.0134

Appendix 11 - Input variables (Coagulant concentration and initial density) and output variables (final density, Brookfield viscosities, Marsh viscosities, pH, conductivities, DR, Marsh gaps and initial and final density gaps) for the runs performed with Al₂(SO₄)₃, for 8 minutes on Clay A clay, using different agitators at 200 and 300 rpm. ^{a)}Impossible to measure

Run	Zone	Coagulant concentration	Dei	nsity (g/c	m³)		l viscosity P)	Marsh v	viscosity (s/quart)	р	Н	conductiv	ity (µS/cm)	DR
	20110	(mg/L)	Initial	Final	Gap	Initial	Final	Initial	Final	Gap	Initial	Final	Initial	Final	(g/cm³)
8	Middle	600	1.0974	1.0905	0.0067	45.5	43.44	62	68	6	10.31	9.72	1366	1425	0.0069
0	Bottom	600	1.1231	1.0972	0.0067	47.76	45.48	62	00	0	10.32	9.92	1360	1434	0.0259
200	Middle	600	1.1097	1.1069	0.0044	80.28	775.2	405	1.84.3)	1 1 4 3)	10.33	9.57	1314	1501	0.0028
26	Bottom	600	1.1361	1.1080	0.0011	85.68	820.8	105	I.M. ^{a)}	I.M. ^{a)}	10.47	9.04	1304	1488	0.0281
20	Middle	600	1.1052	1.1040	0.0000	76.92	567.6	70	404	20	10.42	10.19	1288	1359	0.0012
39	Bottom	600	1.1162	1.1042	0.0002	81.6	632.4	73	101	28	10.46	10.14	1280	1357	0.012
40	Middle	600	1.1013	1.0982	0.004	67.2	703.2	70	400	07	10.43	9.61	1298	1450	0.0031
40	40 Bottom	600	1.1178	1.0972	0.001	67.8	834	73	100	27	10.38	9.08	1277	1457	0.0206

Appendix 12 - Input variables (Coagulant concentration and initial density) and output variables (final density, Brookfield viscosities, Marsh viscosities, pH, conductivities, DR, Marsh gaps and initial and final density gaps) for the runs performed with Al₂(SO₄)₃, with a mixing speed of 200 rpm, for 8 minutes on Clay A clay using internal and external introduction methods at 200 and 300 rpm.

Rui	n Zone	Coagulant concentration	Der	sity (g/d	cm³)		kfield ity (cP)		sh visco (s/quart)	•	р	Н	conductiv	ity (µS/cm)	–
		(mg/L)	Initial	Final	Gap	Initial	Final	Initial	Final	Gap	Initial	Final	Initial	Final	(g/cm ³)
	Middle	600	1.0974	1.0905	0.0067	45.5	43.44	60	60	6	10.31	9.72	1366	1425	0.0069
, °	Bottom		1.1231	1.0972	0.0067	47.76	45.48	62	68	6	10.32	9.92	1360	1434	0.0259
ΕΛ	Middle	600	1.1011	1.0954	0.0003	107	149	70	06	17	1.64	10.27	1112	1192	0.0057
54	54 Bottom	600	1.1103	1.0957	0.0003	95.4	501	79	96	17	10.66	9.95	1111	1207	0.0146

Appendix 13 - Input variables (Coagulant type and initial density) and output variables (final density, Brookfield viscosities, Marsh viscosities, pH, conductivities, DR, Marsh gaps and initial and final density gaps) for the runs performed with different coagulants (Al₂(SO₄)₃, FeSO₄, PFS and (NH₄)₂SO₄) at 600 mg/L with a mixing speed of 250 rpm, for 8 minutes on Clay A clay. *Impossible to measure

Run	Zone	Coagulant	Den	sity (g/d	cm³)	Brool viscosi		Mar	sh visco (s/quart)	•	р	Н	conductivi	ty (µS/cm)	DR
		J	Initial	Final	Gap	Initial	Final	Initial	Final	Gap	Initial	Final	Initial	Final	(g/cm³)
22	Middle	Al ₂ (SO ₄) ₃	1.0987	1.0957	0.0008	72.48	112.4	97	153	56	10.50	9.90	1245	1365	0.003
22	Bottom	A12(3O4)3	1.1109	1.0949	0.0006	71.4	553.2	91	100	36	10.51	9.71	1236	1400	0.016
27	Middle	F080	1.1092	1.0976	0.0025	68.4	110.8	106	162	57	10.45	9.57	1300	1428	0.01157
27	Bottom	FeSO ₄	1.1136	1.0941	0.0035	69.96	236.2	106	163	57	10.49	9.51	1288	1434	0.0195
28	Middle	DEC	1.1109	1.1052	0.0043	126.3	676.8	148	1 N 1 *	I N // *	10.22	9.21	1341	1537	0.0057
28	Bottom	PFS	1.1227	1.1095	0.0043	155.7	704.4	148	I.M.*	I.M.*	10.23	8.36	1339	1565	0.0132
20	Middle	(NILL) CO	1.1061	1.1038	0.0004	67.68	1509	0.0	447	24	10.41	9.90	1315	1816	0.0023
29	Bottom	(NH ₄) ₂ SO ₄	1.1191	1.1034	0.0004	73.8	1698	86	117	31	10.44	9.77	1310	1800	0.0157
57	Middle	AL (CO.)	1.1607	1.1502	0.0008	818.4	730.8	99	85	-14	10.42	9.57	1164	1340	0.0105
57	Bottom	Al ₂ (SO ₄) ₃	1.1600	1.1494	0.0006	859.2	783.6	99	65	-14	10.41	9.48	1175	1344	0.0106
C.F.	Middle	F-00	1.1492	1.1465	0.0000	1827	1020	101	70	00	10.39	8.95	1254	1540	0.0027
65	Bottom	FeSO ₄	1.1538	1.1528	0.0063	1836	1236	101	78	-23	10.35	9.01	1251	1598	0.001
66	Middle	PFS	1.1588	1.1611	0.0032	1407	1221	115	90	-25	10.20	10.03	1314	1483	-0.0023
00	Bottom	PFS	1.1572	1.1643	0.0032	1650	1500	115	90	-25	10.22	9.97	1313	1494	-0.0071
67	Middle	(NH ₄) ₂ SO ₄	1.1595	1.1572	0.0016	1908	2235	91	75	-16	10.14	8.99	1288	1553	0.0023
07	Bottom	(14074)2304	1.1623	1.1588	0.0016	2069	2295	91	70	-10	10.16	8.92	1300	1475	0.0035

Appendix 14 - Input variables (Coagulant concentration and initial density) and output variables (final density, Brookfield viscosities, Marsh viscosities, pH, conductivities, DR, Marsh gaps and initial and final density gaps) for the runs performed with different coagulants (Al₂(SO₄)₃ and PFS) at different concentrations with a mixing speed of 200 rpm, for 8 minutes on Clay A clay. ^{a)}Impossible to measure. ^{b)}Not measured

		Coagula nt	Den	sity (g/cr	m³)	Brook (cF		Mars	sh (s/qu	art)	р	Н		uctivit S/cm)		l	OR (g/cn	n³)	
Run	Zone	ration (mg/L)	Initial	Final	Gap	Initial	Initial	Final	Final	Gap	Initia I	Final	Initial	Final	Values	Mean	Error	Media n	Error
	Тор	VI-(8O)	N.M.b)	N.M.b)		N.M.b	N.M.				N.M.	N.M.	N.M. ^b	N.M.b)	N.M.b)				
R63	Middle	'	1.1592	1.1526	0.00 13	2259	2163	95	88	-7	10.2 9	9.82	N.M. ^b	N.M.b)	0.0066	0.006	0.0001	0.0067	0.0000
	Botto m	mg/L	1.1606	1.1539		2400	2271				10.3	9.84	N.M. ^b	N.M.b)	0.0067				
	Тор	DEC	N.M.b)	N.M.b)		N.M.b	N.M.				N.M.	N.M.	N.M. ^b	N.M.b)	N.M.b)				
R68	Middle		1.1526	1.1498	0.00	1563	1164	114	96	-18	10.2 8	9.74	1325	1425	0.0028	0.005	0.0030	0.0058	0.0000
	Botto mg/L	mg/L	1.1595	1.1507		1509	1338				10.2 2	9.78	1336	1428	0.0088				
	Тор	AL (CO.)	N.M.b)	N.M.b)		N.M.b)	N.M.				N.M.	N.M.	N.M. ^b	N.M.b)	N.M.b)				
R57	Middle		1.1607	1.1502	0.00	818.4	730. 8	99	85	-14	10.4 2	9.57	1164	1340	0.0105	0.010	0.0000	0.0106	0.0000
	Botto m	mg/L	1.1600	1.1494		859.2	783. 6				10.4 1	9.48	1175	1344	0.0106				
	Тор	DEO	N.M.b)	N.M.b)		N.M.b)	N.M.				N.M.	N.M.	N.M. ^b	N.M.b)	N.M.b)				
R65	Middle	PFS, 600	1.1492	1.1465	0.00 63	1827	1020	101	78	-23	10.3 9	8.95	1254	1540	0.0027	0.001	0.0009	0.0018	0.0000
	Botto m	mg/L	1.1538	1.1528		1836	1236				10.3 5	9.01	1251	1598	0.0010				
R70	Тор		N.M.b)	N.M.b)	0.00 29	N.M.b	N.M.	111	I.M.a)	I.M.a -	N.M.	N.M.	N.M. ^b	N.M.b)	N.M.b)	0.060 0	0.0004	0.0600	0.0000

	Middle	Al ₂ (SO ₄)	1.1489	1.0885		1623	11.0 4			10.2	8.57	1336	1873	0.0604				
	Botto m	з, 1000 mg/L	1.1509	1.0914		1593	N.M.			10.2 9	N.M.	1347	N.M.b)	0.0595				
	Тор	PFS,	N.M.b)	N.M.b)		N.M. ^{b)}	N.M.			N.M.	N.M.	N.M. ^b	N.M.b)	N.M.b)	0.074 4	0.0105	0.0744	0.0000
R71	Middle	1000	1.1614	1.0765	0.02 35	1797	8.16	85		10.1	7.53	1366	1924	0.0849				
	Botto m	mg/L	1.1639	1.1000		1767	-			10.1 5	N.M.	1385	N.M.b)	0.0639				
	Тор	Al ₂ (SO ₄)	N.M.b)	1.0059	N 1 N 4	N.M.b)	18.9 6			- N.M. _{b)}	7.29	N.M. ^b	1746	0.1431				
R58	Middle	. 1500	1.1490	N.M.b	N.M. b)*	2022	N.M.	109		10.3 6	N.M.	1155	N.M.b)	N.M.b)				
	Botto m)	1.1516	N.M.b)		2004	N.M.			7	N.M.			0.1476			I.M. ^{a)}	
	Тор	DEC	N.M.b)	1.0039	N.	N.M.b)	5.64			N.M.	7.14	N.M. ^b	1958	N.M.b)				
R69	Middle		1.1515	N.M.b)	N N.M.	1803	N.M.	98	N.M.	10.2 3	N.M.	1338	N.M.b)	N.M.b				
	Botto m	mg/L	1.1525	N.M. ^{b)}	<i>-</i> ,	1953	N.M.			10.2 3	N.M.	1329	N.M.b)	N.M.b				

Appendix 15 - Input variables (flocculant type and initial density) and output variables (final density, Brookfield viscosities, Marsh viscosities, pH, conductivities, DR, Marsh gaps and initial and final density gaps) for the runs performed with Al₂(SO₄)₃ and different flocculants (Microbond 6610 and Telsun 5153) at 150 mg/L with a mixing speed of 200 rpm, for 8 minutes on Clay A clay. ^{a)}Impossible to measure

Run	Zone	Flocculant	Density (g/cm³)	Brookfield (cP)	Marsh (s/quart)	рН	
-----	------	------------	-----------------	-----------------	-----------------	----	--

			Initial	Final	Gap	Initial	Final	Initial	Final	Gap	Initial	Final	DR (g/cm ³)
R57	Middle		1.1607	1.1502	0.1435	818.4	730.8	99	85	14	10.42	9.57	0.0105
K57	Bottom	-	1.1600	1.1494	0.1433	859.2	783.6	99	00	14	10.41	9.48	0.0106
D70	Middle	Missabasal	1.1566	1.0045		1659	1017	440			10.18	9.42	0.1521
R72	Bottom	Microbond	1.1630	I.M.*		1608	I.M.*	112			10.23	I.M. ^{a)}	I.M. ^{a)}
D70	Middle	0040	1.1558	1.0073	IMa)	1323	15.38	104	I.M. ^{a)}	I.M. ^{a)}	10.11	9.01	0.1485
R73	Bottom	6610	1.1580	I.M.*	I.M. ^{a)}	1560	I.M.*	104	1.IVI. ⁴⁷		10.11	I.M. ^{a)}	I.M. ^{a)}
D74	Middle	TalC 5452	1.1601	1.0020		1554	14.04	0.4			10.19	9.10	0.1581
R74	Bottom	TelSun 5153	1.1604	I.M.*		1674	I.M.*	94			10.20	I.M. ^{a)}	I.M. ^{a)}

Appendix 16 - Input variables (flocculant type and initial density) and output variables (final density, Brookfield viscosities, Marsh viscosities, pH, conductivities, DR, Marsh gaps and initial and final density gaps) for the runs performed with Al₂(SO₄)₃ and different flocculants (TelSun 5153, 9233, Telsun N23 and Flonex 934) at 150 mg/L with a mixing speed of 200 rpm, for 8 minutes on Clay A clay. ^{a)}Impossible to measure

Bun	Zone	Flocculant	Den	sity (g/cr	n³)	Brookfi	eld (cP)	Marsh (s/quart)	р	Н	DR
Run	Zone	FIOCCUIAIIL	Initial	Final	Gap	Initial	Final	Initial	Final	Initial	Final	(g/cm3)
	Тор		1.1524	1.0018		1650	26.46			10.14	9.92	0.1506
R83	Middle	Telsun 5153	1.1561	I.M. ^{a)}		1599	I.M. ^{a)}	98		10.22		I.M. ^{a)}
	Bottom		1.1654	1.101.		1635	1.101.57			10.23		1.IVI. ^ω /
	Тор		1.1569	1.0012		1899	37.32			10.20	9.93	0.1557
R87	Middle	9233	1.1580	I.M. ^{a)}		1980	I.M. ^{a)}	83		10.21		I.M. ^{a)}
	Bottom		1.1593	1.IVI. ⁴⁷	I.M. ^{a)}	2016	1.IVI. ⁴⁷		I.M. ^{a)}	10.20		1.IVI. ⁴⁷
	Тор		1.1528	1.1325	I.IVI. ^ω	1509	25.32		1.IVI. ⁴⁷	10.14	I.M.*	0.0203
R89	Middle	Telsun N23	1.1525	LMa)		1554	LMa)	96		10.15		IMa)
	Bottom		1.1574	I.M. ^{a)}		1638	I.M. ^{a)}			10.14		I.M. ^{a)}
	Тор		1.1590	1.1382		1710	30.36			10.10	9.81	0.0208
R90	Middle	Flonex 934	1.1586	I.M.a)		1737	I.M. ^{a)}	78		10.09		I.M.*
	Bottom		1.1575	I.IVI. [∽] /		1836	I.IVI. [~] /			10.07		I.IVI.

Appendix 17 - Input variables (Coagulant, flocculant concentration and initial density) and output variables (final density, Brookfield viscosities, Marsh viscosities, pH, conductivities, DR, Marsh gaps and initial and final density gaps) for the runs performed with Al₂(SO₄)₃ and TelSun 5153 at different concentrations with a mixing speed of 200 rpm, for 8 minutes on Clay A clay. ^{a)}Impossible to measure. ^{b)}Not measured.

Run	Zone	Density (g/cm³)	Brookfield (cP)	Marsh (s/quart)	рН	DR (g/cm³)
-----	------	-----------------	--------------------	-----------------	----	------------

		Coagula nt/ floccula nt concentr ation (mg/L)	Initial	Final	Gap	Initial	Initial	Initial	Final	Gap	Initial	Final	Zone	Mean	Error	Median	Error
	Тор		N.M. ^{b)}	N.M. ^{b)}		N.M.b)	N.M.b)				N.M.	N.M.	N.M.b)	N.M.b)	N.M. ^{b)}		N.M. ^{b)}
62	Middle	100/0	1.1566	1.1576	0.001 5	2166	1887	98	103	5	10.5 8	10.3 1	-0.001			0.0024	
	Bottom		1.1618	1.1561		2106	2085				10.4 1	10.2 6	0.0057				
	Тор		N.M. ^{b)}	N.M. ^{b)}		N.M.b)	N.M.b)				N.M.	N.M.	N.M.b)	N.M.b)	N.M. ^{b)}		N.M.b)
63	Middle	200/0	1.1592	1.1526	00013	2259	2163	95	86	-9	10.2 9	9.82	0.0066			0.0067	
	Bottom		1.1606	1.1539		2400	2271				10.3 0	9.84	0.0067				
	Тор		N.M.b)	N.M. ^{b)}		N.M.b)	N.M.b)				N.M.	N.M.	N.M.b)				
57	Middle	600/0	1.1607	1.1502	0.000	818.4	730.8	99	85	-14	10.4 2	9.57	0.0105	0.0106	0.0000	0.0106	0.0113
	Bottom		1.1600	1.1494		859.2	783.6				10.4 1	9.48	0.0106				
	Тор		1.1529	1.1439		1524	1260				10.1 3	10.0	0.009				
76	Middle	50/75	1.1543	1.1430	0.001	1554	1323	86	71	-15	10.1 6	10.0	0.0113	0.0110	0.0011	0.0113	0.0121
	Bottom		1.1546	1.1420		1554	1377				10.1 6	10.0	0.0126				
	Тор		1.1572	1.1408	0.002	1716	N.M.b)				9.75	9.54	0.0164				
79	Middle	100/37.5	1.1551	1.1397	8	1623		78	I.M. ^{a)}	I.M.a)	9.71	9.49	0.0154	0.0154	0.0005	0.0154	0.0165
	Bottom		1.1570	1.1425		1644					9.71	9.45	0.0145				

	Тор		1.1482	1.1348		1482					10.0 6		0.0134				
80	Middle	150/37.5	1.1497	1.1375	0.005 9	1458		90			10.1 6	N.M.	0.0122	0.0122	0.0007	0.0122	0.0131
	Bottom		1.1543	1.1434		1422					10.1 6		0.0109				
	Тор		1.1614	1.1394	0.000						N.M.	N.M.	0.022				
81	Middle	150/75	1.1604	1.1381	0.000 9	N.M.b)		N.M.b)			5)	5)	0.0223	0.0250	0.0029	0.0223	0.0241
	Bottom		1.1680	1.1372									0.0308				
	Тор		1.1654	1.0018		1761	29.52				10.2 0	9.92	0.1636				
82	Middle	150/300	1.1653	N.M.b)		1800	I.M.a)	84			10.1 6	I.M.a)	I.M.a)				
	Bottom		1.1655	N.M.b)	LMa)	1812	I.M. ^{a)}				10.2 4	I.M.a)	I.M. ^{a)}	LMa)	LM a)	LMa)	LM a)
	Тор		1.1524	1.0018	I.M. ^{a)}	1650	26.46				10.1 4	9.92	0.1506	I.M. ^{a)}	I.M. ^{a)}	I.M. ^{a)}	I.M. ^{a)}
83	Middle	150/150	1.1561	N.M.b)		1599	I.M.a)	98			10.2 2	I.M.a)	I.M. ^{a)}				
	Bottom		1.1654	N.M. ^{b)}		1635	I.M.a)				10.2	I.M.a)	I.M. ^{a)}				
	Тор		1.1607	1.1501		1692	1446				10.2 9	10.0	0.0106				
84	Middle	175/37.5	1.1619	1.1514	0.005 4	1704	1557	87	73	-14	10.2 8	9.98	0.0105	0.0084	0.0022	0.0105	0.0114
	Bottom		1.1609	1.1568		1758	1664				10.2 7	9.95	0.0041				
	Тор		1.1560	1.1475		1554	1242				10.2 3	9.94	0.0085				
78	Middle	200/15	1.1570	1.1474	0.001 1	1530	1221	113	I.M.	a)	10.2 0	9.90	0.0096	0.0106	0.0016	0.0096	0.0103
	Bottom		1.1601	1.1463		1605	1344				10.2 3	9.83	0.0138				
77	Тор	200/37.5	1.1497	1.0016	I.M. ^{a)}	1257	19.92	96			9.83	9.80	0.1481		1.1	∕I . ^{a)}	

	Middle		1.1530	I.M. ^{a)}		1287	I.M.a)		9.80	-	-		
	Bottom		1.1567	1.IVI. ^u		1311	I.M.a)		9.83	-	•		
	Тор		1.1625	1.0015	I.M. ^{a)}	1449	22.68		10.1 0	9.85	0.161		
75	Middle	200/75	1.1635	I.M. ^{a)}		1677	I.M.a)	113	10.2 0	1	1		
	Bottom		1.1648	I.IVI. ^{cr}		1818	I.M.a)		10.2 3	-	-		
	Тор		N.M.**	N.M. ^{b)}		I.M.a)	- I.M. ^{a)}		N.M.	N.M.	0.1581		
74	Middle	600/75	1.1601	1.0020		1554	14.04	94	10.1 9	9.10	I.M. ^{a)}	0.1581	I.M. ^{a)}
	Bottom		1.1604	I.M. ^{a)}		1674	- I.M. ^{a)}		10.2 0	I.M.a)	I.M. ^{a)}		

Appendix 18 - Input variables (initial density, mixing speed and introduction type) and output variables (final density, Brookfield viscosities, Marsh viscosities, pH, conductivities, DR, Marsh gaps and initial and final density gaps) for the runs performed with Al₂(SO₄)₃ and TelSun 5153 at 150 mg/L of 200 rpm, for 8 minutes on Clay A clay. ^{a)}Impossible to measure. ^{b)}Not measured.

Bun	Zana	Coagulant/flocculant	Density	(g/cm ³)	Brookf	ield (cP)	Marsh (s/quart)	į	ЭΗ	DR
Run	Zone	concentration (mg/L)	Initial	Final	Initial	Final	Initial	Final	Initial	Final	(g/cm³)
	Тор		1.1524	1.0018	1650	26.46			10.14	9.92	0.1506
R83	Middle	200 rpm (external)	1.1561	I.M. ^{a)}	1599	I.M. ^{a)}	98		10.22	N.M.b)	N.M. ^{b)}
	Bottom		1.1654	1.101.47	1635	1.101.47			10.23		
	Тор		1.1515	1.0013	2013	37.8			10.22	9.95	0.1502
R86	Middle	200 rpm (internal)	1.1520	I.M. ^{a)}	1899	I.M. ^{a)}	98	I.M.a)	10.22		N.M. ^{b)}
	Bottom		1.1556	1.101.57	1875	1.101.57			10.22	N N.M.b)	IN.IVI.~
	Тор		1.1558	1.0008	2031	94.8*			10.22		0.155
R88	Middle	20 rpm (internal)	1.1560	1.1591	1731	1497	87		10.27	10.21	-0.0031
	Bottom		1.1580	1.1580	1773	1524			10.26	10.21	0

Appendix 19 - Input variables (Coagulant concentration and initial density) and output variables (final density, Brookfield viscosities, Marsh viscosities, pH, conductivities, DR, Marsh gaps and initial and final density gaps) for the runs performed with Al₂(SO₄)₃, with a mixing speed of 200 rpm, for 8 minutes on clay B. ^{a)}Impossible to measure. ^{b)}Not measured.

Run	Zone	Coagulant	Flocculant concentration	Den	sity (g/c	:m³)	Brook	field (cP)	Mars	sh (s/qu	art)	р	Н	condu (µS/	•	DR
Kuli	Zone	(mg/L)	(mg/L)	Initial	Final	Gap	Initial	Initial	Final	Final	Gap	Initial	Final	Initial	Final	(g/cm³)
57	Middle	600	0	1.1607	1.1502	0.0008	818.4	730.8	99	85	14	10.42	9.57	1164	1340	0.0105
37	Bottom	(Terracota)	U	1.1600	1.1494		859.2	783.6	39	65	14	10.41	9.48	1175	1344	0.0106

	Тор			1.1605	1.1608		410.4	393.6				10.60	10.64	544.0	564.0	-0.0003
97	Middle	600 (MCS)	0	1.1611	1.1610	0.001	408.0	397.2	66	68	-2	10.73	10.69	543.0	561.0	0.0001
	Bottom			1.1617	1.1620		411.6	385.2				10.57	10.59	554.0	585.0	-0.0003
	Тор			N.M.**	1.0045		-	-	I.M.a)	I.M.a)	I.M. ^{a)}	N.M.b)	N.M. ^{b)}	N.M. ^{b)}	N.M. ^{b)}	0.1521
72	Middle	600 (Terracota)	75	1.1566	I.M. ^{a)}	I.M. ^{a)}	1659	1017				10.18	9.42	1326	977	N.M.b)
	Bottom	,		1.1630	I.M. ^{a)}		1608	-				10.23	N.M. ^{b)}	1337	977	N.M.b)
	Тор			1.1561	1.1522	0.0039	393	345				10.70	10.52	545	647	0.0039
96	Middle	600 (MCS)	75	1.1569	1.1535	I.M. ^{a)}	400	328.8	63	71	-8	10.70	10.53	554	666	0.0034
	Bottom			1.1576	1.1574	1.IVI. ²³ /	434	330				10.70	10.53	555	674	0.0002
	Тор			1.1452	1.0037	0.1415	2121	17.76		I.M.a)	I.M. ^{a)}	10.31	6.42	1194	1922	0.1415
59	Middle	2000 (Terracota)	0	1.1481	LMa)		2040	I.M.*	96			10.35	N.M. ^{b)}	1193	N.M. ^{b)}	N.M.b)
	Bottom			I.M.*	I.M. ^{a)}		I.M.*	I.M.*				N.M.b)	N.M.b)	N.M.b)	N.M. ^{b)}	N.M.b)
	Тор			1.1503	1.1520	I.M. ^{a)}	435.6	396.0				10.36	10.24	483.0	541.0	-0.0017
108	Middle	2000 (MCS)	0	1.1523	1.1523		445.2	411.6	83			10.34	10.23	510.0	547.0	0.0000
	Bottom			1.1522	1.1540		450.0	412.8				10.31	10.24	522.0	556.0	-0.0018

Appendix 20 - Input variables (Coagulant and flocculant type, concentration and initial density) and output variables (final density, Brookfield viscosities, Marsh viscosities, pH, conductivities, DR, Marsh gaps and initial and final density gaps) for the runs performed with a mixing speed of 200 rpm, for 8 minutes on clay B. ^{a)}Impossible to measure.

D	7	Coagula nt/	Den	sity (g/cn	1 ³)	Broo (c	kfield P)	Mars	h (s/q	uart)	pl	Н		uctivit S/cm)		D	R (g/cm	³)	
Run	Zone	flocculan t	Initial	Final	Gap	Initial	Initial	Initi al	Final	Ga p	Initial	Fina I	Initia I	Final	Values	Mean	Mean Error	Media n	Media n Error
	Тор		1.1612	1.1615		393.6	368.4				10.5 2	10.4 5	556	595	-0.0003				
99	Middle	Microbon d	1.1620	1.1631	0.000	393.8	374.4	67	68	1	10.4 9	10.4 1	569	581	-0.0011	0.000	0.0008	0.0003	0.0004
	Bottom		1.1638	1.1623		394.8	375.6				10.4 7	10.4 4	557	598	0.0015				
	Тор		1.1624	1.1495		390	697.2				10.5 9	10.6 0	538	555	0.0129				
102	Middle	5153	1.1630	1.1510	0.000 5	387.6	710.4	69	81	12	10.6 3	10.5 8	553	558	0.012	0.012 5	0.0003	0.0125	0.0000
	Bottom		1.1640	1.1515		386.4	714				10.6 3	10.6 1	566	561	0.0125				
	Тор		1.1551	1.1550		448.8	462				10.6 1	10.6 0	554	565	0.0001				
101	Middle	Al ₂ (SO ₄) ₃	1.1562	1.1559	I.M.a)	445.2	421.1	80	80	0	10.6 3	10.5 9	557	569	0.0003	0.000 6	0.0004	0.0003	0.0004
	Bottom		1.1574	1.1560		462	421.2				10.6 3	10.5 9	546	563	0.0014				
	Тор		1.1510	1.1395		434	700.7				10.6 9	10.6 5	558	567	0.0115				
95	Middle	Al ₂ (SO ₄) ₃ + 5153	1.1524	1.1401	0.001 1	438	711.1	71	79	8	10.6 9	10.6 5	572	567	0.0123	0.011 6	0.0004	0.0115	0.0002
	Bottom		1.1523	1.1412		434	727.2				10.7 0	10.6 4	555	572	0.0111				
103	Тор	PFS+515	1.1644	1.1538	0.000	404.4	1073	74	I.M. ^{a)}	I.M.	10.6 5	10.6 0	507	534	0.0106	0.010	0.0000	0.0107	0.0000
103	Middle	3	1.1651	1.1544	2	409.2	1014	/4			10.7 1	10.6 0	521	542	0.0107	7	0.0000	0.0107	0.0000

	Bottom		1.1653	1.1546		409.2	922.8				10.6 9	10.6 0	523	539	0.0107				
	Тор		1.1640	1.1551		499.2	750				10.6 1	10.5 9	519	535	0.0089				
104	Middle	FeSO ₄ +5 153	1.1657	1.1553	0.000 4	495.2	750	87	92	5	10.6 3	10.5 9	512	533	0.0104	0.010 1	0.0006	0.0104	0.0004
	Bottom		1.1668	1.1557		498	760.8				10.6 2	10.5 9	505	535	0.0111				

Appendix 21 - Input variables (Coagulant type and concentration and initial density) and output variables (final density, Brookfield viscosities, Marsh viscosities, pH, conductivities, DR, Marsh gaps and initial and final density gaps) for the runs performed NaCl and CaCl₂ with a mixing speed of 200 rpm, for 8 minutes on clay B. ^{a)}Impossible to measure.

			De	ensity (g/d	cm³)	Brookfi	ield (cP)	р	Н	condu (µS/			DR	(g/cm³)		
Run	Zone	Coagulant concentration (mg/L)	Initial	Final	Gap	Initial	Initial	Final	Final	Initial	Final	Zone	Mean	Error	Media n	Error
	Тор		1.142 4	1.1267		417.6	4776	10.1 9	9.58	518	6630	0.0157				
111	Middle	NaCl (584 mg/L)	1.142 9	1.1334	0.0013	427.2	5664	10.3 2	9.56	509	6776	0.0095	0.012 4	0.0018	0.0120	0.0005
	Botto m		1.144 1	1.1321		427.2	5334	10.3 1	9.55	502	6884	0.0120				
	Тор		1.154 2	1.1406		352.8	3196	10.7 2	9.6	559	6850	0.0136				
112	Middle	NaCl (5844 mg/L)	1.156 2	1.1421	0.0023	357.6	3840	10.7 9	9.9	568	6810	0.0141	0.015 3	0.0014	0.0141	0.0015
	Botto m		1.157 9	1.1398		356.4	3138	10.7 5	9.9	567	6750	0.0181				
100	Тор	CaCl ₂ (1110	1.151 2	1.1502	0.0014	484.8	441.6	10.1 6	10.2 9	459.0	493.0	0.0010	0.000	0.0000	0.0000	0.0002
106	Middle		1.151 7	1.1509	0.0011	480.0	452.0	10.3 5	10.2 9	475.0	508.0	0.0008	6	0.0003	0.0008	0.0003

	Botto m		1.152 0	1.1520		472.8	420.0	10.3 4	10.3	463.0	514.0	0.0000				
	Тор		1.153 3	1.1531		392.4	351.6	10.7 1	10.6 8	541.0	618.0	0.0002				
109	Middle	CaCl ₂ (2775 mg/L)	1.154 2	1.1541	0.0008	400.8	352.8	10.7 1	10.6 8	544.0	628.0	0.0001	0.000	0.0006	0.0002	0.0007
	Botto m		1.155 1	1.1533		399.6	351.6	10.7 7	10.6 8	561.0	614.0	0.0018				
	Тор		1.158 9	1.1560		398.4	300.0	10.8 2	10.5 7	540.0	737.0	0.0029				
107	Middle	CaCl ₂ (5549 mg/L)	1.160 3	1.1573	0.0007	402.0	303.6	10.7 5	10.5 7	530.0	732.0	0.0030	0.002 8	0.0002	0.0029	0.0001
	Botto m		1.160 5	1.1580		396.0	309.6	10.6 6	10.5 6	541.0	737.0	0.0025				
105	Тор		1.157 4	1.0026		402.0	2.2	10.8 5	9.20	529.0	7.0	0.1548				
I.M.a	Middle	CaCl ₂ (11100 mg/L)	1.157 7	I.M. ^{a)}	I.M. ^{a)}	404.4	I.M. ^{a)}	10.9 2	I.M.*	523.0	I.M. ^{a)}	I.M. ^{a)}	0.154 8	I.M. ^{a)}	0.1548	0.0000
)	Botto m		1.159 0	1.IVI. ⁹⁷		405.6	1.IVI. ⁹⁷	10.9 1	I.IVI.	530.0						

Appendix 22 - Input variables (Coagulant concentration and initial density) and output variables (final density, Brookfield viscosities, Marsh viscosities, pH, conductivities, DR, Marsh gaps and initial and final density gaps) for the runs performed with Al₂(SO₄)₃, with a mixing speed of 200 rpm, for 8 minutes on clay B without GPlus. ^{a)}Impossible to measure.

Dun	Zono	Coagulant		sity (g/	cm³)	Brookf	ield (cP)		рН	condu (µS/	ctivity cm)		D	R (g/cm³)	
Run	Zone	concentratio n (mg/L)	Initial	Final	Gap	Initial	Initial	Final	Final	Initial	Final	Zone	Mean	Error	Media n	Error
113	Тор	0 (no GPlus)	1.154 9	1.106 7	0.0174	436.8	367.2	10.9 3	10.89	536	513	0.0482	0.036	0.0077	0.0394	0.003
113	Middle	0 (no GPius)	1.160 5	1.122 1	0.0174	544.8	518.4	10.9 9	10.95	539	542	0.0384	1	0.0077	0.0384	0

	Bottom		1.161 2	1.139 5		667.2	589.2	10.9 7	10.94	543	543	0.0217				
	Тор		1.129 0	1.135 0		680.4	483.6	10.8 4	10.43	418	511	-0.006				
115	Middle	300 (no GPlus)	1.130 3	1.123 4	0.0045	698.4	483.6	10.8	10.39	413	515	0.0069	0.002	0.0040	0.0050	0.004
	Bottom		1.132 9	1.127 9		760.8	667.2	10.8	10.36	419	516	0.005				
	Тор		1.160 5	1.160 8		410.4	393.6	10.6 0	10.64	544.0	564.0	-0.0003				
97	Middle	600	1.161 1	1.161 0	0.001	408.0	397.2	10.7 3	10.69	543.0	561.0	0.0001	0.000	0.0001	0.0003	0.000 2
	Bottom		1.161 7	1.162 0		411.6	385.2	10.5 7	10.59	554.0	585.0	-0.0003	2			
	Тор		1.129 3	1.001 7		775.2	29.8	10.5 5	9.76	490.0	745.0	0.1276				
144	Middle	600 (no GPlus)	1.136 9	1.117 2	I.M. ^{a)}	796.8	129.6	10.6 2	9.79	494.0	748.0	0.0197	0.073	I.M. ^{a)}	0.0737	0.000
	Bottom		1.138 2	I.M.*		825.6	I.M. ^{a)} M. *	10.5 4	I.M.a)	494.0	I.M. ^{a)}	I.M. ^{a)}				
	Тор		1.150 3	1.152 0		435.6	396.0	10.3 6	10.24	483.0	541.0	-0.0017				
108	Middle	2000	1.152 3	1.152 3	0.0017	445.2	411.6	10.3 4	10.23	510.0	547.0	0.0000	0.001	0.0006	- 0.0017	0.000 7
	Bottom		1.152 2	1.154 0		450.0	412.8	10.3	10.24	522.0	556.0	-0.0018	2			
110	Тор		1.142 4	1.000		652.8	1.44	10.8 9	4.91	475	1502	0.1423				
I.M. ^{a)} I.M.	Middle	2000 (no GPlus)	1.155 6	I.M.*	I.M. ^{a)}	519.6	I.M. ^{a)}	I.M.a)	I.M.*	478	I.M. ^{a)}	I.M. ^{a)}	0.142 3	I.M. ^{a)}	0.1423	0.000
a)	Bottom		1.156 0	I.M.*		612	I.M. ^{a)}	I.M. ^{a)}	I.M.*	479	I.M. ^{a)}	I.M. ^{a)}				

Appendix 23 - Input variables (Coagulant type and initial density) and output variables (final density, Brookfield viscosities, Marsh viscosities, pH, conductivities, DR, Marsh gaps and initial and final density gaps) for the runs performed with different coagulants with a mixing speed of 200 rpm, for 8 minutes on clay B without Gplus.

Run	Zone	Coagulant	Dens	sity (g/cr	n³)	Brookfi	eld (cP)	р	Н		ctivity (cm)		[OR (g/cm	1 ³)	
114		Joagaiain	Initial	Final	Gap	Initial	Initial	Final	Final	Initial	Final	Zone	Mean	Error	Median	Error
	Тор		1.1326	1.1292		759.6	550.8	10.51	10.08	451	542	0.0034				
141	Middle	Al ₂ (SO ₄) ₃	1.1277	1.1329	0.0053	802.8	674.4	10.39	10.18	454	549	- 0.0052	0.0043	0.0042	0.0052	0.0011
	Bottom		1.1270	1.1382		822	649.2	10.45	10.21	450	545	- 0.0112				
	Тор		1.1236	1.0018		602.4	62.88	10.48	9.75	465	661	0.1218				
142	Middle	PFS	1.1275	1.1392	0.0027	646.8	182.4	10.47	9.75	466	659	- 0.0117	0.0350	0.0434	- 0.0051	0.0528
	Bottom		1.1368	1.1419		746.4	214.8	10.47	9.64	464	641	- 0.0051				
	Тор		1.1270	1.1133		774	872.2	10.36	10.37	490	483	0.0137				
143	Middle	A0410	1.1275	1.1203	0.0004	806.4	855.6	10.40	10.41	478	464	0.0072	0.0106	0.0019	0.0108	0.0003
	Bottom		1.1307	1.1199		770.4	898.8	10.39	10.40	478	464	0.0108				

Appendix 24 - Input variables (flocculant type and initial density) and output variables (final density, Brookfield viscosities, Marsh viscosities, pH, conductivities, DR, Marsh gaps and initial and final density gaps) for the runs performed with NaCl and flocculants, with a mixing speed of 200 rpm, for 8 minutes on clay B

Run Zo	Zone	Flocculant	Den	sity (g/cm	1 ³)	Brookf	ield (cP)	р	Н		ductivity S/cm)		DI	R (g/cm³)	
			Initial	Final	Gap	Initial	Initial	Final	Final	Initial	Final	Zone	Mean	Error	Median	Error

	Тор		1.1400	1.1345		2418	4512	10.49	10.25	532	955	0.0055				
116	Middle	Microbond	1.1433	1.1424	0.0088	2643	4782	10.52	10.22	543	975	0.0009	0.0069	0.0040	0.0055	0.0019
	Bottom		1.1480	1.1336		4773	4920	10.49	10.19	556	984	0.0144				
	Тор		1.1257	1.1266		3048	>6000	10.73	10.51	500	766	-0.0009				
117	Middle	6610	1.1309	1.1264	0.0005	3324	>6000	10.78	10.53	463	834	0.0045	0.0051	0.0036	0.0045	0.0008
	Bottom		1.1386	1.1269		3678	>6000	10.79	10.52	547	856	0.0117				

Appendix 25 - Input variables (flocculant and HCl concentration and initial density) and output variables (final density, Brookfield viscosities, Marsh viscosities, pH, conductivities, DR, Marsh gaps and initial and final density gaps) for the runs performed with 6605, with a mixing speed of 300/50 rpm, for 8 minutes on clay B. a) Impossible to measure.

Dun	Zono	Flocculant/HCI	Der	sity (g/	cm³)	Brookfi	eld (cP)	р	Н	conduc (µS/c	•		Di	R (g/cm³)	ı	
Run	Zone	concentration (mg/L/ mM)	Initial	Final	Gap	Initial	Initial	Final	Final	Initial	Final	Zone	Mean	Error	Media n	Error
	Тор		1.1483	1.1492		4686	4936	10.36	10.48	477	509	-0.0009				
131	Middle	0	1.1481	1.1514	0.0008	5046	5046	10.41	10.51	507	511	-0.0033	0.0003	0.0020	0.0009	0.0008
	Bottom		1.1556	1.1522		5526	5622	10.44	10.51	505	518	0.0034	0.0000		0.0000	
	Тор		1.1486	1.1185		5634	3780	10.53	10.18	516	575	0.0301				
129	Middle	1000/0	1.1434	1.1187	0.0109	5832	3792	10.56	10.20	521	578	0.0247	0.0252	0.0027	0.0247	0.0006
	Bottom		1.1503	1.1296		5976	4416	10.53	10.21	517	574	0.0207				
	Тор		1.1423	1.1117		>6000	5232	10.70	9.75	498	665	0.0306				
127	Middle	1000/2.1	1.1485	1.1312	0.0015	5942	5484	10.72	9.64	581	686	0.0173	0.0245	0.0039	0.0255	0.0014
	Bottom		1.1582	1.1327		>6000	5784	10.71	9.58	487	618	0.0255				

	Тор		1.1387	I.M. a)	I.M. a)	4440	>6000	10.42	10.16	488	588		
134	Middle	1200/0	1.1412			4914	>6000		10.16	493	605		
104		1200/0						-		489			
	Bottom		1.1473			5362	>6000	10.44	10.18	409	612		
	Top		1.1484			5034	>6000	10.32	8.91	548	827		
135	Middle	1200/2.5	1.1524			5478	>6000	10.34	8.98	551	848	I.M. ^{a)}	
	Bottom		1.1545			5478	>6000	10.29	9.02	559	851		
	Тор		1.1447			4711		10.31		503			
132	Middle	1500/3.125	1.1452			5094	I.M. ^{a)}	10.40	I.M. a)	502	I.M. ^{a)}		I.M. ^{a)}
	Bottom		1.1504			5286		10.44		509			
126	Тор		1.1122	0.9996		2520	6	10.49	7.23	523	933	0.1126	
I.M. ^{a)}	Middle	2000/4.2 (5g/L)	1.1350	I.M. ^{a)}		3414	I.M. ^{a)}	10.50	I.M. a)	531		M.*	
1.IVI. "	Bottom		1.1780	1.IVI. ⁴⁷	I.M. ^{a)}	4668	1.101. 9	10.48	I.M. ^{a)}	582] 1.1	VI.	
	Тор		1.1515	1.0013	I.IVI. ^u	>6000	19.5	10.49	7.79	485	1038	0.1502	
130	Middle	2000/4.2 (10 g/L)	1.1511	I.M. ^{a)}		>6000	I.M. ^{a)}	10.54	I.M.*	498		∕ I. ^{a)}	
	Bottom		1.1534	1.IVI. ⁴⁷		>6000	1.IVI. ^ω /	10.50	1.171.	498	1.1	VI/	

Appendix 26 - Input variables (HCl concentration and initial density) and output variables (final density, Brookfield viscosities, Marsh viscosities, pH, conductivities, DR, Marsh gaps and initial and final density gaps) for the runs performed with A0140, with a mixing speed of 300/50 rpm, for 8 minutes on clay B- a) Impossible to measure

Run	Zone	HCI concentratio	Dens	sity (g/cı	m³)	Brook	field (cP)	р	Н	condu (µS/	ctivity cm)		D	R (g/cm	³)	
Kuii	Zone	n (mM)	Initial	Final	Gap	Initial	Initial	Final	Final	Initial	Final	Zone	Mean	Error	Media n	Error
120	Тор	0	1.1535	1.1272	0.002	>6000	>6000	10.52	10.44	482	445	0.0263	0.028	0.0027	0.0263	0.0024
120	Middle	U	1.1554	1.1307	0.002	>6000	>6000	10.49	10.44	488	449	0.0247	1	0.0027	0.0263	0.0024

			l			1							1		1	1
	Bottom		1.1661	1.1327		>6000	>6000	10.45	10.43	496	448	0.0334				
	Тор		1.1217	1.1039		2634	>6000	10.26	9.65	451	470	0.0178				
121	Middle	8.0	1.1321	1.1028	0.0013	3012	>6000	10.26	9.74	456	471	0.0293	0.027 8	0.0054	0.0293	0.0020
	Bottom		1.1403	1.1041		4306	>6000	10.25	9.76	455	473	0.0362				
	Тор		1.1439	1.1080		5514	>6000	10.31	9.37	514	491	0.0359				
122	Middle	1.7	1.1457	1.1176	0.0113	5760	>6000	10.31	9.38	519	557	0.0281	0.036	0.0048	0.0359	0.0004
	Bottom		1.1509	1.1063		>6000	>6000	10.30	9.38	520	591	0.0446	_			
	Тор		1.1443	1.1200		5238	>6000	10.55	9.50	484	659	0.0243				
136	Middle	2.5	1.1456	1.1083	0.0112	5574	>6000	10.53	9.33	494	645	0.0373	0.030	0.0038	0.0298	0.0009
	Bottom		1.1493	1.1195		5808	>6000	10.55	9.27	486	658	0.0298				
	Тор		1.1615	1.1244		55320	292800	10.33	9.11	543	633	0.0371				
152	Middle	2.5 (replica)	1.1644	1.1257	0.0064	47160	>300000	10.43	9.08	531	650	0.0387	0.035 5	0.0024	0.0371	0.0021
	Bottom		1.1628	1.1321		49866	292800	10.44	9.09	539	660	0.0307				
	Тор		1.1555	1.1190		48900	273000	10.62	9.48	525	614	0.0365				
156	Middle	2.5 (16°C)	1.1583	1.1214	0.0062	43140	298300	10.70	9.64	510	624	0.0369	0.040	0.0036	0.0369	0.0044
	Bottom		1.1626	1.1152		52200	427800	10.72	9.63	507	620	0.0474				
	Тор		1.1491	1.1109		31500	628800	10.65	9.21	507	594	0.0382				
157	Middle	2.5 (21°C)	1.1537	1.1073	0.0037	48360	728400	10.64	9.21	532	633	0.0464	0.048	0.0063	0.0464	0.0023
	Bottom		1.1634	1.1036		37320	885600	10.64	9.20	530	633	0.0598] '			
	Тор		1.1582	1.1101		39540	270600	10.46	8.64	521	651	0.0481				
153	Middle	2.9	1.1529	1.1177	0.0001	38820	275700	10.45	8.76	526	710	0.0352	0.041 8	0.0037	0.0420	0.0003
	Bottom		1.1598	1.1178		38700	278700	10.46	8.76	498	710	0.042				
4.40	Тор	2.0	1.1476	1.0692	0.0044	5136	>6000	10.44	8.64	502	721	0.0784	0.057	0.0400	0.0000	0.0000
140	Middle	3.3	1.1487	1.1142	0.0211	5946	>6000	10.43	8.59	505	715	0.0345	9	0.0128	0.0609	0.0039

	Bottom		1.1540	1.0931		>6000	>6000	10.44	8.52	504	716	0.0609				
	Тор		1.1597	1.0898		48360	202500	10.42	8.12	584	813	0.0699				
154	Middle	3.9	1.1623	1.0862	0.0099	42540	200400	10.43	8.09	582	821	0.0761	0.071 4	0.0024	0.0699	0.0020
	Bottom		1.1643	1.0961		40800	276000	10.41	8.09	586	823	0.0682				
	Тор		1.1532	1.0779		42720	286500	10.36	7.69	691	876	0.0753				
155	Middle	4.4	1.1530	1.0994	0.0021	35400	261900	10.36	7.64	601	864	0.0536	0.061 6	0.0069	0.0558	0.0076
	Bottom		1.1531	1.0973		34800	269400	10.36	7.59	608	861	0.0558	Ŭ			
	Тор		1.1580	1.0882		15600	6300	10.53	7.55	578	866	0.0698				
158	Middle	4.7	1.1604	1.1126	0.0183	23760	745280	10.50	7.56	565	867	0.0478	0.061 9	0.0341	0.0681	0.0082
	Bottom		1.1624	1.0943		17340	766800	10.51	7.65	510	859	0.0681				
	Тор		1.1466	1.0001		48720		10.26		598		0.1465				
151	Middle	5	1.1593	I.M. ^{a)}		38580		10.34		624		I.M.*				
	Bottom		1.1481	1.IVI. ⁴⁷	I I.M. ^{a)}	37020	I.M. ^{a)}	10.28	I.M. ^{a)}	622	I.M. ^{a)}	I.M.*		IM a)I.M. ^{a)}	
	Тор		1.1597	0.9974	i I.IVI. ^u	52320	1.IVI. ~/	10.56	ı.lVI. ∽′	563	1.IVI. [/]	0.1623		1.IVI. [~]	′1.1VI. [~] ′	
150	Middle	6.6	1.1601			51480		10.56		558		I.M.*				
	Bottom		1.1612	I.M. ^{a)}		48240		10.55		560		I.M.*				

Appendix 27 - Input variables (flocculant concentration and initial density) and output variables (final density, Brookfield viscosities, Marsh viscosities, pH, conductivities, DR, Marsh gaps and initial and final density gaps) for the runs performed with 6605, with a mixing speed of 300/50 rpm, for 8 minutes on clay B

Run	Zone	Flocculant concentration (mg/L)	Density (g/cm³)			Brookfi	eld (cP)		DR (g/cm³)			
			Initial	Final	Gap	Initial	Initial	Zone	Mean	Error	Median	Error
149	Тор	250	1.1434	1.1491	0	39660	180300	-0.0057	0.0017	0.0039	0.0033	0.0021
	Middle		1.1520	1.1487		32700	135600	0.0033		0.0039	0.0033	0.0021

	Bottom		1.1530	1.1456		33300	181500	0.0074				
	Тор		1.1576	1.1309		44340	1037000	0.0267				
159	Middle	800	1.1570	1.1270	0	46680	765600	0.03	0.0325	0.0042	0.0300	0.0032
	Bottom		1.1595	1.1188		39300	978000	0.0407				
	Тор		1.1615	1.1244		55320	292800	0.0371				
152	Middle	1000	1.1644	1.1257	0	47160	>300000	0.0387	0.0355	0.0024	0.0371	0.0021
	Bottom		1.1628	1.1321		49866	292800	0.0307				
	Тор		1.1457	1.1224		4308	>6000	0.0233				
137	Middle	1500	1.1472	1.1112	0	4452	>6000	0.036	0.0334	0.0053	0.0360	0.0034
	Bottom		1.1492	1.1082		5740	>6000	0.041				

Appendix 28 - Input variables (flocculant and HCl concentration and initial density) and output variables (final density, Brookfield viscosities, Marsh viscosities, pH, conductivities, DR, Marsh gaps and initial and final density gaps) for the runs performed with A0410, with a mixing speed of 300/50 rpm, for 8 minutes on clay B/sand mix

Run	Zone	HCI concentration (mM)	Density (g/cm³)			Brookfi	eld (cP)		DR (g/cm³)			
			Initial	Final	Gap	Initial	Initial	Zone	Mean	Error	Median	Error
	Тор	0 (clay)	1.1535	1.1272	0	>6000	>6000	0.0263	0.0281	0.0027	0.0263	0.0024
120	Middle		1.1554	1.1307		>6000	>6000	0.0247				
	Bottom		1.1661	1.1327		>6000	>6000	0.0334				
	Тор	0.8 (clay)	1.1217	1.1039	0	2634	>6000	0.0178	0.0278	0.0054	0.0293	0.0020
121	Middle		1.1321	1.1028		3012	>6000	0.0293				
	Bottom		1.1403	1.1041		4306	>6000	0.0362				
152	Тор	2.5 (clay)	1.1615	1.1244	0	55320	292800	0.0371	0.0355	0.0024	0.0371	0.0021
	Middle		1.1644	1.1257		47160	>300000	0.0387				0.0021

	Bottom		1.1628	1.1321		49866	292800	0.0307				
160	Тор	0 (clay/sand)	1.2100	1.1800	0	109800	294600	0.030	0.0350	0.0029	0.0350	0.0000
	Middle		1.2200	1.1800		73200	585600	0.040				
	Bottom		1.2200	1.1850		79200	274800	0.035				
	Тор	0.8 (clay/sand)	1.2000	1.1800	0	63000	937200	0.020	0.0267	0.0033	0.0300	0.0044
161	Middle		1.2100	1.1800		56400	853200	0.030				
	Bottom		1.2200	1.1900		59100	763800	0.030				
	Тор	2.5 (clay/sand)	1.2100	1.1650	0	151200	1968000	0.045	0.0433	0.0044	0.0450	0.0022
162	Middle		1.2200	1.1700		153600	1626000	0.050				
	Bottom		1.2150	1.1800		152400	1566000	0.035				

Run	Zone	Coagulant/flocculant	Density (g/cm³)			Brookfi	eld (cP)	DR (g/cm³))	
		concentration (mg/L)	Initial	Final	Gap	Initial	Initial	Zone	Mean	Error	Median	Error
	Тор		1.2000	1.1900	0.0100	52800	2214000	0.01				
R165	Middle	0.2L	1.2100	1.1850		42600	2394000	0.025	0.0167	0.0044	0.0150	0.0022
	Bottom		1.2100	1.1950		43200	2340000	0.015				
	Тор		1.2100	1.1650	0.0100	151200	1968000	0.045				
R162	Middle	0.4L	1.2200	1.1700		153600	1626000	0.050	0.0433	0.0044	0.0450	0.0022
	Bottom		1.2150	1.1800		152400	1566000	0.035				
	Тор		1.2100	1.1500	0.0000	105600	3432000	0.06				
R164	Middle	0.67L	1.2100	1.1600		82800	2382000	0.05	0.0567	0.0033	0.0600	0.0044
	Bottom		1.2200	1.1600		87600	1920000	0.06				
	Тор		1.2100	1.1350	0.0100	128500	978000	0.075				
R163	Middle	1L	1.2100	1.1300		133200	690000	0.08	0.0750	0.0029	0.0750	0.0000
	Bottom		1.2100	1.1400		91200	924000	0.07				